THE HONG KONG POLYTECHNIC UNIVERSITY

CIVIL AND STRUCTURAL ENGINEERING DEPARTMENT

STRUCTURAL CONTROL AND CONDITION ASSESSMENT WITH SUBSTRUCTURE METHOD

YONG DING

B. Sc, M. Sc.

A thesis submitted in partial fulfillment of the requirements for the

Degree of **Doctor of Philosophy**

July, 2011

CERTIFICATE OF ORIGINALITY

I hereby declare that this thesis is my own work and that, to the best of my knowledge and belief, it reproduces no material previously published or written, nor material that has been accepted for the award of my other degree or diploma, except where due acknowledgement has been made in the text.

_______________________________ (Signed)

_________DING Yong____________ (Name of student)

To My Parents

ABSTRACT

Structural condition assessment is a major component in a structural health monitoring system. A large scale structural system may have complex boundary conditions and uncertainties due to the discreteness of geometric and material properties. Models on the boundary conditions and any innovative vibration control device for seismic protection in a large scale civil structure may not be accurate. Another obstacle for large scale civil structural condition assessment is that the current damage detection methods are either insensitive to local structural damage or sensitive to measurement noise. It is difficult to conduct structural condition evaluation for large structures partially because of these points.

Numerous structural condition assessment methods have been proposed. The structural condition assessment methods in frequency domain always need large number of measured data. The methods in time domain are alternative solutions to structural health monitoring which needs as few data as possible. Though a lot of work has been done in this field, there are yet some gaps which limit the application of this kind of method. It is usually difficult to conduct the parameter identification in large scale structural system also due to the computational efficiency, accuracy and convergence. Previous time response sensitivity methods commonly assume the structure is connected rigidly to the base and the base-superstructure interaction is rarely taken into consideration. Most of the sensitivity methods in time domain commonly need the record of the excitation or

need an assumption of the function of the external force time history. Also the initial structural responses, e.g. acceleration, velocity and displacement, are commonly assumed to be zero but they are always unknown and non-zero values. Time-variant structural parameter identification is difficult to be identified with the existing time response sensitivity methods. Efficient structural control can ensure the structural reliability of the structure during the severe earthquake or other harsh environmental load. The integrated system of structural control and model updating would make the structural control algorithm more stable and effective. However, only the integrated system with model updating method in frequency domain has been investigated. This thesis aim to propose a framework to conduct the structural condition assessment and structural control based on substructure methods which could improve the computational effort, perform the general out-put only structural condition evaluation, including load evaluation and damage detection, conduct the time-variant structural condition evaluation and implement the smart structure with the integration of structural control and structural health monitoring.

The time response sensitivity method in time domain with substructure method is an alternative solution to large scale structural condition assessment, which needs as few data as possible. Several components of work in structural condition assessment and structural control are completed in this thesis. Firstly, a substructural external force identification method based on the equation in state space with the First-Order Hold discrete and Tikhonov regularization is presented.

This method makes good use of this limited but accurate analytical information of the target substructure for the inverse identification of moving or static external force acting on the structure. Secondly, a general response sensitivity method based on the two-stage identification for structural model updating considering the nonlinear support-superstructure interaction is developed. The two-stage identification method proposed previously for substructural condition assessment is illustrated, proved and improved. With the two-stage method the interface forces are identified in the first stage and the local damage is detected in the second stage. In this study, a concept of pseudo structure is constructed for illustration and proof. Furthermore, two new computational methods are proposed to improve the first stage identification. A time window force identification method is presented to reduce the computation effort of the first stage identification. The structural responses of the first time step are always supposed as zero with time domain response sensitivity method in previous research work. However, the initial structural responses are unknown and non-zero practically. In general, and a method for the simultaneous identification of the unknown force and initial responses are also presented for the first stage identification. An adaptive regularization method is employed for the model updating in the second stage. Thirdly, a time-variant structural parameter is proposed based on time window identification method. With this method, the abrupt structural damage during the earthquake could be identified. Lastly, a new combined system of adaptive structural control and structural evaluation is proposed. The structural control system is implemented with the LQG which is an effective control method for the vibration mitigation of structures. The structural control is adaptive with the changes of the structural parameters via the structural evaluation system. A modified adaptive regularization method is used in the solution of the structural evaluation via model updating. The combination of the structural control and evaluation is designed as decentralized autonomous to guarantee the reliability under the harsh environmental excitation. The decentralized autonomous control system explores the substructure method which is more efficient in calculation with smaller mass, damping and stiffness matrices for the structural evaluation. All these proposed methods in this thesis are verified by numerical simulation. The two-stage identification method and time-variant damping identification is also verified by laboratory work. Results show that the proposed methods on the structural condition assessment are effective and perform satisfactorily even there is noise in the measurement.

LIST OF PUBLICATIONS

Journal Papers:

Law, S.S. and Ding, Y., (2010), "Substructure Methods for Structural Condition Assessment", *Journal of Sound and Vibration*, 330(15), 3606-3619.

Ding, Y. and Law, S.S., (2010), "Dynamic Load Assessment with Information of A Substructure Only", *Journal of Applied Mechanics*. ASME. (Under review)

Ding, Y. and Law, S.S., (2010), "Structural damping Identification based on an Iterative Regularization Method", *Journal of Sound and Vibration*, 330(10), 2281-2298.

Law, S.S., Li, J. and Ding, Y., (2010), "Structural response reconstruction with transmissibility concept in frequency domain", *Mechanical System and Signal Processing*, 25(3), 952-968.

Ding, Y. and Law, S.S., (2010), "A General Response Sensitivity Method for Substructural Condition Assessment", *Journal of Sound and Vibration*. (Under review)

Conference Papers:

Law, S.S. and Ding, Y., (2009), "Substructure Method of Damage Identification without Input Information", *The 4th International Symposium on Environmental Vibration: Prediction, Monitoring and Evaluation*，1353-1358, Beijing, China.

Law, S.S. and Ding, Y., (2009), "Dynamic Condition Assessment of a Substructure in a Large Civil Infrastructural System", *The 6th National Workshop on Nondestructive Evaluation of Civil Infrastructural System (NDECIS'09) Inspection, Monitoring and Diagnosis of Bridges*, Taiwan, China.

Ding, Y. and Law, S.S., (2010), "Dynamic load assessment of substructure", *The 9 th International Conference of Civil and Environmental Engineering*, Dalian, China.

Ding, Y. and Law, S.S., (2011), "Integration of pseudo negative stiffness control and structural health monitoring for large scale structural system", *Smart Structures/NDE*, SPIE.

Ding, Y. and Law, S.S., (2011), "A New Sensitivity Method for Substructural Condition Assessment", *International Operational Modal Analysis Conference*, Turkey.

ACKNOWLEDGEMENTS

I would like firstly to express my deepest gratitude and foremost to my supervisor, Prof. S. S. Law, for his patient instruction and enlightening guidance, extensive discussion and kindest encouragement throughout my PhD study. I benefit a lot from his research attitude and strategy, high efficiency, critical and creative thinking.

Secondly, I would like to express my gratitude to Prof. Bin Wu from Harbin Institute of Technology where I got my M.Sc. degree. It is his instruction that initiate my research interest and then I have this great opportunity to study in The Hong Kong Polytechnic University.

I am very lucky to have Mr. J. Li, Dr. S. Q. Wu, Miss. K. Liu and Dr. X. Y. Li who are my colleagues for their constructive comments as well as encouraging discussions. I would like to express my gratitude to them for the friendship and for their persistent help to me. Special thanks are extended to Mr. T. T. Wai, Mr. H.Y. Yau, Mr. C.W. Liauw and Mr. C.F. Cheung for their assistance in the laboratory work.

Appreciation is extended to the Hong Kong Polytechnic University, who provides me the financial support which makes my PhD study possible.

Last but not least, I am greatly indebted to my family for their constant support and encouragement.

TABLE OF CONTENTS

LIST OF TABLES

LIST OF FIGURES

CHAPTER 1

INTRODUCTION

1.1 Research Background

During the long-term service, civil engineering structures may be subject to some the hazards or deterioration, such as earthquake typhoon, fire, explosion and long-term fatigue damage. To mitigate the vibration and monitoring the condition important modern structures are always built as smart structures and instrumented with structural health monitoring system and structural vibration control system. Structural vibration control system and structural health monitoring system will play an important role to reduce and predict the potential damage, to ensure the safety and reliability of the structural system and provide detailed guideline for more efficient maintenance after long-term service or hazards.

As the two important components of modern smart structure both of the structural condition assessment and control have received considerable attention respectively from the researchers in the last few decades. The integrated system with the function of structural control and structural health monitoring has also been another active field of the smart structure.

1.1.1 Background of Structural Condition Assessment

Damage detection and model updating are vital aspects of structural condition assessment. The damage of structure could be generally defined as an abnormal change which adversely affects the performance of the system in an comprehensive review paper (Doebling et al. 1998). Increasing interest has been attracted to structural condition assessment due to the natural catastrophes such as earthquake and typhoon, dynamic load, permanent static load and so on. With the successive investigation of researchers the damage will be defined as the changes of materials or geometric properties of systems, including the boundary condition the connectivity, which adversely affects the performance of the system (Farra et al., 2001). A four-level damage detection procedure was proposed by Rytter (1993) as

Level 1: Damage detection Determination of the presence of damage in the structure;

Level 2: Damage localization: Level 1 plus determination of the probable location of the damage;

Level 3: (Damage Quantification): Level 2 plus quantification of the severity of the damage;

Level 4: (Consequence): Level 3 plus prediction of the remaining useful life of the structure.

These four series steps provide a practical guideline to damage detection (Yao and Natke 1994; Park et al. 1997; Stubbs et al. 1998, 2000). This thesis focuses on the second and third level investigation of damage detection. Model updating method is also presented in this thesis which considers the model error as well as abnormal changes of the structural properties. The structural damage in this Thesis is also defined the loss of the stiffness as majority of existing research literatures.

The damage could be classified as linear damage or nonlinear damage. The damage is linear if the initially linear structure still retains the linear elastic property (Doebling et al., 1998). Research in this field has produced substantial literature and numerous has been applied to detect damage in mechanical, aeronautical and civil engineering systems. The damage is nonlinear if the initially linear structure behaves nonlinearly after the damage (Doabling et al., 1998). The nonlinear damage will also be reflected in the structural response and the parameters derived from the structure response. Without considering the nonlinear structural damage, the linear damage identification method would provide unexpected results for the nonlinear damage identification. A detailed report summarizes the nonlinearity identification method (Kerschen, Worden, Vakakis and Golinval 2006). But the literature related to nonlinear parameter identification and nonlinear damage identification is still insufficient for the inverse problem in practical civil engineering.

Visual inspections of the structural damage by experts were commonly used for the structural condition assessment of civil engineering structure in the past. However, time consuming labor works as well as subjective experience are required for the experts' inspection. There are some effective tools for the structural condition assessment. Nondestructive damage evaluation (NDE) methods and technique are also developed in practice, such as acoustic and ultrasonic methods. With the NDE methods local experiment will be done. But these series technique require of a *priori* of the damage location which is always unknown in practice and many defect exists inside the structural component. Moreover, some critical components of the structure are inaccessible to inspect within their service life, such as main pier of offshore platforms, the bottom of floating structures and mid bottom decks of long span bridges and so on. The NDE of structure might disturber the daily service of the civil engineering infrastructures. These kinds of methods cannot be directly applied in the large size civil engineering structures due to these limitations.

The investigation of vibration-based structural condition assessment methods as an effective means for the damage detection attracted considerable attention of researchers recently. It is known that the defect or damage in the structural material property will be reflected in the information of structural responses and the parameters derived from the structural response by Fast Fourier Transformation (Cooley and Tukey, 1965), wavelet analysis and other efficient tools. It is possible to conduct the evaluation for the condition of structural systems with limited number of sensors.

The vibration-based structural condition assessment method could be classified into two broad categories, which are response-based method (Cawley and Adams 1979; Salawu 1997a, 1997b; Uzgider et al. 1993; Zhang et al. 1992, 1993) and modeling-based method (Mottershead et al. 1993; Collins et al. 1974; Abdalla et al. 1998, 2000). With response-based methods, the time consuming analytical model updating work could be avoided. However, the identification of damage location and severity in Level 2 and 3 requires a large number of sensors and time consuming work on data processing. The external excitation is always unknown. The response-based approach needs to consider all damage scenarios which are time consuming and not practical for large size structures. With the modeling-based method, the abnormal changes could be represented analytically by physical parameters, such as mass, stiffness and damping, or the function of them, such as analytical natural frequency, analytical mode shape and analytical modal strain energy, which could be derived from the analytical structural response. The damage could be located and quantified by inverse analysis with the difference between the analytical data and measured data. The pre-event evaluation of structure would provide the guideline to structural design. The post-event condition assessment and successive maintenance could also be fulfilled with the model-based methods. Appropriate compromises are sought by researchers between the accuracy and simplification of the practical engineering problems to reduce the computational time of the structural condition assessment.

Another aspect of structural condition assessment is load environment identification. The dynamic load is an important source causing the damage and the dynamic load environment assessment is an important component in the structural condition assessment and health monitoring of a structure (Balageas 2002; Boller and Staszewski 2004). It is impossible to measure the excitation of the structure directly under most circumstances due to the lack of accessibility to the loading position or the need of a large number of sensors. The dynamic responses of a civil engineering structure subject to time varying loads have been studied for a few decades with indirect method. A lot of force re-constructions or force identification methods have been proposed and analyzed. Various researches in the field of force identification, such as bridge-vehicle interaction problem, wind load identification and base excitation identification can be found (Busby and Trujillo 1998; Kucharski 2000; Law and Chan 1997).

Although the aforementioned research works include most aspects in the dynamic analysis of civil structures and force identification, the force identification method is frequently based on the finite element model which often contains some errors practically. Furthermore, the force identification method is almost based on the Zero-Order Hold discrete in previous studies. The conventional ZOH discretization of the continuous equation of motion gives satisfactory results when the number of external excitation is small and the sampling period is short. However, when the number of unknown external forces increases, particularly with a more complicated structural system, this method may be inaccurate. With the ZOH discrete analysis, the result will be also less accurate when the sampling rate is low. This is because the force is continuous in practice. The First-Order Hold discrete assumption will be closer to the real force time history than the ZOH discrete.

The common type of errors is found in modeling the boundary conditions which affects the accuracy of both the forward and backward analysis result. The analysis of large size civil structures is always subject to the problem of insufficient or incorrect information on the analytical model including the uncertainties of geometric and physical properties, and connections at the boundaries. Research on the inverse problem of damage detection has been conducted with the substructure method in the last two decades. However, few literatures have taken into account the errors and uncertainties in the finite element model of the structure for structural condition assessment. Therefore, in the structural condition assessment and model updating of this Thesis, the uncertainties have to be considered for a full description of the dynamic response of the structural system. The structural condition assessment of a determined structure has to mitigate the uncertainties steadily with the iterative inverse analysis and provides more reliable results to engineers.

1.1.2 Background of Structural Vibration Control

Passive, active, semi-active and hybrid control methods have been actively investigated and implemented in a large number of modern buildings and bridges to mitigate the structural vibration due to the wind or earthquake. Passive control devices, such as base isolation and braces, are widely used in civil engineering structures but they cannot be adaptive to the structural parameters. For more than three decades, researchers have investigated the application of active, hybrid, and semi-active control methods and devices to remove the limitation of passive approaches and to reduce structural responses. Kajima Corporation implemented the first active control to a full scale building in 1989 (Kobori et al. 1990). The aim of the active control is to conduct the structural control during the strong wind and moderate earthquake (Spencer et al. 2003). Hybrid-control strategies of civil engineering structures also have been investigated by many researchers to ensure the control efficiency and reliability of both the structure and control system during the harsh earthquake event (Housner et al. 1997; Adeli and Saleh 1998; Kareem et al. 1999; Nishitani and Inoue 2001; Yang and Dyke 2003; Casciati 2003; Faravelli 1994; Spencer 2003). The hybrid structural control is a combination of the passive control, active control or semi-active control. The hybrid structural system is more reliable than the active control system. The active control can also be work with a limited number of response feedbacks of the sensing system for the hybrid control system during the strong wind or moderate earthquake. The semi-active control and passive control could also reduce the structural response even the failure of active control. Considering the reliability and efficiency, the hybrid control is now generally applied in practical engineering (Faravelli and Spencer 2003).

However, majority of the control strategies are designed for the centralized control system without considering the changes in structural properties in the past. With the centralized control of structural vibration of large system a higher demand will be required on sensing system, controller and actuator. Large number of sensors and actuators are needed for the control of large size structures. Higher requirements of sensors, data transmission facility, the computational hardware, actuators as well as the central controller are needed to be fulfilled (Lunze 1992). The centralized structural control strategies may not be reliable as expected due to the possible failure of the active control function during the severe earthquake. The decentralized control strategy has been proposed to remove these limitations in areas of power transmission network, economic systems and space dynamic systems (Sandel 1978; Ahmadian 1994; Siljak 1996; Bakule 2008). However, research on decentralized structural control for large-scale reports (Lynch and Law 2000; Swartz and Lynch 2006; Wang 2007a, 2007b; Loh et al. 2007) structural systems is still limited.

1.2 Research Objectives

The primary research work presented in this Thesis aims to develop a structural condition assessment with time-invariant or time-variant parameter and to perform a theoretical study of decentralized control strategy with substructure method. The specific objectives of the whole research work will be achieved with the completion of the following aspects:

(1) To develop force identification method for substructure with first-order hold discrete method considering force at a fix-position force and moving

force.

(2) To develop a new two-stage model updating method for structural condition assessment with substructure methods. A general response sensitivity method for substructural model updating is proved and illustrated.

(3) Two new computational methods are proposed to improve the first stage identification. Firstly, a time window force identification method is proposed to reduce the computation effort of the first stage identification. Secondly, in general, a method for the simultaneous identification of the unknown force and initial responses is also presented for the force identification.

(4) Two time-variant structural parameter identification methods are proposed based on Chebyshev polynomial and time window identification method. With this post-event method, the abrupt structural damage and bilinear property of brace during the earthquake could be identified.

(5) A new decentralized autonomous control system with substructure method is presented. The structural control is adaptive with the updating of the structural parameters of the system via the structural evaluation system.

1.3 Major contribution of this thesis

A large-scale structural system may have complex boundary conditions and uncertainties in the material properties. The large-scale structure is complicated and models on the boundary conditions and any innovative device for seismic protection may not be accurate. It is difficult to conduct structural condition evaluation for large structures partial because of these points.

Numerous of structural condition assessment methods have been proposed. The structural methods in frequency domain always need large number of measured data. The structural condition assessment in time domain is an alternative solution to structural health monitoring which needs as few data as possible. Though a lot of work has been done in this field, there are yet some gaps which limit the application of this kind of method. It is usually difficult to conduct the parameter identification in large scale structural system due to the calculation efficiency, accuracy and convergence. Previous time response sensitivity methods commonly assume the structure is connected rigidly to the base and the base-superstructure interaction is never taken into consideration. Most of the sensitivity methods in time domain commonly needs the record of the excitation or needs an assumption of the function of the external force time history. The force identification method is always based on the Zero-Order Hold discrete method which may cause large error to the identification result. Also the structural initial responses, i.e. acceleration, velocity and displacement, are commonly assumed to be zero but they are always unknown and non-zero values. Time-variant structural parameter identification is difficult to be identified with the existing time response sensitivity methods.

Structural control would ensure the structural reliability of the structure during the severe earthquake. The integrated system of structural control and model updating would make the structural control algorithm more stable and effective. However, only the integrated system with model updating method in frequency domain has been investigated. Model updating method in frequency domain commonly needs a large number of measured data from structural system with existing proposed method.

Since the gaps mentioned before, this thesis aim to propose a series method based on substructure methods which could improve the computational effort considering the time-variant or time-invariant model error and damage, perform the general out-put only structural condition assessment, including load identification and damage detection, conduct the time-variant structural condition evaluation and implement the smart structure with the integration of structural control and structural health monitoring.

The response sensitivity method in time domain is an alternative solution to structural condition assessment, which needs as few data as possible. Several components of work in structural condition assessment with substructure method are completed in this thesis. Firstly, a substructural external force identification method based on the equation in state space with the First-Order Hold discrete and Tikhonov regularization is presented. This method makes good use of this limited but accurate analytical information of the structure for the inverse identification of moving or static external force acting on the structure.

Secondly, a general response sensitivity method based on the two-stage identification for structural model updating considering the nonlinear support-superstructure interaction is developed. The two-stage identification method for substructural condition assessment is illustrated, proved and improved. In this study, a concept of pseudo structure is constructed for illustration and proof. Furthermore, two new computational methods are proposed to improve the first stage identification. A time window force identification method is proposed to reduce the computation effort of the first stage identification. The initial structural response, i.e. the acceleration, velocity and displacement at all dofs of the structural system, is always supposed as zero with time domain response sensitivity method in previous research work. However, the initial structural response is unknown and non-zero practically. In general, and a method for the simultaneous identification of the unknown force and initial responses is also presented for the first stage identification. An adaptive regularization method is employed for the model updating in the second stage.

Thirdly, a time-variant structural parameter identification based on Chebyshev polynomial is proposed for damping identification. The time window identification method is developed to conduct the time-variant parameters identification. With this method, the abrupt structural damage during the earthquake could be identified.

Lastly, a new decentralized autonomous control system is proposed. The structural control system is implemented with the LQG which is an effective control method for the vibration mitigation of structures. The structural control is adaptive with the updating of the structural parameters of the system via the structural evaluation system. A modified adaptive regularization method is used in the solution of the structural evaluation via model updating. The autonomous decentralized control system employs the substructure method proposed in this thesis which is more efficient in calculation with smaller mass, damping and stiffness matrices for the structural evaluation.

All these proposed methods in this thesis are verified by numerical simulation. The two-stage identification method and time-variant damping identification is also verified by laboratory work. Results show that the proposed methods on the structural condition assessment are effective and with good performance even there is noise in the measurement.

1.4 Outline of the Thesis

The contents of this Thesis will be divided into eight Chapters. The outline is given as follows:

In Chapter 1, research background will be introduced. The research objectives and the contributions of this thesis are also stated in this Chapter. An outline of the Thesis is presented at the end of this Chapter.

In Chapter 2, a detail literature review on existing research work related to the following topics will be addressed: structural condition assessment, substructural system identification, regularization method for inverse analysis and a review of integrated structural control system. At the end of Chapter 2, the critical issues and limitation of existing structural condition assessment and control methods are presented.

In Chapter 3, a force identification method for a substructure is proposed to identify external forces acting on a portion of a structural system based on the modified First-Order Hold (FOH) Discrete method in state space. A flat plate structure is investigated to illustrate the effectiveness and accuracy of the proposed method. Two cases, force on a fixed-position and moving force, are studied. A plate structure is divided into three substructures with both excitation and measurements in a target substructure. Both the interface forces between the substructures and the excitation forces are unknown and they are identified with the proposed method.

In Chapter 4, two substructure identification methods are proposed to handle two types of assessment problems. For the first problem, the finite element model (FEM) of the whole structure is required and the external forces acting on the structure are identified in state space with FEM of the whole structure. For the second problem, the FEM of the whole structure is assume unknown but the FEM of the target substructure is available. Both the external forces acting on the substructure and the interface forces of the substructure are identified using the FEM of the substructure. In both Scenarios, the perturbations in the substructural parameters are identified with substructure method and the FEM of the substructure is updated in iteration steps. A general response sensitivity method is proposed addressing the deficiency of existing sensitivity method for damage detection/model updating of a substructure with the analogous evolution of a pseudo substructure in the model updating process. Two new computational techniques are proposed to improve the first stage of force identification which are: a time window force identification method to improve the computation efficiency, and a method of simultaneous identification of the interface force and the initial responses in a short time window. The updated results from seismic excitation of a shearing frame structure are shown to be accurate even with measurement noise and unknown initial responses of the structure.

In Chapter 5, two identification methods are proposed for structural time-variant parameters identification. This Chapter reviews on the iterative regularization methods for the system identification and propose a general sensitivity-based method for the identification of both the time-variant and time-invariant damping in a structural system. A new method for the time-variant storey stiffness identification based on windowed measured data is presented. The time history of measured acceleration is divided into short non-overlapping time windows. The structural parameter is taken as invariant in each time window since the period of each time window is very small. This idea originates from of average acceleration step-by-step integration method. A two-phase identification strategy is applied to ensure the physical meaning and convergence of the proposed identification algorithm. In the first phase, the initial structural response is identified with the Tikhonov regularization method. In the second phase, the structural parameter is identified with a modified adaptive regularization method.

In Chapter 6, a new integrated system of structural control and evaluation is proposed. The control system is autonomous and decentralized with each controller independent. A substructural damage detection algorithm is applied for this system, which would be more efficient in calculation. The structural evaluation system in each distributed substructure performs the structural evaluation and the interface force between substructures is updated iteratively in iterations in the time domain. A modified adaptive Tikhonov regularization method is employed in the structural evaluation system for model updating to ensure the physical meaning of structural parameters. The implementation of the integrated system is verified with a 16-storey planar shear frame structure. Results of damage detection are accurate even with 10% measurement noise and the effect of structural control is noted to improve with the updated structural parameters.

In Chapter 7, experimental investigation of the force identification method with FOH discrete method, the two-stage structural condition assessment method and time-variant damping identification method will be presented. A nine-bay cantilever space frame and a two-dimensional frame were fabricated in the laboratory of The Hong Kong Polytechnic University tested for the validation of the proposed methods.

In Chapter 8, conclusions are drawn from the research work presented in the Thesis. Due to the limitation of the time and the author' knowledge, some recommendations on the future work related to the problems of the structural condition assessment and control with substructure methods are addressed.

CHAPTER 2

LITERATURE REVIEW

The structural condition assessment and vibration control include a broad range of topics and cover interdisciplinary subjects, such as civil engineering, mechanical engineering, automation and so on. The investigation of vibration-based structural damage detection was first conducted in offshore oil industry in the 1970s and early 1980s. Due to the harsh environmental changes, such as the marine growth, the measurement noise, and time-variant mass, the early stage investigation of vibration-based damage detection method lacked of success. This attempt to damage detection in structures was suspended in the mid of 1980s. And these methods again attracted increasing interest in the last two decades with the application in mechanical engineering, aerospace engineering and recently in civil engineering with the development of concerning disciplinary. There are two kinds of structural dynamic problems which could be distinguished as the forward problem and inverse problem. The forward problem can be defined as finding the solution of structural system with the known structural model and input. The inverse problem contains two kinds of problems which are to identify the system input with the response, boundary condition and system model and to identify the system model with the given inputs, response and boundary conditions.

This Chapter aims to provide a review of the recent studies on the fields of structural condition assessment and structural control with vibration-based method of civil engineering structures. The literature review on structural condition assessment will focus on the load identification method, damage detection method based on the structural vibration, substructural system identification regularization method and structural control with substructure model updating and damage detection and the review on the structural vibration control will include centralized control and decentralized structural control.

This Chapter mainly covers the following topics. Firstly, a general review on structural condition assessment including load identification, damage detection, model updating will be provided. Secondly, the application of substructure methods in structural condition assessment system identification is presented. Thirdly, the investigation of the effective tool of regularization methods is reviewed. Fourthly, the recent works on integrated system with the function of structural control and structural condition assessment based on decentralized structural control are explored. Finally, critical issues and shortcomings are in existing methods are discussed.

2.1 Structural Condition Assessment

The dynamic structural response analysis and condition assessment of building and bridges subject to external excitation has been studied for decades. Considerable research works on structural performance evaluation, online and offline structural condition assessment can be found in conferences and journals. The structural model updating, damage detection and external excitation evaluation are important components of structural condition assessment. The following reviews on structural condition assessment will focus on these parts.

Structural damage detection and structural model updating have been active research fields in the past three decades (Abdalla et al. 2000). An excellent detailed review report on structural damage detection provided by Doebling et al. (1998) which summarize various types of existing damage detection methods. There are also a lot of methods for loading evaluation. A general summarization of problems of force identification was presented by Stevens (1984) and a review on moving load identification was provided by Fryba (1999). A selected review of the recent developments in structural condition assessment of civil engineering structure will be listed in this Chapter.

2.1.1 Load Identification Methods of Structures

The forward and inverse problems of building and bridges subject to the external excitation have been investigated for a few decades while the inverse problem of the evaluation of the external excitation is only with partial success. The external excitation estimation methods fall into two categories, which are the direct method and indirect method. With the direct method the force transducers are installed where the forces apply. Traditional ways to measure the vehicle axle load by stopping and weighing vehicle using weighbridge or loadometer are expensive and inefficient. Considerable investigations and tests have been carried out since the late 60s and early 70s (Moses 1979; Davis and Sommerville 1987; Freund and Bonaquist 1989; Zhi et al. 1999) to control the overweight vehicles. Two famous research projects, COST 323 and WAVE, were carried out in Europe (Jacob 1994; Jacob and O'Brien 1996). However, the above system can only measure the equivalent static loads but not time history of moving loads. In fact, the dynamic response of a bridge due to moving loads can be significant, and Cebon (1987) concluded that the dynamic wheel loads may increase road surface damage by a factor of two to four over that due to static ones.

With the indirect method other sensors, such as the accelerometers, the strain gauges and Fiber Bragg Grating (FBG) placed on the nodes of structure, are utilized to evaluate the dynamic time history of the force. In general, it is very difficult to measure the external applied force on a structure in real time, while response measurement is more accurate than that of the force. The force identification method provides an alternative method to solve the above problem. Therefore the time-varying force time history identification from measured responses contributed greatly to the indirect methods for force measurement (Steltzner and Kammer 1999). A review on the inverse analysis for indirect force identification methods was presented by Inoue et al. (2001). The identification of fixed-position environmental load is nearly the same with the moving force evaluation but there is no need to consider the time-variant shape function to describe the force position in this problem. The knowledge of the dynamic characteristics of these external forces of structures becomes a requirement in engineering design and structural condition assessment. As mentioned before, the force identification is the second problem of the inverse problem.

Moving force identification and wind load identification are two typical indirect force identification problems. Bridges are subject to the damaging effects of the daily traffics. The structural conditions of the bridge will be affected by the operation loads including the dead load, live load, wind load and seismic load, etc. Among these loads, the moving vehicular axle load plays a vital role in the condition assessment especially for median span bridges. The importance of investigating the moving loads on top of the bridge deck was first recognized in the 19^{th} century. Following the collapses of some railway bridges in Great Britain, engineers and researchers began to pay more attention to the dynamic behavior of the bridge under moving vehicular loads, and further research on new techniques for the bridge design and bridge condition assessment had been carried out (Cantieni 1983, 1992; Chan 1988, 1990). The estimation of moving load on bridge is very important for bridge design and bridge condition assessment. A general summarization of moving load identification has been proposed by Fryba (1999). Various types of structural models include single-/multi-span uniform/non-uniform beam/plate/shell with elastic/non-elastic structural Young's modulus, with/without prestressed force. The overweight moving load may cause excessive damages to the bridge structure and may even result in great collapse. The accurate evaluation of moving load, reliable assessment of bridge condition and effective control of the transportation network become a crucial problem and it draws attention of many researchers (Chan 1999; Law et al. 2008; Busby and Trujillo 1998; Kucharski 2000; Zhu and Law 2000, 2001, 2002).

The wind action on a structure is very similar to that with moving vehicles passing on top of a bridge deck. The wind load effect on the structures has also been investigated extensively (Simiu 1996). When a proper wind load model is adopted, the responses of the structure can be formulated explicitly as a function of the wind load, and the wind load can then be identified from the structural responses in the inverse analysis. Chen and Li (2001) estimate the wind load acting on a shear building system using a general statistical average algorithm based on the system responses, including the displacements, velocities and accelerations from all degrees of freedom (DOFs), and with unknown structural parameters. Wind load identification is usually based on the basic wind pressure calculated from the long term records of wind speed and direction data in the area of structure and the statistical information, considering the surface roughness of the ground, coefficient of the shape of the structure for the wind load, coefficient of wind pressure variation with height and the magnifying effect caused by the fluctuating wind components and so on (Kolousek 1984). Chen and Li (2001) estimate the wind load acting on a shear building system using a general statistical average algorithm based on the system responses, including the displacements, velocities and accelerations from all degrees of freedom (DOFs), and with unknown structural parameters.

Except the moving force, wind load there are also some other types of forces, such as cable forces on the power transmission tower, suspension force on the bridges and so on. They are also important for the structural design, evaluation and maintenance. Enormous methods have been proposed for the identification of these forces, including deterministic methods, stochastic methods and methods based on artificial intelligence (Uhl 2007). The deterministic methods require the model of the structural system and the identification results strongly depend on the accuracy of the model. The estimation of model parameters is based on the input measurement only or input/output measurement. The structural responses with low noise level and accurate system model could help improve the identification result. The identification of the time-variant structural parameter could also modify the load identification result in case of the time-variant structural system with deterministic method. Stochastic methods require the statistical relationship between the input and output. The relationship is evaluated based on the experimental measurement of the input and output the structural system and with relationship the estimation of the external excitation. Regression model is commonly used in the force identification. And a dedicated procedure of the regression model for load identification has been presented by Uhl (1998). Artificial intelligence has also been used in load identification with artificial neural-network algorithms, fuzzy algorithms and genetic algorithms. The learn process is required to recognized and learn the pattern between the load and the structural responses. In the learning process large number of data and the accurate measurement are required. The learn process from the practical structure could be substituted by numerical simulation due to the difficulty of the force direct measurement.

The deterministic method includes two main classes of frequency domain method and time domain method (Simonian 1981; Anger 1990; Cannon et al. 1986; Law et al. 1999). The frequency response function based on least squares approach is the most widely used and these series methods can be applied in various force identification problems with the spectral analysis. Frequency response function and measured responses are always required for the force identification method in frequency domain to obtain the spectrum of excitation force. The identification of the external force could be conducted mutual energy theorem proved by Heaviside in 1892. With the measured response and the FRF matrix, the inverse analysis of the external excitation could be conducted through their product. The time history of the dynamic force at the expected frequency can be calculated with the inverse Fourier transform on the previous multiplying. The modal superposition technique is typically used to decompose the equation of motion of the system in which the response of structure is represented by a set of modal shapes with different amplitudes. The equation of motion of a dynamic system, which is a partial differential equation, is transformed into a set of ordinary differential equations which can be easily solved by numerical methods such as the Newmark-β method.

Method in time domain could identify the force with the relation between the system and responses of the structural system with the known force position and in form of convolution integral. This method was firstly proposed by Law et al. (1997) for the moving force identification and the relationship of moving axle force and modal response is formulated in form of convolution integral. The discrete form of equation of motion of the system for each vibration mode can be obtained by assuming the time history of moving forces to be step functions in small time intervals which is also the Zero-Order Hold discrete method (Busby and Trujillo 1998). The time history of the external forces on a simply supported beam can be identified by solving the time discrete equations. The application of this method on identifying the moving forces on a multi-span continuous bridge was investigated by Zhu and Law (2000, 2001, 2002). The research was also extended to study the possibility of identifying axle loads when applied to real bridge-vehicle system with road surface roughness and incomplete vehicle speed. Experimental tests showed that the method can identify individual axle loads travelling at non-uniform speed with small error (Zhu and Law 2003). The effect of bearing stiffness on the bridge support was also included in this moving force identification procedure by Zhu and Law (2006).

There are some conventional methods applied in the load identification. In many practical engineering problems, the boundary conditions are not known and the locations of loads are known. In these problems, the target is limited to identify the time history and amplitude of the time history of the external forces.

With both the time domain method and frequency method, the least-squares method is commonly used in the procedure of identification. The least-squares methods, singular value decomposition (TSVD) based least-squares methods and Tikhonov regularization methods (Law et al. 2001) for the force identification have been investigated in numerous of reference (Yu and Chan 2003).

2.1.2 Damage Detection Methods Based on the Structural Vibration

Structural damage could be defined as the reduction of structural loading-bear capacity structural. The structural damages always result from environmental loadings such as earthquake, wind, snow and ice and the corrosion from the rain and moisture. As mentioned before, conventional Non-Destructive Tests includes: penetration, magnetic particle, eddy current, ultrasonic, and radiographic tests. Optimization method has also been applied to the optimal matrix (Rodden 1967; Brock 1968; Baruch 1978). These traditional methods bear several limitations when testing in practical engineering due to the penetration depth, the *priori* of the damage location and inaccessibility of the damage location. In this section, a review of structural damage detection and model updating parameters will be conducted in two aspects, which are time-invariant parameters identification and time-variant parameters identification.

2.1.2.1 Time-invariant Damage Identification

The vibration-based damage index methods as a kind of generally applied method in engineering possesses the merit that they can be simply realized in engineering problems. In this process, the structural parameters are assumed as invariant when the damage is small. Damage index methods use changes in natural frequencies, mode shapes or other modal parameters calculated from the measured response to detect damage and can avoid the limitations above. With the difference between the modal data from the damaged and the intact structures or analytical model information on the damage location and even the extent could be obtained. However, these kinds of methods always do not provide the quantitative information about the structural damage. Existing approaches could be classified into the following categories based on the parameters used in the damage detection: (1) methods with the shifts of natural frequency; (2) methods with the mode shape changes; (3) methods with the variation of mode shape curvatures; (4) methods using modal flexibility changes; (5) methods using modal strain energy changes; and (6) methods using frequency response function.

Methods based on Natural Frequency

In the early stage of damage detection only the shifts of the frequency is the most effective and reliable method due to the easy implementation of the natural frequency measurement and immature modal analysis methods. A comprehensive review on the damage detection with the changes of natural frequency was presented by Salawu in 1997. Two types of damage detection methods conducted with the shifts of the frequency. The first type method is forward problem. With the first type method, the analytical frequency changes of all damage cases are compared with the measured frequency shifts and the best match is supposed as the suspect one (Vandiver 1975, 1977). This kind of method was used in offshore structures in 1970s (Vandiver 1975, 1977; Wojnarowski, et al. 1977). With the direct comparison of natural frequency only the location of damage could be found. Cawley and Adams (1979) employed the ratio of the frequency changes to detect the damage in composite materials. The ratio between the frequency shift of the *i*th and *j*th mode is denoted as $\delta\omega_i / \delta\omega_j$. However this method could only detect the position of the damage but cannot quantify the damage severity as presented by Lu (2005) and Li (2008). And the method is limited to the single damage scenario. A formulation could be used to illustrate the problem. The change of the *i*th modal frequency could be represented as a function of the severity vector $\boldsymbol{\alpha}$ and position vector s of the damage as follows

$$\delta\omega_i = f_i(\boldsymbol{\alpha}, \mathbf{s}) \tag{2.1}$$

With Taylor series expansion ignoring the higher order terms Eq. (2.1) can be written as

$$\delta\omega_i = \frac{\partial f_i(\boldsymbol{\alpha}, \mathbf{s})}{\partial \boldsymbol{\alpha}} \boldsymbol{\alpha} \tag{2.2}$$

Considering the damage severity as small value then $\delta\omega_i / \delta\omega_j$ can be calculated as

$$\frac{\delta\omega_i}{\delta\omega_j} = \frac{\partial f_i(\mathbf{0}, \mathbf{s}) / \partial \boldsymbol{\alpha}}{\partial f_j(\mathbf{0}, \mathbf{s}) / \partial \boldsymbol{\alpha}} \Big|_{\boldsymbol{\alpha}=\mathbf{0}} \tag{2.3}$$

When the ratio between different natural frequency shifts of simulated analytical damage scenario matches the experimental measurement, the possible damage site is located. The ratios of frequency changes are also adopted for damage detection by Friswell et al. (1994). A series of damage scenarios are assumed. The ratios are calculated for several low modes of the experimental structure and the analytical damaged structure with intact structural model. When the damage scenario of analytical structure matches the inspected structure, the damage scenario is supposed as the suspect one. The shifts pattern of a deterministic mode could be applied to identify the structural parameters changes. Messina et al. (1996) proposed a parameter defined as Damage Location Assurance Criterion for the location j calculated as

$$DLAC = \frac{|\Delta\mathbf{f}^T \cdot \delta\mathbf{f}_j|^2}{(\Delta\mathbf{f}^T \cdot \Delta\mathbf{f}) \cdot (\delta\mathbf{f}_j^T \cdot \delta\mathbf{f}_j)} \tag{2.4}$$

where $\Delta\mathbf{f}$ is the measured frequency change vector of structure with single damage, $\delta\mathbf{f}_j$ is the theoretical frequency change vector for a damage of a known level at location j. The location with highest value of $DLAC$ is regard as the damage location. The method mentioned above was constrained to the single damage identification. The multiple damage detection was proposed and calculated with the parameter of multiple damage location assurance criterion. The size of the damage is also formulate as

$$DLAC = \frac{|\Delta\mathbf{f}^T \cdot \delta\mathbf{f}_j(\delta D)|^2}{(\Delta\mathbf{f}^T \cdot \Delta\mathbf{f}) \cdot ((\delta\mathbf{f}_j\delta D)^T \cdot \delta\mathbf{f}_j\delta D)} \tag{2.5}$$

where δD is the stiffness reduction factor.

The second method with the shifts of frequency is inverse problem. In the second method, the damage location and severity detection is formulated and calculated as inverse problem for model updating. Lifshiz and Rotem (1969) conducted the damage detection with inverse analysis from the shifts of the natural frequency and found that the modulus changes related to the structural natural frequency shifts. The method with natural frequency sensitivity with respect to the structural damage was developed in 1990s. A large number of studies were conducted based on the sensitivity analysis of modal frequency to structural damage (Stubbs and Osegueda 1990). Penny et al. (1993) proposed a method to detect the damage by the experimental measurement and the analytical simulated cases with the idea of error function and least-squares. They also found the identification results with frequency shifts methods are sensitive to measurement noise (Penny et al., 1993; Messina et al., 1996; Farrar et al. 1994). Friswell et al. (1994) presented a damage detection method based on a known likely damage scenarios. An accurate model is assumed and the ratios of frequency changes of low modes are calculated for all the postulated damage scenarios. The corresponding ratios are also calculated for the inspected structure. A power law relation is used to fit these two sets of values. When the damage scenario of the real structure match to the set of assumed damages, the correct type of damage will produce a fit depicted by a unity-slope line. For all other types of damage, the fit will be inexact. Salawu (1997a) proposed a global damage integrity index that is based on a weighted ratio of the damaged natural frequency to the undamaged natural frequency. The weights could reflect the relative sensitivity of each mode to the different damage location. The local integrity index is calculated by weighting the global index with the square of the ratio of damaged mode amplitude to the intact mode amplitude on a particular measurement point.

Currently, it is practical to conduct damage detection with frequency shifts when the measurement could be performed in an acceptable environment. New established closed-form sensitivity equation relating the change in stiffness and shifts in natural frequency was established by Xu et al. (2004) which was verified by numerical simulation and laboratory work.

The advantages of application with frequency shifts possess could be summarized as the number of sensors is not large and the measured natural frequency is subjected to less measurement noise than other modal parameters. It is possible to implement the long term structural health monitoring with the frequency-based method. However, there are some significant limitations with this kind of methods although ongoing and future work may help resolve these difficulties. The low sensitivity of the natural frequency shifts to structural damage requires small error in measurement and large level of damage. Furthermore, as a global characteristic of structural system, shifts of frequency could reflect the existence of structural properties changes to some extent but these shifts cannot clearly illustrate the local damage. In other words, the frequencies cannot provide clear information to locate and quantify the local characteristics of structure. Higher modal frequencies are more sensitive to the structural changes however the higher modal frequencies are difficult to measure due to the measurement noise and less contribution to the response.

Methods based on Mode Shapes

A numerical study was conducted numerically to obtain the natural frequencies and modal shapes by Yuen (1985) with a finite element model of uniform cross-sectioned cantilever. In this study the systematic approach was used to locate the damage position according the changes in mode shape and mode-shape-slope parameters. It is shown that the changes in the eigenvector definitely relate to the location and severity of structural damage.

The structural changes will cause the changes in mode shapes in the vicinity of damage components. Two generally used methods are the comparison of the modal assurance criterion (MAC) proposed by West (1984) the coordinate modal assurance criterion (COMAC) from the measurement before and after damage. MAC indicates the correlation between two sets of mode shapes obtained from the measurement before and after the damage while COMAC indicates the correlation between the modes shapes on selected measurement point of the structure. MAC is calculated as

$$MAC(\phi_r \phi_s) = \frac{|\phi_r^T \phi_s|^2}{\phi_r^T \phi_r \phi_s^T \phi_s} \tag{2.6}$$

where ϕ_s and ϕ_r are selected any two eigenvectors of a structural system. In the cases of model updating, the mode shape pairs from a tested structure and its corresponding analytical model are used to calculate the MAC values. It is noted that the value of MAC ranges from 0 to 1 with a value of 1 to indicating identical mode shapes and 0.0 for orthogonal ones. COMAC (Lieven and Ewins 1988) is calculated

$$COMAC(\phi_r \phi_s) = \frac{[\sum_{r=1}^{N} | \phi_{k,r}^{A} \phi_{k,r}^{B} |]^2}{\sum_{r=1}^{N} (\phi_{k,r}^{A})^2 \sum_{r=1}^{N} (\phi_{k,r}^{B})^2} \tag{2.7}$$

where k and t denotes the coordinate index and mode index respectively, A and B denote the state after and before the structural damage. It is noted that the calculation of COMAC involves not only the mode indices but also the structural DOFs and coordinate information.

Rizos et al. (1990) developed the analytical model of a cantilever beam with a transverse surface crack extending uniformly along the width to locate and quantify the damage. In this study open crack (Abdel et al. 1999, 2001) model was applied and compatibility condition between the two sections was derived based on the crack-strain-energy function. The beam was excited at a natural frequency and the vibration magnitudes were measured on two points. It shows that the crack location can be found and depth can be estimated with satisfactory accuracy from the measured amplitudes, the respective vibration frequency and an analytical solution of the dynamic response. In the study by Bakir et al. (2007) the MAC values and the relative differences of the frequencies was minimized to update a multi-storey complex structure with a complicated damage pattern.

Stubbs et al. (1990) reported an investigation of a scale model of offshore platform structure with damage and found that the changes of mode shapes could not be related to damage in this study. Fox (1992) presented a comparison study between identification results with natural frequency and mode shape data. A simple case of a uniform beam with a crack was considered. And results from finite element analysis and from experimental modal analysis were presented. The study showed that the single vibration mode such as the MAC was relatively not sensitive to the saw cut damage. A node-line MAC, a MAC with measurement point close to a node for one particular mode is more sensitive indicator of mode shape changes caused by damage. Simply graphical comparison of the relative changes in mode shapes proved to be the effective way to detect the damage location at resonant frequencies and with measured mode shapes. To locate the damage, a simple method of correlating the node point which show relatively little changes in resonant frequencies with the corresponding peak amplitude points in modes which show large changes at resonant frequencies was proposed. A method of scaling the relative changes in mode shape to identify the location of the damage was also proposed by Fox. Based on the changes in mode shapes Mayes (1992, 1995) proposed a method known as structural translational and rotational error checking (STREC). With the ratios of relative modal displacements, STREC assessed the difference of structural stiffness between two different sets of DOFs. With STREC, the stiffness comparison of the tested structure and analytical model or the comparison of two tested structure could be obtain. Srinivasan and Kot (1992) found the changes of mode shapes were more sensitive to the damage than resonant frequency on the shell structure. The damage could be quantified with the value of MAC comparing the damage and intact mode shapes. Lam et al. (1995) defined a mode shape normalized by the change in natural frequency of another mode as a “damage signature” which is only a function of crack location. A set of possible signatures is computed analytically considering all possible damage states. The measured signatures were selected when they gave the best match to the measurements using the MAC.

Based on the concept of MAC, Lieven and Ewins (1988) proposed COMAC calculated as Eq. (2.7). Kim et al. (1992) investigated the MAC and its variation due to the structural damage. With the Partial MAC in conjunction and COMAC the location of damage could be isolated. Ko et al. (1994) presented a method that used a combination of MAC, COMAC and sensitivity analysis to detect damage in steel frame structures. The sensitivities of the analytical mode shapes to particular damage locations were computed to determine which DOF is most relevant. The author distinguished the mode shape pairs which could be used for damage detection with the analysis of MAC calculated from the damaged structure and intact structure. The results demonstrated that not all mode pairs were effective to conduct the damage detection and the indication of damage might be masked by some modes that were not sensitive to the damage. Messina et al. (1998) developed a method which is an extension of the multiple damage location assurance criterions (MDLAC) by using incomplete mode shape instead of modal frequency. A plane truss structure is analyzed as a numerical example to compare the performance of the proposed method with the multiple damage location assurance criterions. Results indicate that the new method is more accurate and robust in damage localization with or without noise effect. The result of Salawu and Williams (1994) also showed experimentally that a selected mode shapes could be applied for the damage detection but not all the mode shapes perform as good indicator. Salawu and Williams (1994) showed that the values of MAC can be utilized to indicate which modes are sensitive to the damage.

The damage detection methods with mode shapes combined with other parameters are also investigated. A method was proposed by Skjaeraek et al. (1996) to localize structural damage in reinforced concrete (RC) structures excited by earthquake using the two lowest smoothed frequencies and mode shape coordinates which are used as an input via a substructure iteration technique. The optimal sensor placement issue for the damage detection has also been examined. Incomplete measurement was used for damaged structural elements identification by Cobb and Liebst (1997). Optimization method was applied in this method to minimize the deviations between the measured and analytical modal frequencies and partial mode shapes. Damage could be identified by determining the element stiffness changes to match the measured data of the damaged structure. Parloo et al. (2003) used mode shape sensitivities to damage detection with calculated sensitivities matrix from the experimentally determined mode shapes. Therefore, the finite element model for the test structure is not necessary. Pascual et al. (2005) proposed a new method in form of the expansion of mode shape for damage assessment and they obtained satisfactory results.

As the previous literature shown, critical issues with mode-shapes based on damage index method contain that the location of the selection of mode, the optimal placement of limited number of sensors. Mode shapes inherently reflect the spatial information of the structural changes while only high mode shapes, which are difficult to obtain, are sensitive to changes of structure

Methods based on Mode Shape Curvatures/Strain Mode Shapes

The changes in structural parameters could be reflected in the mode shapes, however, the corresponding changes in mode shapes are not sensitive to the changes in structural parameters. New parameters developed from mode shape derivatives, such as curvatures, were used as an alternative tool to for damage detection. The curvature of beam is firstly calculated as

$$\varepsilon=\frac{y}{R}=\kappa y \tag{2.8}$$

where ε is strain, R is radius of curvature and κ is curvature. It is noted that there is a direct relationship between curvature and bending strain for beams, plates, and shells and the curvature can be obtained by strain measurement.

Pandey et al (1991) presented that the changes of mode shape curvature can be used for damage detection for a simply supported beam model they considered. With finite central difference method and the analytical modal displacements curvature values at measurement point i can be calculated as

$$\kappa_i = (\varphi_{i+1} - 2\varphi_i + \varphi_{i-1}) / h^2 \tag{2.9}$$

where h is the length of the element. The analytical finite element model is not needed if the response of intact structure can be measured. But the rotational components cannot be obtained through the measurement of displacement responses or acceleration responses.

Ratcliffe (1997) developed the method based on mode shape data and this method did not require a *priori* knowledge of the undamaged structure. When damage is severe (a localized thickness reduction of more than 10%), this method can identify the location of damage successfully with a finite difference approximation of Laplace's differential operator to the mode shape. However, when damage is not severe, processing of the Laplacian output is required before the location can be determined. Testing locations are required close to each other and testing points are in good enough or large errors will be aroused by central difference method. Chance et al. (1994) found that errors will be introduced when numerical curvature of mode shapes may arise. Nwosu et al (1995) investigated the strain changes with a crack in a tubular T-joint. These data can be measured at a relatively large distance from the crack.

Abdo and Hori (2002) presented that rotation of mode shapes may be available to the damage detection. They conduct a simulation with a beam and the numerical results of their studies clarify that the rotation of mode shape contains the characteristic of the damage localization even though the displacement modes cannot localize the damage. The simulation results also indicate that the rotations of modes are robust in multi-damage with different damage level. Furthermore, the method with the changes in the rotation of mode shape does not need very fine grid of measurements to detect and locate damage, effectively.

There are some drawbacks in applications with the mode shapes and their derivatives. Firstly, a large number of sensors are required with mode shapes or mode shape curvatures. Secondly, the measurement of mode shape or their derivates are sensitive to the measurement noise and uncertainties on structural system. Thirdly, the rotational mode shapes are still difficult to measure though they are more sensitive to structural parameter changes. Lastly, all these method only based on mode shapes or curvature techniques cannot be practically applied to large size structural system.

Methods based on Flexibility Matrix Changes

Another class of damage detection methods with flexibility matrix to estimate changes structure stiffness was proposed. The flexibility matrix can be derived from the mass-normalized measured mode shapes and frequencies and with this method the flexibility matrix is also called modal flexibility. Generally, damage is identified with the comparison of flexibility matrices synthesized from the modes of the damaged structure and undamaged structure or FEM of structure. The modal flexibility can be approximately estimated from a few lower modes data of the structure which overcome the drawback of incomplete measurement of modes. Therefore, many research works focused on this type of methods.

Raghavendrachar et al. (1994) and Aktan (1994) illustrated the method with modal flexibility as a tool for nondestructive evaluation of bridge-foundation-soil systems. In their study, the modal flexibility is found to be more sensitive to the local damages than natural frequencies or mode shapes. Pandey and Biswas (1994) presented a damage detection and localization method based on variation in the measured flexibility of the structure. Numerical example and experimental work with linear local damages were conducted with this proposed method. Results showed that the estimation of the damage location and severity could be obtained from just the first two measured modes of the structure. Toksoy and Aktan (1994) proposed a bridge-condition assessment method for evaluating the global state of health. This method was formulated based on modal flexibility directly obtained by measured modal test data. The method was proven and experimental and numerical investigations were conducted to a three-span reinforced-concrete high-way bridge. They observed that anomalies in the deflection profile can indicate damage even without a baseline data set.

Zhang and Aktan (1995 and 1998) studied the derivative of modal flexibility, called uniform load surface (ULS), which is defined as the deformation shape of the structure subjected to a uniform unit load. In their study, the effect of truncation error on modal flexibility was investigated through a numerical example and the experimental results from a three-span highway bridge. They concluded that modal flexibility coefficient, especially the off-diagonal terms of the matrix where the loading location is different from the deflection location, are very sensitive to the frequency band used. Wu and Law (2004) developed a damage detection method with variation of uniform load surface (ULS) curvature for two-dimensional plate structures. A new approach to compute the ULS curvature was proposed based on the Chebyshev polynomial approximation, instead of the central difference method. In their studies it is found that the ULS curvature is sensitive to the presence of local damages, even with truncated, incomplete, and noisy measurements.

Methods based on Modal Strain Energy Changes

The combination of the finite element model and mode shapes was developed by some research to conduct the damage detection and some more damage indicators, such as modal strain energy changes was proposed. Some studies indicated that damage detection method based on modal strain energy changes is efficient to localize structural damage. The general definition of modal strain energy of a structure with respect to the *i*-th mode can be expressed as

$$MSE_i = \frac{1}{2}\phi_i^T \mathbf{K}\phi_i \tag{2.10}$$

where ϕ is the modal displacement shape of the *i*th mode, and $\mathbf{K}$ is the stiffness matrix of the structural system.

Yao et al. (1992) presented a method to detect damage with the concept of strain mode shape. It is assumed in their studies that a new state of force equilibrium is realized when structure subject to damage and this change of force distribution can be noted from the modal strain energy of the structure before and after the damage. However, internal force redistribution is different between different modes. Therefore different outcomes will be attained with different testing modes. Topole and Stubbs (1995) adopted method for damage detection with limited modal parameters of the damage structure. Stubbs and Kim (1996) improved this method and utilized the modal strain energy to localize and quantify the damage without baseline modal properties. Stubbs and Kim (1996) improved the method by using the modal strain energy to localize and estimate the severity of the damage without baseline modal parameters.

Law et al. (1998) developed the use of modal strain energy named Elemental Energy Quotient (EEQ). The EEQ of the *j*th element and the *i*th mode is defined as

$$MSE_i = \frac{\phi_i^T \mathbf{K}_j^e \phi_i}{\phi_i^T \mathbf{M}_j^e \phi_i} \tag{2.11}$$

where $\mathbf{K}^e_j$ is the *j*th elemental stiffness matrix, $\mathbf{M}^e_j$ is the *j*th elemental mass matrix. Shi et al. (1998) and Abdel (2001) proposed the concept of the Elemental Modal Strain Energy (EMSE) to detect the location of damage. This method makes use of the change of modal strain energy in each structural element before and after the occurrence of damage. Information required in the identification is the measured mode shapes and elemental stiffness matrix only without knowledge of the complete stiffness and mass matrices of the structure. The Modal Strain Energy Change Ratio (MSECR) could be a meaningful indicator for damage localization. The authors also presented two damage quantification algorithms based on sensitivity analysis of modal strain energy (Shi et al. 2000a, 2000b; Shi et al. 2002).

Methods based on Frequency Response Function (FRF)

Considering indirect calculation of modal data from the polluted measurement the FRF data is more reliable and reasonable than the measured modal data for the damage detection. The FRF can be used for the damage detection.

Samman et al (1991) used a pattern recognition method to study the changes in FRF signals for structural damage detection. In their studies a scaled model of a highway bridge was used to investigate the change in FRF signals caused by the development of cracks in its girders. Wang and Liou (1991) proposed a new method to identify joint parameters with two set of measured FRFs of a substructure with and without the effect of joints. Numerical simulation and experiments are used to verify the proposed method with some strategies to overcome the adverse effects of noise. Law et al (1992) developed the sensitivity based on the change in FRF at any point, rather than just at the resonances. Therefore, many points of the FRF around the resonances are considered and a least-squares method is applied to identify the changes in physical parameters. Wu et al. (1992) used a back prop neural network with the first 200 points of the frequency response function as input to identify the damage in a three-storey building model. Chaudhry and Ganino (1994) utilized measured FRF data over a specified frequency range as input to a back prop neural network to identify the presence and severity of delamination in debonded beams. Park et al. (2003) proposed detection technique based upon an incompletely measured experimental model but based upon incompletely measured frequency responses without accurate finite element model. Their work also discusses frequency regions where the suggested method works satisfactorily. Ni et al. (2006) presented an experimental investigation of seismic damage in a 38-storey tall building model with measured FRFs and neural networks. Juan and Dyke (2000) presented and experimentally verified a new technique to identify damage based on changes in the component transfer functions of the structure or transfer function between the floors of a structure.

The structural input information is commonly required in the identification of frequency response function of structure. This is quite difficult for large civil engineering structures. Furthermore, there is still no good method to select interested frequency bound and mitigate the adverse effect of the noise.

Sensitivity-based Damage Detection Method

The sensitivity-based method is another class of method for structural damage detection which is based on the first-order Taylor series expansion. An objective function is defined and optimization method is applied to minimize the function of residual errors caused by structural matrices perturbations. The residual r_i denoting the difference of parameters between the damaged structure and those of the initial structure. The parameters could include the frequencies, mode shapes, modal strain energy and the response in time history and so on. A linearized relation between the sensitivity matrix **S,** the perturbation in the unknowns, δp and **r** can be expressed as

$$\mathbf{r} = \mathbf{S}\delta\mathbf{p} \tag{2.12}$$

Jahn (1948) derived the complete formulae for eigenvalue and eigenvector sensitivities in a first-order Taylor series for a standard eigenproblem to improve an approximate set of eigenvalues and eigenvectors. That method was also illustrated by a numerical example. The theory was then extended by Fox and Kapoor (1968) to the case of generalized symmetric eigenvalue problems by considering changes of physical parameters in the mass and stiffness matrices. In their studies exact expressions for the rates of change of eigenvalues and eigenvectors with respect to the design parameters of the actual structure was presented and it is indicated that these derivatives can be used successfully to approximate the analysis of new structural designs. The proposed method later named as 'modal method' requires all the modes of the system to be available in order to calculate the required eigenvalue and eigenvector sensitivities which is sometimes computationally expensive especially for matrix of large dimension. To overcome this probelm, Nelson (1976) developed a simplified procedure to determine the derivatives of eigenvectors of *n*th order which can generally applied to symmetric or nonsymmetric systems. The improved method just requires knowledge of one eigenvalue and its associated left and right eignvector.

Collins et al. (1974) applied the eigen-sensitivity analysis to FEM updating firstly. Based on the work of Collins et al. Chen and Garba (1980) proposed a method to calculate the Jacobian matrix with a matrix perturbation method. Hajela and Soeiro (1990) investigated the inverse problem of damage identification with the sensitivity method and nonlinear optimization technique. Lin et al (1995) improved the inverse eignsensitivity method for structural model updating employing both analytical and experimental modal. The sensitivity of the modal strain energy (MSE) to damage is also derived and used in damage identification (Shi et al., 2000b). Abdel (2001) studied the application using the sensitivity-based updating approaches, in which the sensitivity of the natural frequencies, mode shapes and modal curvatures to damage are combined to construct the sensitivity matrix. A structural damage detection method through the sensitivity-based finite element model updating procedure was presented by Hemez and Farhat (1995). They formulated the sensitivities at the element level. This allows the identification to focus on the structural members susceptible to damage, and also improves the computational efficiency comparing with the sensitivity analysis in system level.

The methods for damage detection reviewed above are based on the modal parameters in frequency domain. Sensitivity method in time domain has been investigated and applied extensively for damage detection based on structural response in time domain without the need of modal extraction procedure which may cause the loss of information and affect the results of damage identification. Law et al. (2005) developed the sensitivity-based damage detection method basing on the wavelet packet energy of the measured accelerations and the method can identify damage of a structure from a few measurement locations. Law and Li (2006) used the wavelet coefficient sensitivity of structural response with respect to a system parameter for structural condition assessment. The sensitivity matrix of response with respect to the structural parameters is derived to locate and quantify local damages with as few as a single sensor (Zhu and Law 2007a, 2007b). Lu and Law (2007b) identified the external excitations and the local damage of the structure simultaneously. Sensitivity method based on a new adaptive regularization method has been proposed by Li and Law (2010). A plane truss was studied numerically and the results indicated that method can satisfactorily conduct the structural damage detection even with measurement noise.

2.1.2.2 Time-variant Structural Parameter

Numerous methods have been developed for time-variant structural condition assessment and model updating in the past. Kerschen et al. (2006) reviewed the investigations on the time-variant structural parameter identification have also been conducted for linear or nonlinear structures over the last two decades. Shi et al. (2007) studied a linear time-varying multiple degrees-of-freedom system identification method based on Hilbert transformation and empirical mode decomposition was proposed. The time-variant parameters on a shear frame structure could be identified fairly accurate with measurement noise while some fluctuations are found in the identification results.

The Kalman filter is an effective mean to system parameter identification and input estimation for a linear or nonlinear structure. Haykin et al. (1997) investigated two forms of the extended recursive least-squares algorithm were considered for the identification of system parameter and the tracking of a chirped sinusoid in additive noise. Other time-variant parameter identification methods were also proposed. Yang et al. (2004) proposed an online identification of nonlinear hysteretic structure with an adaptive track techniques based on least-squares estimation proposed. Nonlinear normal modes analysis considering the nonlinearity of structural system was stated by Kerschen et al. (2009). Tang et al. (2006) proposed an online sequential weighted least-squares support vector machine technique to quantify the structural parameter changes when the measurement involves damage events based on the work of Yang et al. (2004). Yang at al. (2007) proposed an adaptive tracking technique based on extended Kalman filter for structural parameters and their changes identification which could consider the nonlinear components of structure. Li and Law (2009) investigate the dynamic response sensitivity method and proposed a moving time window to identify the time-variant damping ratio. The time-variant damping ratio can be identified accurately though there are some fluctuations near the abrupt changes of the damping ratio. Jin et al. (2000) conducted nonlinear finite element analysis with an energy index approach for damage detection in highway bridges.

These methods reviewed above remove the assumption that the time of occurrence of the anomalies is known *a priori*. Hence, these methods could be applied to conduct the structural condition assessment online. However, most existing methods for time-variant parameter identification do not consider the uncertainties in the structural parameters or measurements. Comparing to the time-invariant structural parameters identification method, the number of time-variant structural identification method is still limited for the engineering inverse problems.

2.2 Substructural System Identification

The substructure methods allow structural condition assessment of large or complex structures, which might be evaluated with global methods due to the insufficient information. Local characteristics, which may have no significant impact on the whole system, can be identified with substructure methods. With the substructure methods distributed or parallel structural analysis could be conducted. Due to these advantages substructure methods have been applied extensively for structural condition assessment in the field of aerospace engineering, mechanical engineering and civil engineering.

Increasing interest has been focused on this topic in the last two decades due to the leap of computation power with modern computer. The large and complex structural system can be divided into smaller substructures for separate assessment with a reduced number of unknown parameters. Substructural synthesis method has been applied to analyze complex structures since 1960s. In this section, a review on substructure method in structural condition assessment will be presented in frequency domain and time domain.

2.2.1 Substructural Condition Assessment Methods in Frequency Domain

The frequency response function is widely used in experimental substructure method. The equation of motion could be written as

$$\mathbf{M}\ddot{\mathbf{x}} + \mathbf{C}\dot{\mathbf{x}} + \mathbf{K}\mathbf{x} = \mathbf{F} \tag{2.13}$$

with the compatibility condition and equilibrium condition

$$\mathbf{B}\mathbf{x} = \mathbf{0},\ \mathbf{L}^T(\mathbf{g}) = \mathbf{0} \tag{2.14}$$

where **B** operate on the interface DOFs and is the Boolean matrix when the interface force matching with each other among the substructures and matrix **L** is a geometric operator to connect the DOFs in the global structure with those in the independent substructures. Performing Fourier transform on the equation above the governing equation in frequency domain be obtain as

$$\mathbf{B}\mathbf{x} = \mathbf{0},\ \mathbf{L}^T(\mathbf{g}) = \mathbf{0} \tag{2.15}$$

$$\begin{cases} \mathbf{H}^P(\omega)\mathbf{x}(\omega) = \mathbf{f}(\omega) + \mathbf{g}(\omega) \\ \mathbf{B}\mathbf{x}(\omega) = 0 \\ \mathbf{L}\mathbf{g}(\omega) = 0 \end{cases} \tag{2.16}$$

where **x**(ω), **f**(ω) and **g**(ω) denote the amplitude of the harmonic response and forces, $\mathbf{H}^P$ is a bleck-diagonal matrix containing the dynamic stiffness matrices of the substructures as

$$\mathbf{H}^P(\omega) = -\omega^2\mathbf{M}^P + j\omega\mathbf{C}^P + \mathbf{K}^P \tag{2.17}$$

Equation (2.12) can be written in coupled form as

$$\begin{bmatrix} \mathbf{H}^P & \mathbf{B}^T \\ \mathbf{B} & \mathbf{0} \end{bmatrix} \begin{Bmatrix} x \\ \tau \end{Bmatrix} = \begin{Bmatrix} f \\ \mathbf{0} \end{Bmatrix} \tag{2.18}$$

where ω is omitted for brevity. The displacement can be obtained as

$$\mathbf{x} = (\mathbf{H}^P)^{-1}\mathbf{f} - (\mathbf{H}^P)^{-1}\mathbf{B}^T(\mathbf{B}(\mathbf{H}^P)^{-1}\mathbf{B}^T)^{-1}\mathbf{B}(\mathbf{H}^P)^{-1}\mathbf{f} \tag{2.19}$$

The frequency domain substructure methods primarily use the coupling dynamic stiffness $\mathbf{H}^{\mathrm{P}}$ while the dynamic stiffness matrix $\mathbf{H}^{\mathrm{P}}$ is difficult to obtain. It is commonly obtained with the inverting the measured receptance matrix and ususlly carrided out as coupling the impedance matrix $(\mathbf{H}^{\mathrm{P}})^{-1}$ (Imregun and Robb 1992, 1993; D'Ambrogio et al. 2004).

The assembled matrix can be expressed as

$$\begin{bmatrix} \mathbf{M}^P & \mathbf{0}^T \\ \mathbf{0} & \mathbf{0} \end{bmatrix} \begin{Bmatrix} \ddot{\mathbf{x}} \\ \boldsymbol{\tau} \end{Bmatrix} + \begin{bmatrix} \mathbf{C}^P & \mathbf{0}^T \\ \mathbf{0} & \mathbf{0} \end{bmatrix} \begin{Bmatrix} \dot{\mathbf{x}} \\ \boldsymbol{\tau} \end{Bmatrix} + \begin{bmatrix} \mathbf{K}^P & \mathbf{B}^T \\ \mathbf{B} & \mathbf{0} \end{bmatrix} \begin{Bmatrix} x \\ \boldsymbol{\tau} \end{Bmatrix} = \begin{Bmatrix} \mathbf{f} \\ \mathbf{0} \end{Bmatrix} \tag{2.20}$$

The Equation (2.15) can be decoupled in with the following equation

$$\mathbf{x} = \Phi\mathbf{q} \tag{2.21}$$

where Φ is mode shapes matrix. The undamped eigenproblem with dynamic substructure method could be obtained as

$$\begin{bmatrix} \mathbf{K}^P & \mathbf{B}^T \\ \mathbf{B} & \mathbf{0} \end{bmatrix} \boldsymbol{\Phi}^P q - \lambda \begin{bmatrix} \mathbf{M}^P & \mathbf{0}^T \\ \mathbf{0} & \mathbf{0} \end{bmatrix} \boldsymbol{\Phi}^P q = \begin{Bmatrix} \mathbf{0} \\ \mathbf{0} \end{Bmatrix} \tag{2.22}$$

The main idea of substructure method in frequency domain could be summarized as to extract the eigensolutions and eigensensitivities (Kron 1963).

2.2.2 Substructural Condition Assessment Methods in Time Domain

Koh et al. (1991) proposed a substructure method to estimate the structural parameters in time domain. The equation of motion of the substructure considered can be written as

$$\begin{bmatrix}\mathbf{M}_{IB} & \mathbf{M}_{II}\end{bmatrix}\begin{Bmatrix}\ddot{\mathbf{x}}_B \\ \ddot{\mathbf{x}}_I\end{Bmatrix}+\begin{bmatrix}\mathbf{C}_{IB} & \mathbf{C}_{II}\end{bmatrix}\begin{Bmatrix}\dot{\mathbf{x}}_B \\ \dot{\mathbf{x}}_I\end{Bmatrix}+\begin{bmatrix}\mathbf{K}_{IB} & \mathbf{K}_{II}\end{bmatrix}\begin{Bmatrix}\mathbf{x}_B \\ \mathbf{x}_I\end{Bmatrix}=\{\mathbf{f}\} \tag{2.23}$$

where subscript I and B denote the internal coordinates and interface boundary coordinates of a substructure, respectively. Koh et al. (1991) formulated and solve the equation of motion for the substructures with the extended Kalman filter and a weighed global iteration algorithm. The substructures with or without overlapping members were considered respectively. Koh et al. (2003) proposed the quasi-static displacement vector to release the requirement of measured displacement and velocity at the interface of substructures and only the acceleration measurement on the interface is required.

Yun and Lee (1997) proposed a substructural identification method with application of an extended Kalman method. In their research, the state and observation equation with and without overlapping members for the identification of structural parameters are solved respectively. An auto-regressive moving average method with stochastic input model has been presented for substructure measurements with noise. Yun and Bahng (2000) adopted a neural network for substructural identification of a complex system.

Tee et al. (2005) proposed two system identification methods for substructures. The first one adopted first-order state space formulation in state space with eigensystem realization algorithm and the Kalman filter identification method. The identification was conducted in the global level to obtain the second order model parameters. The second one conducted both the first-order and second order identification at substructural level. Koh et al. (2006) and Tee et al (2009) also applied the condensation method for substructural identification. With the condensation method, fewer sensors are required for the structural measurement. Yang et al. (2007) and Huang et al. (2008) also applied substructure method in the proposed sequential nonlinear least-square estimation with only a limited number of response data.

Time domain identification with substructure methods have also been used for the simultaneous identification of structural parameters and input time history of the applied excitation (Sandesha and Shankar 2008). The substructural parameters, including the unknown interface forces at the ends of the substructure, were identified iteratively. The method proposed by Sandesh (2008) requires the measurement of accelerations at all the interior DOFs but not interface DOFs of the substructure. The effect of noisy data was also studied. Even with measurement noise, the proposed substructural method could identify the structural parameters with appreciable accuracy and with a considerable saving of CPU time. Damage identification method for a plate was proposed with an inverse time domain formulation Sandesha (2009). The time domain acceleration responses need to be measured at certain locations which includes the acceleration at the interface as well as certain points at the interior DOFs. Since the computational effort of identification using the global finite element model of the plate proved prohibitive, the substructure method was used. The substructure was condensed of the rotary DOF's for increased computational improvement. The Genetic Algorithm (GA) and Particle Swarm Optimization (PSO) were used to solve the inverse problem. In their study, the PSO algorithm proved superior to GA in convergence and accuracy.

2.3 Regularization Methods

Since the relationship between the vibration parameter **R** and the fractional stiffness change parameter $\boldsymbol{\alpha}$ is nonlinear, a nonlinear model updating technique, like the Gauss-Newton method, is required. The Gauss-Newton method in the damage detection procedure can be described as

$$\mathbf{R}(\boldsymbol{\alpha}_d) = \mathbf{R}(\boldsymbol{\alpha}_0) + \mathbf{S}(\boldsymbol{\alpha}_0)\Delta\boldsymbol{\alpha}_1 + \mathbf{S}(\boldsymbol{\alpha}_0 + \Delta\boldsymbol{\alpha}_1)\Delta\boldsymbol{\alpha}_2 + \cdots \tag{2.24}$$

where subscript d denotes the damage state, subscript 0 denotes the initial state of the structural parameter and **S** denotes the sensitivity matrix. Ignoring the higher terms the Equation (2.24) can be written as

$$\mathbf{R}(\boldsymbol{\alpha}_d) = \mathbf{R}(\boldsymbol{\alpha}_0) + \mathbf{S}(\boldsymbol{\alpha}_0)\Delta\boldsymbol{\alpha}_1 \tag{2.25}$$

The damage identification equation for the (k+1)th iteration can be written as

$$\Delta\mathbf{R}_k = \mathbf{S}_k\Delta\boldsymbol{\alpha}_{k+1} \tag{2.26}$$

where $\mathbf{S}_0 = \mathbf{S}(\boldsymbol{\alpha}_0)$, $\mathbf{S}_1 = \mathbf{S}(\boldsymbol{\alpha}_0 + \Delta\boldsymbol{\alpha}_1)$, $\Delta\mathbf{R}_k = \mathbf{R}(\boldsymbol{\alpha}_{k+1}) - \mathbf{R}(\boldsymbol{\alpha}_k)$.

A problem is well-posed if its solution exits, is unique, and continuously depends on errors present in problem formulation. If the problem fails to fulfill any of these conditions, then it is said to be ill-posed. Like many other inverse problems, model updating involved in Equation (2.26), which could also be used for damage detection, may be ill-posed. Regularization techniques are needed to provide bounds to the solution. Research in this area has built on the early work of Tikhonov (1977), and Tikhonov regularization is performed as

$$J(\Delta\mathbf{x}, \lambda) = \left\| \mathbf{S} \cdot \Delta\boldsymbol{\alpha} - \Delta\mathbf{R} \right\|_2^2 + \lambda^2 \left\| \Delta\boldsymbol{\alpha} \right\|_2^2 \tag{2.27}$$

The basic idea is to minimize the cost function in Equation (2.27) by searching for a solution $\Delta\mathbf{x}$. The two terms are balanced with the value of the regularization parameter λ. Hansen (1992, 1998) have proposed regularization methods for obtaining a solution to the inverse problem It is shown that a stable solution scheme can be achieved by imposing certain constraints with adjustable a *priori* weighting parameters.

The two most widely used regularization methods are Tikhonov regularization (Tikhonov 1995) and truncated singular value decomposition (Weber et al. 2009). Tikhonov parameter was determined through trial-and-error in the early application to system identification and model updating (Rothwell and Drachman 1989; Ojalvo and Ting 1990; Mottershead and Foster 1991; Fregolent et al. 1996). Busby and Trujillo (1997) applied both the L-curve method and generalized cross validation (GCV) to choose the optimal regularization parameter. Ziaei-Rad and Imregun (1999) summarized the performance of existing regularization method applied to model updating. Mares et al. (2002) investigated the robust estimation technique and Tikhonov regularization method for the output-error-based model updating with measured modal parameters.

Truncated SVD is another form of regularization by truncating the last several small singular values to improve the conditioning of matrix. In effect, the TSVD technique can be described as a filter that helps overcome the instability by filtering out the smallest singular values of the matrix. A trial-and-error procedure is used by Mottershead and Foster (1991) to determine the truncation parameter. Ren (2005) presented a method for determination of the truncation level. However, similar to the regularization method the difficulty is the determination of the truncation parameter.

The most frequently used conditions (Friswell and Mottershead 1995) are: (a) $\boldsymbol{\alpha} \to \mathbf{0}$, which means that the parameter values will be small; (b) $\boldsymbol{\alpha} \to \boldsymbol{\alpha}_0$, which means that the total parameter changes with respect to the reference model will be small and (c) $\Delta\boldsymbol{\alpha}^{k+1} \to 0$, which denotes that the parameter increment between iterations will be small. In the above conditions, the parameter variations or the updated parameters are bounded with a fixed reference vector. Li and Law (2010) proposed an adaptive regularization method. In their study, the discrimination of possible damaged elements and undamaged elements is done from results obtained in previous iterations via a new side condition. Their method aims to limit the local change in damaged structural elements in each iteration and to force the variation of other undamaged elements close to zero. A simulation of a thirty-one bar plane truss was investigated and the results indicated that method are greatly improved even with large noise contamination in the measurement

2.4 Structural Vibration Control

Over the last three decades, the research and application of structural control system have attacked considerable attention. Before the concept of structural control was imported into civil engineering the concepts of vibration absorption and vibration damping and the techniques were developed to aircraft during the Second World War. From 1960s great efforts have been undertaken to develop passive, active, semi-active and hybrid structural control algorithm into a workable technology (Soong and Spencer 2000). These structural control algorithm and devices have been extensively investigated and implemented in a large number of modern buildings and bridges to mitigate the structural vibration due to the wind or earthquake.

Passive energy dissipation systems or control devices, such as base isolation and braces, are widely used in civil engineering structures to enhancing the damping, stiffness. These devices could both service as dissipation devices during the earthquake and rehabilitation of aging structures (Soong et al. 2005; Constantinou et al. 1998). They are characterized by their capability to energy dissipation and strength enhancement.

In accordance to the way of energy dissipation the passive devices could be classified as base isolation system, vibration absorbing system and vibration damping system. The base isolation system is commonly installed between the foundation and superstructure to absorb the earthquake input energy and mitigate the vibration of superstructure. The base isolations always have a large stiffness in vertical direction and flexible stiffness in horizontal direction with a high damping elastomeric bearing (Pong et al. 1994a, 1994b, 1994c; Constantinou et al. 1992). Tuned mass damper (TMD), tuned liquid damper (TLD) and tuned liquid column damper (TLCD) are typical vibration absorbing devices. With these devices, the earthquake input is transformed into kinetic energy of moving mass or liquid (Kareem, 1994). Metallic damper, friction damper and viscoelastic damper are typical vibration damping devices (Skinner et al. 1980; Whittaker et al. 1991; Pall et al 1980; Soong 2005). Passive devices possess many advantages including the low cost, no requirement of external energy input and stable performance during the earthquake. But they cannot be adaptive to the structural parameters.

For more than three decades, researchers have investigated the application of active, hybrid, and semi-active control methods and devices to remove the limitation of passive approaches and to reduce structural responses. Compared with the passive control system, the active control system has a relatively short history. Kajima Corporation implemented the first active control to a full scale building in 1989 (Kobori et al. 1991). Purely active structural control system consists of three parts, which are sensors, devices to possess the measured response and calculate the control force, and actuators to implement the control force. The aim of the active control is to conduct the structural control during the strong wind and moderate earthquake (Spencer et al. 2003). Considerable optimal control algorithms have been investigated to implement the structural control under different conditions (Skelton 1988; Soong 1990; Widrow and Lehr 1990; Zadeh 1965). The advantages of active control includes the insensitivity to site condition and excitation, flexibility to control algorithm and selectivity to control objectives such as the safety of structure or human comfort on platform. Despite the advantages mentioned above, the active control systems require external power, large control force. The semi-active control devices which are commonly viewed as controllable passive devices can partially overcome the limitation of the active control system. The difference between the active control devices and semi-active control devices is that the semi-control devices do not directly add energy to the structural system.

Hybrid-control strategies of civil engineering structures also have been investigated by many researchers to ensure the control efficiency and reliability of both the structure and control system during the harsh earthquake event (Housner et al. 1997; Adeli and Saleh 1998; Kareem et al. 1999; Nishitani and Inoue 2001; Yang and Dyke 2003; Casciati 2003; Faravelli and Spencer 2003). The hybrid structural control is a combination of the passive control, active control or semi-active control. The hybrid structural system is more reliable than the active control system. The active control can also be work with a limited number of response feedbacks of the sensing system for the hybrid control system during the strong wind or moderate earthquake. The main benefit of the semi-active control devices and hybrid control devices is that they could also reduce the structural response even the failure of active control. Considering the reliability and efficiency, the hybrid control is now generally applied in practical engineering (Faravelli and Spencer 2003).

Majority of research works stated above on the structural control strategies were designed for the centralized control system and did not consider the changes in structural properties in the past. In a centralized structural control system, the structural responses measured by sensor system in a structure are transmitted into a central controller where the value of control force are determined and then transmitted to all actuators in a central manner. To conduct the centralized structural vibration control of large system, a higher demand will be required on sensing system, controller and actuator. Large number of sensors and actuators are needed for the control of large size structures. Higher requirements of sensors, data transmission facility, the computational hardware, actuators as well as the central controller are needed to be fulfilled (Lunze 1992). The centralized structural control strategies may not be reliable as expected due to the possible failure of the active control function during the severe earthquake. Sandel (1978), Ahmadian (1994), and Bakule (2008) proposed the decentralized control strategies to remove these limitations in areas of power transmission network, economic systems and space dynamic systems. However, research on decentralized structural control for large-scale structural systems is still limited.

With the development of the techniques of structural control and structural health monitoring the combination of these two techniques is necessary considering the changes in structural system. All of the passive control, semi-active control, active control and hybrid control could be applied in this integrated system. The integration of structural parameter identification and semi-active control has been investigated by Xu and Chen (2007a, 2007b). They proposed the concept of an integrated system with semi-active friction dampers and parameter identification system. Their research indicated that the integrated system is efficient to conduct the structural control with updated structural model. The integrated system is centralized and the parameter identification is conducted in frequency domain which needs a large number of measurement data. The on-line implementation of structural control and evaluation of a large scale structure are difficult due to the complicated computation with matrices. Moreover, the reliability of the structural control and evaluation results will also reduce in a large scale structural system during severe earthquake with centralized control system.

2.5 Critical Issues and Shortcomings in Existing Methods of Structural Condition Assessment and Structural Control

Although the vibration based structural condition assessment and structural control have investigated intensively, there are a number of issues that need to be addressed to make this method more practical so that this method could be commonly applied to engineering problems. The structural control and condition assessment is still extremely difficult due to the large and complex structure system with the considerable proposed methods. Output-only strategies are required for the practical engineering inverse problem (Lardies, 1998; Li et al. 1999a, 1999b). These issues includes the computational burden related with the structural model updating and force identification, the uncertainty in the measured vibration data and in the structural model, the incompleteness of measurement data, the ill-conditioning in inverse problem and the effect of the varying operational and environmental conditions.

Firstly, it is difficult to locate the local abnormality with global measurement for a large scale structural system (Brownjohn, 2007; Farrar and Worden 2007). The changes of global dynamic properties may not be sensitive enough to the local changes. A study by Worden et al. (2005) indicated that those indices sensitive to local damage are also sensitive to environmental conditions and measurement noise.

Secondly, complex boundary conditions and uncertainties exist due to the discreteness of components in the finite element model and variability in the material properties. Models on the boundary conditions and any innovative device for seismic protection in a large-scale civil structure may not be accurate. These uncertainties may render the optimization process ill-conditioned (Friswell et al. 2007). Large number of unknowns may adverse the convergence property in inverse analysis.

Thirdly, substructure methods could reduce the number of unknown parameters and improve the computational efficiency. However, the substructure methods bear the problem of incompleteness of measurement data and the measurement location. Many techniques work very well in example cases but perform poorly when subject to the measurement limitations imposed by practical modal testing. These limitations usually arise because of the fact that the further bear limitation of the number of sensor and sensor position. Most of the substructure methods in time domain commonly need the record of the excitation or needs certain point measurement, such as interface DOFs or all responses of interior DOFs.

Fourthly, structural control would ensure the structural reliability of the structure during the severe earthquake. The integrated system of structural control and model updating would make the structural control algorithm more stable and effective. However, only the integrated system with model updating method in frequency domain has been investigated. Since the gaps illustrated before, this thesis aim to propose a series method based on substructure method which could improve the computational effort, perform the general out-put only structural condition evaluation, including load evaluation and damage detection, conduct the time-variant structural condition evaluation and implement the smart structure with the integration of structural control and structural health monitoring.

Based on the existing problems and shortcomings in structural condition assessment and structural control, the aspects below deserve further exploration. The time response sensitivity method in time domain with substructure methods is an alternative solution to structural condition assessment, which needs as few data as possible. A fairly accurate substructural external force identification method is needed to develop to identify both the interface force and external force without accurate model of the boundary condition. A general response sensitivity method based on the two-stage identification for substructural model updating is needed to be developed with general sensor placement. A time-variant parameters identification method is developed without the exact time of the damage and initial structural response. A new combined system of adaptive structural control and structural evaluation is developed with the effective structural control and structural condition assessment.

CHAPTER 3

SUBSTRUCTURAL FORCE IDENTIFICATION

3.1 Introduction

The dynamic load environment assessment is the first kind of inverse problem as mentioned in Chapter 2. Dynamic load assessment is an important component in the structural condition assessment and health monitoring of a structure. It is impossible to measure the excitation of the structure directly under most circumstances due to the lack of accessibility to the loading position or the need of a large number of sensors. A lot of force re-constructions methods or force identification methods have been proposed and analyzed (Law and Chan 1997; Busby and Trujillo 1995; Kucharski 2000). The force identification method is frequently based on the finite element model which is often inaccurate. There are some model errors in the finite element model. The most common type of errors is found in modeling the boundary conditions which affects the accuracy of both the forward and backward analysis result. And most existing methods have not considered the real boundary conditions of the structure. Research on the inverse problem has been conducted with the substructure method in the last two decades. However, very few literatures have taken into account the error in the finite element model of the structure.

A lot of force re-constructions or force identification methods have been proposed and analyzed with regularization method. The equation for the force identification has been formulated in state space (Trujillo and Busby 1997; Law, Bu and Zhu 2005; Law and Fang 2001) and directly solved with regularization method with the Zero-Order Hold (ZOH) Discrete method. The external forces acting on the structure can be identified when the number of external force is small. Others have employed the ZOH discrete method and first-order regularization in force identification based on the dynamic programming method, but the computation is very time consuming (Trujillo and Busby 1997; Law and Fang 2001). The discretization of the continuous state space equation will influence the accuracy of the calculated response especially the acceleration. It would subsequently affect the assessment result in an inverse problem. However, there is few literatures discussing on the accuracy of force identification based on different discretization methods of the continuous function.

The conventional ZOH discretization of the continuous equation of motion gives satisfactory results when the number of external excitation is small (Law and Fang 2001; Trujillo and Busby 1997). However, when the number of external forces that need to be identified increases, particularly with a more complicated structural system, this method is not accurate.

Engineering analysis with a large-scale structure always has the problem of insufficient and incorrect information on the analytical model of the structure including connections at the boundaries. It is, however, much easier to have an accurate model of a portion of the structure through detail and vigorous desktop study and field inspection. The method proposed in this Chapter attempts to make good use of this limited but accurate analytical information of the structure for the inverse identification of external forces acting on the structure. A force identification strategy is proposed to identify external forces acting on a portion of a structural system based on the modified FOH discrete method of the state space equation. The structure could be divided into substructures with both the excitation and measurements in each target substructure. Both the interface forces between the substructures and the excitation on each target substructure are taken as unknown and they will be identified with the proposed method. It is noted that there may be a large number of forces to be identified.

This Chapter will present the development of the indirect assessment method with substructure methods. With this method the interface forces as well as external excitation could be identified and FOH discrete method could provide a more accurate identification results than the ZOH discrete method. The equation of motion of substructure for the forward problem is given in Section 3.2. Basic theory of the ZOH discrete method, FOH discrete method and the force identification method with substructure technique based on FOH discrete method will be illustrated in Section 3.3. The implementation procedure for the force identification including the identification of force at a fixed position and moving will be presented respectively in Section 3.4. Numerical simulation will be conducted in Section 3.5 which includes comparisons of the forward analysis and inverse analysis with the ZOH discrete method and FOH discrete method. A discussion on the effect of the number of sensors will be provided in Section 3.6. A summary will be given at the end of this Chapter.

3.2 Dynamic Responses of a Substructure

If a structure is subject to external excitation, the equation of motion of the structural system can be written as

$$\mathbf{M}\ddot{\mathbf{x}} + \mathbf{C}\dot{\mathbf{x}} + \mathbf{K}\mathbf{x} = \mathbf{L}\mathbf{F} \tag{3.1}$$

where matrices **M**, **C**, and **K** are the mass, damping and stiffness matrixes of the structural system respectively. **F** is the vector of external excitation forces on the structure and **L** is the mapping matrix for the input excitation forces. $\ddot{\mathbf{x}}$, $\dot{\mathbf{x}}$ and $\mathbf{x}$ are vectors of acceleration, velocity and displacement of the structural system respectively. Rayleigh damping is assumed for the structure,

$$\mathbf{C} = a_1 \cdot \mathbf{M} + a_2 \cdot \mathbf{K} \tag{3.2}$$

where a_1 and a_2 are the damping coefficients.

The whole structural system can be divided into substructures with one substructure selected as the target substructure for assessment as shown in Figure 3.1 with the substructures linked at the interface dofs. Equation (3.1) can be rewritten as

$$\begin{bmatrix} \mathbf{M}_{rr} & \mathbf{M}_{ri} & \mathbf{0} \\ \mathbf{M}_{ir} & \mathbf{M}_{ii} & \mathbf{M}_{is} \\ \mathbf{0} & \mathbf{M}_{si} & \mathbf{M}_{ss} \end{bmatrix} \begin{Bmatrix} \ddot{\mathbf{x}}_r \\ \ddot{\mathbf{x}}_i \\ \ddot{\mathbf{x}}_s \end{Bmatrix} + \begin{bmatrix} \mathbf{C}_{rr} & \mathbf{C}_{ri} & \mathbf{0} \\ \mathbf{C}_{ir} & \mathbf{C}_{ii} & \mathbf{C}_{is} \\ \mathbf{0} & \mathbf{C}_{si} & \mathbf{C}_{ss} \end{bmatrix} \begin{Bmatrix} \dot{\mathbf{x}}_r \\ \dot{\mathbf{x}}_i \\ \dot{\mathbf{x}}_s \end{Bmatrix} + \begin{bmatrix} \mathbf{K}_{rr} & \mathbf{K}_{ri} & 0 \\ \mathbf{K}_{ir} & \mathbf{K}_{ii} & \mathbf{K}_{is} \\ 0 & \mathbf{K}_{si} & \mathbf{K}_{ss} \end{bmatrix} \begin{Bmatrix} \mathbf{x}_r \\ \mathbf{x}_i \\ \mathbf{x}_s \end{Bmatrix} = \begin{Bmatrix} \mathbf{L}_r\mathbf{F}_r \\ \mathbf{L}_i\mathbf{F}_i \\ \mathbf{L}_s\mathbf{F}_s \end{Bmatrix} \tag{3.3}$$

where the subscripts s, i and r denote the DOFs of Substructure 1, the interface DOFs between the substructures and the DOFs of Substructure 2 respectively.

Equation (3.1) can then be rewritten as

$$(\mathbf{M}_{w,r}+\mathbf{M}_{w,s})\ddot{\mathbf{x}}+(\mathbf{C}_{w,r}+\mathbf{C}_{w,s})\dot{\mathbf{x}}+(\mathbf{K}_{w,r}+\mathbf{K}_{w,s})\mathbf{x}=\mathbf{LF} \tag{3.4}$$

where

$$\mathbf{M}_{w,r}=\begin{bmatrix}\mathbf{M}_{rr} & \mathbf{M}_{ri} & \mathbf{0}\\ \mathbf{M}_{ir} & \mathbf{M}_{ii}^{'} & \mathbf{0}\\ \mathbf{0} & \mathbf{0} & \mathbf{0}\end{bmatrix},\ \mathbf{C}_{w,r}=\begin{bmatrix}\mathbf{C}_{rr} & \mathbf{C}_{ri} & \mathbf{0}\\ \mathbf{C}_{ir} & \mathbf{C}_{ii}^{'} & \mathbf{0}\\ \mathbf{0} & \mathbf{0} & \mathbf{0}\end{bmatrix},\ \mathbf{K}_{w,r}=\begin{bmatrix}\mathbf{K}_{rr} & \mathbf{K}_{ri} & \mathbf{0}\\ \mathbf{K}_{ir} & \mathbf{K}_{ii}^{'} & \mathbf{0}\\ \mathbf{0} & \mathbf{0} & \mathbf{0}\end{bmatrix}$$

$$\mathbf{M}_{w,s}=\begin{bmatrix}\mathbf{0} & \mathbf{0} & \mathbf{0}\\ \mathbf{0} & \mathbf{M}_{ii}^{''} & \mathbf{M}_{is}\\ \mathbf{0} & \mathbf{M}_{si} & \mathbf{M}_{ss}\end{bmatrix},\ \mathbf{C}_{w,s}=\begin{bmatrix}\mathbf{0} & \mathbf{0} & \mathbf{0}\\ \mathbf{0} & \mathbf{C}_{ii}^{''} & \mathbf{C}_{is}\\ \mathbf{0} & \mathbf{C}_{si} & \mathbf{C}_{ss}\end{bmatrix},\ \mathbf{K}_{w,s}=\begin{bmatrix}\mathbf{0} & \mathbf{0} & \mathbf{0}\\ \mathbf{0} & \mathbf{K}_{ii}^{''} & \mathbf{K}_{is}\\ \mathbf{0} & \mathbf{K}_{si} & \mathbf{K}_{ss}\end{bmatrix}$$

and the single and double quotation marks denote the contribution of the system matrices associated with the interface DOFs to Substructures 1 and 2 respectively. The following equations of motion of the substructures can be derived from Equations (3.3) and (3.4) including the contributions from the interface DOFs.

$$\begin{bmatrix}\mathbf{M}_{rr} & \mathbf{M}_{ri} & \mathbf{0}\\ \mathbf{M}_{ir} & \mathbf{M}_{ii}^{'} & \mathbf{0}\\ \mathbf{0} & \mathbf{0} & \mathbf{0}\end{bmatrix}\begin{Bmatrix}\ddot{\mathbf{x}}_r\\ \ddot{\mathbf{x}}_i\\ \ddot{\mathbf{x}}_s\end{Bmatrix}+\begin{bmatrix}\mathbf{C}_{rr} & \mathbf{C}_{ri} & \mathbf{0}\\ C_{ir} & C_{ii}^{'} & \mathbf{0}\\ \mathbf{0} & \mathbf{0} & \mathbf{0}\end{bmatrix}\begin{Bmatrix}\dot{\mathbf{x}}_r\\ \dot{\mathbf{x}}_i\\ \dot{\mathbf{x}}_s\end{Bmatrix}+\begin{bmatrix}\mathbf{K}_{rr} & \mathbf{K}_{ri} & \mathbf{0}\\ \mathbf{K}_{ir} & \mathbf{K}_{ii}^{'} & \mathbf{0}\\ \mathbf{0} & \mathbf{0} & \mathbf{0}\end{bmatrix}\begin{Bmatrix}\mathbf{x}_r\\ \mathbf{x}_i\\ \mathbf{x}_s\end{Bmatrix}=\begin{Bmatrix}\mathbf{L}_r\mathbf{F}_r\\ \mathbf{L}_i\mathbf{F}_i\\ \mathbf{0}\end{Bmatrix} \tag{3.5}$$

$$\begin{bmatrix}\mathbf{0} & \mathbf{0} & \mathbf{0}\\ \mathbf{0} & \mathbf{M}_{ii}^{''} & \mathbf{M}_{is}\\ \mathbf{0} & \mathbf{M}_{si} & \mathbf{M}_{ss}\end{bmatrix}\begin{Bmatrix}\ddot{\mathbf{x}}_r\\ \ddot{\mathbf{x}}_i\\ \ddot{\mathbf{x}}_s\end{Bmatrix}+\begin{bmatrix}\mathbf{0} & \mathbf{0} & \mathbf{0}\\ \mathbf{0} & \mathbf{C}_{ii}^{''} & \mathbf{C}_{is}\\ \mathbf{0} & \mathbf{C}_{si} & \mathbf{C}_{ss}\end{bmatrix}\begin{Bmatrix}\dot{\mathbf{x}}_r\\ \dot{\mathbf{x}}_i\\ \dot{\mathbf{x}}_s\end{Bmatrix}+\begin{bmatrix}\mathbf{0} & \mathbf{0} & \mathbf{0}\\ \mathbf{0} & \mathbf{K}_{ii}^{''} & \mathbf{K}_{is}\\ \mathbf{0} & \mathbf{K}_{si} & \mathbf{K}_{ss}\end{bmatrix}\begin{Bmatrix}\mathbf{x}_r\\ \mathbf{x}_i\\ \mathbf{x}_s\end{Bmatrix}=\begin{Bmatrix}0\\ \mathbf{L}_i^{''}\mathbf{F}_i^{''}\\ \mathbf{L}_s\mathbf{F}_s\end{Bmatrix} \tag{3.6}$$

$$\mathbf{L}_i^{''}\mathbf{F}_i^{''}+\mathbf{L}_i^{'}\mathbf{F}_i^{'}=\mathbf{L}_i\mathbf{F}_i \tag{3.7}$$

where $\mathbf{L}_i^{'}$ and $\mathbf{L}_i^{''}$ are the mapping matrices for the force vectors $\mathbf{F}_i^{'}$ and $\mathbf{F}_i^{''}$ respectively.

The equation of motion of the Substructure 1 with '*s*' DOFs can be extracted from Equation (3.6) as

$$\begin{bmatrix}\mathbf{0} & \mathbf{M}_{si} & \mathbf{M}_{ss}\end{bmatrix}\begin{Bmatrix}\ddot{\mathbf{x}}_r\\ \ddot{\mathbf{x}}_i\\ \ddot{\mathbf{x}}_s\end{Bmatrix}+\begin{bmatrix}\mathbf{0} & \mathbf{C}_{si} & \mathbf{C}_{ss}\end{bmatrix}\begin{Bmatrix}\dot{\mathbf{x}}_r\\ \dot{\mathbf{x}}_i\\ \dot{\mathbf{x}}_s\end{Bmatrix}+\begin{bmatrix}\mathbf{0} & \mathbf{K}_{si} & \mathbf{K}_{ss}\end{bmatrix}\begin{Bmatrix}\mathbf{x}_r\\ \mathbf{x}_i\\ \mathbf{x}_s\end{Bmatrix}=\{\mathbf{L}_s\mathbf{F}_s\} \tag{3.8}$$

Rewrite Equation (3.8) into

$$\mathbf{M}_{ss}\ddot{\mathbf{x}}_s + \mathbf{C}_{ss}\dot{\mathbf{x}}_s + \mathbf{K}_{ss}\mathbf{x}_s = \mathbf{L}_s\mathbf{F}_s - (\mathbf{M}_{si}\ddot{\mathbf{x}}_i + \mathbf{C}_{si}\dot{\mathbf{x}}_i + \mathbf{K}_{si}\mathbf{x}_i) \tag{3.9}$$

The right-hand-side of Equation (3.9) consists of two parts. The first term $\mathbf{L}_s\mathbf{F}_s$ is the vector of external forces and the second term $-(\mathbf{M}_{si}\ddot{\mathbf{x}}_i + \mathbf{C}_{si}\dot{\mathbf{x}}_i + \mathbf{K}_{si}\mathbf{x}_i)$ is the vector of internal forces associated with the interface DOFs. In fact, vector $-(\mathbf{M}_{si}\ddot{\mathbf{x}}_i + \mathbf{C}_{si}\dot{\mathbf{x}}_i + \mathbf{K}_{si}\mathbf{x}_i)$ consists of the interface forces which can be taken as another set of external forces acting on the substructure.

3.3 Force Identification of the Target Substructure

3.3.1 ZOH Discrete Method in Force Identification

The equation of motion of the structural system shown in Equation (3.1) can be expressed in the state space as following

$$\dot{\mathbf{z}} = \mathbf{A}^C\mathbf{z} + \mathbf{B}^C\mathbf{L}\cdot\mathbf{F} \tag{3.10}$$

where $\mathbf{z} = \begin{bmatrix} \mathbf{x} \\ \dot{\mathbf{x}} \end{bmatrix}$, $\mathbf{A}^C = \begin{bmatrix} \mathbf{0} & \mathbf{I} \\ -\mathbf{M}^{-1}\mathbf{K} & -\mathbf{M}^{-1}\mathbf{C} \end{bmatrix}$ and $\mathbf{B}^C = \begin{bmatrix} \mathbf{0} \\ \mathbf{M}^{-1} \end{bmatrix}$ and the superscript ^{C} denotes matrices for the continuous system. Vector $\mathbf{y}(t) \in \mathbf{R}^{ns\times 1}$ is assumed to represent the output of the structural system and it is assembled from the measurements with

$$\mathbf{y} = \mathbf{R}_a\ddot{\mathbf{x}} + \mathbf{R}_v\dot{\mathbf{x}} + \mathbf{R}_d\mathbf{x} \tag{3.11}$$

where $\mathbf{R}_a$, $\mathbf{R}_v$ and $\mathbf{R}_d \in \mathbf{R}^{m\times ndof}$ are the output influence matrices for the measured acceleration, velocity and displacement respectively, m is the dimension of the measured responses and *ndof* is the number of dofs of the structure. Equation (3.11) can be rewritten as

$$\mathbf{y} = \mathbf{R}^C \mathbf{z} + \mathbf{D}^C \cdot \mathbf{L} \cdot \mathbf{F} \tag{3.12}$$

where $\mathbf{R}^C = [\mathbf{R}_d - \mathbf{R}_a \mathbf{M}^{-1}\mathbf{K} \quad \mathbf{R}_v - \mathbf{R}_a \mathbf{M}^{-1}\mathbf{C}]$ and $\mathbf{D}^C = \mathbf{R}_a \mathbf{M}^{-1}$. When the external force is known or measured, the value of state variable z and y can be calculated accurately. However, in practice, the measurement data is discrete and the continuous state equation is required to be transformed into discrete equation.

Based on the ZOH discrete method (Franklin, Powell and Workman 1998), Equations (3.10) and (3.12) can be converted into the following discrete equations as

$$\mathbf{z}(j+1) = \mathbf{A}^D \mathbf{z}(j) + \mathbf{B}^D \cdot \mathbf{L} \cdot \mathbf{F}(j) \tag{3.13}$$

$$\mathbf{y}(j) = \mathbf{H}\mathbf{z}(j) + \mathbf{J} \times \mathbf{L} \times \mathbf{F}(j) \quad (j = 1,2,\cdots,N) \tag{3.14}$$

where superscript ^{D} denotes the matrices for the discrete structural system. N is the total number of sampling points, dt is the time step between the state variables $\mathbf{z}(j)$ and $\mathbf{z}(j+1)$, $\mathbf{A}^D = \exp(\mathbf{A}^C \cdot dt)$, $\mathbf{B}^D = (\mathbf{A}^C)^{-1}(\mathbf{A}^D - \mathbf{I})\mathbf{B}^C$, $\mathbf{H} = \mathbf{R}^C$ and $\mathbf{J} = \mathbf{D}^C$.

The output $\mathbf{y}(j)$ is solved from Equations (3.13) and (3.14) with zero initial conditions of responses in terms of the previous input $\mathbf{F}(k),\ (k = 0,1,\cdots,j)$ and we have

$$\mathbf{y}(j) = \sum_{k=0}^{j} \mathbf{H}_k \cdot \mathbf{L} \cdot \mathbf{F}(j-k) \tag{3.15}$$

where $\mathbf{H}_0 = \mathbf{J}$ and $\mathbf{H}_k = \mathbf{H}(\mathbf{A}^D)^{(k-1)}\mathbf{B}^D$.

The constants in matrix H_k in Equation (3.15) are the system Markov parameters. Equation (3.15) can be rewritten to give the matrix convolution equation as

$$\mathbf{Y} = \mathbf{H}_L\mathbf{F} \tag{3.16}$$

where $\mathbf{H}_L = \begin{bmatrix} \mathbf{H}_0 & \mathbf{0} & \cdots & \mathbf{0} \\ \mathbf{H}_1 & \mathbf{H}_0 & \cdots & \mathbf{0} \\ \vdots & \vdots & \ddots & \mathbf{0} \\ \mathbf{H}_{N-1} & \mathbf{H}_{N-2} & \cdots & \mathbf{H}_0 \end{bmatrix}\mathbf{L}_S$, $\mathbf{L}_S = \begin{bmatrix} \mathbf{L} & \mathbf{0} & \cdots & \mathbf{0} \\ \mathbf{0} & L & \cdots & \mathbf{0} \\ \vdots & \vdots & \ddots & \mathbf{0} \\ \mathbf{0} & \mathbf{0} & \cdots & \mathbf{L} \end{bmatrix}$,

$\mathbf{Y} = \left\{ \mathbf{y}(0)^T \quad \mathbf{y}(1)^T \quad \cdots \quad \mathbf{y}(N-1)^T \right\}^T$,

$\mathbf{F} = \left\{ \mathbf{F}(0)^T \quad \mathbf{F}(1)^T \quad \cdots \quad \mathbf{F}(N-1)^T \right\}^T$.

Matrix $\mathbf{H}_L$ is constant for a specific structural system, and the response vector $\mathbf{Y}$ can be derived from the measured responses. The external force vector $\mathbf{F}$ can be identified from Equation (3.16) which is an ill-posed inverse problem in structural mechanics.

3.3.2 Triangle FOH Discrete Method

When the number of external forces increases, the influence of these forces on the response of the structural system increases correspondingly, and an inaccurate matrix $\mathbf{B}^D$ will result with large error in the state variable. This is because the force in a sampling period has been assumed to be constant as shown in Equation (3.13). This discretization within a sampling period is treated differently in the FOH discrete method, namely the triangle hold discrete method, where the discrete data is interpolated as

$$u(t) = u(i) + \frac{u(i+1) - u(i)}{T}(t - iT) \qquad (iT \le t \le (i+1)T \quad i = 1, 2 \cdots N-1) \tag{3.17}$$

where T is the sampling period.

$$\mathbf{u} = \mathbf{LF} \tag{3.18}$$

Define the unite impulse function δ as

$$\delta(t) = \begin{cases} +\infty & t = 0 \\ 0 & t \neq 0 \end{cases} \tag{3.19}$$

where $\int_{-\infty}^{+\infty} \delta(t)dt = 1$.

The impulse response and block diagram of the modified FOH are shown in Appendix A. The Laplace transformation of the extrapolation filter (Franklin, Powell and Workman 1998) that follows the impulse sampling is

$$H_{tri}(s) = \frac{e^{Ts} - 2 + e^{-Ts}}{Ts^2} \tag{3.20}$$

Based on the block diagram in Appendix A, the state variables v and w are defined as

$$v = w / T \tag{3.21}$$

$$\dot{w} = u(t+T)\delta(t+T) - 2u(t)\delta(t) + u(t-T)\delta(t-T) \tag{3.22}$$

where $\delta(t)$ is the unit impulse shown in Equation (3.19). It can be shown from the integration of Equations (3.21) and (3.22) that $v(i)=u(i)$ and $w(i)=u(i+1)-u(i)$, and a new state space equation can be derived as

$$\begin{bmatrix} \dot{\mathbf{z}} \\ \dot{\mathbf{v}} \\ \dot{\mathbf{w}} \end{bmatrix} = \begin{bmatrix} \mathbf{A}^C & \mathbf{B}^C & 0 \\ 0 & 0 & 1/T \\ 0 & 0 & 0 \end{bmatrix} \begin{bmatrix} \mathbf{z} \\ \mathbf{v} \\ \mathbf{w} \end{bmatrix} + \begin{bmatrix} 0 \\ 0 \\ 1 \end{bmatrix} \overline{u} \tag{3.23}$$

where $\overline{u}$ as shown in Appendix A can be taken as the input impulse function. The matrix on right-hand-side of the Equation (3.23) is defined as

$$\mathbf{F}_T = \begin{bmatrix} \mathbf{A}_C & \mathbf{B}_C & \mathbf{0} \\ \mathbf{0} & \mathbf{0} & 1/T \\ \mathbf{0} & \mathbf{0} & \mathbf{0} \end{bmatrix} \tag{3.24}$$

If the one step solution to Equation (3.23) is written as

$$\zeta(iT+1) = e^{F_T T}\zeta(iT) \tag{3.25}$$

then

$$\exp(\mathbf{F}_T T) = \begin{bmatrix} \mathbf{\Phi} & \mathbf{\Gamma}_1 & \mathbf{\Gamma}_2 \\ \mathbf{0} & \mathbf{1} & \mathbf{0} \\ \mathbf{0} & \mathbf{0} & \mathbf{1} \end{bmatrix} \tag{3.26}$$

The equation in variable x can be written as

$$\mathbf{x}(i+1) = \mathbf{\Phi}x(i) + \mathbf{\Gamma}_1 v(i) + \mathbf{\Gamma}_2 w(i) \tag{3.27}$$

If a new state is defined as $\mathbf{z}(i) = \mathbf{x}(i) - \mathbf{\Gamma}_2\mathbf{u}(i)$, Equation (3.27) for the modified FOH can be rewritten as

$$\mathbf{z}(i+1) = \mathbf{A}^D\mathbf{z}(i) + \mathbf{B}^D\mathbf{u}(i) \tag{3.28}$$

The output equation is

$$\mathbf{y}(i) = \mathbf{C}^D\mathbf{z}(i) + \mathbf{D}^D\mathbf{u}(i) \tag{3.29}$$

The parameter for the state equation can then be represented as

$$\begin{aligned} A^D &= \Phi, \\ B^D &= \mathbf{\Gamma}_1 + \Phi\mathbf{\Gamma}_2 - \mathbf{\Gamma}_2, \\ C^D &= H, \\ D^D &= J + H\mathbf{\Gamma}_2 \end{aligned} \tag{3.30}$$

Based on the above modified FOH discrete method, the force identification can be conducted following Equations (3.10) to (3.16) with more accurate results than the previous ZOH discrete method as shown in the following studies.

3.3.3 Force Identification based on the FOH Discrete Method

The external force identification based on the FOH discrete method can also be written in the form of Equation (3.16) which is ill-posed. A straightforward least-squares solution will produce unbounded solution. Regularization method would provide an improved solution to the ill-posed problem. The damped least-squares method proposed by Tikhonov (1963) is adopted to give bounds to this problem. Equation (3.31) shows the application of the regularization method in force identification as

$$\mathbf{H}_L{}^T\mathbf{Y} = (\mathbf{H}_L{}^T\mathbf{H}_L + \lambda \mathrm{I})\mathbf{P} \tag{3.31}$$

where λ is the non-negative damping coefficient governing the participation of the least-squares error in the solution. Solving Equation (3.31) is equivalent to minimizing the function

$$J(P,\lambda) = \left\|\mathbf{H}_L\mathbf{P} - \mathbf{Y}\right\|^2 + \lambda\left\|\mathbf{P}\right\|^2 \tag{3.32}$$

The L-curve method proposed by Hansen (1992) is applied in this Chapter to find the optimal regularization parameter λ. The relative percentage error in the identified external forces can be calculated as

$$error = \frac{\left\|\mathbf{F}_{id} - \mathbf{F}_{true}\right\|}{\left\|\mathbf{F}_{true}\right\|} \times 100\% \tag{3.33}$$

where $\mathbf{F}_{true}$ is the real force acting on the substructure and $\mathbf{F}_{id}$ is the identified external force.

When there is no noise in the measured response, the external forces can be identified fairly accurately. However, the identified force will fluctuate close to the real force when there is measurement noise. To mitigate the influence of noise, the Chebyshev Polynomial can be applied to approximate the time history of response as

$$\ddot{\mathbf{x}}_k = \sum_{m=1}^{Nm} c_m^k \mathbf{T}_m^k(t) \tag{3.34}$$

where k indicates the k th measured response and N_m denotes the number of terms of the Chebyshev Polynomial. The coefficient of the Chebyshev Polynomial c_m^k can be taken as unknowns in the curve fitting via the regularization method. The influence of noise can be moderated to certain extent through the iterative updating of the polynomial coefficients. Eighty terms of the polynomial is selected in this study when the position of the excitation force is fixed.

3.3.4 Moving Force Identification

When a vertically acting external force is acting on a flat plate finite element, the equivalent nodal force of the plate element can be represent though the shape function as

$$\begin{aligned}
N_1(\zeta, y) &= (1+2\zeta / l_x)(1-\zeta / l_x)^2(1+2y/l_y)(1-y/l_y)^2 \\
N_2(\zeta, y) &= (1+2\zeta / l_x)(1-\zeta / l_x)^2(y/l_y)(1-y/l_y)^2 l_y \\
N_3(\zeta, \eta) &= -(1-\zeta)^2\zeta(1+2\eta)(1-\eta)^2 l_x \\
N_4(\zeta, \eta) &= (1+2\zeta)(1-\zeta)^2(3-2\eta)\eta^2 \\
N_5(\zeta, \eta) &= (1+2\zeta)(1-\zeta)^2(1-\eta)\eta^2 l_y \\
N_6(\zeta, \eta) &= -\zeta(1-\zeta)^2(3-2\eta)\eta^2 l_x \\
N_7(\zeta, \eta) &= (3-2\zeta)\zeta^2(3-2\eta)\eta^2 \\
N_8(\zeta, \eta) &= -(3-2\zeta)\zeta^2(1-\eta)\eta^2 l_y \\
N_9(\zeta, \eta) &= -(1-\zeta)\zeta^2(3-2\eta)\eta^2 l_x \\
N_{10}(\zeta, \eta) &= (3-2\zeta)\zeta^2(1+2\eta)(1-\eta)^2 \\
N_{11}(\zeta, \eta) &= (3-2\zeta)\zeta^2\eta(1-\eta)^2 l_y \\
N_{12}(\zeta, \eta) &= (1-\zeta)\zeta^2(1+2\eta)(1-\eta)^2 l_x
\end{aligned} \tag{3.35}$$

where x and y are the local coordinates in the i th element, l_x and l_y are the length and width of the plate element and $\eta = y / l_y$, $\zeta = x / l_x$ proposed by Wu (2006).

The nodal force vector only consists of force F_z and moments M_x and M_y as $\mathbf{F}=\{F_z, M_x, M_y\}^T$. The equivalent nodal forces at the four nodes of the plate element can be shown as follows:

$$\begin{aligned}
&f_{1,z} = N_1 \cdot F \quad M_{1,x} = N_2 \cdot F \quad M_{1,y} = N_3 \cdot F \\
&f_{2,z} = N_4 \cdot F \quad M_{2,x} = N_5 \cdot F \quad M_{2,y} = N_6 \cdot F \\
&f_{3,z} = N_7 \cdot F \quad M_{3,x} = N_8 \cdot F \quad M_{3,y} = N_9 \cdot F \\
&f_{4,z} = N_{10} \cdot F \quad M_{4,x} = N_{11} \cdot F \quad M_{4,y} = N_{12} \cdot F
\end{aligned} \tag{3.36}$$

Though the mapping matrix L of the force is time-variant for a moving force, the interface forces can also be identified simultaneously through Equations (3.31) and (3.32). The mapping matrix $\mathbf{L}_s$ will take up the following form as

$$\mathbf{L}_S = \begin{bmatrix} \mathbf{L}_1 & \mathbf{0} & \cdots & \mathbf{0} \\ \mathbf{0} & \mathbf{L}_2 & \cdots & \mathbf{0} \\ \vdots & \vdots & \ddots & \mathbf{0} \\ \mathbf{0} & \mathbf{0} & \cdots & \mathbf{L}_N \end{bmatrix} \tag{3.37}$$

where $\mathbf{L}_k$ is the mapping matrix at the location of the k th sampling point.

3.4 Implementation Procedure

Step 1: Divide the structure into substructures and obtain the mass, damping and stiffness matrices of the target substructure.

Step 2: Conduct dynamic measurement on the substructure.

Step 3: Obtain the matrix of system Markov parameters from the finite element model of the substructure based on the FOH discrete method from Equations (3.29) and (3.30). If the force is a moving force, matrix $\mathbf{H}_L$ is obtained from Equation (3.16).

Step 4: Identify the forces acting on the substructure including the interface forces through the damped least-squares method in Equation (3.31) based on the FEM of the substructure.

It should be noted that this approach of force identification only needs the finite element model of the target substructure.

3.5 Simulation Study with a Flat Plate Structure

In this section, force identification of a plate structure is investigated in state space with the ZOH and the FOH discrete method. A 32m×9m flat plate made of concrete is investigated to verify the proposed method of substructural force identification. The flat plate shown in Figure 3.2 is divided into 16×3=48 elements with size 2.0m×3.0m each. The substructure in the middle of the plate consists of 24 elements is taken as the target substructure in this simulation. The thickness of the plate is 0.15m and is fix-supported along its two short edges. The mass density, elastic modulus of material and Poisson ratio are 2500 kg/m^3, 3.25×10^{10} N/m^2 and 0.2 respectively. The plate is assumed to exhibit Rayleigh damping and the damping ratios of the first two modes are taken to be 0.01 and 0.005 respectively.

Mindlin plate element could be used to investigate the moderately thick shell with thickness-to-width ratio as 1/10. When the shell is thick, high-order of the shear deformation should be considered because the Mindlin's solution is only for the moderately thick shell element (Reissner, 1945; Mindlin, 1951; Lim et al. 1995). The thickness-to-width ratio in this study is about 1.67% (0.15/9) which is thinner than moderately thick shell element. For simplicity, the shear deformation is not considered in this thesis. But for practical engineering problem, the forward and inverse analysis should take the shear deformation into consideration for higher accuracy if the plate is thick enough. It should be noted that the formulation and implementation procedure in this Section is generally proposed.

3.5.1 Accuracy of Response from the Discrete State Space Function

The response of the substructure is calculated in state space assuming zero initial structural response of the structure. The acceleration of the flat plate structure at Node 13 is calculated to investigate the accuracy of the time response in state space. The response of the substructure is solved through the state space Equations (3.29) and (3.30) with the known external force at Node 14 and the interface forces calculated from the finite element model of the whole structure. Figure 3.3 gives comparison of the acceleration at Node 13 obtained from the ZOH discrete method and modified FOH discrete method. The calculated acceleration from the ZOH discrete method differs greatly from the acceleration calculated from using the Matlab command ‘lsim’ which serves as the reference response, while the acceleration calculated from the FOH discrete method is very close to the reference acceleration. The FOH discrete method is noted to be accurate with linear interpolation of the force between sampling points as shown in Figure 3.4.

The vertical responses at all the nodes of the substructure are calculated from the FOH state space equation and the ZOH state space equation with sampling rates of 200 and 500 Hz. The results are compared with the reference solution from Matlab command ‘lism’ in Figure 5 for 500 Hz sampling rate. The norm of errors of solution from ZOH state space equation and FOH state space equation are shown in Table 3.1. It is noted from Figure 3.5 and results from 200 Hz sampling rate (not shown) that the solution based on both the ZOH and FOH discrete methods will become more accurate when the sampling rate increases. Comparison in Table 3.1 shows that the solution based on FOH discrete method is more accurate than the solution calculated from ZOH discrete method of the state space equation. Therefore, it is recommended that the FOH discrete method be applied in the force identification in state space with relatively large sampling rate.

3.5.2 Force Identification

3.5.2.1 Fixed Position Force

The acceleration in the z-direction under the applied force at Node 14 are calculated at Nodes 1-8, 9-20 and 29-36 and there are 28 “measured” accelerations for the force identification. Zero initial conditions are assumed for the structure. An external force acts vertically along the z-direction on the flat plate structure at Node 14 and is modeled as

$$F(t) = 500(\sin(30\pi t + 0.3\pi) + \sin(45\pi t + 0.2\pi) + \sin(55\pi t + 0.16\pi))N \quad (3.38)$$

The 24 interface forces and the excitation force on the target substructure are evaluated with the force identification method based on FOH discrete methods in state space. The force identification results based on the FOH discrete method are shown in Figure 3.6. The identified force time histories at the interface and the excitation force almost overlap with the true curves indicating the accuracy of the proposed method. Sampling rate is 1000Hz and the data from the first 0.3s of the time history of the force is used for the identification.

When there is noise in the "measured" response, the polluted response is simulated by adding a random component to the "measured" responses as

$$\ddot{\mathbf{x}}_m = \ddot{\mathbf{x}} + E_P N_{noise} \sigma(\ddot{\mathbf{x}}) \quad (3.39)$$

where E_{p} is the percentage noise level, N_{noise} is a standard normal distribution vector with zero mean and unit standard deviation, $\sigma(\ddot{x})$ is the standard deviation of the "measured" acceleration response. When there is 5% noise in the measured response, the identified force time histories from FOH discrete method is shown alongside the true forces in Figure 3.7. The identified forces are close to the true forces but with more variations in the moments M_x. This may be due to the lacking of angular acceleration information in the "measured" response. The relative error in the identified forces is calculated as 11.56%. However the applied force at Node 14 is accurately identified and is almost overlapping with the true force.

3.5.2.2 Moving Force on a Substructure

A second scenario is studied with a force moving along the y-direction of the plate between the two ends of the substructure at 40 meter per second as shown in Figure 2. The force time history is

$$\mathbf{F}(t) = (150\sin(5\pi t + 0.3\pi) + 100\sin(10\pi t + 0.2\pi))N \tag{3.39}$$

The acceleration in the z-direction under the applied moving force are calculated at Nodes 1-4, 6, 7, 9, 10, 11, 12, 14, 15, 18, 19, 22, 23, 25, 26, 27, 28, 30, 31, 33-36 and the first 0.4 s of responses are used for the force identification. These responses are arbitrarily selected for the study. In this simulation, the force start from the beginning of substructure but not the beginning of the whole structure. The moving force can be identified as shown in Figure 3.8 without noise in the measurement and in Figure 3.9 with 6% noise in the measurement. The results show that the proposed method is accurate with the identification of a moving force. For the case with polluted measurements, the error in the initial value of the identified force affects the first part of the identified force time history. The second halve of the identified time history is almost overlapping with the true force with the reduction of initial value effect indicating the accuracy of the proposed method with polluted measurement.

3.5.2.3 Moving Force on the Whole Structure

The third simulation is more general, in which the moving force moves from one end to the other end of the whole structure. The force time history is set as

$$F(t) = (130\sin(5\pi t + 0.3\pi) + 120\sin(15\pi t + 0.2\pi) + 110\sin(20\pi t + 0.1\pi))N$$

The "measured" acceleration responses are identical as those for the second simulation and 0.8s of the acceleration is used to evaluate the moving force. The sampling rate in this simulation is 100 Hz for a reduced computation effort. In this general case, the identified moving force on the substructure without noise in the 'measured' acceleration is shown in Figure 3.10, and the one with 5% noise in the measured response is shown in Figure 3.11. In the first 0.2s and last 0.2s, only the interface forces are acting on the substructure and therefore the identified moving force is zero. The results in this simulation show that the moving force identification is not sensitive to the measurement noise. The proposed method can be recommended for large bridge system without considering too much the errors and uncertainties in the finite element model of the structure.

3.6 Discussion on the Number of Sensors

In the simulation studies of this Chapter, the number of sensors is more than the number of unknown forces. When the number of sensors is less than the number of the external forces, the solution to the Equation (3.16) will not be unique. However, the regularization method always makes sure that the number of the equation is equal to the number of the unknowns as noted in Equation (3.31). $\mathbf{H}_L$ is an *Nsensor*×*Nunknownf* matrix with *Nsensor* being the number of the measured discrete data and *Nunknownf* is the number of the unknowns in external forces. Therefore, as noted in Equation (3.16) *Nsensor* is also the number of equation considering the size of $\mathbf{H}_L$. Through the regularization method as Equation (3.31), the number of the equation is changed to *Nunknownf*. Therefore, a small change in the number of sensors will not have great influence in the identification result in general, and the uniqueness of the solution can be ensured by the regularization method and the optimal parameter λ. When there is noise in the measurement, it is recommended that the number of the sensors is more than or equal to the number of the external forces. When the number of the measured acceleration is reduced to 18 and only the acceleration at Nodes 1, 4, 6, 7, 10, 11, 14, 15, 18, 19, 22, 23, 26, 27, 30, 31, 33, 36 are calculated as measured response without noise, the moving force can also be identified with 0.77% error. If the number of the measured acceleration is reduced to 14, nearly half of the number of the external force, and the accelerations at Node 1, 4, 6, 9, 12, 15, 18, 19, 22, 25, 28, 31, 33, 36 are used for the force identification, the error will become large in the identified moving force as shown in Figure 3.12. It may be concluded that less information from the system will result in the larger optimal parameter λ, which will make the force identification not very accurate.

3.7 Conclusions

Engineering analysis with a large-scale structure always has the problem of insufficient and incorrect information on the analytical model of the structure including connections at the boundaries. It is, however, much easier to have an accurate model of a portion of the structure through detail and vigorous desktop study and field inspection. A method is proposed in this Chapter to make good use of this limited but accurate analytical information of the structure for the inverse identification of external force acting on the structure.

A substructural external force identification method based on the equation in state space with the FOH discrete and Tikhonov regularization is presented in this Chapter. This method only needs measurements in time domain, such as acceleration, and information on the finite element model of a substructure. Its effectiveness is illustrated with the identification of a time varying force acting at a fixed location and a time varying moving force on top of a flat plate structure.

In the forward problem of dynamic response prediction and the inverse problem of force identification, the FOH discrete method is shown to be more accurate than the ZOH discrete method due to the interpolation of the force between adjacent sampling points. Both the interface forces and the excitation force can be identified fairly accurately based on the FOH discrete method in state space even with polluted measurements with 6% noise. It is recommended in practice that the sampling rate should be set relatively high for an improved accuracy. It is also noted that there is a large number of forces to be identified in the problem and yet the applied force can be obtained with good accuracy.

Table 3.1 – Error of solution of state space equation

Sampling rate	Error (ZOH)(%)	Error (FOH)(%)
200	178.6	11.72
500	78.12	5.65

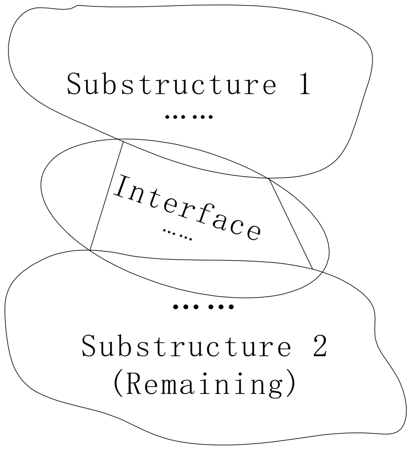

Figure 3.1 - Structure and substructures

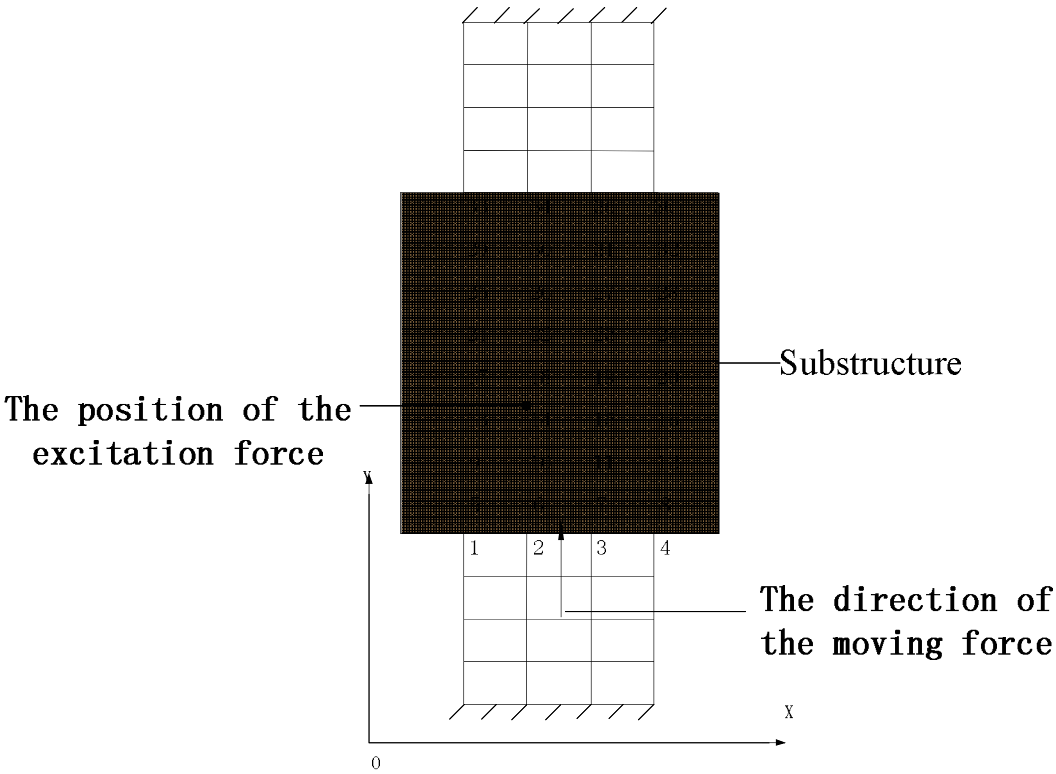

Figure 3.2 - 32m×9m flat plate structure

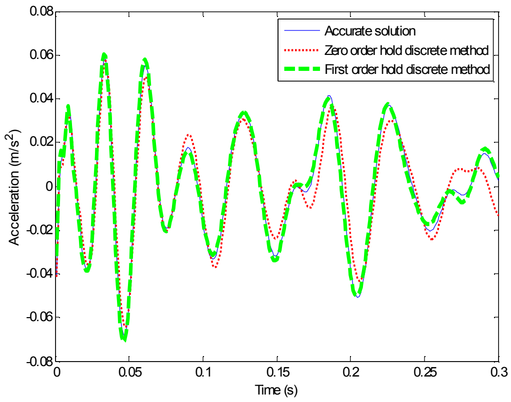

(a) Acceleration in *z*-direction

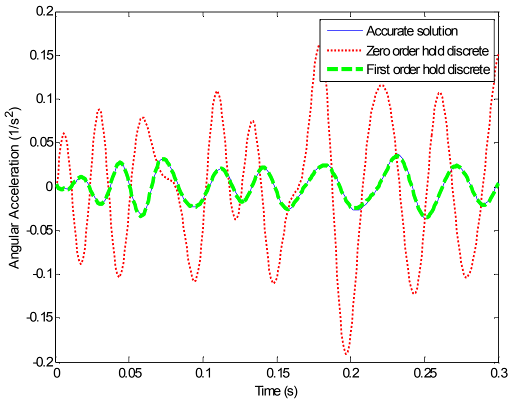

(b) Angular acceleration in plane *x*-*z*

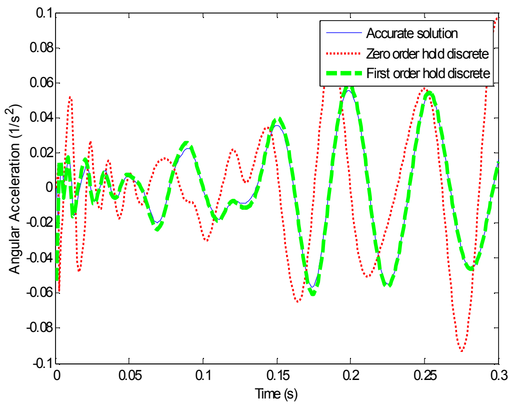

(c) Angular acceleration in plane *y*-*z*

Figure 3.3 - Structural response on Node 13

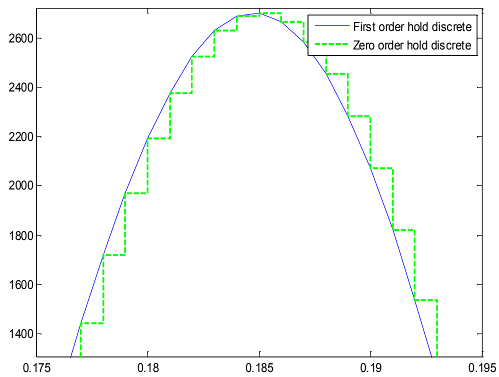

Figure 3.4 - Discretization at a peak of the applied force at Node 14 from ZOH and FOH discrete method

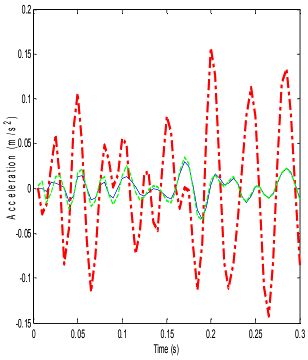

(1) Node 1

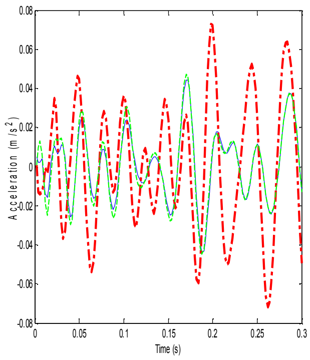

(2) Node 2

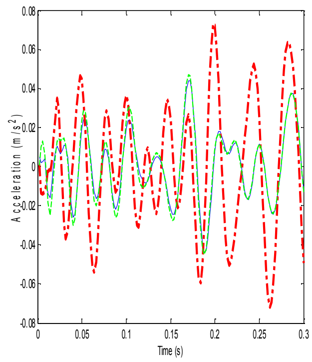

(3) Node 3

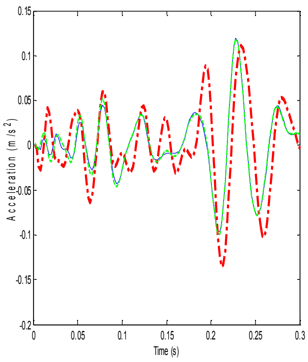

(4) Node 4

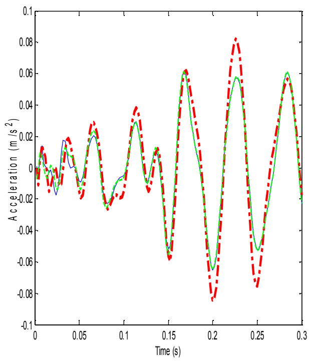

(5) Node 8

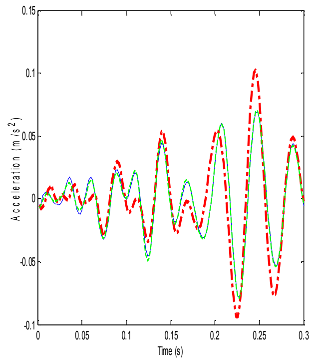

(6) Node 9

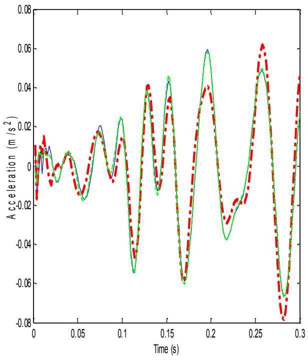

(7) Node 10

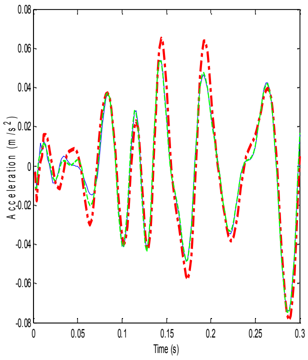

(8) Node 11

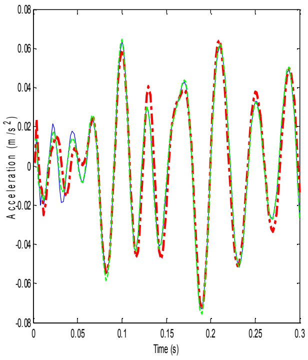

(9) Node 12

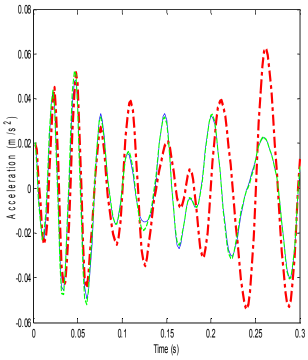

(10) Node 13

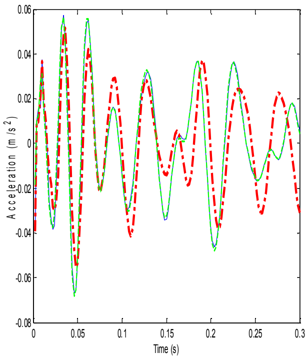

(11) Node 14

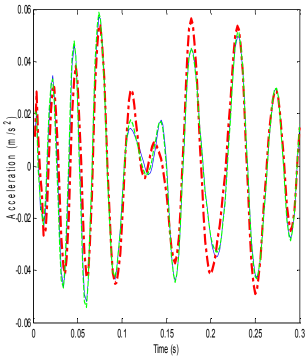

(12) Node 15

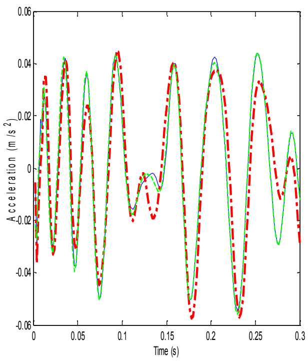

(13) Node 16

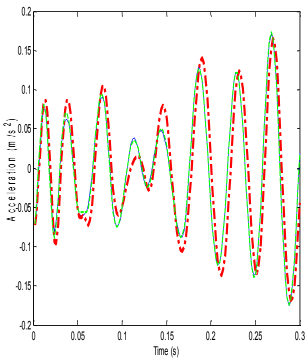

(14) Node 17

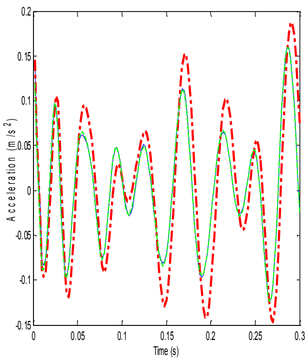

(15) Node 18

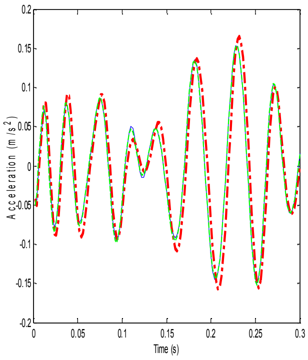

(16) Node 19

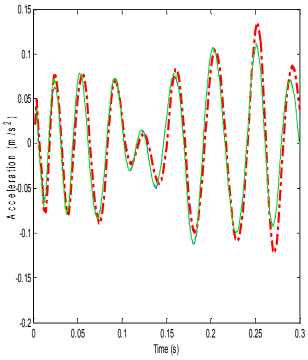

(17) Node 20

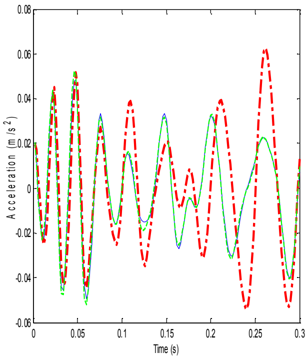

(18) Node 21

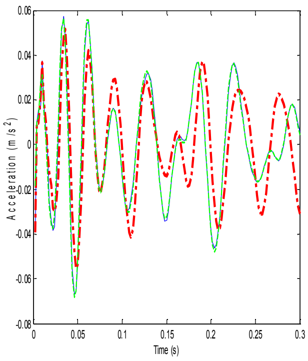

(19) Node 22

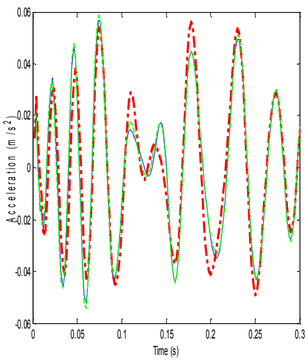

(20) Node 23

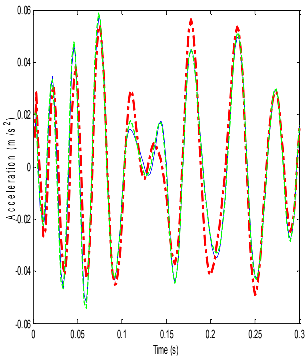

(21) Node 24

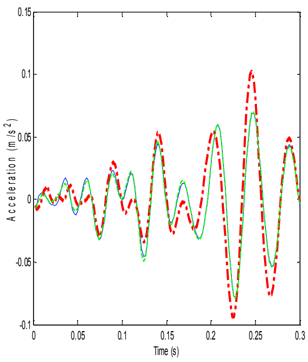

(22) Node 25

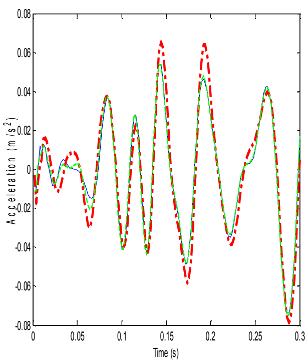

(23) Node 26

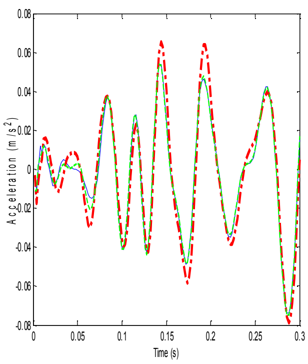

(24) Node 27

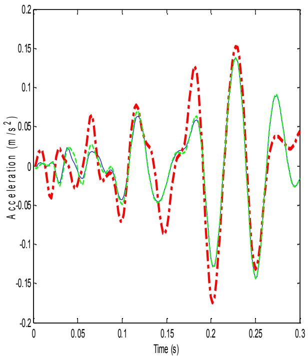

(25) Node 33

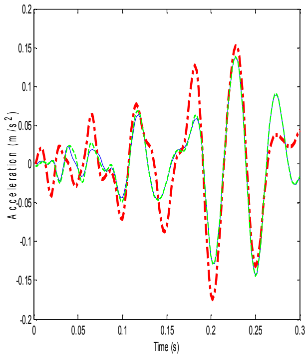

(26) Node 34

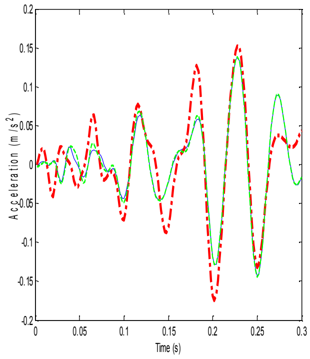

(27) Node 35

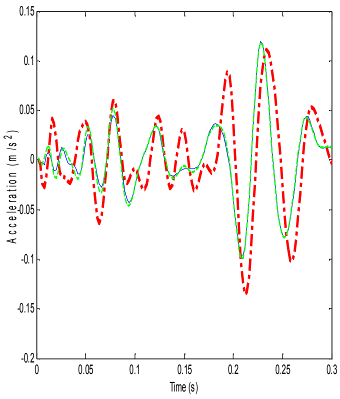

(27) Node 36

Figure 3.5 - Structural response of z-direction with 500 Hz sampling rate (______accurate, ... from ZOH, _._._ from FOH)

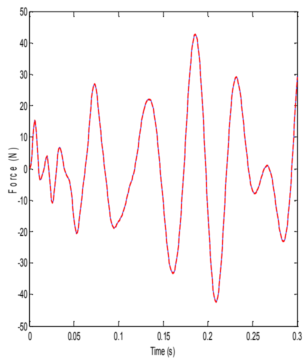

(1) Node 1 F_z

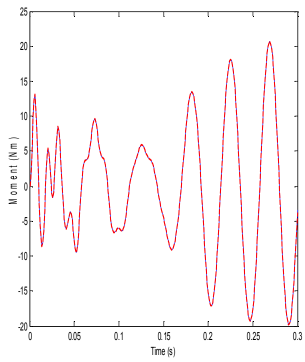

(2) Node 1 M_x

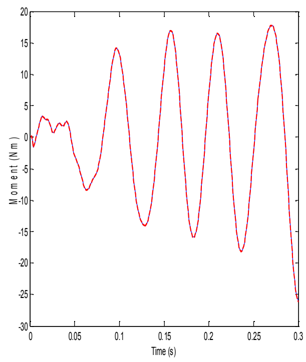

(3) Node 1 M_y

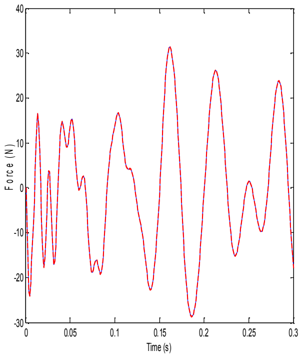

(4) Node 2 F_z

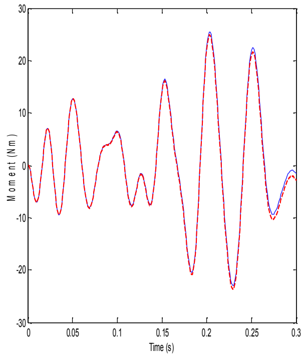

(5) Node 2 M_x

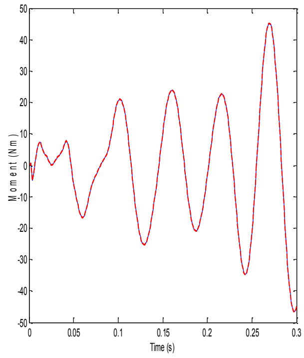

(6) Node 2 M_y

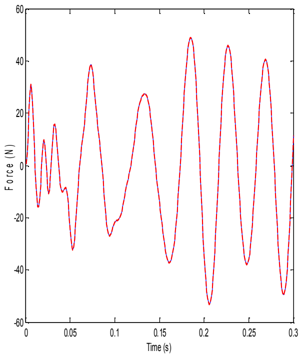

(4) Node 2 F_z

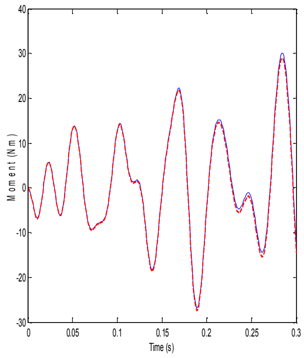

(5) Node 2 M_x

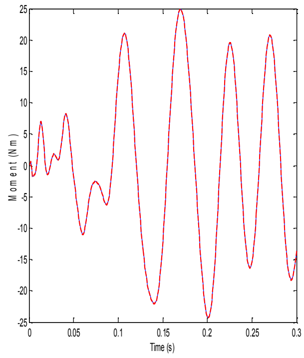

(6) Node 2 M_y

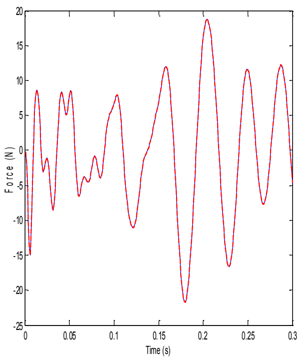

(10) Node 4 F_z

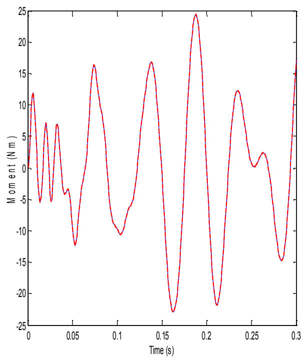

(11) Node 4 M_x

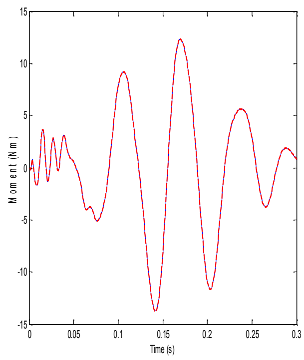

(12) Node 4 M_y

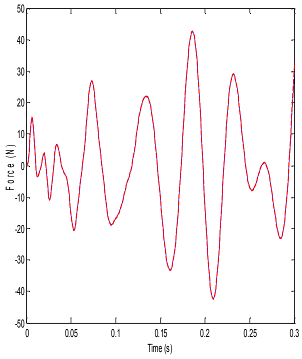

(13) Node 33 F_z

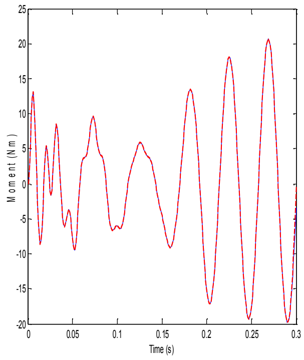

(14) Node 33 M_x

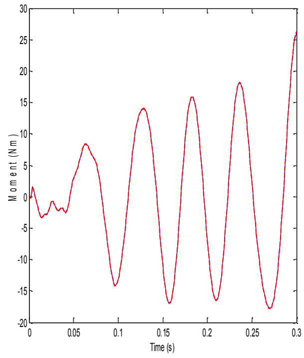

(15) Node 33 M_y

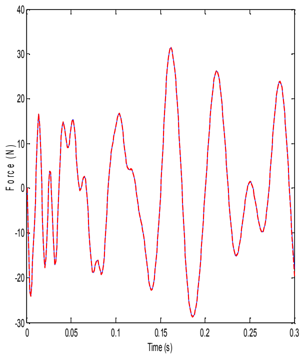

(16) Node 34 F_z

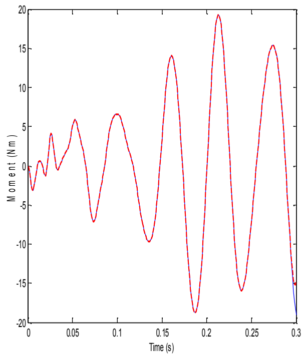

(17) Node 34 M_x

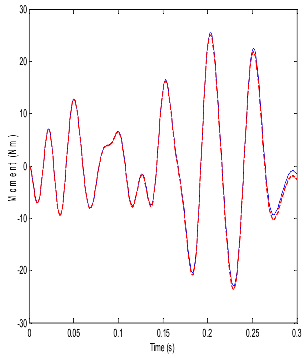

(18) Node 34 M_y

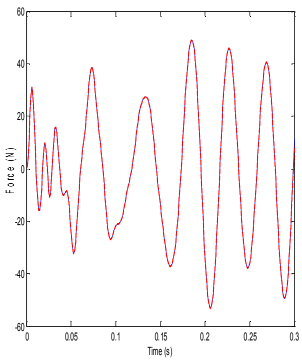

(19) Node 35 F_z

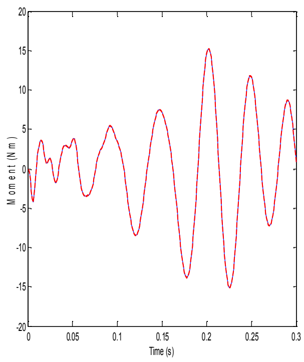

(20) Node 35 M_x

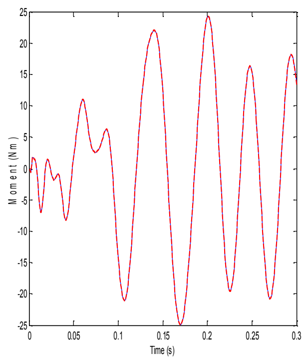

(21) Node 35 M_y

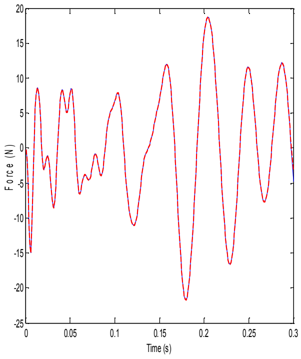

(22) Node 36 F_z

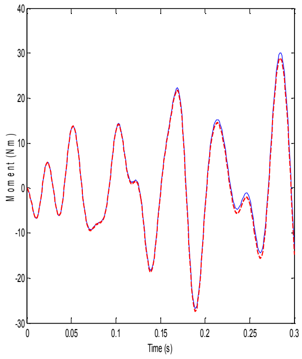

(23) Node 36 M_x

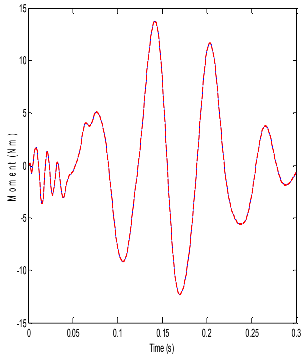

(24) Node 36 M_y

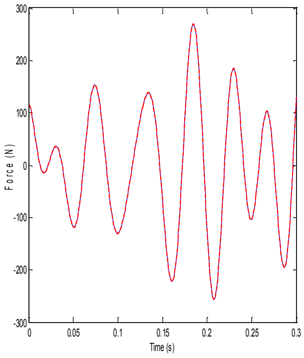

(25) Node 14 F

Figure 3.6 - Identified external forces based on the modified FOH discrete method without noise (____ real force; ---- identified force)

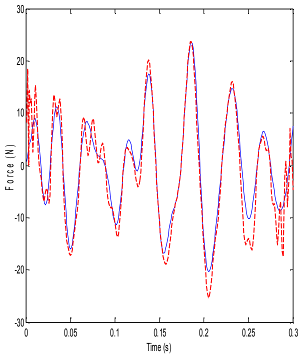

(1) Node 1 F_z

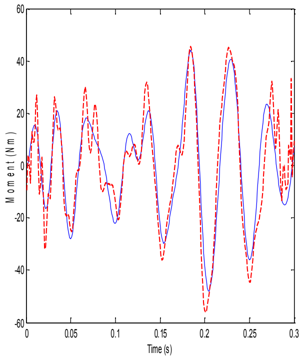

(2) Node 1 M_x

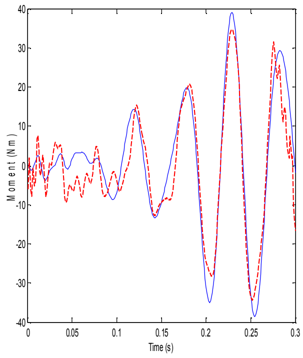

(3) Node 1 M_y

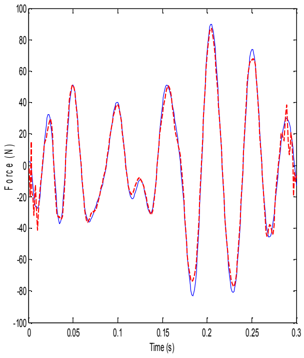

(4) Node 2 F_z

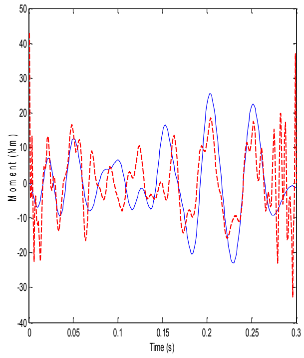

(5) Node 2 M_x

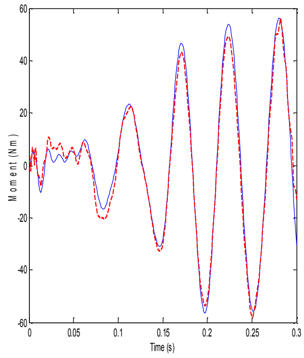

(6) Node 2 M_y

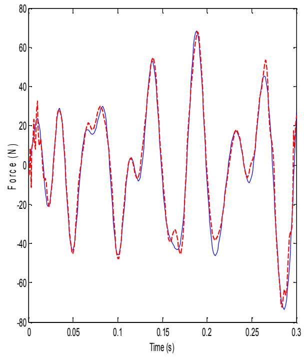

(7) Node 3 F_z

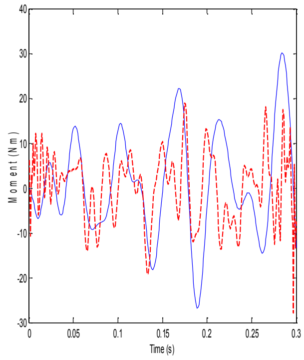

(8) Node 3 M_x

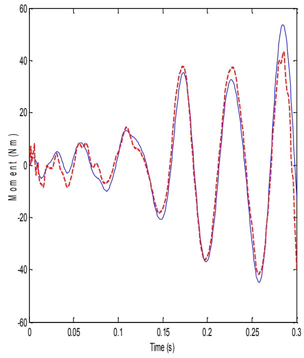

(9) Node 3 M_y

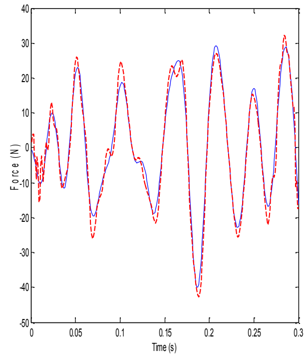

(10) Node 4 F_z

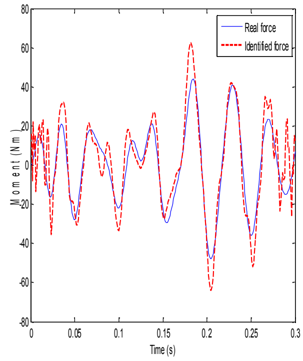

(11) Node 4 M_x

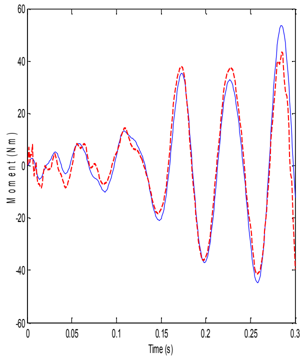

(12) Node 4 M_y

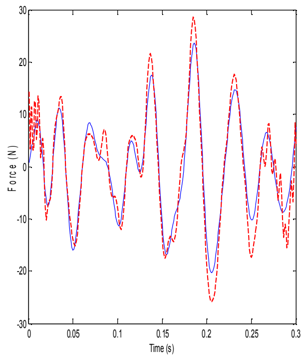

(13) Node 33 F_z

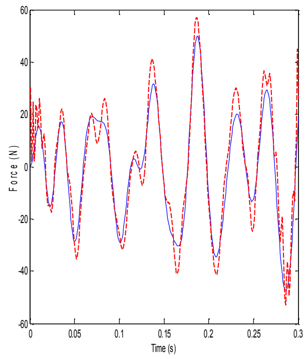

(14) Node 33 M_x

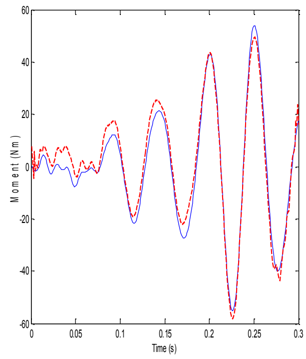

(15) Node 33 M_y

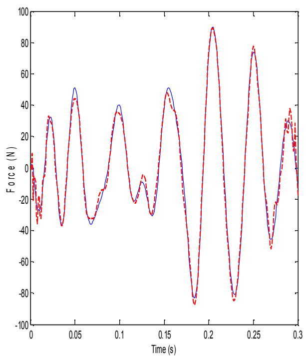

(16) Node 34 F_z

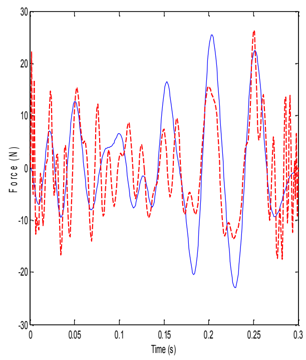

(17) Node 34 M_x

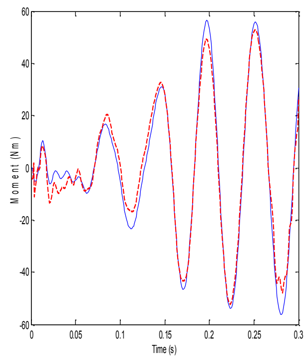

(18) Node 34 M_y

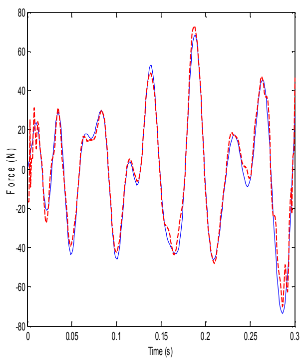

(19) Node 35 F_z

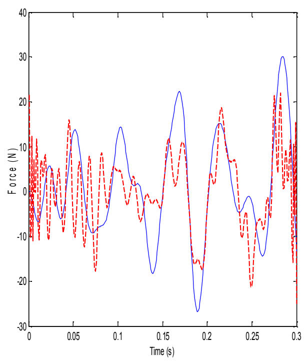

(20) Node 35 M_x

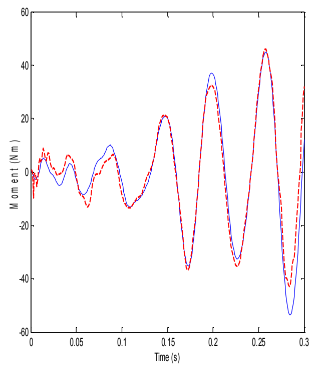

(21) Node 35 M_y

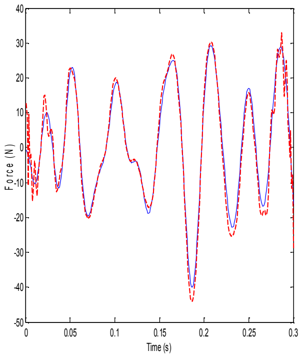

(22) Node 36 F_z

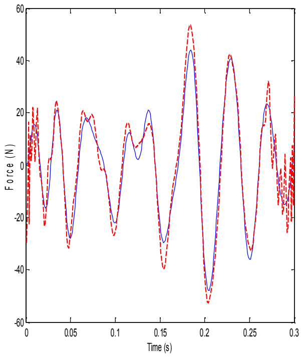

(23) Node 36 M_x

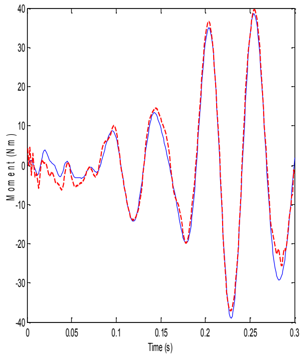

(24) Node 36 M_y

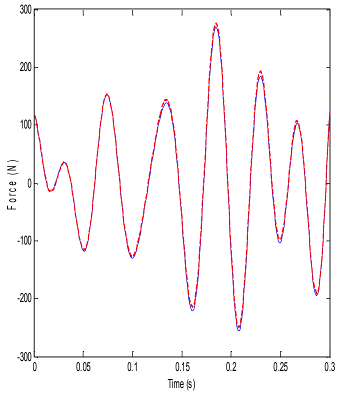

(25) Node 14 F

Figure 3.7 - Identified forces based on the modified FOH discrete method with 5% noise (____ real force, ---- identified force)

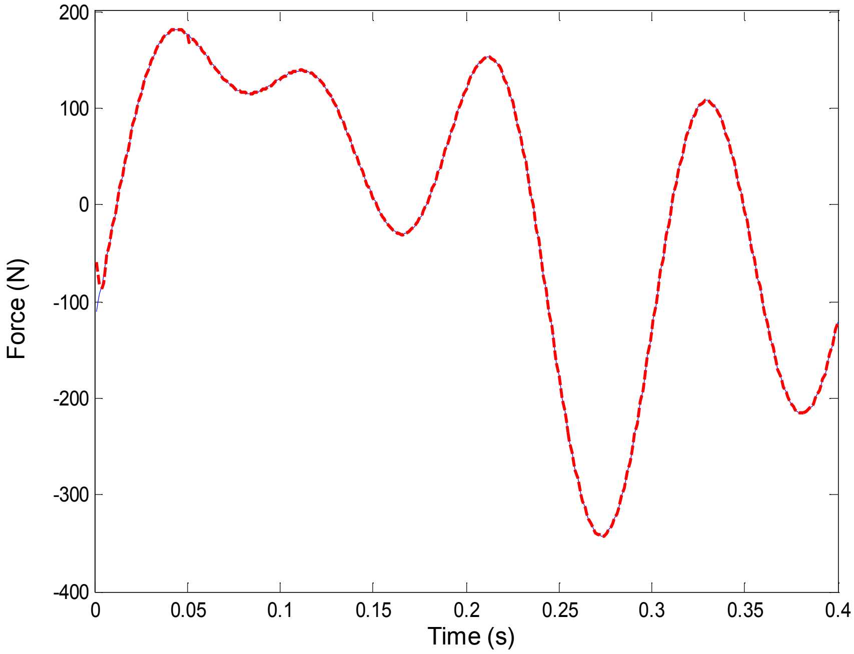

Figure 3.8 - Identified moving forces based on the modified FOH discrete method without noise without noise (____ real force, ---- identified force)

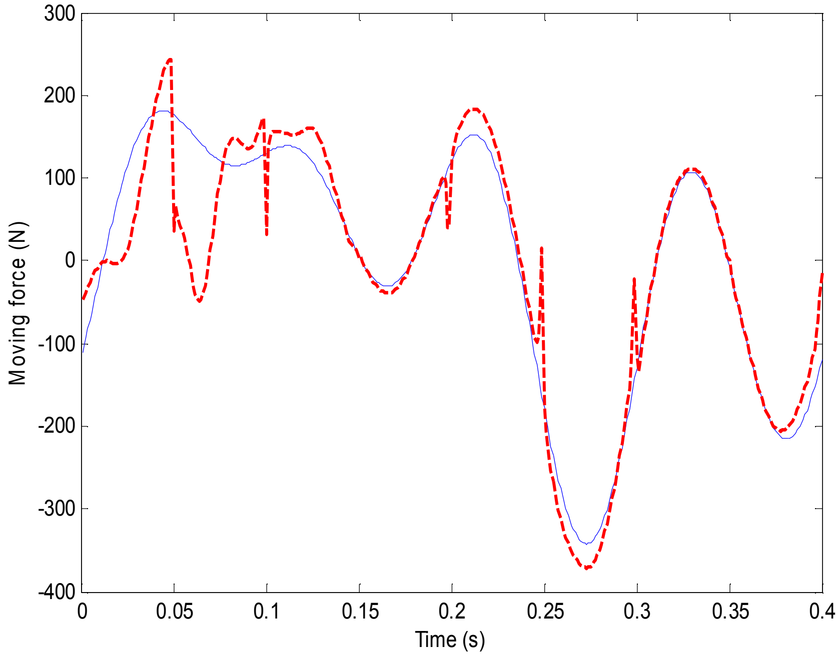

Figure 3.9 - Identified moving forces based on the modified FOH discrete method with 6% noise (____ real force, ---- identified force)

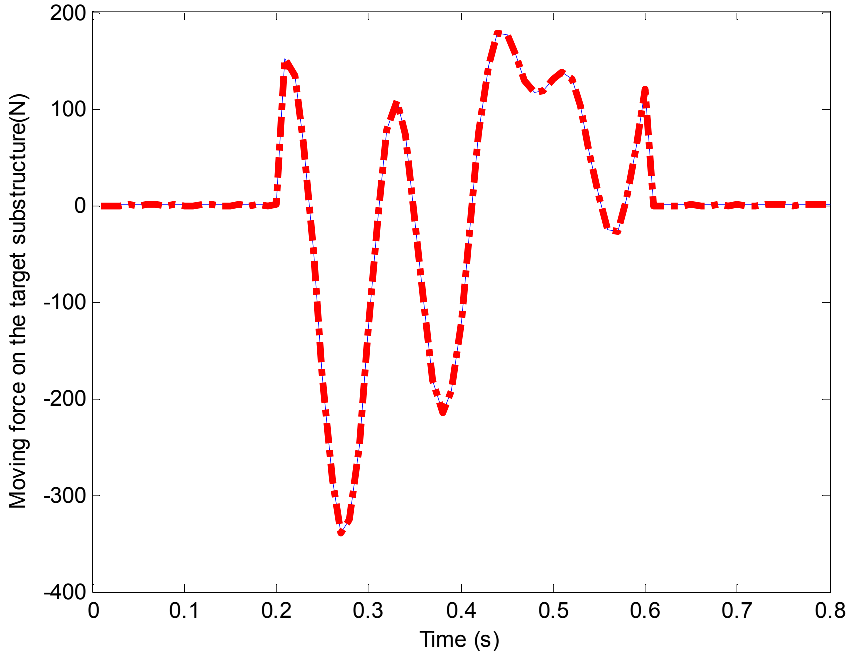

Figure 3.10 - Identified moving forces based on the modified FOH discrete method without noise (____ real force, ---- identified force)

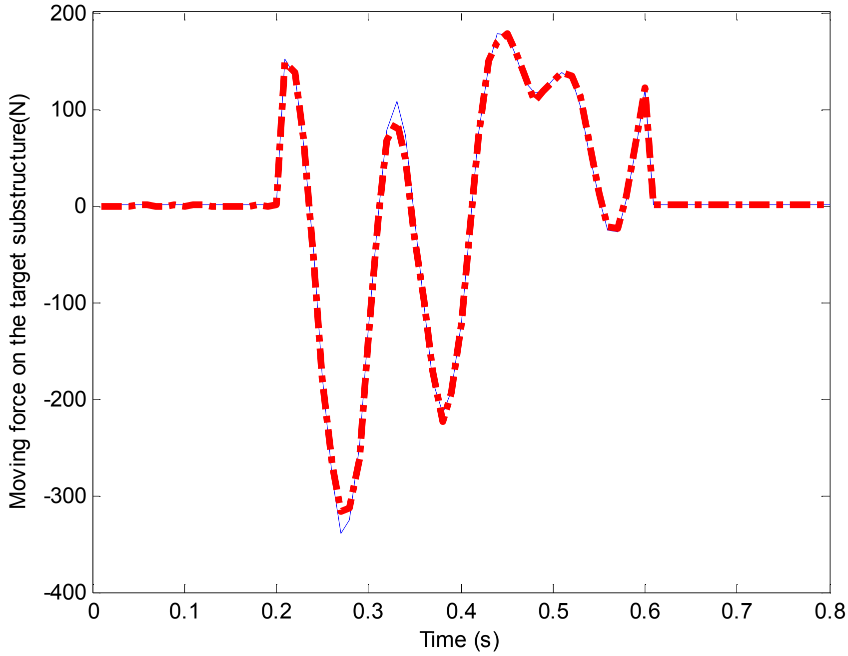

Figure 3.11 - Identified moving forces based on the modified FOH discrete method with 5% noise (___ real force, ---- identified force)

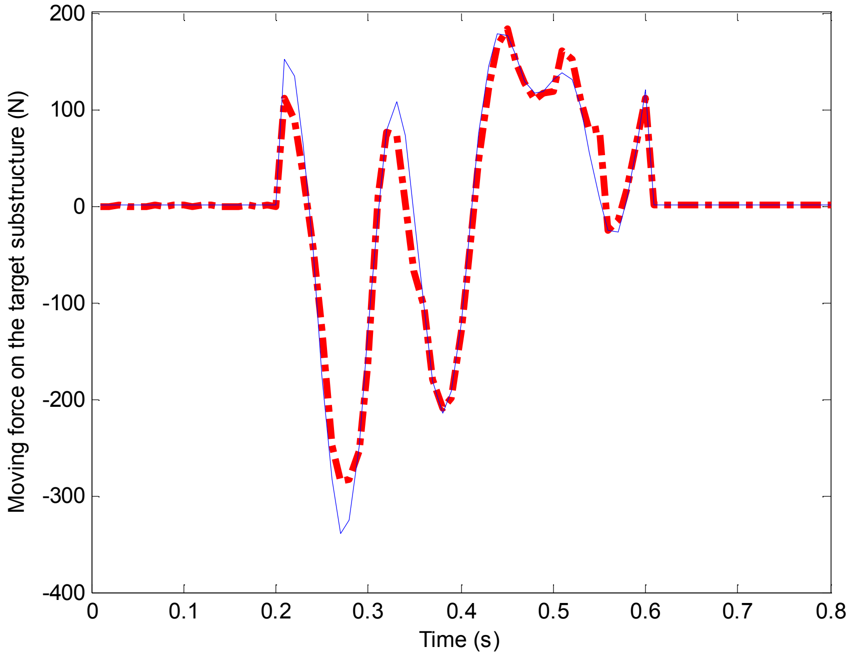

Figure 3.12 Identified moving forces based on the modified FOH discrete method with 14 sensors without noise (___ real force, ---- identified force)

CHAPTER 4

TWO-STAGE METHODS FOR DAMAGE DETECTION OF SUBSTRUCTURES

4.1 Introduction

Chapter 3 proposed a methodology for the substructural dynamic load assessment without the information on boundary conditions and without damage or model error on the target substructure. In this Chapter, a new two-stage structural condition assessment method will be proposed and implemented to conduct the structural condition assessment even when there is model error or local damage on the structure. A large scale structural system may have complex boundary conditions and uncertainties due to the discreteness of components in the finite element model and variability in the material properties. Models on the boundary conditions of a structure and any innovative device for seismic protection of a structure may be inaccurate, and it is difficult to conduct model updating for a large structure.

In the past few decades, many methods have been developed for structural model updating and damage detection. These methods can be broadly classified into three categories which are time domain method, frequency-domain method and time-frequency domain method as listed in Chapter 2. It is commonly known that measured responses from a structure could be used to assess the conditions of the structure with information on the location and features of local damages. However, when the structural system is very large and complex, it is impossible to gather sufficient responses for the assessment. The assessment of the structural system may also be difficult and inaccurate due to the large size of the analytical model in the computation with poor convergence and efficiency.

To improve the computational efficiency and convergence property, the substructure method introduced in Chapter 3 is an alternative tool to conduct the inverse analysis for large size structures. Increasing interest has been focused on this topic in the last two decades due to the leap of computation power with modern computer. The large and complex structural system can be divided into smaller substructures for separate assessment with a reduced number of unknown parameters. Substructural synthesis method has been applied to analyze complex structures since 1960s by Hurty. A substructural identification method has been proposed by Koh et al. (1991) with application of an extended Kalman method to solve the state and observation equation with and without overlapping members for the identification of structural parameters. An auto-regressive moving average method with stochastic input model has been presented by Yun and Lee (1997) for substructure measurements with noise.

Condensation method can also be applied to damage identification to reduce the computational time. The reduction of DOFs of a structure can be achieved by applying the Guyan static condensation method which, however, does not take the dynamic property of structure into account. The iterative Improved Reduced System (IRS) method (Friswell 1995) has also been applied in the numerical simulations, but the response of the condensed finite element model is not always matching closely to the response from the original finite element model. The dynamic responses of the condensed model of the structure cannot accurately represent those of the original structure. It is noted that the dynamic responses of the substructure could be accurately simulated if the interface conditions of the substructure could be accurately modeled.

Sensitivity method in time domain has been investigated and applied extensively for damage detection. The sensitivity matrix of response with respect to the structural parameters is derived to locate and quantify local damages with as few as a single sensor (Zhu and Law 2007; Lu and Law 2007a). Lu and Law identified the external excitations and the local damage of the structure simultaneously (Lu and Law 2007b). A general response sensitivity method is proposed addressing the deficiency of existing sensitivity method for damage detection/model updating of a substructure (Ding and Law 2010) with the analogous evolution of a pseudo substructure in the model updating process. This method takes into account the inaccurate modeling or lack of information on the nonlinear boundary conditions.

In Chapter 3, a force identification method was proposed to identify the external force and interface forces. This Chapter will develop a two-stage structural condition assessment method with substructure methods without measurement of the input. Both the excitation and structural parameter could be identified with this method. An introduction to the equations of motion for the structural system and each substructural system is given in Section 4.2. Existing response sensitivity method will be presented and a general response sensitivity method for substructural condition assessment is proposed in Section 4.3. In Section 4.4, two new computational techniques are proposed to improve the first stage of force identification which are: (a) a time window force identification method to improve the computation efficiency, and (b) a method of simultaneous identification of the interface force and the initial responses in a time segment, i.e. the acceleration, velocity and displacement, at all DOFs of the structural system. In Section 4.5, two procedures of implementation for substructure identification methods are proposed to handle two types of assessment problems. For the first problem (Scenario A), the finite element model (FEM) of the whole structure is required and for the second problem (Scenario B), only the FEM of the target substructure is available. Two types of numerical simulations are conducted in Section 4.6 including linear interface force and nonlinear interface force. A discussion and conclusion are given in Section 4.7.

4.2 Structural and Substructural Dynamic Responses

The structural system is assumed to be linear as shown in Figure (4.1). The equation of motion of the structural system can be partitioned as

$$\begin{bmatrix} \mathbf{M}_{ss} & \mathbf{M}_{sr} \\ \mathbf{M}_{rs} & \mathbf{M}_{rr} \end{bmatrix} \begin{bmatrix} \ddot{\mathbf{x}}_s \\ \ddot{\mathbf{x}}_r \end{bmatrix} + \begin{bmatrix} \mathbf{C}_{ss} & \mathbf{C}_{sr} \\ \mathbf{C}_{rs} & \mathbf{C}_{rr} \end{bmatrix} \begin{bmatrix} \dot{\mathbf{x}}_s \\ \dot{\mathbf{x}}_r \end{bmatrix} + \begin{bmatrix} \mathbf{K}_{ss} & \mathbf{K}_{sr} \\ \mathbf{K}_{rs} & \mathbf{K}_{rr} \end{bmatrix} \begin{bmatrix} \mathbf{x}_s \\ \mathbf{x}_r \end{bmatrix} = \begin{bmatrix} -(\mathbf{MG})_s \\ -(\mathbf{MG})_r \end{bmatrix} \ddot{x}_g + \begin{bmatrix} \mathbf{L}_s \mathbf{F}_s \\ \mathbf{L}_r \mathbf{F}_r \end{bmatrix} \tag{4.1}$$

where the subscript s denotes Substructure 1 above the support and soil mass, and subscript r denotes Substructure 2 which is the rest of the structural system. Subscripts sr and rs denote the interface dofs of the structure. In the following study, Substructure 1 is selected to be the target substructure for model updating. It is noted that Substructure 2 consisting of the ground support and soil mass may behave nonlinearly. Moreover, the finite element model of Substructure 2 may not be accurately known in practice. The equation of motion of Substructure 1 includes the interaction with Substructure 2 as

$$\mathbf{M}_{ss}\ddot{\mathbf{x}}_s + \mathbf{C}_{ss}\dot{\mathbf{x}}_s + \mathbf{K}_{ss}\mathbf{x}_s = -(\mathbf{MG})_s \ddot{x}_g + \mathbf{L}_s\mathbf{F}_s - (\mathbf{M}_{sr}\ddot{\mathbf{x}}_r + \mathbf{C}_{sr}\dot{\mathbf{x}}_r + \mathbf{K}_{sr}\mathbf{x}_r) \tag{4.2}$$

where the term $-(\mathbf{M}_{sr}\ddot{\mathbf{x}}_r + \mathbf{C}_{sr}\dot{\mathbf{x}}_r + \mathbf{K}_{sr}\mathbf{x}_r)$ represents the set of interface forces between the two substructures. Usually the interface forces cannot be accurately represented by $-(\mathbf{M}_{sr}\ddot{\mathbf{x}}_r + \mathbf{C}_{sr}\dot{\mathbf{x}}_r + \mathbf{K}_{sr}\mathbf{x}_r)$ as an accurate finite element model of the interface is always difficult to achieve or the interface forces may be a nonlinear function of the responses. Equation (4) can in general be written as

$$\mathbf{M}_{ss}\ddot{\mathbf{x}}_s + \mathbf{C}_{ss}\dot{\mathbf{x}}_s + \mathbf{K}_{ss}\mathbf{x}_s = -(\mathbf{MG})_s \ddot{x}_g + \mathbf{L}_s\mathbf{F}_s + \mathbf{F}_{in} \tag{4.3}$$

where $\mathbf{F}_{in}$ denotes the interface forces.

4.3 Sensitivity Methods

4.3.1 Existing Response Sensitivity Method

Existing time domain response sensitivity method always assumes a set of well-known boundary conditions or with boundaries of the structure modeled with an extremely large stiffness (Zhang et al. 2010; Li et al. 2011). For the frame structure shown in Figure 4.1, only Substructure 1 is considered since the responses of Substructure 2 at the interface, i.e. $\ddot{\mathbf{x}}_r$, $\dot{\mathbf{x}}_r$ and $\mathbf{x}_r$, are assumed to be zero or close to zero. The term $\mathbf{F}_{in}$ in Equation (4.3) is ignored and the equation of motion of the substructure becomes

$$\mathbf{M}_{ss}\ddot{\mathbf{x}}_s + \mathbf{C}_{ss}\dot{\mathbf{x}}_s + \mathbf{K}_{ss}\mathbf{x}_s = -(\mathbf{MG})_s \ddot{x}_g + \mathbf{L}_s\mathbf{F}_s \tag{4.4}$$

Assuming the damage extent of the ith element in the superstructure is represented by a reduction factor, α_i, a change of the global stiffness matrix of Substructure 1 can be described as

$$\Delta\mathbf{K} = \sum_{i=1}^{Ne} \alpha_i \mathbf{K}_i \tag{4.5}$$

where Ne denotes the number of finite elements of the superstructure.

Performing differentiation to both sides of Equation (4.5) with respect to the structural parameters α_i, existing sensitivity method would give directly

$$\mathbf{M}_{ss}\frac{\partial\ddot{\mathbf{x}}_s}{\partial\alpha_i} + \mathbf{C}_{ss}\frac{\partial\dot{\mathbf{x}}_s}{\partial\alpha_i} + \mathbf{K}_{ss}\frac{\partial\mathbf{x}_s}{\partial\alpha_i} = -\frac{\partial\mathbf{K}_{ss}}{\partial\alpha_i}\mathbf{x}_s - a_2\frac{\partial\mathbf{K}_{ss}}{\partial\alpha_i}\dot{\mathbf{x}}_s \tag{4.6}$$

The system is assumed to be at rest initially. The responses $\ddot{\mathbf{x}}$, $\dot{\mathbf{x}}$ and $\mathbf{x}$ are obtained by the step-by-step time integration method from Equation (4.4). The convergence property is presented in Appendix B for the integrity of thesis. They are then substituted into Equation (4.6). The sensitivity matrices $\partial\ddot{\mathbf{x}}_s/\partial\alpha_i, \partial\dot{\mathbf{x}}_s/\partial\alpha_i, \partial\mathbf{x}_s/\partial\alpha_i$ can then be solved similarly by the step-by-step time integration Newmark-β method from Equation (4.6). The local anomalies of the structure can then be found with the sensitivity method with different optimization tools.

4.3.2 The General Response Sensitivity Method

In practice, rigid boundary conditions of a substructure are rare and the nonlinear boundary conditions are difficult to model correctly. The inclusion of the actual boundary conditions in the model updating may produce significant effect on the updating results. Figure 4.2 shows a structural system with base isolation which may behave nonlinearly under lateral load. When the interaction between the support and superstructure is taken into consideration, existing sensitivity method described in Section 4.2 is not applicable for the model updating as shown below.

The interface force $\mathbf{F}_{in}$ in Equation (4.3) is known to be a function of the structural parameters α_i when the interaction between two substructures is included. Applying differentiation with respect to the structural parameter α_i to both sides of Equation (4.3), we get

$$\mathbf{M}_{ss}\frac{\partial \ddot{\mathbf{x}}_s}{\partial \alpha_i} + \mathbf{C}_{ss}\frac{\partial \dot{\mathbf{x}}_s}{\partial \alpha_i} + \mathbf{K}_{ss}\frac{\partial \mathbf{x}_s}{\partial \alpha_i} = -\frac{\partial \mathbf{K}_{ss}}{\partial \alpha_i}\mathbf{x}_s - a_2\frac{\partial \mathbf{K}_{ss}}{\partial \alpha_i}\dot{\mathbf{x}}_s + \frac{\partial \mathbf{F}_{in}}{\partial \alpha_i} \tag{4.7}$$

Equation (4.7) is different from Equation (4.6) with an extra term $\partial \mathbf{F}_{in} / \partial \alpha_i$ on the right-hand-side. The sensitivities matrices $\partial \ddot{\mathbf{x}}_s / \partial \alpha_i$, $\partial \dot{\mathbf{x}}_s / \partial \alpha_i , \partial \mathbf{x}_s / \partial \alpha_i$ are coupled with $\partial \mathbf{F}_{in} / \partial \alpha_i$ and all of them are derivatives with respect to α_i. They cannot be obtained by the Newmark-β method. It can, however, be solved with the general sensitivity method described below.

The general sensitivity method is based on the evolution of a pseudo structural system in the iterative model updating process. The pseudo structural system illustrated in Figure 4.3 consists of Substructure 1 in the initial intact state with the interface forces when the whole structure is under the effect of earthquake excitation. The pseudo system is subject to the interface forces and the external excitation forces, $\boldsymbol{F}_{pseudo}$, *which are identical to those acting on the real Substructure 1 with local anomalies* during the data collection for model updating. The response of the pseudo structure in the kth updating iteration, $\mathbf{z}_k$, can be represented as

$$\begin{aligned} &\mathbf{z}_k = f(\mathbf{F}_{pseudo}, \boldsymbol{\alpha}_k) \quad (k = 1, 2, 3\cdots) \\ &\boldsymbol{\alpha}_1 = \mathbf{0} \end{aligned} \tag{4.8}$$

Since $\mathbf{F}_{pseudo}$ remains the same in subsequent iterations of model updating, Equation (4.8) is then rewritten as a function of damaged target Substructure 1. The response of the pseudo structure in the updating can therefore be represented as

$$\begin{aligned} &\mathbf{z}_k = f(\boldsymbol{\alpha}_k) \quad (k = 1, 2, 3\cdots) \\ &\boldsymbol{\alpha}_1 = \mathbf{0} \end{aligned} \tag{4.9}$$

The equation of motion of the pseudo structural system can therefore be represented similar to Equation (4.3) as

$$\mathbf{M}_{ss}\ddot{\mathbf{x}}_s + \mathbf{C}_{ss}\dot{\mathbf{x}}_s + \mathbf{K}_{ss}\mathbf{x}_s = -(\mathbf{MG})_s\ddot{x}_g + \mathbf{L}_s\mathbf{F}_s + (\mathbf{F}_{in})_{damage} \tag{4.10}$$

where subscript *damage* denotes the interface forces corresponding to the damage state of the substructure, and $(\mathbf{F}_{in})_{damage}$ is not a function of the stiffness reduction factor α_i. Hence, the equation of derivatives in Equation (4.7) becomes Equation

(4.6) which can be solved to find the corresponding response sensitivity matrices. The model updating of the real structure is analogous to the model updating of the pseudo structure.

In the following studies, the "measured" response, $\ddot{\mathbf{x}}_m$, is obtained as the analytical solution of the equation of motion in Equation (4.10) from the finite element model including local anomalies. If acceleration is taken as the "measured" information, the Taylor series expansion on the difference between the "measured" response and the calculated response, $\ddot{\mathbf{x}}$, from Equation (4.10) can be written as

$$\ddot{\mathbf{x}}_m - \ddot{\mathbf{x}} = \frac{\partial \ddot{\mathbf{x}}}{\partial \boldsymbol{\alpha}} \cdot \boldsymbol{\alpha} + o(\boldsymbol{\alpha}^2) \tag{4.11}$$

where $o(\boldsymbol{\alpha}^2)$ is the residual term of the series expansion. The unknown stiffness reduction vector $\boldsymbol{\alpha}$ can be calculated from Equation (4.11) with an optimization method. It should be noted that the identification equation has no requirement of zero initial values for the solution as discussed in Section 4.4.2 below.

4.4 The Computation Algorithm

The present study takes both the interface forces and the local damages of the structure as unknowns, and they will be identified in an iterative optimization. A two-stage method with two new computational techniques is described below for the iterative substructural model updating.

4.4.1 Identification of the Interface Force in the First Stage

The equation of motion of the structure in Equation (3.10) can be expressed in the state space considering the external force and excitation as

$$\dot{\mathbf{z}} = \mathbf{A}^C z + \mathbf{B}^C(-\mathbf{MG}\ddot{\mathbf{x}}_g + \mathbf{L}\cdot\mathbf{F}) \tag{4.12}$$

Vector of output of the structural system can be expressed as a combination of acceleration, velocity and displacement measurements as

$$\mathbf{y} = \mathbf{R}_a\ddot{\mathbf{x}} + \mathbf{R}_v\dot{\mathbf{x}} + \mathbf{R}_d\mathbf{x} \tag{4.13}$$

with $\mathbf{R}_a$, $\mathbf{R}_v$ and $\mathbf{R}_d \in \mathbf{R}^{m\times Ndof}$ which are the output influence matrices for the measured acceleration, velocity and displacement respectively, *m* is the dimension of the measured responses and *Ndof* is the number of DOFs of the structure. Equation (4.13) can be rewritten as

$$\mathbf{y} = \mathbf{Rz} + \mathbf{D}\cdot(-\mathbf{M}\ddot{x}_g + \mathbf{L}\cdot\mathbf{F}) \tag{4.14}$$

where $\mathbf{R} = [\mathbf{R}_d - \mathbf{R}_a\mathbf{M}^{-1}\mathbf{K} \quad \mathbf{R}_v - \mathbf{R}_a\mathbf{M}^{-1}\mathbf{C}]$ and $\mathbf{D} = \mathbf{R}_a\mathbf{M}^{-1}$.

Equations (4.12) and (4.14) can be converted into the following discrete equations as

$$\mathbf{z}(j+1) = \mathbf{A}^D\mathbf{z}(j) + \mathbf{B}^D\cdot(-\mathbf{MG}\ddot{\mathbf{x}}_g + \mathbf{L}\cdot\mathbf{F}(j)) \tag{4.15}$$

$$\mathbf{y}(j) = \mathbf{Rz}(j) + \mathbf{D}\cdot(-\mathbf{M}\ddot{\mathbf{x}}_g + \mathbf{L}\cdot\mathbf{F}(j)) \quad (j = 1,2,\cdots,N) \tag{4.16}$$

Superscript *D* denotes that the matrices are for the discrete structural system. *N* is the total number of sampling points, *dt* is the time step between the state variables $\mathbf{z}(j)$ and $\mathbf{z}(j+1)$, and $\mathbf{A}^D = \exp(\mathbf{A}^C\cdot dt)$, $\mathbf{B}^D = (\mathbf{A}^C)^{-1}(\mathbf{A}^D - \mathbf{I})\mathbf{B}^C$ which are the same as illustrated in Chapter 3.

The output $\mathbf{y}(j)$ can be expressed in terms of the previous input $\mathbf{F}(k), (k = 0, 1, \cdots, j)$ and $\ddot{\mathbf{x}}_g$ from Equations (4.15) and (4.16) with zero initial responses as follows

$$\mathbf{y}(j) = \sum_{k=0}^{j} \mathbf{H}_k \cdot (-\mathbf{MG}\ddot{\mathbf{x}}_g(j-k) + \mathbf{L} \cdot \mathbf{F}(j-k)) \tag{4.17}$$

where $\mathbf{H}_0 = \mathbf{D}$ and $\mathbf{H}_k = \mathbf{RA}_{k-1}^{D}\mathbf{B}$. The constants in matrix $\mathbf{H}_k$ in Equation (4.17) are the system Markov parameters. Equation (4.17) can be rewritten as

$$\mathbf{Y} - \mathbf{H}_G \ddot{\mathbf{x}}_g = \mathbf{H}_L \mathbf{F} \tag{4.18}$$

where $\mathbf{H}_L = \begin{bmatrix} \mathbf{H}_0 & 0 & \cdots & 0 \\ \mathbf{H}_1 & \mathbf{H}_0 & \cdots & 0 \\ \vdots & \vdots & \ddots & 0 \\ \mathbf{H}_{N-1} & \mathbf{H}_{N-2} & \cdots & \mathbf{H}_0 \end{bmatrix} \mathbf{L}_S, \quad \mathbf{L}_S = \begin{bmatrix} \mathbf{L} & 0 & \cdots & 0 \\ 0 & \mathbf{L} & \cdots & 0 \\ \vdots & \vdots & \ddots & 0 \\ 0 & 0 & \cdots & \mathbf{L} \end{bmatrix}$,

$\mathbf{H}_G = \begin{bmatrix} \mathbf{H}_0 & 0 & \cdots & 0 \\ \mathbf{H}_1 & \mathbf{H}_0 & \cdots & 0 \\ \vdots & \vdots & \ddots & 0 \\ \mathbf{H}_{N-1} & \mathbf{H}_{N-2} & \cdots & \mathbf{H}_0 \end{bmatrix} \mathbf{G}_S, \quad \mathbf{G}_S = \begin{bmatrix} -\mathbf{MG} & 0 & \cdots & 0 \\ 0 & -\mathbf{MG} & \cdots & 0 \\ \vdots & \vdots & \ddots & 0 \\ 0 & 0 & \cdots & -\mathbf{MG} \end{bmatrix}$,

$\mathbf{Y} = \left\{ \mathbf{y}(0)^T \quad \mathbf{y}(1)^T \quad \cdots \quad \mathbf{y}(N-1)^T \right\}^T$, $\mathbf{F} = \left\{ \mathbf{F}(0)^T \quad \mathbf{F}(1)^T \quad \cdots \quad \mathbf{F}(N-1)^T \right\}^T$.

Matrix $\mathbf{H}_L$ is constant for a system, and the response vector $\mathbf{Y}$ can be formulated from the measured responses. The identification equation for the vector of forces can be written in least-squares sense as

$$\mathbf{F} = (\mathbf{H}_L{}^T \mathbf{H}_L)^{-1} \mathbf{H}_L{}^T (\mathbf{Y} - \mathbf{H}_G \ddot{\mathbf{x}}_g) \tag{4.19}$$

Regularization method would provide an improved solution to the ill-posed problem in Equation (4.19), and the damped least-squares method (Tikhonov 1963; Law, Bu and Zhu 2005; Hansen 1992) is adopted to give bounds to the problem. Equation (4.20) shows the application of the regularization method in force identification as

$$\begin{aligned}\mathbf{H}_L{}^T(\mathbf{Y}-\mathbf{H}_G\ddot{\mathbf{x}}_g) &= (\mathbf{H}_L{}^T\mathbf{H}_L+\lambda\mathbf{I})\mathbf{F} \\ \mathbf{F} &= (\mathbf{H}_L{}^T\mathbf{H}_L+\lambda\mathbf{I})^{-1}\mathbf{H}_L{}^T(\mathbf{Y}-\mathbf{H}_G\ddot{\mathbf{x}}_g)\end{aligned} \tag{4.20}$$

where λ is the non-negative damping coefficient governing the participation of the least-squares error in the solution. This force identification procedure is the same as presented in Section 3.4.

4.4.2 New Strategies for the First Stage Identification

4.4.2.1 Time Window Force Identification

The size of matrix $\mathbf{H}_L$ is proportional to the number of sampling points in the measured data and the number of unknowns in the time history of forces. Calculation with a large matrix $\mathbf{H}_L$ is time consuming and can cause computation error. In this study, the measured data is divided into several time segments and the time history of the unknown interface forces will be identified in each time segment. The initial response values in each segment are calculated from the identified forces of the previous segment. With the proposed method, the interface forces in all time segments are identified separately in the first stage, while in the second stage the local anomalies are identified with the complete measured response time history.

4.4.2.2 Identification of Non-zero Initial Responses

When the initial response of the structure is not zero, the time history of responses of a structure is a function of the initial state, external forces and structural parameters. The response vector can therefore be represented as

$$\mathbf{Y} = \boldsymbol{f}(\mathbf{Y}_0, \mathbf{F}, \boldsymbol{\alpha}) \tag{4.21}$$

where $\mathbf{Y}_0$ is the initial responses of the structural system. When the structural system is linear, the responses of the structure can be considered as the summation of free vibration due to the non-zero initial responses and the forced vibration due to external excitations. Equation (4.21) can be rewritten as

$$\mathbf{Y} = \mathbf{Y}_{fr} + \mathbf{Y}_{fo} = \boldsymbol{g}(\mathbf{Y}_0, \boldsymbol{\alpha}) + \boldsymbol{h}(\mathbf{F}, \boldsymbol{\alpha}) \tag{4.22}$$

where $\mathbf{Y}_{fr} = g(\mathbf{Y_0}, \boldsymbol{\alpha})$and $\mathbf{Y}_{fo} = h(\mathbf{F}, \boldsymbol{\alpha})$ are respectively the responses of free vibration and forced vibration.

Considering the free vibration only, the initial response of the structure could be represented as the summation of all mode shapes of the structure as

$$\mathbf{Y}_0 = \begin{bmatrix} \boldsymbol{\Phi} & \mathbf{0} \\ \mathbf{0} & \boldsymbol{\Phi} \end{bmatrix} \boldsymbol{\beta} \tag{4.23}$$

where $\boldsymbol{\Phi}$ is the normalized mode shape matrix of the structure and $\boldsymbol{\beta}$ is a $(2\times Ndof)\times 1$ unknown vector of contribution coefficients of the vibration modes. Initial response vector $\mathbf{Y}_0$ has dimensions $(2\times Ndof)\times 1$ consisting of the displacements and velocities. It is noted that the acceleration can be computed based on the equation of motion. The total response due to free vibration and forced vibration of the structure could be represented as

$$\mathbf{Y} = \mathbf{Y}_{ini}\boldsymbol{\beta} + \mathbf{H}_L\mathbf{F} \tag{4.24}$$

where $\mathbf{Y}_{ini}$ is the free vibration response vector of the structure arising from the vector of initial response at all DOFs of the structure. Equation (4.24) can be written as:

$$\mathbf{Y} = \begin{bmatrix} \mathbf{Y}_{ini} & \mathbf{H}_L \end{bmatrix} \begin{bmatrix} \boldsymbol{\beta} \\ \mathbf{F} \end{bmatrix} \tag{4.25}$$

It is noted that the last vector in Equation (4.25) consists of the unknown force coefficients and the contributing coefficient vector $\boldsymbol{\beta}$ on the initial response of the system, and it can be obtained with any optimization method.

4.4.2.3 Model Updating with Adaptive Regularization Method

Iterative regularization methods are usually adopted in practical inverse problems, such as load identification, model updating and damage detection. The objective function in the problem of model updating in Equation (4.11) with Tikhonov regularization method is defined as

$$J(\Delta\boldsymbol{\alpha}^{k+1}, \lambda) = \left\| \mathbf{S}^k \Delta\boldsymbol{\alpha}^{k+1} - \Delta\ddot{\mathbf{x}}^k \right\|^2 + \lambda^2 \left\| \Delta\alpha^{k+1} \right\|^2 \tag{4.26}$$

where $\mathbf{S}$ is the sensitivity matrix calculated from Equation (4.6) and k denotes the kth iteration of the identification.

Inverse problem is always ill-posed and measurement noise may have adverse effect in the process of identification. The iterative identification methods should be able to ensure the significance of the structural parameters and mitigate the unfavorable effect of noise in the identification. An adaptive regularization method with an adaptive upper limit on the identified damage based on results from last iteration step is adopted. The objective function of the optimization is expressed as

$$J(\Delta\boldsymbol{\alpha}^{k+1}, \lambda_\alpha) = \left\| \mathbf{S}^k \Delta\boldsymbol{\alpha}^{k+1} - \Delta\ddot{\mathbf{x}}^k \right\| + \lambda_\alpha^{\ 2} \left\| \sum_{i=1}^{k+1} \Delta\boldsymbol{\alpha}^i - \boldsymbol{\alpha}^{k,*} \right\| \tag{4.27}$$

where $\boldsymbol{\alpha}^{k,*}$ is a value to coordinate the constraint of the solution in the i th iteration in the model updating process. Parameter $\boldsymbol{\alpha}^{k,*}$ can be defined as

$$(\alpha^{k,*})_j = \begin{cases} 0 & \text{if } (\sum_{i=1}^{k} \Delta\alpha^k)_j > 0 \\ (\sum_{i=1}^{k} \Delta\alpha^k)_j & \text{if } (\sum_{i=1}^{k} \Delta\alpha^k)_j < 0 \end{cases} \tag{4.28}$$

where the subscript j denotes the j th element of the target structure. $(\sum_{i=1}^{k} \Delta\alpha^k)_j$ is the cumulative identified change of stiffness. The local anomaly can then be calculated iteratively with the identified optimal parameter λ as

$$\begin{aligned} \Delta\boldsymbol{\alpha}^{k+1} &= ((\frac{\partial \ddot{\mathbf{x}}}{\partial \boldsymbol{\alpha}^k})^T \frac{\partial \ddot{\mathbf{x}}}{\partial \boldsymbol{\alpha}^k} + \lambda^2 \mathbf{I}_\alpha)^{-1} (\frac{\partial \ddot{\mathbf{x}}}{\partial \boldsymbol{\alpha}^k})^T (\ddot{\mathbf{x}}_m^k - \ddot{\mathbf{x}}^k) \\ \boldsymbol{\alpha}_{k+1} &= \boldsymbol{\alpha}_k + \Delta\boldsymbol{\alpha}^k \end{aligned} \tag{4.29}$$

At the end of the model updating, the pseudo structure should have been updated such that the interface forces and the FEM are identically to those of the damage state of the structure.

4.5 Implementation Procedure

4.5.1 For Scenario A when the FEM of the Whole Structure is Known

When the FEM of the whole structure is known, the implementation procedure of the two-stage identification is described as follows

Step 1: Conduct dynamic measurement on the structure.

Step 2: The matrix of system Markov parameters, $\mathbf{H}_L$ in Equation (4.18), is obtained from finite element model of the structural system.

Step 3: The external forces are obtained from the damped least-squares method in

Equation (4.20).

Step 4: Divide the structure into substructures and obtain the mass, damping and stiffness matrices of the target substructure.

Step 5: Compute the interface forces from the intact finite element model under the action of the identified external forces.

Step 6: Compute responses of the substructure from Equation (4.3) and the sensitivity of responses with respect to structural parameters of the substructure from Equation (4.6).

Step 7: The changes of the substructure parameters are calculated by damped least-squares method in Equation (4.29) from the sensitivity of the responses of the substructure.

Step 8: Update the finite element model.

Step 9: Repeat Steps 6 to 8 until the convergence condition in Equation (4.30) is met.

The convergence criteria is defined as

$$\left\| \frac{\Delta\alpha_{k+1} - \Delta\alpha_k}{\Delta\alpha_{k+1}} \right\| \le Tol \tag{4.30}$$

where k denotes the number of iteration and Tol is a small prescribed value which is taken equal to 10^{-6} for all studies in this work.

Step 10: The two-stage identification procedure can be repeated by updating the parameters of the whole structure and repeat Steps 2 to 9 for a higher accuracy.

4.5.2 For Scenario B when only the FEM of the Substructure is Known

Step 1: Obtain the mass, damping and stiffness matrices of the target sub-structure only.

Step 2: Construct the pseudo structural system.

Step 3: Conduct measurement on the target sub-structure.

Step 4: Identify the interface forces of the pseudo structural system starting with the intact model of the pseudo sub-structure in state space as Equation (4.18).

Step 5: Compute responses of the pseudo structure with the intact finite element model from Equation (4.10) with the identified interface forces.

Step 6: The response sensitivities with respect to the stiffness reduction factor α_n of the sub-structure $\partial \ddot{\mathbf{x}}_i / \partial \alpha_n, \partial \dot{\mathbf{x}}_i / \partial \alpha_n$ and $\partial \mathbf{x}_i / \partial \alpha_n$ are calculated from Equation (4.6).

Step 7: The local changes of the parameters α_n of the pseudo sub-structure are calculated from Equation (4.29) with the sensitivity matrix calculated in Step 6.

Step 8: Update the FEM of the pseudo structure.

Step 9: Repeat Steps 4 to 7 if the convergence criteria in Equation (4.30) is not met. Otherwise the computation stops.

4.6 Numerical Simulation Studies

4.6.1 Simulation Study of a Linear Structure

A two-dimensional 50-meter high planar truss structure shown in Figure 4.4 is investigated to illustrate the proposed methods. It is a simplified model of a popular type of power transmission tower structure in China. The truss structure consists of 14 nodes each with two DOFs. The two ends of each truss element are assumed hinged and the structure is found on rigid supports at Nodes 1 and 2 with hinges. It has five levels with 10m high each.

The truss structure is divided into two substructures. Substructure 1 contains nodes from 1 to 4 and the elements between them and Substructure 2 consists of nodes from 7 to 14 and the elements between them. Nodes 5 and 6 are the interface nodes. When they are mapped with the substructure domains in Equations (3.5) and (3.6) in Chapter 3, Substructures 1 and 2 corresponds to domains *r* and *s* respectively while Nodes 5 and 6 belong to domain *i*. The matrices with superscript ‘ are for members between Nodes 5 and 6 and Substructure 1 while those matrices with superscript “ are for members between Nodes 5 and 6 and Substructure 2. The element numbers of Substructure 2 are also shown in Figure 4.5. Local damages are assumed to be 10% reduction in the elemental stiffnesses for elements 8 and 11 of Substructure 2. The mass density of material is 7.8×10^3 kg/m^3 and the elastic modulus of material is 2.06 GPA. The cross-sectional area of each truss element is 3.5×10^{-3}m^2.

Dynamic external forces are assumed to act horizontally on Substructure 2 at Nodes 13 and 14 as shown in Figure 4.5. The external forces are modeled as

$$F_{13}(t) = 65\sin(30\pi t + 0.3\pi) + 60\sin(60\pi t + 0.143\pi) + 55\sin(80\pi t + 0.12\pi) \qquad N$$
$$F_{14}(t) = 60\sin(40\pi t + 0.4\pi) + 55\sin(70\pi t + 0.167\pi) + 50\sin(90\pi t + 0.11\pi) \qquad N$$

When there is noise in the "measured" response, the polluted response is simulated by adding a random component to the "measured" responses as Equation (3.39).

The error of identification of the interface forces and the local damages are calculated as

$$error1 = \frac{\left\| F_{id} - F_{true} \right\|}{\left\| F_{true} \right\|} \times 100\% \tag{4.31}$$

$$error2 = \frac{\left\| \alpha_{id} - \alpha_{true} \right\|}{\left\| \alpha_{true} \right\|} \times 100\% \tag{4.32}$$

4.6.1.1 Two-stage Assessment for Scenario A

External forces acting on the structure are identified from Equation (4.20). The sampling rate is 1000 Hz and 0.5s of the horizontal acceleration at Nodes 9, 10, 11 and 12 are 'measured' for studies in Scenario A. The identified forces are shown in Figures 4.6 and 4.7 for cases without and with 10% noise in the "measured" responses respectively. The error of identification calculated from Equations (4.31) and (4.32). The optimized regularization parameters under different noise levels are shown in Table 4.1. The force identification accuracy is noted decreasing with increasing noise level in the responses. However, results in Figure 4.7 show that the external forces are not sensitive to noise and they are fairly accurately identified even with 10% noise based on the FEM of the whole structure.

The damage detection of a substructure requires the knowledge on the responses at the interface DOFs for the calculation of the interface forces. The dynamic responses of the substructure are then calculated from Equation (4.10) for the identification of the local damages of the substructure from Equation (4.29). The accuracy of using the damaged and intact finite element model in the calculation of the interface forces is studied for the case without measurement noise in the responses ”measured” at Nodes 9 to 12. The identified interface forces at Nodes 5 and 6 from both finite element models are plotted in Figures 4.8(a) to 4.8(d). They are found almost overlapping with each other indicating that the use of the intact finite element model is accurate enough for the estimation of the interface forces of the whole structure.

The identified external forces from the first stage of the method based on the FEM are used for the second stage of damage detection. When there is no noise in the measured responses of the structure, the result of damage detection shown in Figure 4.9 is very good indicating the formulation of the substructure damage detection problem is accurate.

The assessment results for the cases with 10% noise level are shown in Figure 4.10. The error of identified results is noted to increase with increasing noise level. However in the case with 10% noise level in the measured acceleration, the local damages can still be identified fairly accurately with good location information and two small false positives in Elements 7 and 14.

The results on the external forces and local damages are quite good in the above studies and there is no need to update the finite element model of the structure and repeat with another iteration of force and damage identification.

4.6.1.2 Two-stage Assessment for Scenario B

When only the FEM of the target substructure is known, the interface forces of the substructure are taken as external forces acting on the substructure which can also be identified from Equation (4.20). However, with the increasing number of the external forces, force identification may not be accurate and converging due to the influence of the measurement noise. To moderate the influence of noise, the measured response is least-squares fitted with the Chebyshev Polynomial. The number of terms in the Chebyshev Polynomial also has an effect on the accuracy of approximation. A study is made on the optimal number of terms for the polynomial to have the best fit of the response. An iterative method with regularization is used for the study. The error curve for using 120 terms in the polynomial is shown in Figure 4.11(a). The error with reference to the unpolluted response is smallest after the first iteration of identification, and it becomes larger with more iterations. Figure 4.11(b) shows the error curve for using 80 terms in the polynomial and the error becomes smaller with increasing iterations. Therefore 80 terms are adopted in the Chebyshev Polynomial approximation in the following studies. The comparison of the unpolluted response, polluted response and the curve-fitting approximated response of the horizontal acceleration at Node 13 on one of the curve peaks in Figure 4.12 shows that the approximation is well done.

Figures 4.13(a) and 4.13(b) show the external force identification results based on the FEM of the target substructure without noise where both vertical and horizontal 'measured' accelerations from Nodes 9, 11 and 14 are used for the external forces identification and the sampling rate is also set as 1000 Hz. Information from six sensors is used to identify the six unknown forces. The identified forces with 10% noise are shown in Figures 4.14(a) and (b). The external forces can also be identified fairly accurately based on the Chebyshev Polynomial approximation and the identification results converge with the damped least-square method.

The errors of the identified external forces of the substructure with 10% noise are 17.9% and 14.4% for the cases without and with approximations in the 'measured' responses. The approximation of the polluted response of the structure can effectively reduce the identification errors from noisy measurements. Comparison of the above with results in Table 4.2 shows that the error of the identified external forces based on the whole structure is smaller than that based on the substructure FEM. That is because the interface forces are treated as external forces in the latter identification. The measurement noise would have more adverse effect when there are more unknowns in the force identification. When the FEM of the whole structure is available, the first identification method (Scenario A) is recommended for the evaluation of the structural conditions.

When only the FEM of the substructure is known, the external forces and the interface forces of the substructure have been identified. All the responses at the nodes of the substructure can then be calculated through the equation of motion of the substructure. It is obvious that any model error in other parts outside the target substructure does not have any influence on the assessment result. The identified external forces from last study are used for damage detection of the substructure.

When there is noise in the measurement, the responses of the substructure are also moderated with Chebyshev Polynomial as Equation (3.34) in Chapter 3. The assessment results for the cases without noise and with 10% noise are shown in Figures 4.15 and 4.16 respectively. The errors in the identified results are larger compared to those in Figures 4.9 and 4.10 for Scenario A. This is due to the larger errors in the identified external forces and interface forces. However, the results are noted not sensitive to the noise level due to the Chebyshev Polynomial approximation. In the case of 10% noise level in the measured acceleration, the location and the severity of the substructure can still be identified fairly accurately with few false positives.

4.6.2 Simulation with a Nonlinear Structure

A fifteen-storey planar shear frame structure with nonlinear base isolations as shown in Figure 4.17 is investigated to illustrate the general response sensitivity method. The base isolation between the structure and the foundation is represented with a bilinear hysteresis model. The vertical stiffness of the base isolation is assumed as infinitely large. The relationship between the force and horizontal displacement is shown in Figure 4.18 where α_b =0.15 is the ratio of the post-yield stiffness to pre-yield elastic stiffness defined by K_E, and d_y is the yielding displacement. The horizontal restoring force of the isolation is defined as

$$F_b = \alpha_b K_E x_b + (1-\alpha_b) K_E z_b \tag{4.33}$$

where subscript b denotes the base isolation, x_b is the horizontal deformation, and z_b is the horizontal elastic storey drift between ground floor and first floor, K_E =0.1 $\times 10^8$ N/m and d_y =0.01 m. The mass of each floor is 4×10^5 kg and the stiffness of each floor is 2×10^8 N/m.

The structure is assumed subject to the N-S El-Centro 1940 earthquake ground motion with the peak ground acceleration scaled to 0.3g. The sampling rate of acceleration measurement is 100Hz. Six scenarios with 10% reduction of stiffness in 8th floor and 13th floor are studied and they are shown in Table 4.3. The calculated horizontal acceleration responses from Equation (4.10) at the 1th, 5th and 10th floors are taken as the "measured" responses for all these six scenarios. Additionally, the horizontal displacement of the 1st floor is also used in the first stage of force identification in the last two scenarios. This is because the constant shift value in the time history of external forces can be difficult to identify with acceleration response only.

In the first four scenarios, 6 seconds of "measured" data are used for the model updating. The "measured" data for the last two scenarios begin at 1.5s after the earthquake excitation and only two seconds of data are utilized for the initial response identification, interface force identification and damage detection. The "measured" data is divided into four segments for the time window force identification in Scenarios 3 and 4 while the whole set of data is used for the other scenarios. There is only one interface force at the nonlinear base isolation to be identified in all scenarios due to symmetry.

Note that the base isolations are performing nonlinearly with the hysteretic curves shown in Figure 4.19. When there is noise in the "measured" response, the polluted response is simulated with the Equation (3.39). The error of identification of the interface forces and the local damages are calculated as

$$error\,1 = \frac{\left\| F_{id} - F_{true} \right\|}{\left\| F_{true} \right\|} \times 100\% \tag{4.34}$$

$$error\,2 = \frac{\left\| \alpha_{id} - \alpha_{true} \right\|}{\left\| \alpha_{true} \right\|} \times 100\% \tag{4.35}$$

where $\mathbf{F}_{id}$ and $\boldsymbol{\alpha}_{id}$ are the identified interface forces and local damages respectively and $\mathbf{F}_{true}$ and $\boldsymbol{\alpha}_{true}$ are the real interface force and local damages of the structure respectively.

In the first two scenarios, the number of unknowns in the first stage is 600 and the measured data is 3×600 which is also the number of equations. The size of matrix $\mathbf{H}_L$ is 1800×600. The number of equations is much larger than the number of unknowns in these two scenarios. In each time segment for force identification of the third and fourth scenarios, there are 150 unknowns and 3×150 equations. The size of matrix $\mathbf{H}_L$ is 450×150 which is one-sixteenth the size of $\mathbf{H}_L$ in the first two scenarios. In the last two scenarios the number of unknowns in the first stage is (200+2×15)=230 and the number of equations is 4×200.

In the second stage of structural model updating, there are 15 unknowns in all six scenarios. The number of equations is 1800 in the first four Scenarios and 600 in the last two Scenarios. The identification problems in this study are all over-determined.

The error of identification for both the interface forces and the local damages as well as the computation time required for each Scenario are shown in Table 4.4 together with the required number of iterations. The results of model updating are shown in Figures 4.20 to 4.25. The stiffnesses shown are the storey stiffnesses of the multi-storey frame.

Figures 4.20 and 4.21 show that the proposed method without measurement noise can identify the damage very accurately but with a very long calculation time as shown in Table 4.4. The calculation of interface forces is time consuming with a large number of unknowns and a large matrix $\mathbf{H}_L$. Difference is noted at the peaks of the force time history in Figure 4.21 when there is 10% measurement noise. However the position and severity of damage could still be found accurately as shown in Figure 4.21. The errors in force identification and damage detection calculated with Equations (4.34) and (4.35) are shown in Table 4.4. The measurement noise and accuracy in the identified forces are noted affecting the damage detection result.

When the time window identification method is applied in Scenarios 3 and 4, the computation time is reduced significantly as shown in Table 4.4. The interface force and the damage can be identified accurately as shown in Figures 4.22 and

4.23 when there is no measurement noise. The errors of identification shown in Table 4.4 for the identified force are comparable to those from the case without using the time window force identification method. The identified results for damage are slightly poorer than those for Scenarios 1 and 2 but the damage location can still be identified. This may be due to the cumulative errors in the calculated initial responses in each time segment.

The initial responses, the interface forces and the local damages are all identified together in Scenarios 5 and 6. The initial responses and the interface forces are identified in the first stage and the local damage is identified in the second stage with the proposed method. Figures 4.24 and 4.25 are the identification results without and with 10% measurement noise respectively. The norm of the damage detection error in Table 4.4 is large compared with those for Scenarios 1 to 4. The large errors in the damage detection as shown in Figure 25 are due to both the errors of identification in the initial responses and the interface force. However, the local damage could still be localized with the polluted measurement.

4.7 Conclusions

A general response sensitivity method based on two-stage identification is proposed with the idea of substructure model updating in the time domain. The proposed method is analogous to the evolution of a pseudo structure with iterative model updating. Two substructural damage detection methods are presented to identify external excitations and local damages iteratively in a substructure with time domain information. In the first method, the finite element model of the whole structure is required and a selected substructure is assessed for its structural conditions. In the second method, only the finite element model of the selected substructure is required with the dynamic measurement and excitation within the same substructure. Exact knowledge on the boundary conditions of the substructure is not necessary. The second method allows a damage detection strategy with distributed sensors in a substructure grouped into a cluster as shown in Figure 4.26. A cluster head is assigned to coordinate the sensor nodes in its cluster and to collect the measured data from the nodes. The identification algorithm is embedded into the on-board computational core of each cluster head in the sensor network for the detection of local damage in that substructure. The damage detection could be conducted simultaneously with parallel computing.

Two new techniques of time windows force identification and initial response identification are also proposed to improve the computation efficiency with force identification. These improvements enable a more flexible application of the sensitivity approach in engineering practice. The errors in the first stage of force identification are found contributing to the error in the second stage of damage detection. However, the location of damage could still be identified from polluted measurement with the adaptive regularization method.

Table 4.1 - Error of force identification and regularization parameters

Noise level (%)	Error *(%)*	Optimal λ
0	0.73	10^{-5}
1	2.1	10^{-5}
5	7.6	1.083×10^{-5}
10	13.0	2.276×10^{-5}

Table 4.2 - Error of force identification and regularization parameters

Noise level (%)	Error (%)	Optimal λ
0	0.02	0.008
1	2.10	0.089
5	2.66	0. 10
10	2.84	0. 30

Table 4.3- Damage Scenarios

Damage scenarios	Initial response	Time Window Force identification	Noise level (%)
1	zero	No	0
2			10
3		Yes	0
4			10
5	unknown	No	0
6			10

Table 4.4 - Condition assessment results

Damage Scenarios	Errors (%)		Required computation time (s)	Number of iterations
	Force Identification	Damage detection		
1	5.55×10^{-3}	8.37×10^{-2}	1493	93
2	13.920	24.04	1511	106
3	9.4×10^{-3}	0.042	94	92
4	14.360	32.97	97	104
5	2.7×10^{-3}	0.030	111	53
6	9.470	62.25	113	58

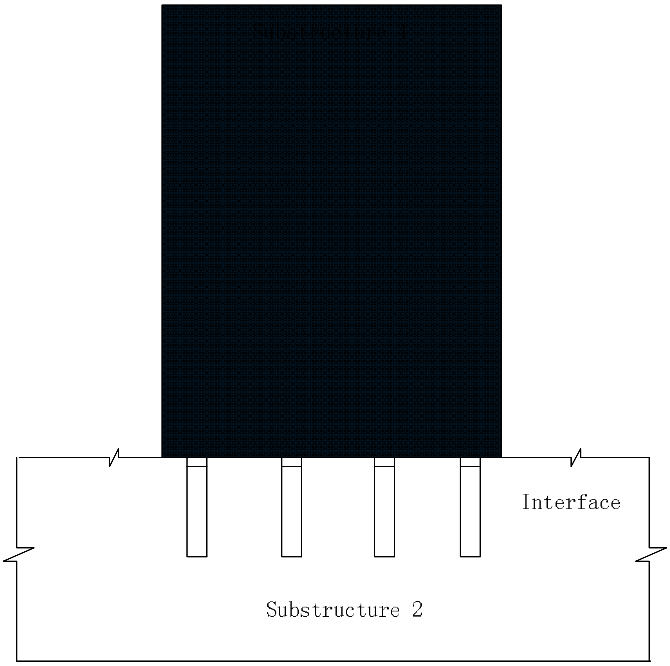

Figure 4.1- Structure and substructures

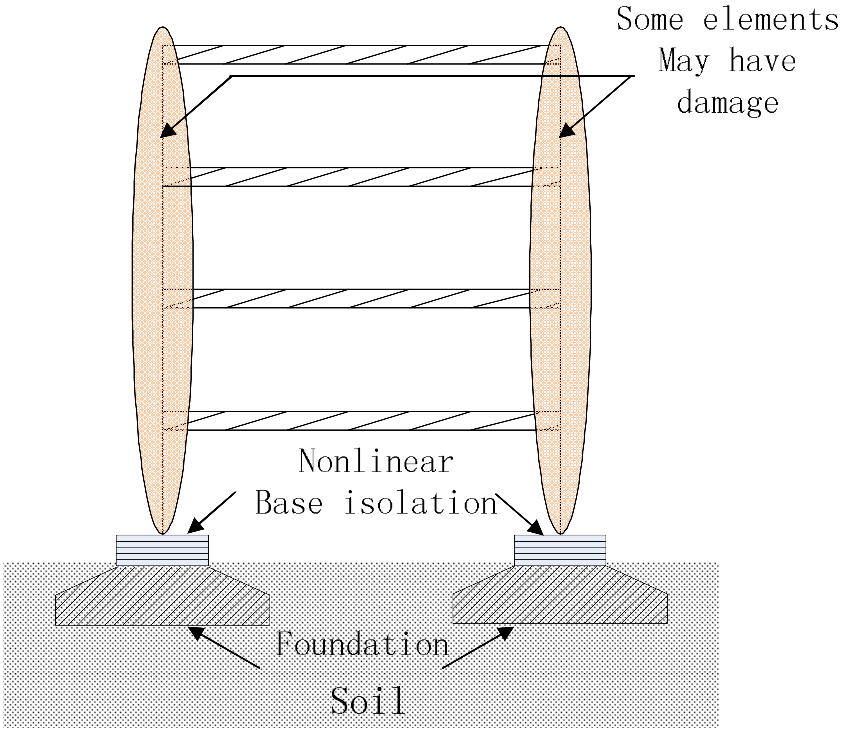

Figure 4.2 - Structural system with base isolation

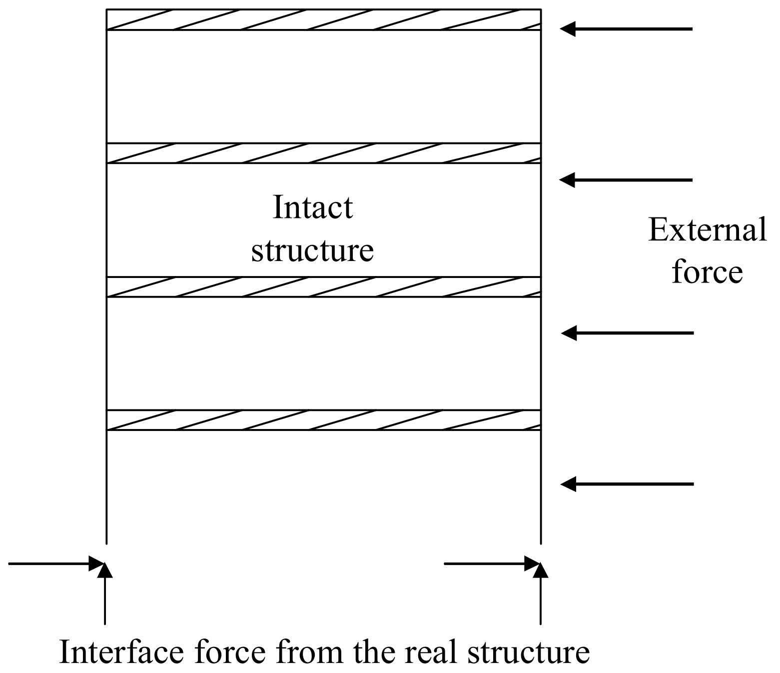

Figure 4.3 - Pseudo target structure

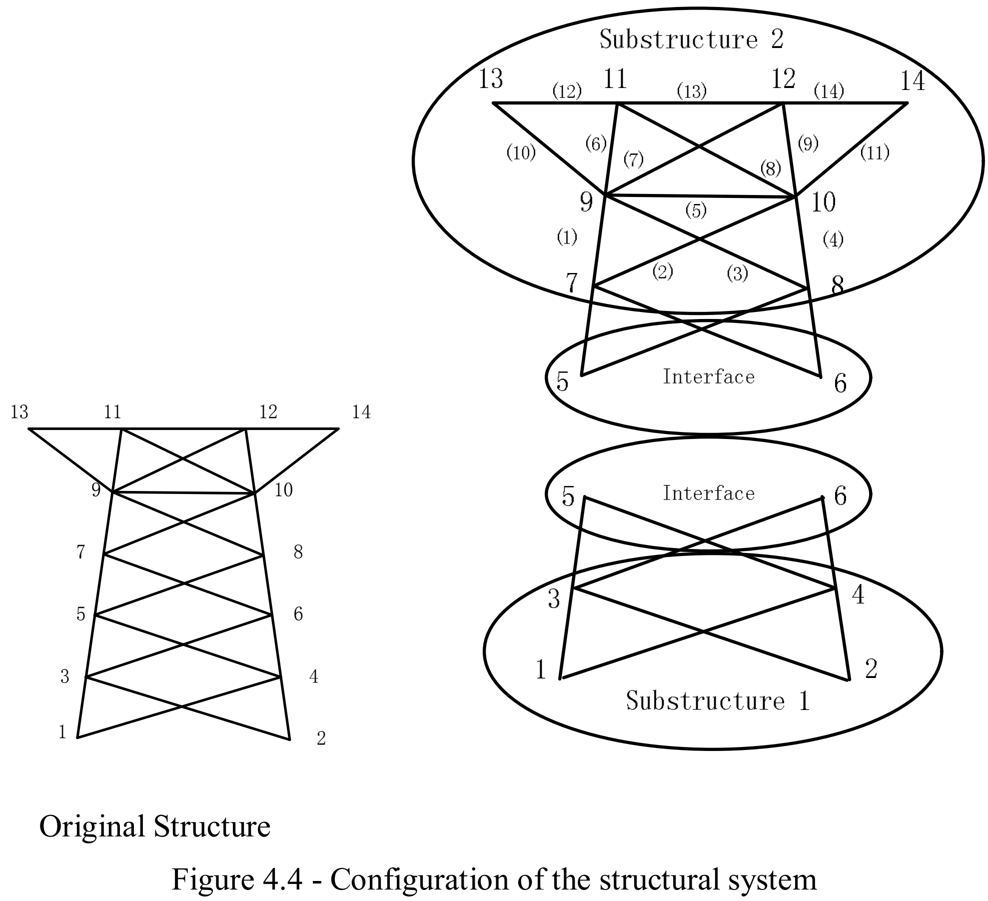

Figure 4.4 - Configuration of the structural system

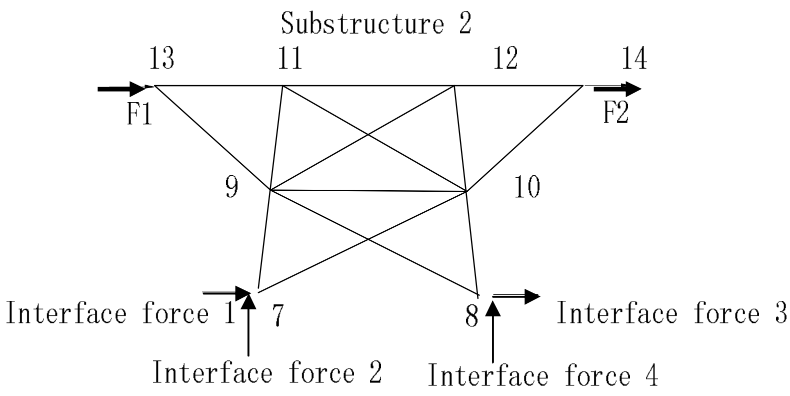

Figure 4.5 - Selected Substructure and External Forces

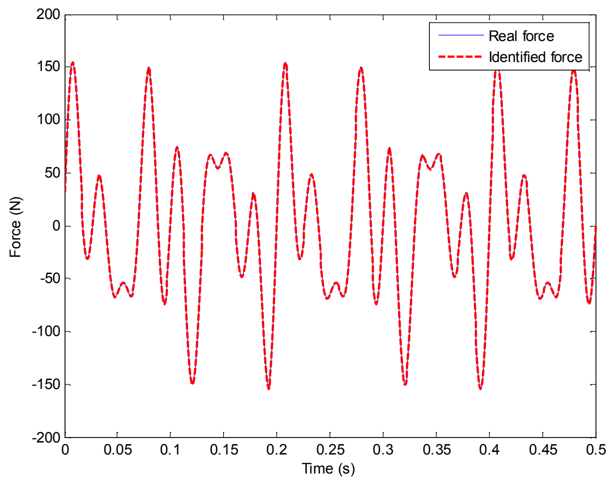

Figure 4.6 (a) - Identified force at Node 13 of Scenario A without noise

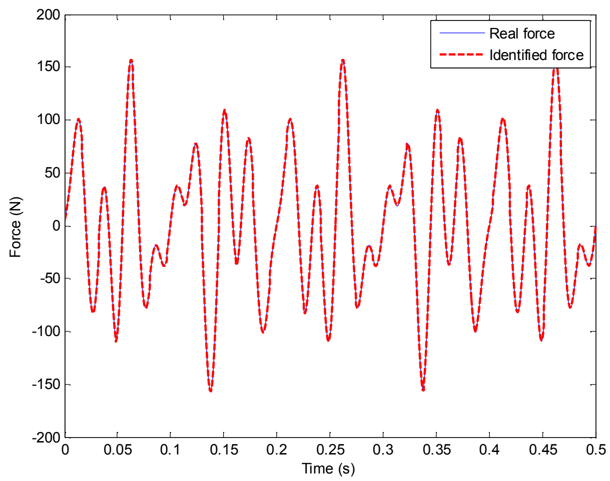

Figure 4.6 (b) - Identified force at Node 14 of Scenario A without noise

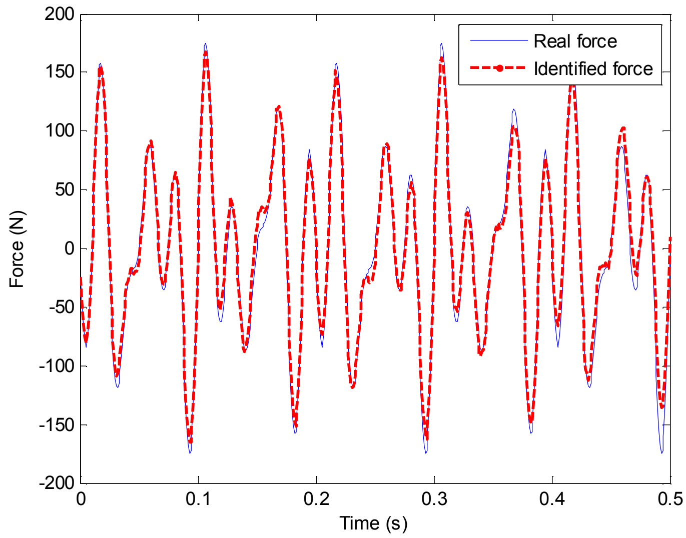

Figure 4.7 (a) - Identified force at Node 13 of Scenario A with 10% noise

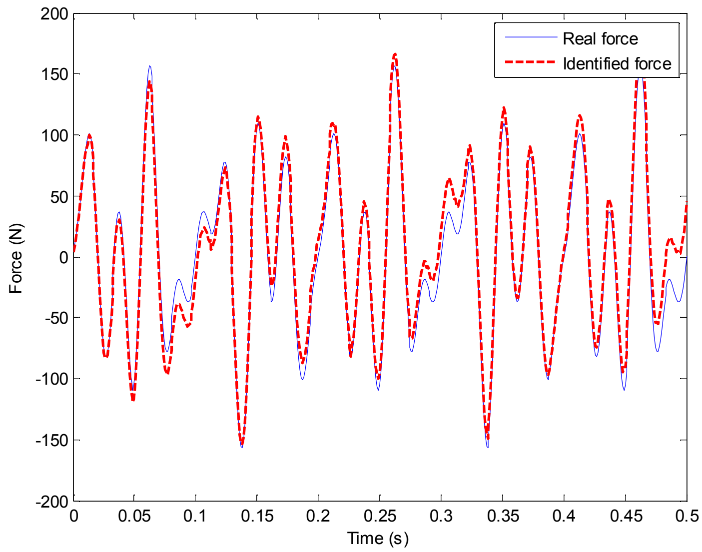

Figure 4.7 (b) - Identified force at Node 14 of Scenario A with 10% noise

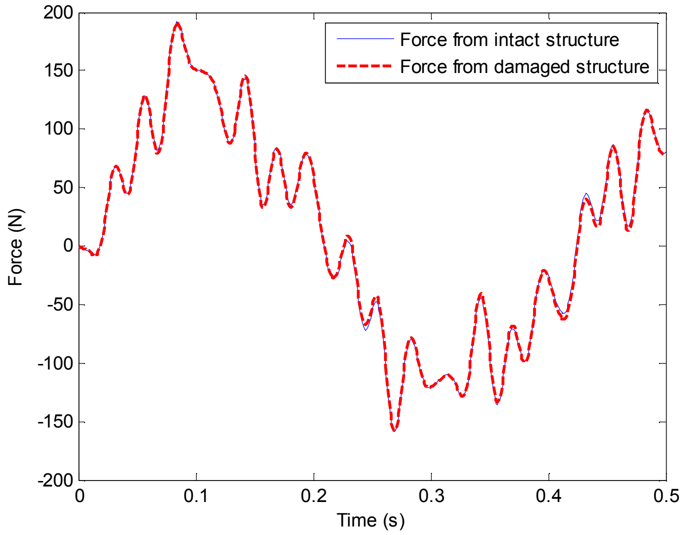

Figure 4.8 (a) - Horizontal interface force comparison at Node 5

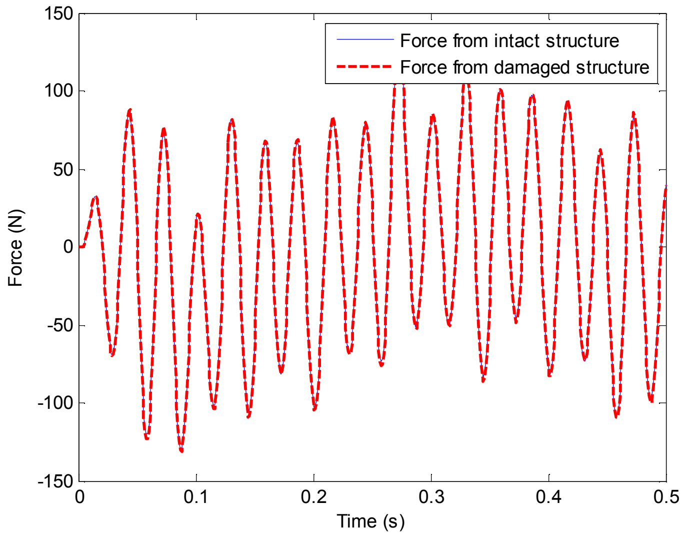

Figure 4.8 (b) - Vertical interface force comparison at Node 5

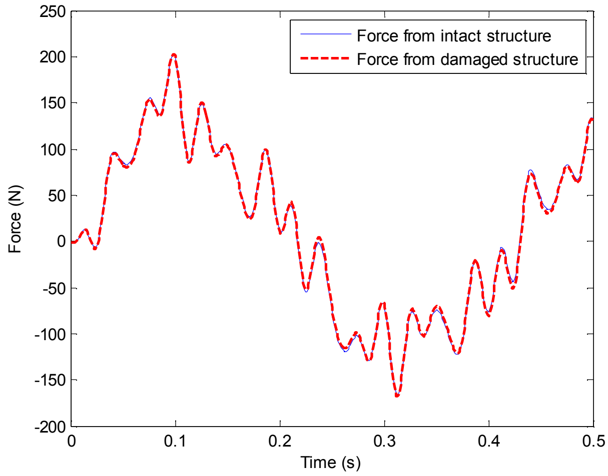

Figure 4.8 (c) - Horizontal interface force comparison at Node 6

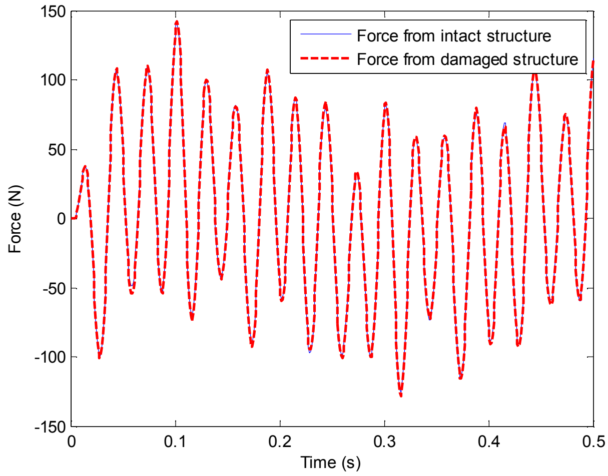

Figure 4.8 (d) - Vertical interface force comparison at Node 6

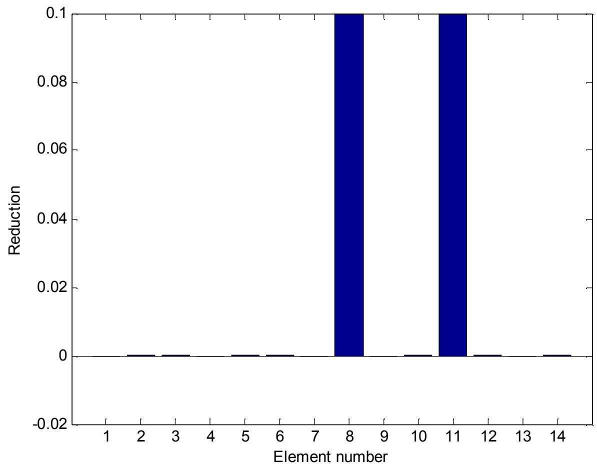

Figure 4.9 - Identified damages of Scenario A without noise

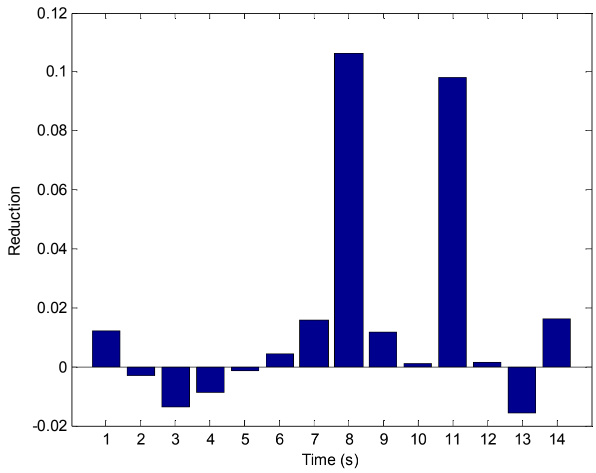

Figure 4.10 - Identified damages of Scenario A with 10% noise

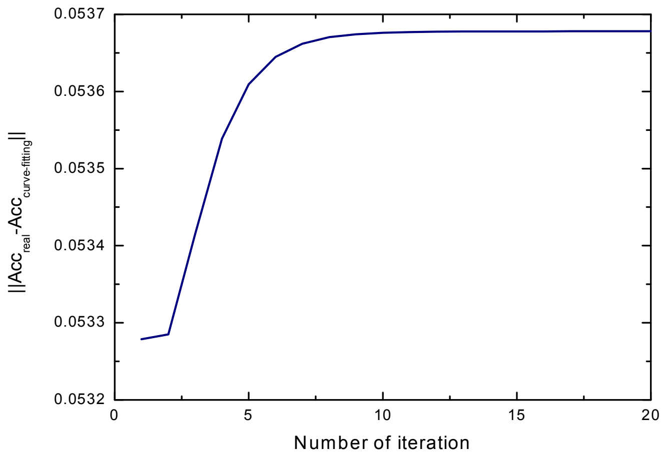

Figure 4.11 (a) - Error versus number of iteration with 120 terms

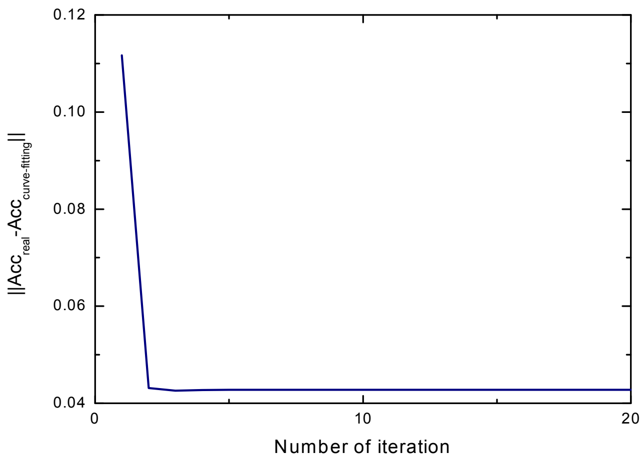

Figure 4.11 (b) - Error versus number of iteration with 80 terms

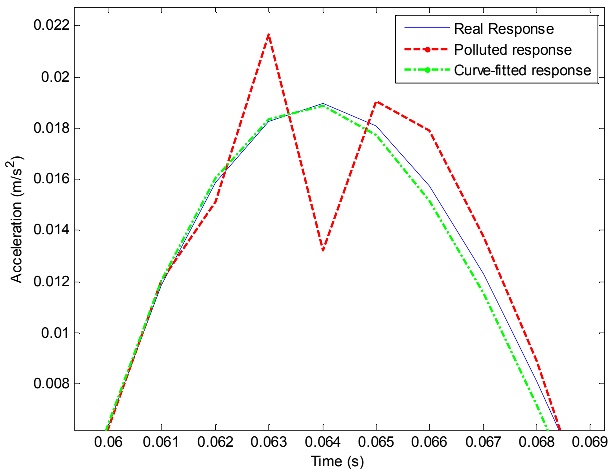

Figure 4.12 - Comparison of horizontal response at Node 13 with 80 terms

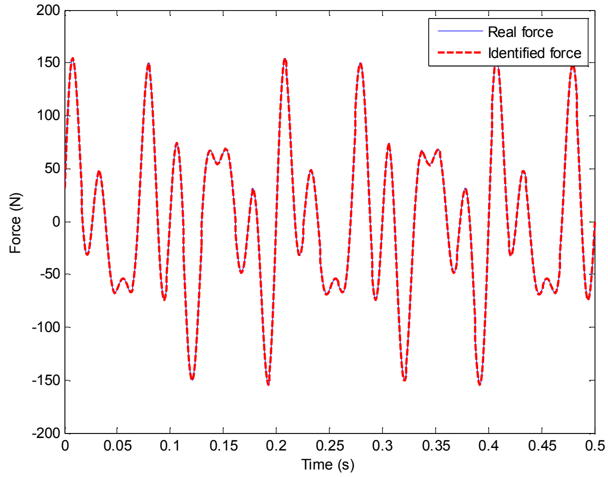

Figure 4.13 (a) - Identified force at Node 13 of Scenario B without noise

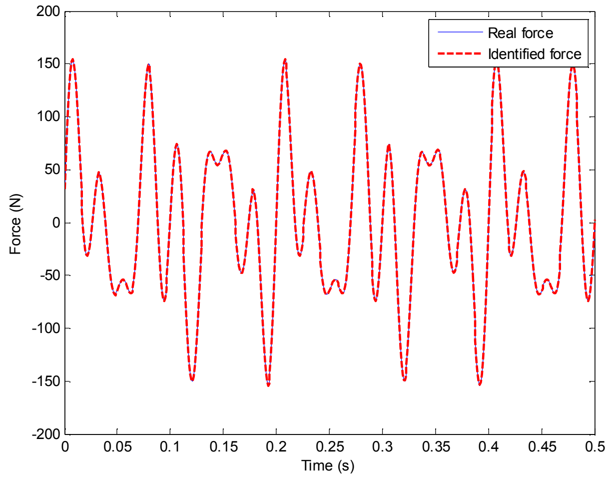

Figure 4.13 (b) - Identified force at Node 15 of Scenario B without noise

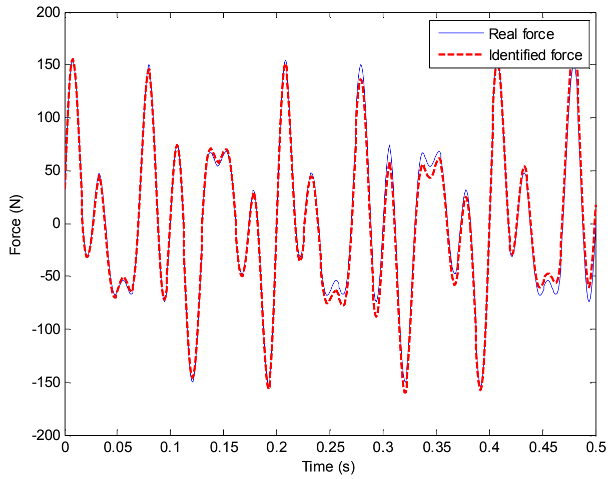

Figure 4.14 (a) - Identified force at Node 13 of Scenario B with 10% noise

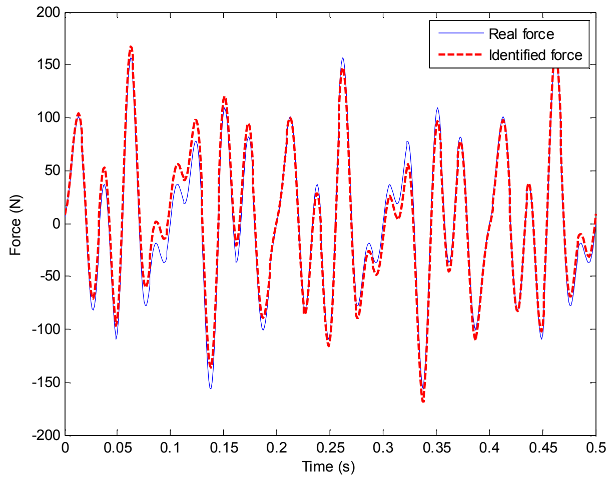

Figure 4.14 (b) - Identified force at Node 15 of Scenario with 10% noise B

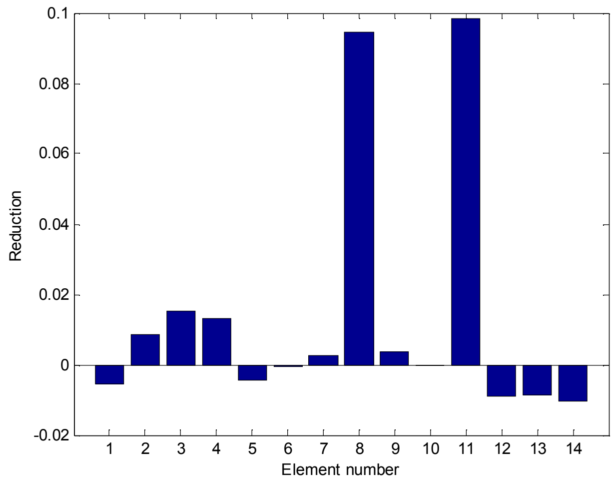

Figure 4.15 - Identified damages of Scenario B without noise

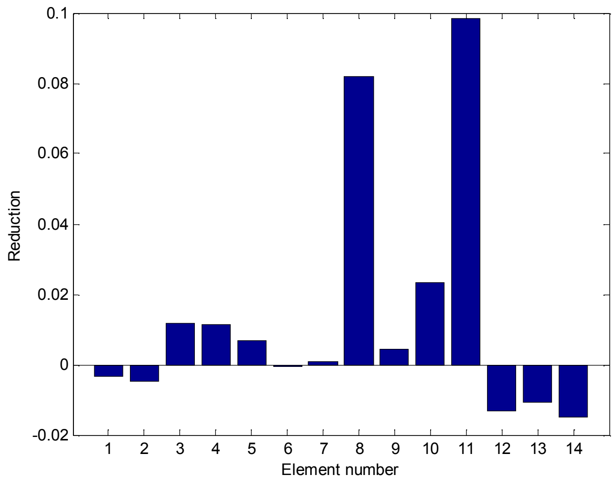

Figure 4.16 - Identified damages of Scenario B with 10% noise

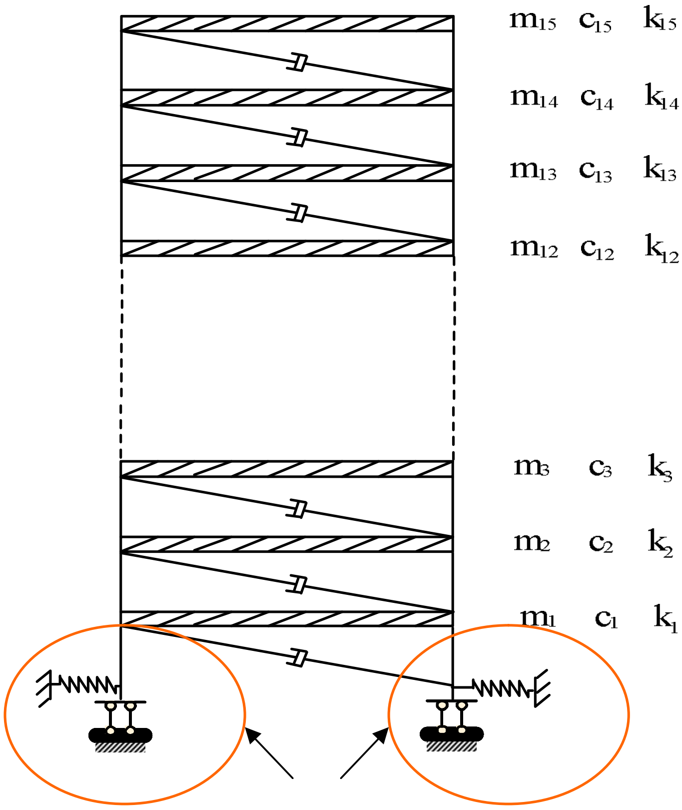

Figure 4.17 - Fifteen-storey shear frame

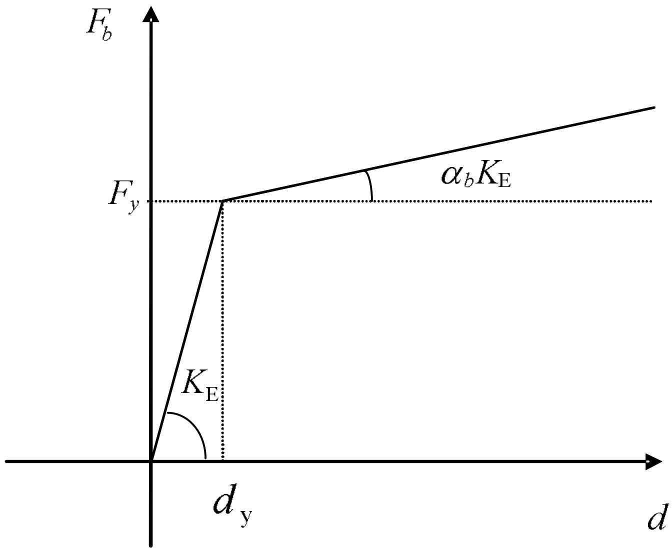

Figure 4.18 - Relationship between force and displacement of bilinear restoring force model

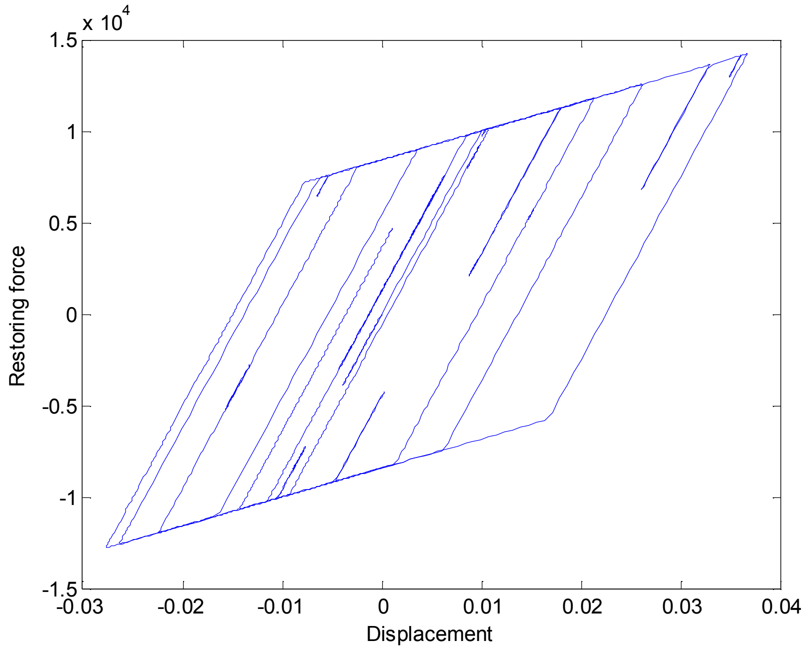

Figure 4.19 - Hysteresis loop of the base isolation

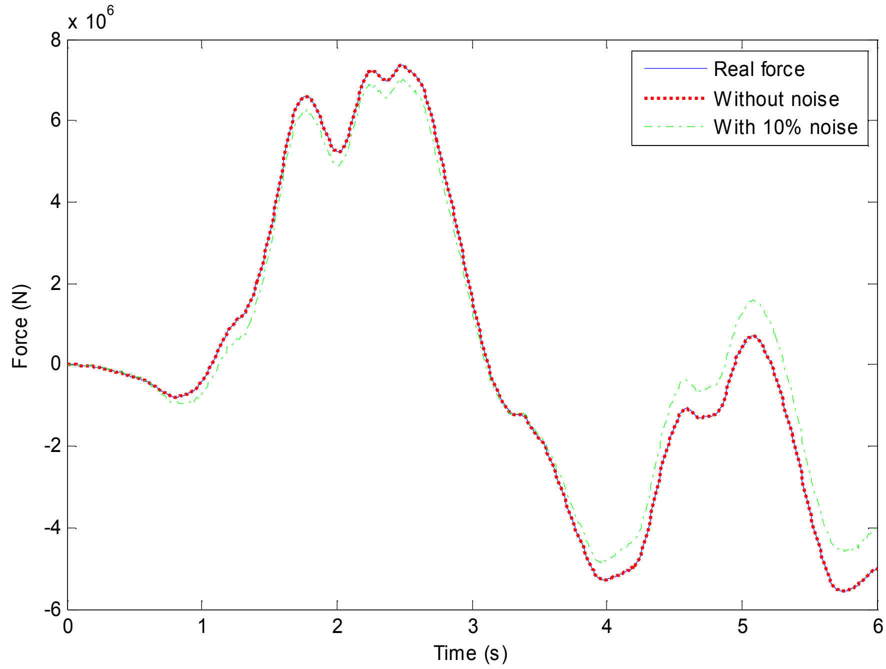

Figure 4.20 - Identified forces of Scenarios 1 and 2

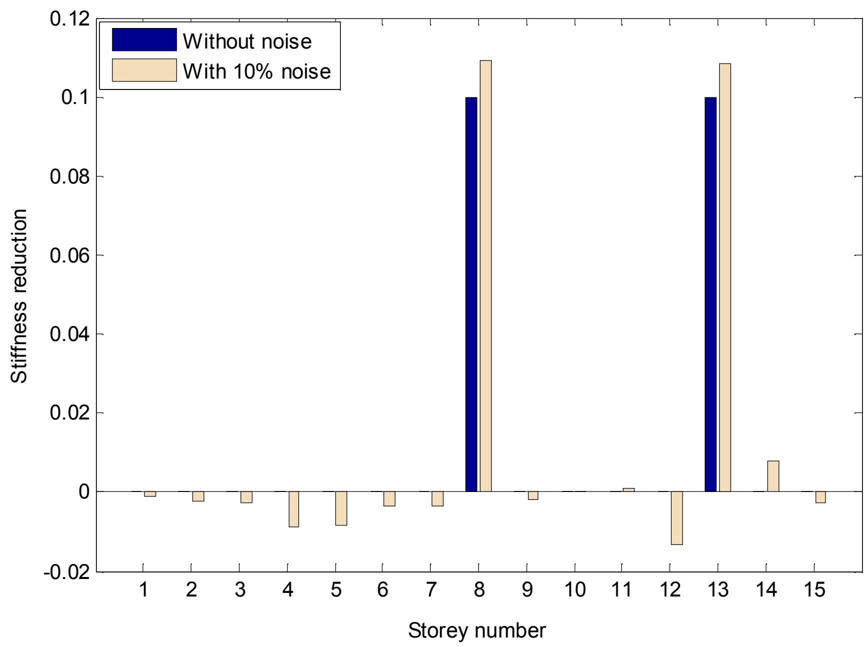

Figure 4.21 - Identified damages of Scenarios 1 and 2

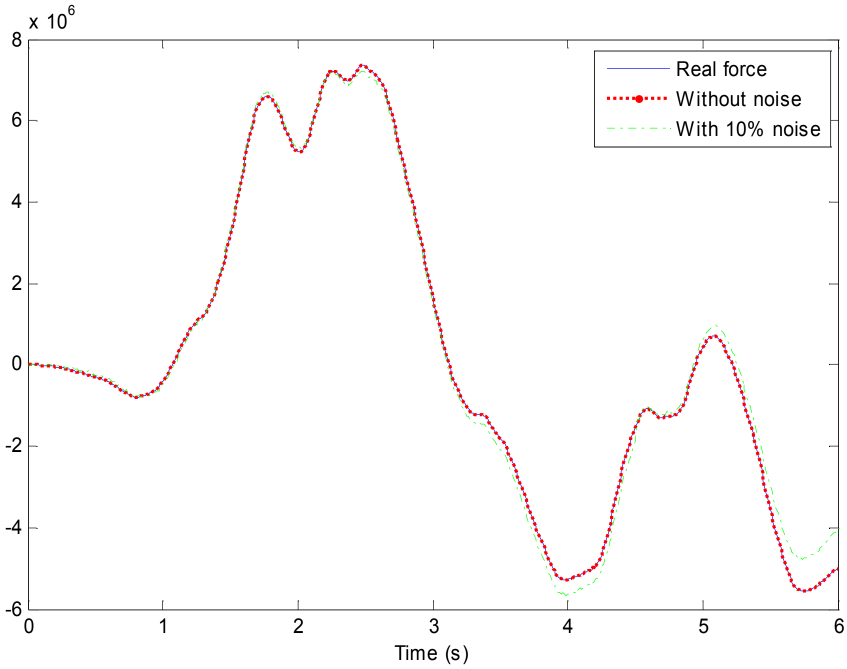

Figure 4.22 - Identified forces of Scenarios 3 and 4

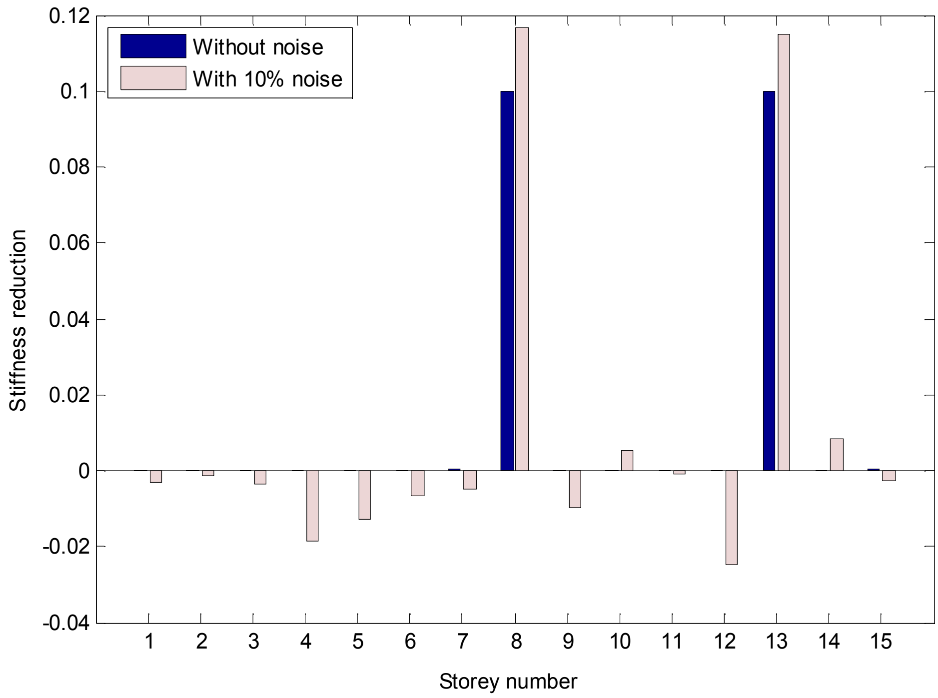

Figure 4.23 - Identified damages of Scenarios 3 and 4

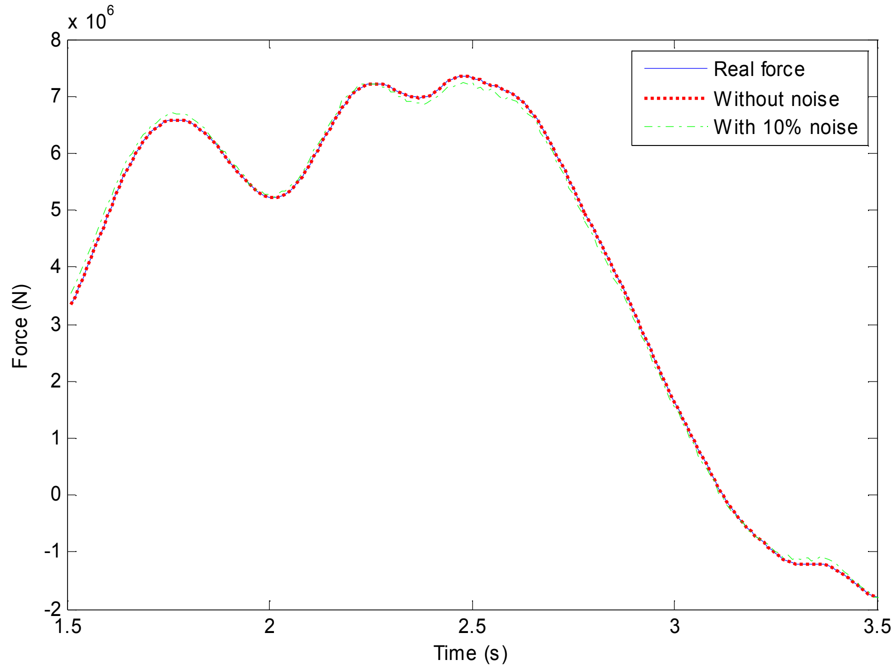

Figure 4.24 - Identified forces of Scenarios 5 and 6

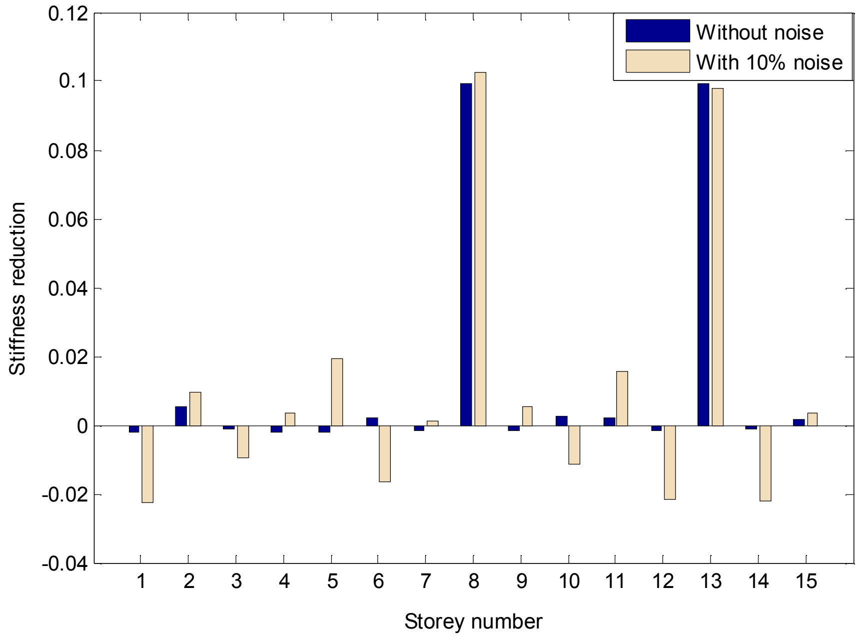

Figure 4.25 - Identified damages of Scenarios 5 and 6

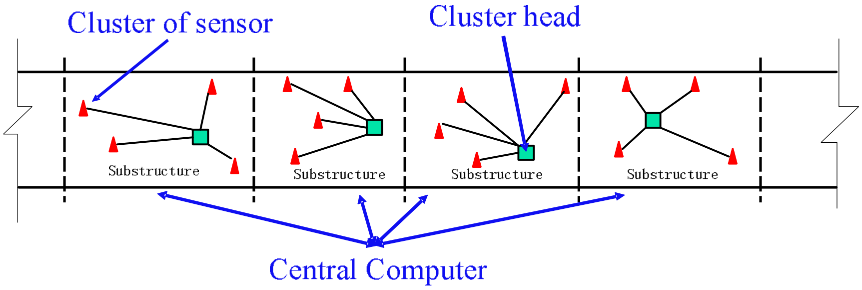

Figure 4.26 - Distributed sensors network

CHAPTER 5

TIME-VARIANT STRUCTURAL PARAMETER IDENTIFICATION

5.1 Introduction

Chapter 4 proposed a new substructural condition assessment approach with a general response sensitivity method and provided a proof and illustration for the proposed method considering the nonlinear component of the structure. All the methods proposed for structural condition assessment in Chapter 4 were for time-invariant structural system. In practical engineering problem, the structural parameters are always time-variant during the strong wind or seismic excitation.

Numerous methods have been developed for time-variant structural condition assessment and model updating in the past. Investigations on the time-variant structural parameter identification have also been conducted for linear or nonlinear structures over the last two decades (Kerschen, Worden, Vakakis and Golinval 2006). A linear time-varying multiple degrees-of-freedom system identification method based on the Hilbert transformation and empirical mode decomposition was proposed (Shi, Law and Li 2007) while some fluctuations are found in the identification results. The Kalman filter is an effective means of system parameter identification and input estimation for a linear or nonlinear structure. Two forms of the extended recursive least-squares algorithm were considered for the identification of system parameter and the tracking of a chirped sinusoid with additive noise (Haykin, Sayed, Zeidler, Yee and Wei 1997). Other time-variant parameter identification methods were also proposed, such as, the online identification of nonlinear hysteretic structure with an adaptive tracking techniques based on least-squares estimation (Yang and Lin 2004), nonlinear normal modes analysis which considered the nonlinearity of structural system (Kerschen, Peeters, Golinval and Vakakis 2009a, 2009b) an online sequential weighted least-squares support vector machine technique to quantify the structural parameter changes when the measurement involves damage events (Tang, Xue, Chen, and Sato 2006), an adaptive tracking technique based on extended Kalman filter for structural parameters and their changes identification (Yang, Pan and Lin 2007), the dynamic response sensitivity method (Li and Law 2009) with a moving time window (Zhu and Law 2007). These methods remove the assumption that the time of occurrence of the anomalies is known *a priori*. Hence, these methods could be applied to conduct the structural condition assessment online. However, most existing methods for time-variant parameter identification do not consider the uncertainties in the structural parameters or measurements.

In this Chapter, two identification methods are proposed for structural time-variant parameters identification. Section 5.2 reviews on the iterative regularization methods for the system identification and propose a general sensitivity-based method for the identification of both the time-variant and time-invariant damping in a structural system. In Section 5.3 a new method for the time-variant parameter identification based on windowed measured data is presented. Section 5.4 provides the conclusion of this Chapter.

5.2 Time-Variant Damping Identification

Damping plays an important role in the dynamic behavior of a structural system. It is, however, difficult to measure and is always a subject of active research. The identification of damping can be conducted by direct or indirect means, and it requires an appropriate damping model and an effective damping identification method. Several damping models have been proposed, such as the Rayleigh damping proposed by Rayleigh (1877), Caughey damping (Caughey and O'Kelly 1965), and the modal damping (Hasselman 1972). Rayleigh damping model is commonly used in engineering practice due to its simplicity. The Caughey damping model includes more coefficients in its description and is more accurate than the Rayleigh damping which is, in fact, a two-term Caughey damping approximation. However, with the large number of coefficients in the Caughey damping model, inappropriate damping coefficients may lead to a negative modal damping ratio which cannot exist in nature. The modal damping model is more general and the damping matrix can be expressed in terms of the mode shape matrix, modal damping ratios and the modal angular frequencies.

The problem of damping identification has been reported previously

(Rayleigh 1877; Caughey and O'Kelly 1965; Hasselman 1972) and most of the application studies adopted the classical Rayleigh damping in the modeling of a structural system (Chu, Soong and Reinborn 2006). Methods in the frequency domain include the matrix method and modal method (Phani and Woodhouse 2007). Others in the time domain are the logarithmic-decrement method, Ibrahim time-domain (ITD) method proposed by Ibrahim and Mikulcik (1977), Station time domain algorithm (STD) method proposed by Ibrahim (1986) and modal damping ratio identification method (Li and Law 2009). A wavelet-based approach has been studied for a one-degree-of-freedom (DOF) nonlinear system (Joseph et al. 2005). Reference by Prandina, Mottershead and Bonisoli (2009a) revisited several selected approaches of damping identification and compared their performances in numerical study with a cantilever beam. There is also literature investigating multiple DOFs systems (Prandina, Mottershead and Bonisoli 2009b) with the energy balance approach. It is known that a complex structural system always has uncertainties in the material property and boundary condition leading to difficulties in the modeling of the damping properties.

The time domain methods could be applied in large scale structural system with the advantages of requiring a small number of sensors. Reference (Shi, Law and Xu 2009) has investigated damping in systems of multiple DOFs based on the Hilbert transform and the empirical mode decomposition with forced vibration response data. The methodology is verified with the simulation of a 2-DOFs system and a four-storey shear frame structure. Reference (Shi, Law and Li 2007) also conducted the time-varying damping identification with the subspace-based method and a 2-DOFs lump mass model is numerically studied to verify the proposed method. Fluctuations are found in the time histories of the identified results.

The vibration-based structural health monitoring has become an increasingly attractive research area. Accurate knowledge on the property of the structural system would contribute greatly to the success of the structural health monitoring and vibration-based structural condition assessment. The damping property of a structure will influence the structural health monitoring results at different stages of the service life of the structure. It is noted that the direct identification of each factor in the damping matrix is difficult in a complex structure. Appropriate damping model is therefore necessary for the identification of a complex structural system with a large number of DOFs. Modal damping ratio identification with a time domain method has been proposed (Li and Law 2009) where identification of an abrupt change of the modal damping has been investigated with a moving window applied to the "measured" data. The results for damping in the higher modes, such as the last five modes in the study of Li and Law (2009), are not very accurate even in numerical simulation without measurement noise. This Chapter proposed the time-variant Rayleigh damping and modal damping identification method which could be applied to large scale structural system. The time-variant damping is represented by the Chebyshev polynomial. The proposed method will be verified with numerical studies and laboratory work.

5.2.1 The Iterative Regularization Methods

Many methods have been proposed for the system parameter identification. The parameters can be identified with regularization method which is an efficient tool for the discrete ill-posed inverse problem (Tikhonov 1963; Hansen 1992). One typical type of discrete ill-posed problems is $\mathbf{Ax} = \mathbf{b}$ with $\min\|\mathbf{Ax} - \mathbf{b}\|$. The singular values of matrix $\mathbf{A}$ will be close to zero if the matrix is ill-conditioned. This type of problem is very common in the load assessment and structural parameter identification. An efficient iterative technique is needed for the regularization method as the identified results may diverge due to errors in the initial structural model or measurement noise (Hansen 1992). The Newton's method, Quasi-Newton method, Gauss-Newton method, and Levenberg-Marquardt methods are all suitable (Levenberg 1944; Marquardt 1963; Fan 2003; Dan, Yamashita and Fukushima 2002) for solving an iterative regularization solution, and some of them have good numerical stability with quadratic rate of convergence (Levenberg 1944). But real engineering problems are very different from numerical simulation due to the existence of model errors or measurement noise which affects the stability and convergence of the solution.

Iteration method is usually adopted in the model updating process with Newton's method, Quasi-Newton method, Gauss-Newton method or Levenberg-Marquardt method where the last one is a modified Gauss-Newton method. In Newton's method, the system equation can be written as

$$F(\boldsymbol{\theta}^k) = -J(\boldsymbol{\theta}^k)(\delta\boldsymbol{\theta})^k \tag{5.1}$$

$$\boldsymbol{\theta}^{k+1} = \boldsymbol{\theta}^k + \delta\boldsymbol{\theta}^k \tag{5.2}$$

where $F(\boldsymbol{\theta}^k)$ is the structural response which is a function of the excitation and the system parameters, and k denotes the k th iteration step. $J(\boldsymbol{\theta}^k) = F'(\boldsymbol{\theta}^k)$ is the Jacobian of F at the point $\boldsymbol{\theta}^k$. $F'(\boldsymbol{\theta}^k)$ is the differentiation of structural response with respect to structural parameter vector $\boldsymbol{\theta}$. The response $F(\boldsymbol{\theta}^k)$ can be obtained through the equation of motion of the structural system via the step-by-step time integration. However, there are limitations when the classical Newton method is used in the structural condition assessment. Firstly, the accuracy of identification results is related to the initial values of iteration and the noise level (Li and Law 2009). Secondly, the Jacobian of $\mathbf{F}$ in each iteration step should be a square matrix and nonsingular. However, the identification problem is ill-posed in most cases and $J(\boldsymbol{\theta}^k)$ is not always a square matrix. When this occurs, Gauss-Newton method can be used instead in the form of

$$(J(\boldsymbol{\theta}^k))^T F(\boldsymbol{\theta}^k) = -(J(\boldsymbol{\theta}^k))^T J(\boldsymbol{\theta}^k)(\delta\boldsymbol{\theta}^k) \tag{5.3}$$

Gauss-Newton method also requires the initial values to be close to the solution but this is not practical for real application with uncertainties and model errors particularly in a large scale structural system. The inverse of the matrix $(J(\boldsymbol{\theta}^k))^T J(\boldsymbol{\theta}^k)$ can be obtained from Moore-Penrose inverse when $(J(\boldsymbol{\theta}^k))^T J(\boldsymbol{\theta}^k)$ is singular. Various numerical regularization techniques have been applied to investigate this ill-posed problem, and Equation (5.3) can be written as

$$(J(\boldsymbol{\theta}^k))^T F(\boldsymbol{\theta}^k) = -((J(\boldsymbol{\theta}^k))^T J(\boldsymbol{\theta}^k) + \lambda \mathbf{I})(\delta \boldsymbol{\theta}^k) \tag{5.4}$$

which is usually named as the Tikhonov Regularization. The optimal parameter λ can be sought through the L-curve method or the generalized cross-validation method (Golub, Heath and Wahaba 1979). To find the solution of Equation (5.4) is equivalent to finding the optimal parameter λ in the minimization of the following objective function as

$$J = \left\| F(\boldsymbol{\theta}^k) \right\| + \lambda \left\| \boldsymbol{\theta}^k \right\| \tag{5.5}$$

A fairly accurate solution of Equation (5.1) can be obtained through the regularized Gauss-Newton method. Hansen. (1998) presented this direct regularization method and gave a comparison of numerical results with other ways dependent on the initial value. When there is noise in the measurement or error in the finite element model, the identified result may diverge with an inappropriate regularization parameter leading to an inaccurate solution. The ill-posed problem in practice always needs a constraint to ensure the physical meaning of the identified parameters. Such a constraint has been proposed on the iterative increment (Hassiotis and Garrett 1995). A projected least-squares algorithm for the positive quadratic programming has been implemented by Lai (2005) where the unconstrained minimization solution of the quadratic objective function is firstly computed as the initial value and it is subsequently projected on the boundaries of the constraints.

A general iterative regularization method is proposed in this study with an additional constraint on the identified parameters. New limits are proposed and added to the structural parameter considering the physical meaning. The initial values are all set equal to zero. The unconstrained solution of the objective function is firstly calculated and the summation of solution is projected on the boundary of constraints (Lai 2005; Lin 2007). The subsequent iterations are therefore not dependent on the initial value. The modified iterative method considering the physical meaning of the parameter is shown as

$$\delta\boldsymbol{\theta}^k = -((J(\boldsymbol{\theta}^k))^T J(\boldsymbol{\theta}^k) + \lambda\mathbf{I})^{-1}(J(\boldsymbol{\theta}))^T F(\boldsymbol{\theta}^k) \tag{5.6}$$

$$\boldsymbol{\theta}^{k+1} = \boldsymbol{\theta}^k + diag(\beta)\cdot\delta\boldsymbol{\theta}^k \tag{5.7}$$

where θ^k is the modified iterative vector and $diag(\beta)$ is a diagonal matrix with

$$\beta_i^k = \begin{cases} (\alpha_{low}\theta_{r,i}\text{-}\theta_i^k)/\delta\theta_i^k & \text{if } \theta_i^k + \delta\theta_i^k < \alpha_{low}\theta_{r,i} \\ 1 & \text{if } \alpha_{low}\theta_{r,i} < \theta_i^k + \delta\theta_i^k < \alpha_{up}\theta_{r,i} \\ (\alpha_{up}\theta_{r,i} - \theta_i^k)/\delta\theta_i^k & \text{if } \theta_i^k + \delta\theta_i^k > \alpha_{up}\theta_{r,i} \end{cases} \tag{5.8}$$

and α_{low} and α_{up} denote the lower and upper fractions to define the limits of the constraint on the summation of the solution, and their selection would affect the convergence rate of computation. k denotes the number of the iteration step and i denotes the i th factor in the diagonal matrix. $\theta_{r,i}$ is the ith factor in the reference vector, which can be defined or determined according to the real problem under study. The above constraint can be generalized as

$$\gamma = \begin{cases} 1 & \text{if } \max(\boldsymbol{\theta}^{k+1}) < \theta_{up} \text{ and } \min(\boldsymbol{\theta}^{k+1}) > \theta_{low} \\ \dfrac{\alpha}{\max(\dfrac{\max(\boldsymbol{\theta}^{k+1}) - \theta_{up}}{\delta\boldsymbol{\theta}^k}, \dfrac{\theta_{low} - \min(\boldsymbol{\theta}^{k+1})}{\delta\boldsymbol{\theta}^k})} & \text{or else} \end{cases} \tag{5.9}$$

where γ is a scalar coefficient on the increment in an iteration instead of $diag(\beta)$ in Equation (5.7). $\theta_{up} = \alpha_{up}\theta_r$ is the upper limit and $\theta_{low} = \alpha_{low}\theta_r$ is the lower limit of the constraint respectively. α is a coefficient less than unity and equals to 0.5 in simulations of this Chapter. The convergence property with the constraint in Equations (5.8) and (5.9) has been demonstrated by Fletcher (1987). The proposed iterative regularization method with new limits considering the physical meaning of parameter as described in Equations (5.6) to (5.9) will be applied to identify the damping of the structure in the following studies.

The error of the converged solution for Equation (5.1) can be written as

$$\mathbf{x}_{error} = \mathbf{x}_{mea} - \mathbf{x}_{cal} \tag{5.10}$$

where $\mathbf{x}_{mea}$ is the measured response from the structure, $\mathbf{x}_{cal} = F(\boldsymbol{\theta})$ is the calculated response from the updated parameters of the structural system and $\mathbf{x}_{error}$ is the vector of difference between the measured response and the re-constructed response.

Different damping models are reviewed in the following paragraphs. Structural responses based on these damping models are calculated from the equation of motion of the structure and they are subsequently used in the inverse analysis of damping identification. The stiffness and mass matrices of the structural system are assumed unchanged in the following studies.

5.2.2 The Time-invariant Rayleigh Damping

As the equation of motion, classical Rayleigh damping is assumed as a linear combination of the stiffness and mass matrices with the form $\mathbf{C} = a_1\mathbf{M} + a_2\mathbf{K}$, where a_1 and a_2 are the coefficients of Rayleigh damping. Performing differentiation to both sides of Equation (5.11) with respect to the parameters a_i, we have

$$\mathbf{M}\frac{\partial \ddot{\mathbf{x}}}{\partial a_1}+(a_1\mathbf{M}+a_2\mathbf{K})\frac{\partial \dot{\mathbf{x}}}{\partial a_1}+\mathbf{K}\frac{\partial \mathbf{x}}{\partial a_1}=-\mathbf{M}\dot{\mathbf{x}} \tag{5.11}$$

$$\mathbf{M}\frac{\partial \ddot{\mathbf{x}}}{\partial a_2}+(a_1\mathbf{M}+a_2\mathbf{K})\frac{\partial \dot{\mathbf{x}}}{\partial a_2}+\mathbf{K}\frac{\partial \mathbf{x}}{\partial a_2}=-\mathbf{K}\dot{\mathbf{x}} \tag{5.12}$$

The responses of the structure are calculated from equation of motion. The sensitivities $\partial\ddot{\mathbf{x}}/\partial a_i$, $\partial\dot{\mathbf{x}}/\partial a_i$ and $\partial\mathbf{x}/\partial a_i$ with respect to the Rayleigh damping coefficients can then be solved by step-by-step time integration Newmark-β method from Equations (5.11) and (5.12). Equation (5.6) can therefore be rewritten as

$$\begin{bmatrix}\delta a_1\\ \delta a_2\end{bmatrix}=\left(\left[\frac{\partial \ddot{\mathbf{x}}}{\partial a_1}\ \frac{\partial \ddot{\mathbf{x}}}{\partial a_2}\right]^T\left[\frac{\partial \ddot{\mathbf{x}}}{\partial a_1}\ \frac{\partial \ddot{\mathbf{x}}}{\partial a_2}\right]+\lambda\mathbf{I}\right)^{-1}\left(\left[\frac{\partial \ddot{\mathbf{x}}}{\partial a_1}\ \frac{\partial \ddot{\mathbf{x}}}{\partial a_2}\right]^T(\ddot{\mathbf{x}}_{mea}-\ddot{\mathbf{x}}_{cal})\right) \tag{5.13}$$

Since the i th modal damping ratio of the structure ξ_i should be larger than zero, the constraint in Equation (5.9) on the vector $[a_1\ a_2]^T$ is given as follows:

$$\gamma=\begin{cases}1 & \text{if}\ \ \max(\xi^{k+1})<\xi_{up}\ \text{and}\ \min(\xi^{k+1})>\xi_{low}\\ \dfrac{\alpha}{\max\left(\left(\dfrac{\max(\xi^{k+1})-\xi_{up}}{\delta\xi^k}\right),\dfrac{\xi_{low}-\min(\xi^{k+1})}{\delta\xi^k}\right)} & \text{or else}\end{cases} \tag{5.14}$$

where ξ_i is the i th modal damping ratio, ξ_{low} and ξ_{up} are the lower and upper limits and they are set equal to 0.0 and 1.0 respectively in this Chapter. It is noted that a structure cannot take up a negative damping nor an over-damped structure would exist in nature. The initial values of a_1 and a_2 are equal to zero. The constraint in Equation (5.14) ensures the physical meaning of the Rayleigh damping and the modal damping ratio is not lost in the updating process, i.e. the identification result can always give a positive modal damping ratio.

5.2.3 The Time-variant Rayleigh Damping

The Rayleigh coefficients are assumed as time-variant with

$$\mathbf{C}(t) = a_1(t)\mathbf{M} + a_2(t)\mathbf{K} \tag{5.15}$$

and the time history of the coefficients are modeled by the Chebyshev orthogonal polynomial as

$$\mathbf{a}(t) = \mathbf{c}\mathbf{T}(\mathrm{t}) \tag{5.16}$$

$$\mathbf{T}(t) = \begin{bmatrix} \mathbf{T}_1(t)\mathbf{M} \\ \mathbf{T}_2(t)\mathbf{K} \end{bmatrix} \tag{5.17}$$

where $a_1(t) = \sum_{m=1}^{N_m} c_{m,1} T_{m,1}(t)$, $a_2(t) = \sum_{m=1}^{N_m} c_{m,2} T_{m,2}(t)$, N_m is the number of terms of the polynomial, $\mathbf{c}$ is the coefficient matrix, $T_{m,1}$ and $T_{m,2}$ are the time basis of the orthogonal polynomial for $a_1(t)$ and $a_2(t)$ and $\mathbf{a}=[a_1\ a_2]^{\mathrm{T}}$ is a vector of the Rayleigh damping coefficients.

The equation of motion of the structure can be written as

$$\mathbf{M}\ddot{\mathbf{x}}(t) + (\sum_{m=1}^{N_m} c_{m,1} T_{m,1}(t)\mathbf{M} + \sum_{m=1}^{N_m} c_{m,2} T_{m,2}(t)\mathbf{K})\dot{\mathbf{x}}(t) + \mathbf{K}\mathbf{x}(t) = \mathbf{L}\mathbf{F}(t) \tag{5.18}$$

Performing differentiation to both sides of Equation (5.18) with respect to $c_{m,i}$, we have

$$\mathbf{M}\frac{\partial \ddot{\mathbf{x}}(t)}{\partial c_{m,1}} + \sum_{m=1}^{Nm}(c_{m,1}T_{m,1}(t)\mathbf{M} + c_{m,2}T_{m,2}(t)\mathbf{K})\frac{\partial \dot{\mathbf{x}}(t)}{\partial c_{m,1}} + \mathrm{K}\frac{\partial \mathbf{x}(t)}{\partial c_{m,1}} = -T_{m,1}(t)\mathbf{M}\dot{\mathbf{x}}(t) \tag{5.19}$$

$$\mathbf{M}\frac{\partial \ddot{\mathbf{x}}(t)}{\partial c_{m,2}} + \sum_{m=1}^{Nm}(c_{m,1}T_{m,1}(t)\mathbf{M} + c_{m,2}T_{m,2}(t)\mathbf{K})\frac{\partial \dot{\mathbf{x}}(t)}{\partial c_{m,2}} + \mathbf{K}\frac{\partial \mathbf{x}(t)}{\partial c_{m,2}} = -T_{m,2}(t)\mathbf{K}\dot{\mathbf{x}}(t) \tag{5.20}$$

The responses of the structure are calculated from equation of motion. The sensitivities $\partial \ddot{\mathbf{x}}(t)/\partial c_{m,i}$, $\partial \dot{\mathbf{x}}(t)/\partial c_{m,i}$ and $\partial \mathbf{x}(t)/\partial c_{m,i}$ with respect to the

Chebyshey polynomial coefficients can then be solved by step-by-step Newmark-β integration method from Equations (5.19) and (5.20). Equation (5.6) can be rewritten for this case as

$$\delta\mathbf{c} = ((\frac{\partial\ddot{\mathbf{x}}}{\partial\mathbf{c}})^T \frac{\partial\ddot{\mathbf{x}}}{\partial\mathbf{c}} + \lambda\mathbf{I})^{-1}((\frac{\partial\ddot{\mathbf{x}}}{\partial\mathbf{c}})^T (\ddot{\mathbf{x}}_{mea} - \ddot{\mathbf{x}}_{cal})) \tag{5.21}$$

It is noted that the damping of the structure can be written in a more convenient form as

$$\mathbf{C} = (\mathbf{\Phi}^T)^{-1} \begin{bmatrix} \ddots & & \\ & 2\xi_n\omega_n & \\ & & \ddots \end{bmatrix} \mathbf{\Phi}^{-1} \tag{5.22}$$

where $\mathbf{\Phi}$ is the mode shape matrix, ω_n is the angular frequency for the nth mode of the structure. The time-varying damping model can be modeled, in general, as follows for the damping identification. In the k+1th iterative step, the modal damping ratio can be represented as

$$\boldsymbol{\xi}^{k+1} = \boldsymbol{\xi}^k + \delta\boldsymbol{\xi}^k \tag{5.23}$$

where $\delta\xi^k$ is the iterative increment of the modal damping ratio vector at the kth step, which can be written according Equation (5.22) as

$$\delta\boldsymbol{\xi}^k = \mathbf{\Phi}^T(\delta\mathbf{c}\,\mathbf{T}(t))\mathbf{\Phi} \begin{bmatrix} \ddots & & \\ & 1/(2\omega_n) & \\ & & \ddots \end{bmatrix} \qquad (n = 1, 2 \cdots Ndof) \tag{5.24}$$

where $\delta\mathbf{c}$ is expressed in Equation (5.21) and $Ndof$ is the number of DOFs of the structure. The constraint on the modal damping ratio can also be defined as Equation (5.14), and the iterative formulation can be modified according to Equation (5.7) as

$$\mathbf{c}^{k+1} = \mathbf{c}^k + \gamma\,\delta\mathbf{c}^k \tag{5.25}$$

It should be noted that the time-variant Rayleigh damping model can also represent the time-invariant Rayleigh damping as there is a time constant term in the Chebyshev polynomial.

5.2.4 Time-variant Modal Damping

If the structural damping is described in terms of more than two modes, i.e. it is assumed as the general form of the Cauchy damping with

$$\mathbf{C} = \mathbf{M}\sum_{l=0}^{J-1} a_l [\mathbf{M}^{-1}\mathbf{K}]^l \tag{5.26}$$

where a_l is the lth coefficient of the Caughey damping. The sensitivity of response of the structure with respect to the coefficients of Caughey damping can be derived based on the equation of motion as

$$\mathbf{M}\frac{\partial \ddot{\mathbf{x}}}{\partial a_l} + (\mathbf{M}\sum_{l=0}^{J-1} a_l [\mathbf{M}^{-1}\mathbf{K}]^l)\frac{\partial \dot{\mathbf{x}}}{\partial a_l} + \mathbf{K}\frac{\partial \mathbf{x}}{\partial a_l} = -\mathbf{M}[\mathbf{M}^{-1}\mathbf{K}]^l \dot{\mathbf{x}} \tag{5.27}$$

However, there is a high possibility that an inappropriate Caughey damping coefficient may lead to negative modal damping ratios of the structure.

Modal damping is a more general damping model and is briefly described in this section for damping identification. Time-invariant modal damping identification has been investigated previously (Li and Law 2009) and it is expressed in terms of the mode shape matrix and modal damping ratios as

$$\mathbf{C} = \mathbf{M}(\sum_{n=1}^{Ndof} \frac{2\xi_n \omega_n}{\mathrm{M}_n} \mathbf{\Phi}_n \mathbf{\Phi}_n^T)\mathbf{M} \tag{5.28}$$

where Φ_n and $\mathbf{M}_n$ are the n th mode shape vector and modal mass respectively. The modal damping of the structure can be assumed as time-variant damping represented as

$$\mathbf{C}(t) = \mathbf{M}(\sum_{n=1}^{Ndof} \frac{2\xi_n(t)\omega_n}{M_n} \mathbf{\Phi}_n \mathbf{\Phi}_n^T)\mathbf{M} \tag{5.29}$$

with

$$\xi_n(t) = \sum_{m=1}^{N_m} (c_{m,n} T_{m,n}(t)) \tag{5.30}$$

or

$$\boldsymbol{\xi}(t) = \mathbf{c}\mathbf{T}_{\mathrm{m}}(t) \tag{5.31}$$

where $\xi_n(t)$ is the n th time-variant modal damping ratio. $\mathbf{c}$ is a matrix of the Chebyshev Polynomial coefficients and $\mathbf{T}_m(t)$ is a matrix of the Chebyshev Polynomial. The sensitivity of the response of the structure with respect to the coefficients $c_{m,n}$ of the modal damping ratio can be derived based on the equation of motion as

$$\mathbf{M}\frac{\partial \ddot{\mathbf{x}}}{\partial c_{m,n}} + \mathbf{C}(t)\frac{\partial \dot{\mathbf{x}}}{\partial c_{m,n}} + \mathbf{K}\frac{\partial \mathbf{x}}{\partial c_{m,n}} = -\frac{\partial \mathbf{C}(t)}{\partial c_{m,n}}\dot{\mathbf{x}} \tag{5.32}$$

The sensitivity of the damping matrix can be computed as

$$\frac{\partial \mathbf{C}(t)}{\partial c_{m,n}} = \mathbf{M}(\frac{2T_{m,n}(t)}{M_n}\omega_n \mathbf{\Phi}_n \mathbf{\Phi}_n^T)\mathbf{M} \tag{5.33}$$

Based on the sensitivity matrix $\partial \ddot{\mathbf{x}} / \partial c_{m,n}^n$ with respect to the coefficients, the time-variant Chebyshev polynomial coefficients can be calculated through the iterative regularization method as shown in Equation (5.6) which is rewritten for this case as

$$\delta \mathbf{c} = ((\frac{\partial \ddot{\mathbf{x}}}{\partial \mathbf{c}})^T \frac{\partial \ddot{\mathbf{x}}}{\partial \mathbf{c}} + \lambda \mathbf{I})^{-1} (\frac{\partial \ddot{\mathbf{x}}}{\partial \mathbf{c}})^T (\ddot{\mathbf{x}}_{mea} - \ddot{\mathbf{x}}_{cal}) \tag{5.34}$$

Since

$$\delta \boldsymbol{\xi}^{k} = \delta \mathbf{c}^{k} \ \mathbf{T}_{m}(t) \tag{5.35}$$

and the iterative procedure can be implemented similar to Equation (5.25) as

$$\mathbf{c}^{k+1} = \mathbf{c}^{k} + \gamma \ \delta \mathbf{c}^{k} \tag{5.36}$$

It should be noted that modal damping is equivalent to Caughey damping when the number of parameters of Caughey damping is equal to the number of the DOFs of the structure.

5.2.5 Numerical Simulation Studies

A nine-bay cantilever space frame structure is investigated numerically with the three damping models described in Sections 5.2.2 to 5.2.4 to illustrate the effectiveness of the proposed iterative regularization identification method. The space frame consists of 69 three-dimensional Euler-Bernoulli beam elements and 29 nodes each of which has six DOFs as shown in Figure 5.1. The total number of DOFs of the structure is 178. The structural members are rigidly joined together. The distance between the centers of each pair of adjacent nodes is 0.5m. The whole cantilever space frame structure is joined to a rigid support at three nodes. Large stiffnesses of 10^6kN/m and 10^6kN-m/rad are used to model the translational and rotational flexibilities at the support DOFs. The property of material of the structure is shown in Table 5.1 and the first 8 natural frequencies are 5.141, 10.935, 15.066, 19.841, 27.566, 39.746, 52.553 and 60.618Hz respectively. The mode shapes are referred to reference of Li and Law (2008). Free vibration of the structure was obtained by a sudden release of a 3.72 kg mass hanging at Node 29 of the structure. The sampling rate is 1000Hz and one second of acceleration record is used for the simulation studies except otherwise stated.

5.2.5.1 Time-invariant Rayleigh Damping Identification

The damping of the structure is assumed as time-invariant Rayleigh damping and is calculated from the first two modal frequencies and modal damping ratios as

$$\begin{bmatrix} a_1 \\ a_2 \end{bmatrix} = 2\begin{bmatrix} 1/\omega_1 & \omega_1 \\ 1/\omega_2 & \omega_2 \end{bmatrix}^{-1}\begin{bmatrix} \xi_1 \\ \xi_2 \end{bmatrix} \tag{5.37}$$

where ξ_1 and ξ_2 are the first two modal damping ratios assumed as 0.05. The response of the structure in the forward problem is then calculated through the step-by-step time integration method. The calculated vertical response at Node 18 serves as the 'measured' response in the inverse problem of damping identification.

The error of identification is defined as

$$error_{Ray} = \left\| coeff_{id} - coeff_{real} \right\| / \left\| coeff_{real} \right\| \times 100\% \tag{5.38}$$

where $coeff_{id}$ is the vector of identified Rayleigh coefficients and $coeff_{real}$ is the vector of real set of Rayleigh coefficients. Two cases, without and with 10% white noise in the calculated acceleration, are studied and the error of identification calculated from Equation (5.38) are respectively 4.97×10^{-5}% and 0.76%. Figure 5.2 shows the curves of real and reconstructed responses at Node 18 with updated damping and they are almost overlapping even in the case with

10% white noise in the measurement. The Rayleigh damping can be identified with high accuracy even with 10% noise in the measurement.

5.2.5.2 Time-variant Rayleigh Damping Identification

In this section, two time-variant Rayleigh damping models are explored. The time varying Rayleigh damping coefficients are modeled in the forward problem as

$$a_{tva,n}(t) = a_{tin,n} \sum_{m=1}^{N_m} c_{m,n} T_{m,n}(t) \tag{5.39a}$$

$$c_{m,n} = (1+\frac{m}{30}) \times \frac{1}{10^{1.5(m-1)}} \tag{5.39b}$$

where $a_{tin,n}$ is the n th factor of the of Rayleigh damping coefficient vector calculated from Equation (5.37), $a_{tva,n}$ is the n th factor of the time-variant Rayleigh damping coefficient vector. The second term on the right-hand-side of Equation (5.39b) ensures the damping value is higher for higher order terms; the second term ensures the fluctuation for higher order terms will be decreasing. The resulting Rayleigh damping coefficients are increasing monotonously as shown in Figure 5.3. The influence of higher order terms in Equations (5.39a) and (5.39b) is constrained with increasing value of m and the time histories of the Rayleigh damping coefficients are close to a quadratic function. N_m is taken equal to six, and a one second record of the acceleration from Node 18 serves as the 'measured' response. Similarly, the 'measured' acceleration and the acceleration calculated from the identified damping with and without noise are shown in Figure 5.4. The error of the re-constructed acceleration is very small when there is 10% white noise in the measurement and the reconstructed acceleration and the 'measured' response are nearly overlapping. The norm of errors between the re-constructed response and the 'measured' response calculated from Equation (5.38) are 8.616×10^{-4}% and 14.69% for the cases without and with 10% noise respectively. These results show that the time-variant assumption on damping may be a more general damping model for identification though the measurement noise would influence the identification result much more than that obtained from the time-invariant Rayleigh damping model. The damping can be identified but with a slightly reduced accuracy which may be due to the large number of terms to be identified in the time-variant damping model.

Next, the time-variant Rayleigh damping is represented with a fast-varying representation as shown in Figure 5.5 for the two coefficients. The fluctuating time histories of the Rayleigh damping coefficients should ideally need more terms in the Chebyshev polynomial for representation (N_m equals to 6 in this study) and they are subsequently taken as unknowns in the inverse problem. The error between the identified time-variant Rayleigh damping and the real damping are 9.05×10-4% and 15.12% for the cases without noise and with 10% noise respectively.

5.2.5.3 Time-variant Modal Damping Identification

In this section, three types of time-variant modal damping models are explored. The sampling rate is changed to 200 Hz. The time-variant modal damping is modeled for the study as

$$\xi_n(t) = \sum_{m=1}^{N_m} c_{m,n} T_{m,n}(t) \tag{5.40a}$$

$$c_{m,n} = (0.05 + \frac{(n-1)^2}{1000}) \times (1 + \frac{m-1}{40}) \times \frac{1}{10^{1.5(m-1)}} \tag{5.40b}$$

where n denotes the n th mode and m denotes the m th term of the Chebyshev polynomial. The first term on the right-hand-side of Equation (5.40b) ensures the damping value does not deviate too much from 0.05; the second term ensures the damping value is higher for higher order terms; the last term ensures the fluctuation for higher order terms will be decreasing. Each modal damping ratio increases monotonously with time as shown in Figure 5.6 for the first eight modes. This form of modeling the damping ratio in Equations (5.40a) and (5.40b) can reduce the contribution of higher order terms of the Chebyshev polynomial in the time-variant modal damping which ensures a monotonous increase of the damping ratio with time.

Case 1

The first eight modal damping are targeted for identification and the remaining higher modal damping is assumed constant at zero. The error of damping ratio in identification is calculated as

$$error_{ratio,im} = \left\| DR_{id,im} - DR_{real,im} \right\| / \left\| DR_{real,im} \right\| \times 100\% \tag{5.41}$$

where $DR_{id,im}$ is the identified damping ratio of the im th mode and $DR_{real,im}$ is the real modal damping of the im th mode. Only the damping ratio of vertical mode can be identified from the 'measured' vertical acceleration at Node 18 and the error of identification is shown in Table 5.2.

The error of identification from vertical responses at Nodes 18 and 23 is shown in Table 5.3. The ‘measured’ vertical response from Node 18 of the structure and the re-constructed response at the same DOF based on the identified damping ratio are shown in Figure 5.7 showing some large errors at the peaks of the response curves when there is 10% noise. The convergence curves are shown in Figure 5.8 with and without 10% noise in the measurement. The error in acceleration is calculated as $error = \|\ddot{\mathbf{x}}_{mea} - \ddot{\mathbf{x}}_{cal}\| / \|\ddot{\mathbf{x}}_{mea}\| \times 100\%$. The error of identification reduces monotonically when there is no noise in the measurement while it fluctuates with decreasing magnitude at increasing iterative step when there is measurement noise. All the above results show that the time-variant modal damping can be identified accurately with the proposed iterative regularization method. Moreover, it should be noted that the time-variant modal damping identification method can also be applied to identify the time-invariant damping in practice.

Case 2

In this case only the modal damping ratios of the first fifteen modes are considered in the identification and the damping ratios of the other higher modes are assumed to be zeros. The error of identification for each modal damping calculated from Equation (5.41) is shown in Figure 5.9 when there is no noise in the measurement. The damping ratios of the first fifteen modes are identified very accurately. This indicates that the proposed method can detect the higher order modal damping even though they have very small participation in the structural response.

Case 3

A fluctuating modal damping ratio is studied in which the damping ratio is slow-varying but increasing with time. The time histories of the first eight modal damping ratios are shown in Figure 5.10 and the remaining higher modal damping is assumed constant at zero. The 'measured' response for the identification is the vertical acceleration at Nodes 18 and 23. The error of identification calculated according to Equation (5.41) between the identified damping ratio and the real modal damping is respectively 8.76×10^{-7}% and 8.13% for the cases without noise and with 10% white noise in the measurement.

5.3 Time-variant Stiffness Identification with Uncertainty in Structure

A structure may suffer from abrupt damages when under severe earthquake and some structural components may perform nonlinearly. It is therefore important to evaluate the condition of structural components and the load bearing capacity of the structural system after the earthquake. However, it is difficult to judge when and where the damage occurs based on the measurements from the structural system. It is also a tough work to assess the severity of the damage. Moreover, the measurement is always polluted by noise and the analysis results are commonly influenced by model error.

Sensitivity methods in time domain have been investigated and applied extensively for time-invariant parameter identification of linear structures. The sensitivity matrix of response with respect to the structural parameters is derived to locate and quantify the damage (Li and Law 2010) or damping ratio in reference (Lu and Law 2007). It has been demonstrated that only a few sensors are needed for the damage detection with the sensitivity method in time domain. The simultaneous identification of the external excitation and the local damage has been implemented by Lu and Law with sensitivity method (Ding and Law 2011). Time-variant damping ratio identification method has been presented with Chebyshev polynomial or a moving time window by Li and Law (2010). However, these literatures did not consider the non-zero initial structural response or the nonlinearity of structure, both of which would influence the identification result. In this Section, a method will be proposed to identify the time-variant parameters including the linear components and nonlinear components.

A new time window identification method was proposed in Section 4.4.2 without the information of initial structural response for time-invariant linear system. In this Section, the time window identification method will be extended to apply to the time-variant structure even the structure with bilinear components. The time history of measured acceleration is divided into short non-overlapping time windows. The initial structural responses are unknown and the structural parameters are assumed to be invariant in each of these short time windows. This idea originates from the average acceleration step-by-step integration method. A new two-phase identification strategy is developed to ensure the physical meaning and convergence of the proposed identification algorithm. In the first phase, the initial structural response is identified with the Tikhonov regularization method and in the second phase, the structural parameter is identified with a modified adaptive regularization method. Three types of structures subject to seismic ground motion are investigated to validate the proposed method, i.e. a linear shear frame with abrupt damage, a linear shear frame with nonlinear base isolation on the first floor and a shear frame with seismic resisting bracing on each floor.

5.3.1 Sensitivity Method for the Time-variant Structural Parameters Identification

5.3.1.1 Discrete Time History of Time-variant Structural Parameter

The structural parameter is always time-variant during a seismic event or under the strong wind. Considering the time-variant stiffness of the structural system, the equation of motion can be written as

$$\mathbf{M}\ddot{\mathbf{x}}(t)+\mathbf{C}\dot{\mathbf{x}}(t)+\mathbf{K}(t)\mathbf{x}(t)=-\mathbf{MG}\ddot{x}_g(t) \tag{5.42}$$

where $\ddot{\mathbf{x}}(t)$, $\dot{\mathbf{x}}(t)$, $\mathbf{x}(t)$, $\mathbf{K}$(t) and $\ddot{\mathbf{x}}_g(t)$ are all time-variant. When the stiffness of the structure is nonlinear, Equation (5.42) could be written as

$$\mathbf{M}\ddot{\mathbf{x}}(t)+\mathbf{C}\dot{\mathbf{x}}(t)+\mathbf{K}(t,x)\mathbf{x}(t)=-\mathbf{MG}\ddot{x}_g(t) \tag{5.43}$$

The continuous equation of motion of the structural system could be discretized in the nth short time window and the equation of motion can be written as

$$\mathbf{M}\ddot{\mathbf{x}}(t)_n + \mathbf{C}\dot{\mathbf{x}}(t)_n + \mathbf{K}(t,x)_n \mathbf{x}(t)_n = -\mathbf{M}\mathbf{G}\ddot{x}_g(t)_n \tag{5.44}$$

where subscript n denotes the nth time window. In this study, it is assumed that the structural parameter is a constant in each short time window.

5.3.1.2 Identification in a Time Window

A general method is presented in this section to identify the initial structural responses and parameter in each time window. The time history responses $\mathbf{Y}$ is a function of the initial structural response $\mathbf{Y}_0$, external force $\mathbf{F}$ and structural parameter $\boldsymbol{\alpha}$. The response vector can therefore be represented as

$$\mathbf{Y} = \boldsymbol{f}(\mathbf{Y}_0, \mathbf{F}, \boldsymbol{\alpha}) \tag{5.45}$$

The responses of the structure can be considered as the summation of free vibration due to the non-zero initial responses and the forced vibration in each time segments. Equation (5.45) can be rewritten as

$$\mathbf{Y}_{\boldsymbol{m}} = \mathbf{Y}_{\boldsymbol{fr}} + \mathbf{Y}_{\boldsymbol{fo}} = \boldsymbol{g}(\mathbf{Y}_0, \boldsymbol{\alpha}) + \boldsymbol{h}(\mathbf{F}, \boldsymbol{\alpha}) \tag{5.46}$$

where subscript m denotes the measured response, $\mathbf{Y}_{fr} = \boldsymbol{g}(\mathbf{Y}_0,\boldsymbol{\alpha})$ and $\mathbf{Y}_{fo} = \boldsymbol{h}(\mathbf{F}, \boldsymbol{\alpha})$ are respectively the responses of free vibration and forced vibration response. Considering the free vibration only, the initial structural response could be represented as the summation of all mass-normalized mode shapes of the structure which is the same as Equation (4.23). Considering the structural model error the total response as shown in Equation (5.46) due to free vibration and forced vibration of the structure could be represented as

$$\mathbf{Y}_m = \mathbf{Y}_{fo} + \mathbf{Y}_{ini}\boldsymbol{\beta} + \mathbf{S}\Delta\boldsymbol{\alpha} \tag{5.47}$$

where $\mathbf{Y}_{ini}$ is the free vibration response vector of the structure arising from the vector of initial response at all dofs of the structure. Equation (5.47) can be written as

$$\mathbf{Y}_m - \mathbf{Y}_{fo} = \begin{bmatrix} \mathbf{Y}_{ini} & \mathbf{S} \end{bmatrix} \begin{bmatrix} \boldsymbol{\beta} \\ \Delta\boldsymbol{\alpha} \end{bmatrix} \tag{5.48}$$

It is noted that the unknown vector on the right-hand-side of Equation (5.48) consists of the coefficient vector $\boldsymbol{\beta}$ and the stiffness change coefficients. A two phase algorithm is proposed in next section for the identification of these unknown parameters.

5.3.2 Identification with Modified Adaptive Regularization Method

Iterative regularization methods are usually adopted in practical inverse problems, such as model updating and force identification. The problem in Equation (5.48) could be directly solved by iterative Tikhonov regularization with the following objective function

$$J(\Delta\boldsymbol{\alpha}^{k+1}, \boldsymbol{\beta}^{k+1}, \lambda) = \left\| \mathbf{Y}_{fr}^{k} \boldsymbol{\beta}^{k+1} + \mathbf{S}^{k} \Delta\boldsymbol{\alpha}^{k+1} - \Delta\ddot{\mathbf{x}}^{k} \right\|^2 + \lambda^2 \left\| \begin{bmatrix} \boldsymbol{\beta}^{k+1} & \Delta\boldsymbol{\alpha}^{k+1} \end{bmatrix}^T \right\|^2 \tag{5.49}$$

where $\mathbf{S}$ is the sensitivity matrix calculated from Equation (4.6) in Chapter 4 and k denotes the kth iteration of the identification. Inverse problem is always ill-posed and measurement noise may have adverse effect in the process of model updating. But the convergence and physical meaning of structural parameters cannot be guaranteed due to the adverse influence of measurement noise.

A two phase identification algorithm is described as follows. The initial structural response is identified in the first phase while the structural parameter is identified in the second phase. Therefore, the iterative Tikhonov regularization method is directly applied with the objective function

$$J(\Delta\boldsymbol{\beta}^{k+1},\lambda)=\left\|\mathbf{Y}_{fr}^{k}\boldsymbol{\beta}^{k+1}-\Delta\ddot{\mathbf{x}}^{k}\right\|^{2}+\lambda^{2}\left\|\boldsymbol{\beta}^{k+1}\right\|^{2} \tag{5.50}$$

A modified adaptive regularization method is utilized in the second phase. An adaptive regularization method has been proposed as presented by Li and Law (2010) with an adaptive limit on the summation of the identified changes based on results of last iteration steps. The objective function of optimization in the model updating is expressed as

$$J(\Delta\boldsymbol{\alpha}^{k+1},\lambda_{\alpha})=\left\|\mathbf{S}^{k}\Delta\boldsymbol{\alpha}^{k+1}-\Delta\ddot{\mathbf{x}}^{k}\right\|+\lambda_{\alpha}{}^{2}\left\|\sum_{i=1}^{k+1}\Delta\boldsymbol{\alpha}^{i}-\boldsymbol{\alpha}^{k,*}\right\| \tag{5.51}$$

where $\boldsymbol{\alpha}^{k,*}$ is a value to coordinate the constraint of the solution in the i th iteration in the damage detection process. Parameter $\boldsymbol{\alpha}^{k,*}$ can be defined as

$$(\alpha^{k,*})_{j}=\begin{cases}0 & \text{if } \left(\sum_{i=1}^{k}\Delta\alpha^{k}\right)_{j}>0\\ \left(\sum_{i=1}^{k}\Delta\alpha^{k}\right)_{j} & \text{if } \left(\sum_{i=1}^{k}\Delta\alpha^{k}\right)_{j}<0\end{cases} \tag{5.52}$$

where the subscript j denotes the j th element of the structure. $\left(\sum_{i=1}^{k}\Delta\alpha^{k}\right)_{j}$ is the cumulative identified change of stiffness. The local damage can then be detected iteratively with the obtained optimal parameter λ_{a}^{2} as

$$\begin{aligned}\Delta\boldsymbol{\alpha}^{k+1}&=\left(\left(\frac{\partial\ddot{\mathbf{x}}}{\partial\boldsymbol{\alpha}^{k}}\right)^{T}\frac{\partial\ddot{\mathbf{x}}}{\partial\boldsymbol{\alpha}^{k}}+\lambda_{a}^{2}\mathbf{I}_{\alpha}\right)^{-1}\left(\frac{\partial\ddot{\mathbf{x}}}{\partial\boldsymbol{\alpha}^{k}}\right)^{T}(\ddot{\mathbf{x}}_{m}^{k}-\ddot{\mathbf{x}}^{k})\\ \boldsymbol{\alpha}_{k+1}&=\boldsymbol{\alpha}_{k}+\Delta\boldsymbol{\alpha}^{k}\end{aligned} \tag{5.53}$$

However, this method could only detect the changes of the structure with a fairly accurate initial analytical model. If there is positive model error involved, they cannot be identified with this method as noted in Equations (5.51) and (5.52). It is assumed in this study that the Young's modulus of material follows a normal distribution, and the parameter is simulated in the same way as the uncertainties of measurement as shown in Equation (3.39). The standard deviation of Young's modulus is taken to be 0.05 times of its mean value in this study. The above adaptive regularization method is modified to take care of the model errors. The initial stiffness of the structural elements is increased by a positive factor of 1.3 such that the identified stiffness change will all have negative values. The adaptive regularization method could then be applied for damage detection via model updating with different values of initial model errors.

5.3.3 Implementation Procedure

Step 1: Obtain the mass, damping and stiffness matrices of the initial structural model, which may be inaccurate.

Step 2: Conduct measurement on the structure.

Step 3: Divide the measurement time history into different non-overlapping short time segments.

Step 4: Identify initial structural response of the first time segment with Tikhonov regularization method.

Step 5: Identify structural parameter with the proposed modified adaptive regularization method in the first segment.

Step 6: Repeat Steps 4 and 5 until the following convergence criteria are met.

$$\left\| \frac{\Delta\boldsymbol{\alpha}_{k+1} - \Delta\boldsymbol{\alpha}_k}{\Delta\boldsymbol{\alpha}_{k+1}} \right\| \le Tol_1 \text{ and } \left\| \frac{\boldsymbol{\beta}_{k+1} - \boldsymbol{\beta}_k}{\boldsymbol{\beta}_{k+1}} \right\| \le Tol_2 \tag{5.54}$$

where k denotes the number of iteration and Tol_1 and Tol_2 are the prescribed value which are taken as 10^{-4} for all studies in this work.

Step 7: Repeat Steps 4 to 6 for the next time segment. The responses at the last time instant of the last time segment are taken as the initial estimation of the initial responses of the new time segment.

5.3.4 Numerical Simulation Studies

There are three cases of time-variant parameter identification studied in this Section, one of which is a linear frame with abrupt damage and the other two cases are for a linear frame with nonlinear dissipative components. The mass of each storey is 4×10^5 kg and the stiffness of each floor is 2×10^8 N/m. The base excitation is the earthquake ground motion record of N-S El-Centro (1940) with the peak ground acceleration scaled to 0.3g. The sampling rate of measurement is 2000Hz. There are 800 sampling points in each time window and of 0.4 s duration there are 75 windows in the whole time duration. When there is noise in the "measured" response, the polluted response is simulated by adding a normal random term to the unpolluted structural responses as Equation (3.39) in Chapter 3.

5.3.4.1 Shear Frame with Abrupt Damage

In the first case, a linear shear frame structure described above with

15-storeys and rigid base connection as shown in Figure 5.11 is investigated. A numerical simulation study with 5% initial model error in the FEM modeled as the measurement noise as shown in Equation (3.39) and 20% abrupt reduction of stiffness in the 2^{nd} and 5^{th} floor is conducted. The time of occurrence of the abrupt stiffness reduction is 2s from the beginning of the excitation. The horizontal accelerations at the 3^{rd}, 6^{th} 10^{th} and 15^{th} floor floors are taken as the "measured" responses.

Figures 5.12(a) and 5.12(b) are comparisons of the real stiffness time histories and the identified stiffness time histories of the 2^{nd} and 5^{th} floor. The time of occurrence, location and severity of the abrupt damage could be identified accurately without noise in the measurement. The identified structural stiffness at the end of the 30s duration is shown as Figure 5.13 with very accurate results. Figures 5.14(a) and 5.14(b) gives the comparison of the stiffness time history identification results of the 2^{nd} and 5^{th} floor with 10% measurement noise. The identified damage extent and location are acceptable with 10% measurement noise although there is a large error at the beginning of the time history and some small fluctuations in the stiffness time history. Figure 5.15 shows the identified structural stiffness at the end of the 30s duration when there is 10% measurement noise. It is noted that the error of stiffness identification is a little bit larger than that obtained from measurement without noise.

5.3.4.2 Shear Frame with Nonlinear Seismic Isolations

This case studies the same frame structure described earlier with 10-storeys as shown in Figure 5.16 with additional base isolation to the first floor. A bilinear stiffness model is used to simulate the base isolation with the relationship between the restoring force and horizontal displacement shown in Figure 4.18. The horizontal restoring force of the isolation is defined as Equation (4.32) in Chapter 4 where K_E =2 $\times 10^7$ N/m and d_y =0.01 m. The horizontal acceleration responses at the 3rd, 6th and 10th floor are taken as 'measured' response.

This numerical simulation study also includes initial model error in the finite element model. There is 5% model error but no stiffness reduction in the main structure above the base isolation. Again 30s of measured data divided into 75 short time segments is used for the identification. Figure 5.16 shows that the time history of the nonlinear storey stiffness of the first floor could be identified accurately without measurement noise. But there are some small errors when there is softening effect of the base isolation. Figure 5.17 is the identified result when there is 10% measurement noise. There are notable yet small fluctuations in the identified stiffness time history with large errors at the beginning of the time history. However the identification result is fairly accurate and acceptable. The identification results of time-invariant parameters are not listed and the norm of the identification error of time-invariant parameter is 1.95%.

5.3.4.3 Shear Frame with Nonlinear Seismic Isolations

The linear frame structure described above with 10-storey and bracing member in each floor as shown in Figure 5.18 is investigated. The bracing members are also simulated with a bilinear stiffness model with α_b =0.05, K_E =5

$\times 10^7$ N/m and d_y =0.015 m. The horizontal acceleration responses at the 3rd, 5th, 8th and 10th floor are taken as measured response. Figure 5.19 and Figure 5.20 are the identification results without and with 10% measurement noise respectively. Results indicate that all the bracing members exhibit the bilinear performance during the earthquake excitation. The time history of the nonlinear storey stiffness at each floor could be identified accurately when there is no noise. The fluctuation is, however, larger than that found in Section 5.3.4.2 when both nonlinear stiffness and measurement noise exist. However the results still show clearly the bilinear stiffness and their time of occurrence.

5.3.5 Discussions

In the first phase of identification in Section 5.3.4.1, the number of unknowns is 30 denoting the number of unknown initial displacement and velocity at all storeys of the structure, and the number of measured data is 4×800 which is also the number of equations for the identification in each time segment. The size of matrix $\mathbf{Y}_{ini}$ is 3200×30. In the second phase of this case study, the number of unknown is 15 which is the number of unknown storey stiffness and the size of the sensitivity matrix **S** is 3200×15 matrix.

In Section 5.3.4.2, the number of the measured data is also 4×800. The size of matrix $\mathbf{Y}_{ini}$ is 3200×20 and the size of **S** is 3200×10. The number of equations and unknowns in Section 5.3.4.3 is the same as that in Section 5.3.4.2. In these three cases, the number of equations is much larger than the number of unknowns and they are all over-determined problems. It is demonstrated from the numerical simulations that the time-variant parameters could be identified with the identification problem linearlized in a small time window

5.4 Conclusions

In this Chapter, new methods are proposed for time-variant damping identification and time-variant stiffness identification. Damping identification is conducted firstly. Rayleigh damping is very suitable for engineering purpose but it is not accurate enough for dynamic analysis of a structure. Modal damping is noted to be very promising for structural condition assessment and is a general damping model.

Three damping models, time-invariant Rayleigh damping, the time-variant Rayleigh damping and time-variant modal damping, are investigated in this Chapter and an iterative regularization identification method is proposed to identify these three types of damping. A constraint is added to ensure the physical significance of the modal damping ratio in the solution process. Chebyshev polynomial is employed in this Chapter to approximate the time-variant Rayleigh damping coefficients and modal damping ratios. Only a few terms in the polynomial is required as the structural damping will not usually change rapidly with time. In the numerical simulation, the forward problem and inverse problem employ the same damping model. The damping can be identified with accurate result even with 10% noise in the measurement. However, the modal damping model is more general and accurate for modeling the structural dynamics as illustrated in the experimental verification.

When the modal damping ratios are difficult to estimate or there is some innovative energy dissipation devices installed in the structural system, it is suggested that the damping can be initially assumed as time-invariant Rayleigh damping for a rough estimation to form a set of reference values for the subsequent more accurate time-variant damping identification. It is also recommended that the time-variant modal damping be utilized for the long-term structural health monitoring because there may be significant changes in the damping mechanism with time due to the changing environmental conditions and structure in the service life of the structure.

Secondly, a time-variant parameter identification method is developed with short time duration of data. Exact knowledge or assumption on the initial structural responses is not necessary. A two-phase identification algorithm is presented to conduct the identification in each time segment. In the first phase, the initial structural response is identified with iterative Tikhonov regularization method while the structural model is updated with a modified adaptive regularization method. The time of occurrence, location and severity of local change in the storey stiffness can be identified with acceptable results even when the measurement is polluted with noise. This linearlized approach with in short time duration not only could identify the linear abrupt loss of stiffness but also could identify the nonlinear stiffness, and it could be applied to the structural condition assessment in the event of a severe earthquake.

Table 5.1 - Material and geometrical properties of members

Properties	Member
Young modulus (N/m^2)	2.10×10^{11}
Area (m^2)	6.597×10^{-5}
Density (kg/m^3)	$1.2126\times10^{+4}$
Poisson ratio	0.3
Mass of ball bolt (kg)	0.232
Additional Mass at the joints (kg)	0.16
Moment of area I_y (m^4)	3.645×10^{-9}
Moment of area I_z (m^4)	3.645×10^{-9}
Torsional rigidity J [m^4]	7.290×10^{-9}

Table 5.2 - Error of identification from Node 18 without noise (time-variant modal damping)

Mode number	Error (%)
1H	*
1V	5.191×10^{-9}
2H	*
1T	*
3H	*
4H	*
5H	*
2V	2.1906×10^{-4}

(H - horizontal mode; T: torsional mode; V: vertical mode)

Table 5.3(a) - Error of identification from Nodes 18 and 23without noise
(time-variant modal damping)

Mode number	Error (%)
1H	5.7938×10^{-10}
1V	3.5733×10^{-9}
2H	2.7590×10^{-6}
1T	3.3668×10^{-8}
3H	7.3473×10^{-7}
4H	1.0896×10^{-4}
5H	2.8547×10^{-6}
2V	5.4876×10^{-7}

(H - horizontal mode; T: torsional mode; V: vertical mode)

Table 5.3(b) - Error of identification from Nodes 18 and 23with 10% noise
(time-variant modal damping)

Mode number	Error (%)
1H	1.010
1V	23.92
2H	1.78
1T	7.86
3H	2.11
4H	10.96
5H	9.29
2V	5.67

(H - horizontal mode; T: torsional mode; V: vertical mode)

Table 5.4 - Number of unknowns and equations for different types of damping identification in both Simulation and Experiment

Damping model	Number of unknowns	Number of equations
Time-invariant Rayleigh damping	2	1000
Time-variant Rayleigh damping	$2\times6=12$	1000
Time-variant modal damping	$8\times6=48$	200

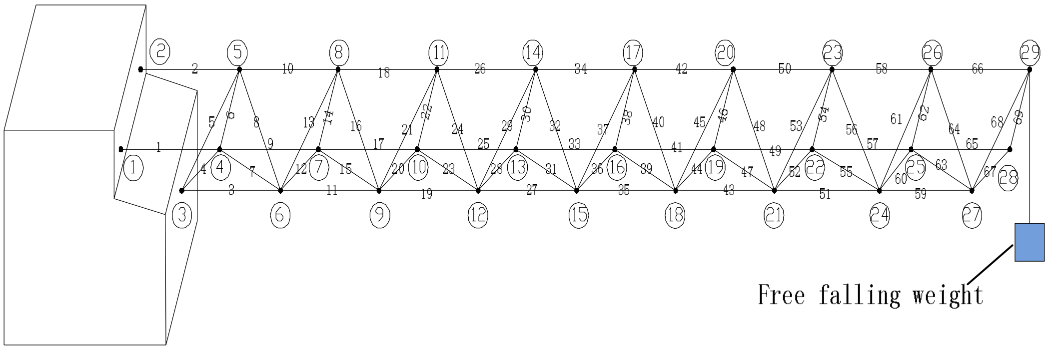

Figure 5.1 - A nine-bay space frame structure hanging with a free falling mass

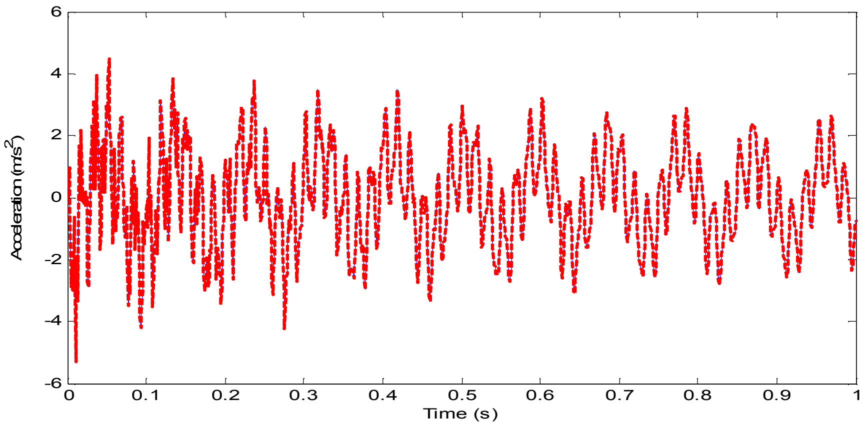

(a) without noise

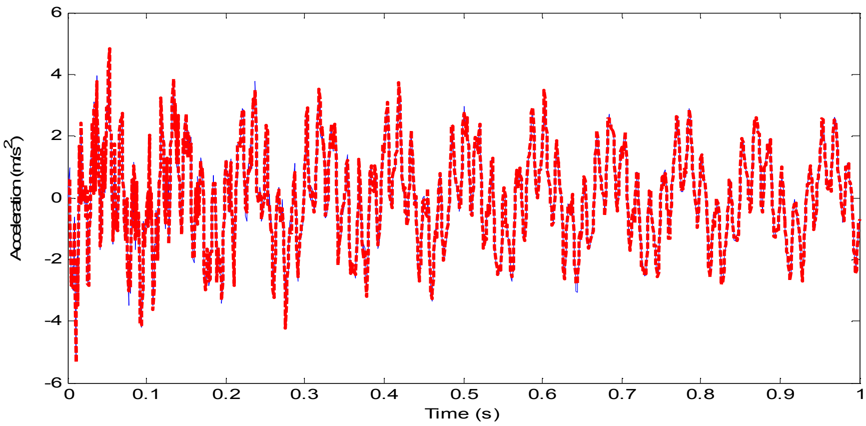

(b) with 10% noise

Figure 5.2 - Comparison of acceleration on Node 18 with time-invariant Rayleigh damping (___real, ---- reconstructed)

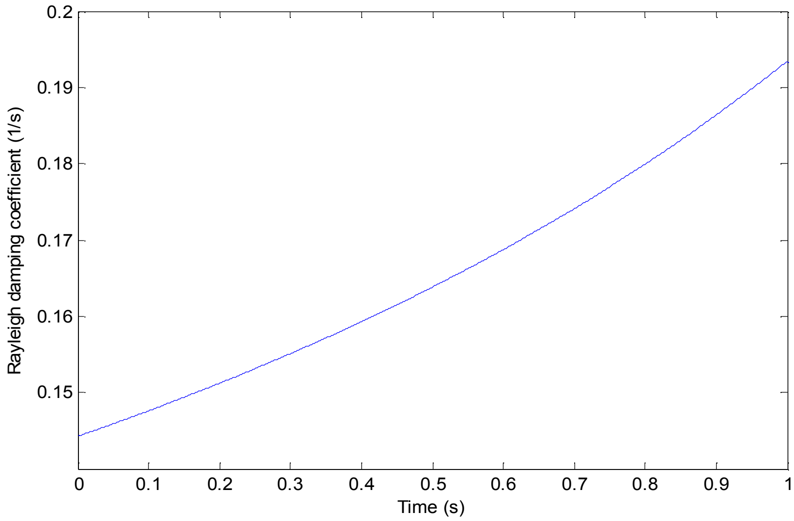

(a) Coefficient a_1

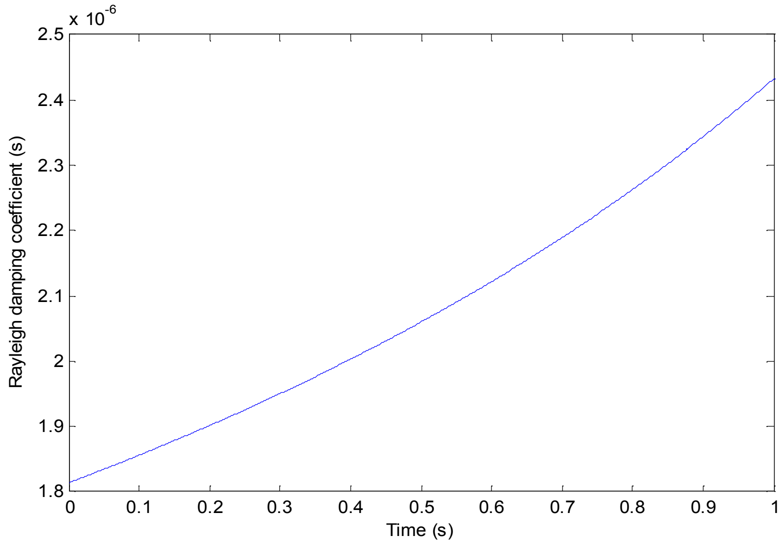

(b) Coefficient a_2

Figure 5.3 - Monotonous time history of Rayleigh damping coefficients

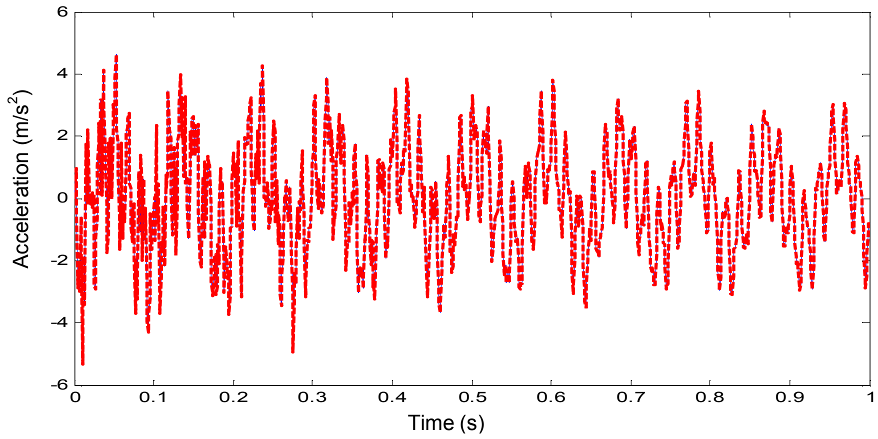

(a) without noise

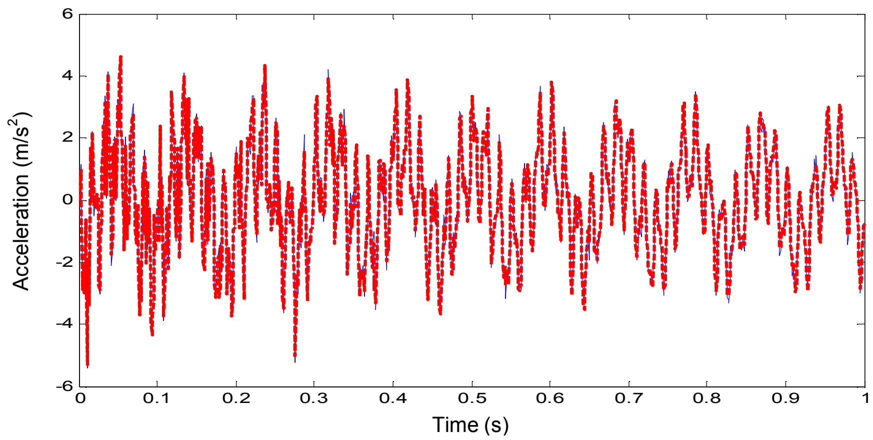

(b) with 10% noise

Figure 5.4 - Comparison of acceleration at Node 18 with time-variant Rayleigh damping (___real, ---- reconstructed)

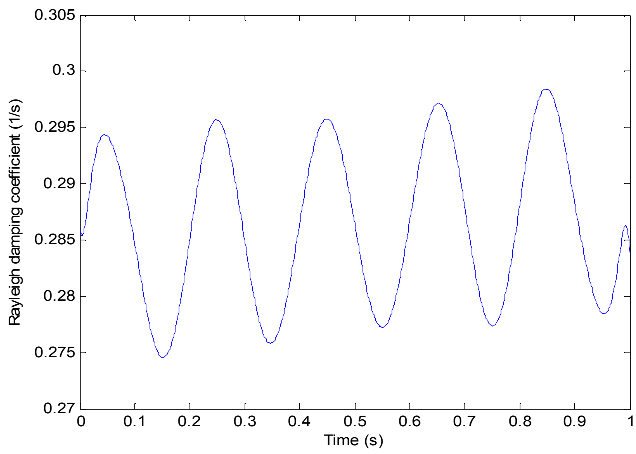

(a) Coefficient a_1

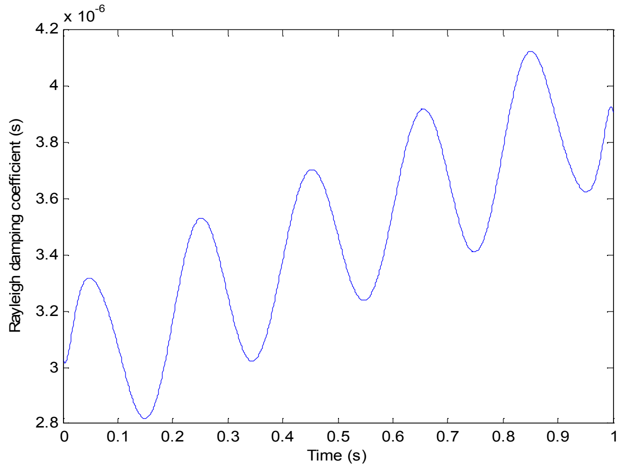

(b) Coefficient a_2

Figure 5.5 - Fluctuating time history of Rayleigh damping coefficients

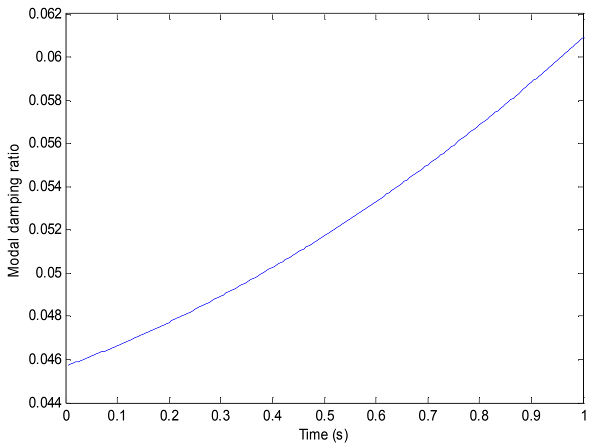

(a) The first mode

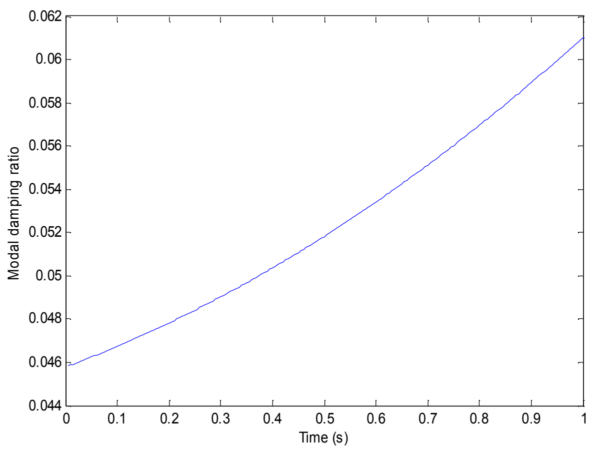

(b) The second mode

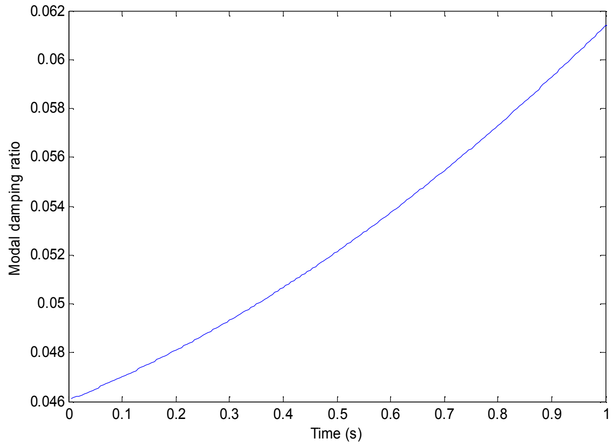

(c) The third mode

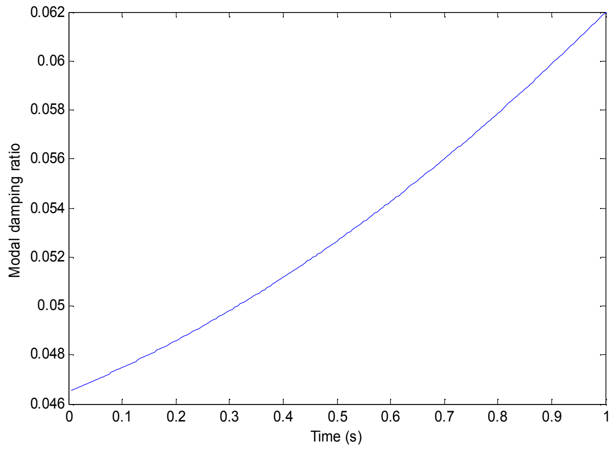

(d) The fourth mode

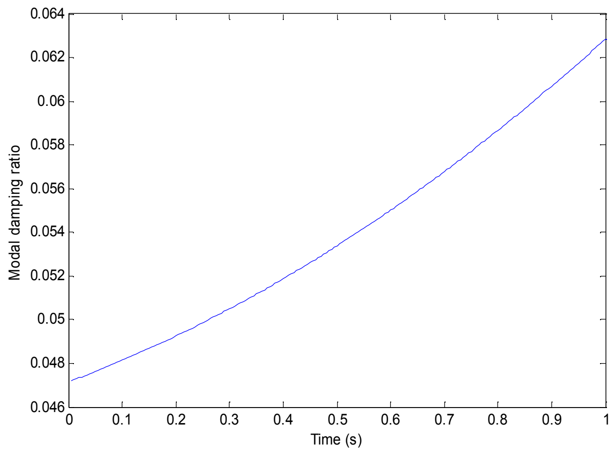

(e) The fifth mode

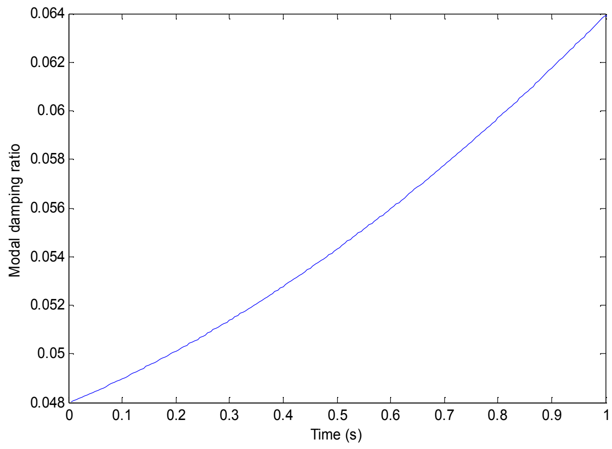

(f) The sixth mode

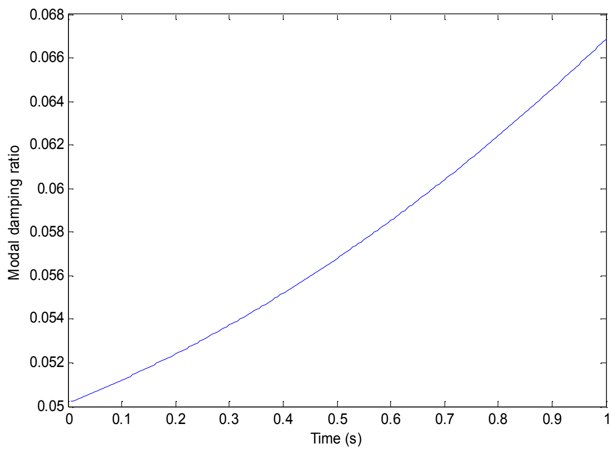

(g) The seventh mode

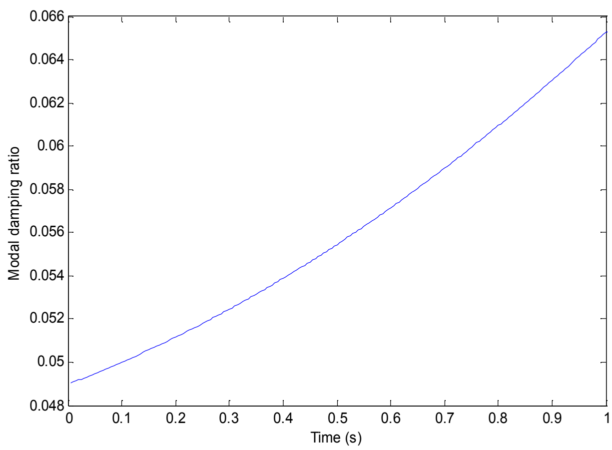

(h) The eighth mode

Figure 5.6 - Time history of the modal damping ratios

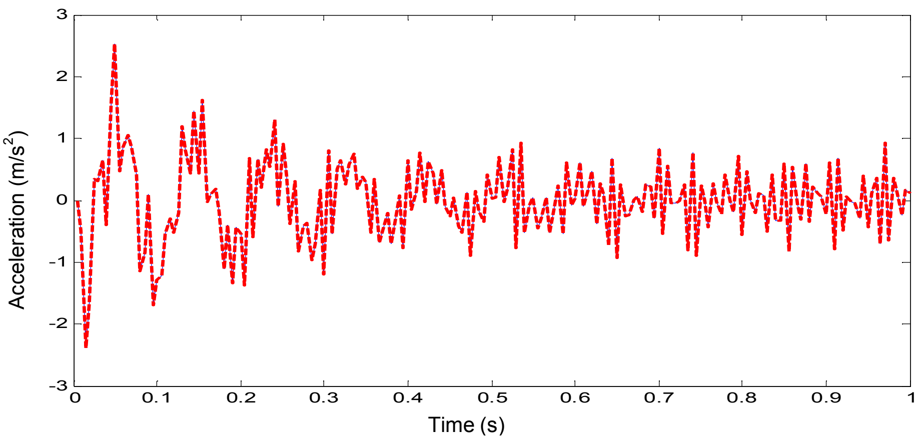

(a) without noise

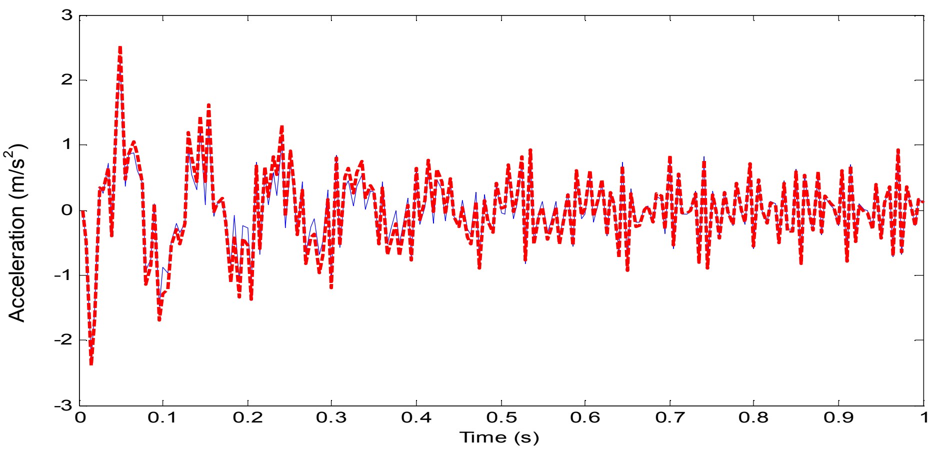

(b) with 10% noise

Figure 5.7 - Comparison of acceleration at Node 18 with time-variant modal damping (___real, ---- reconstructed)

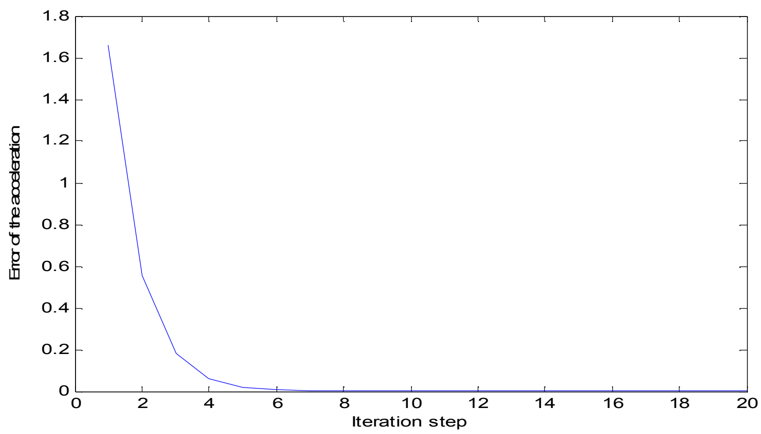

(a) Without noise

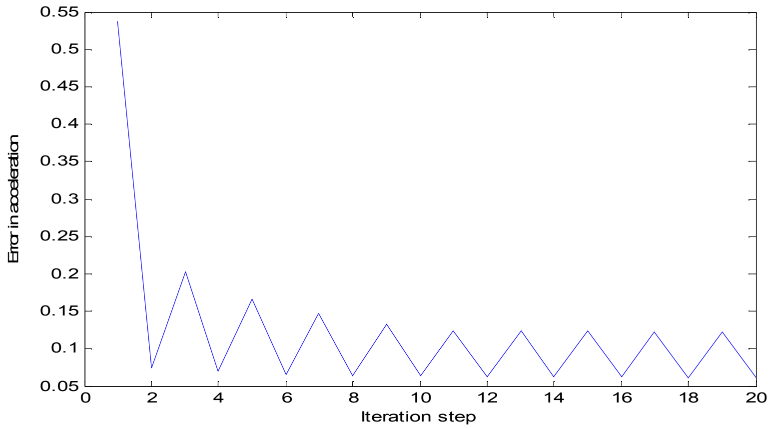

(b) With 10% noise

Figure 5.8 - Convergence curves with iteration step in modal damping identification

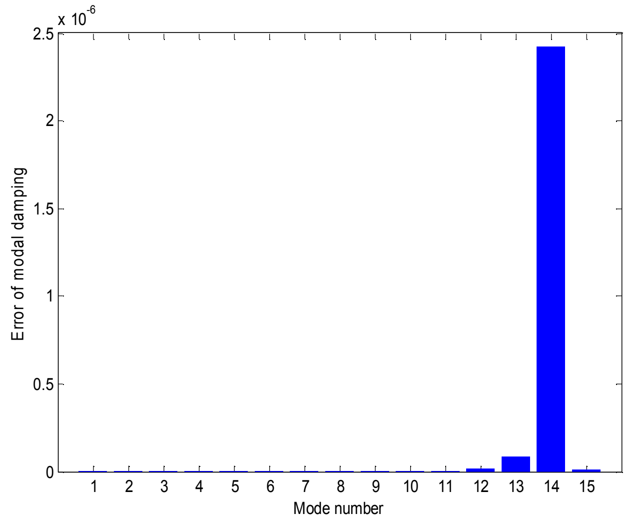

Figure 5.9 - Norm of the error in the coefficient of the modal damping ratio after 50 iterative steps

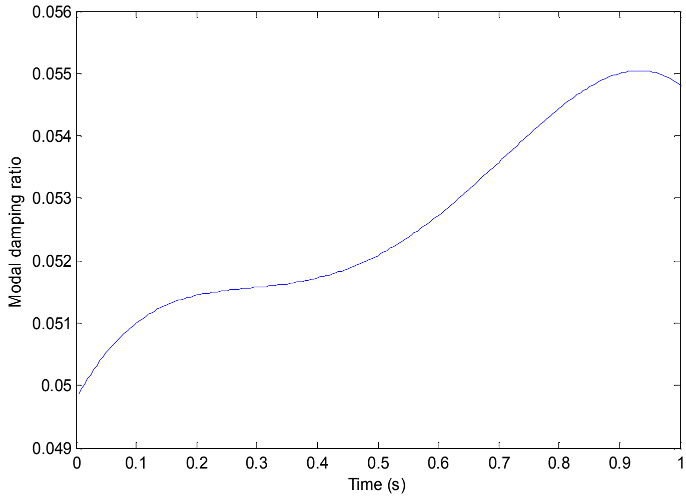

(a) The first mode

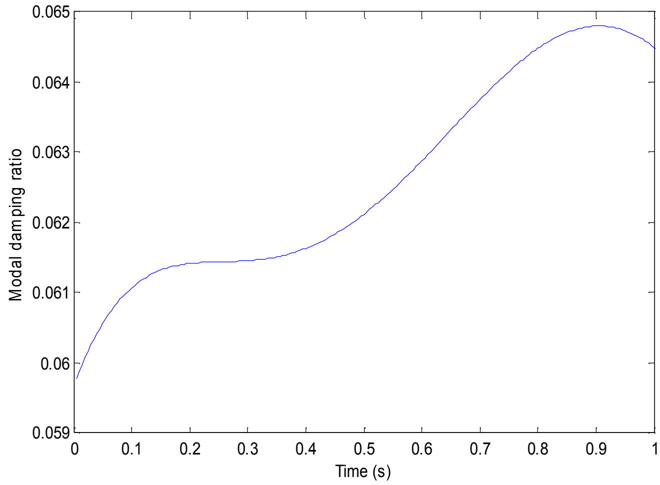

(b) The second mode

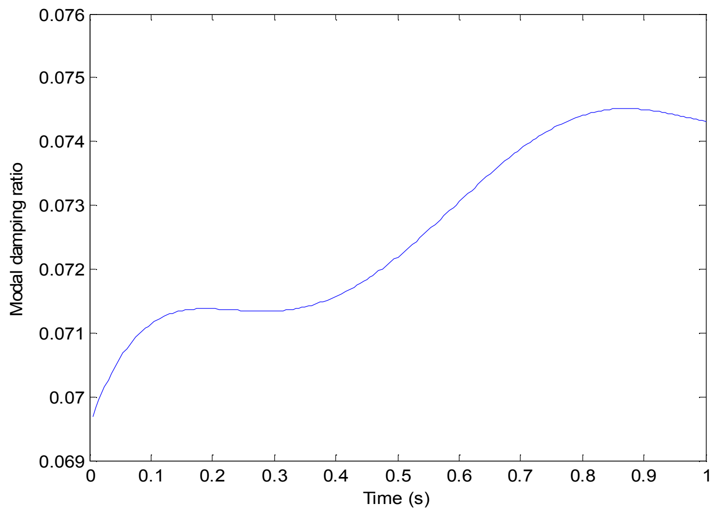

(c) The third mode

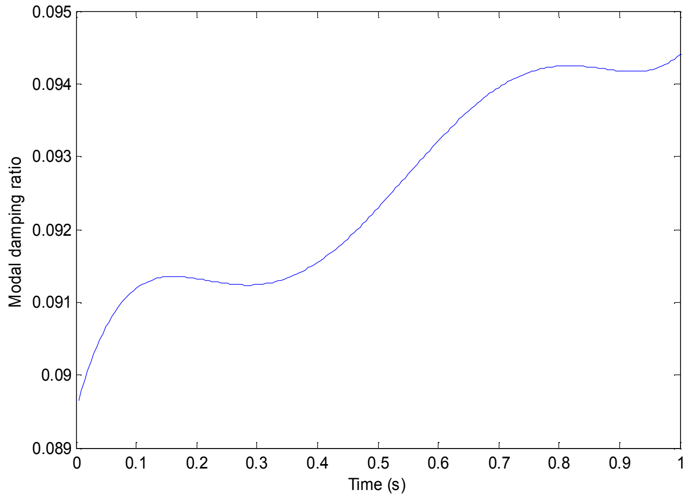

(d) The fourth mode

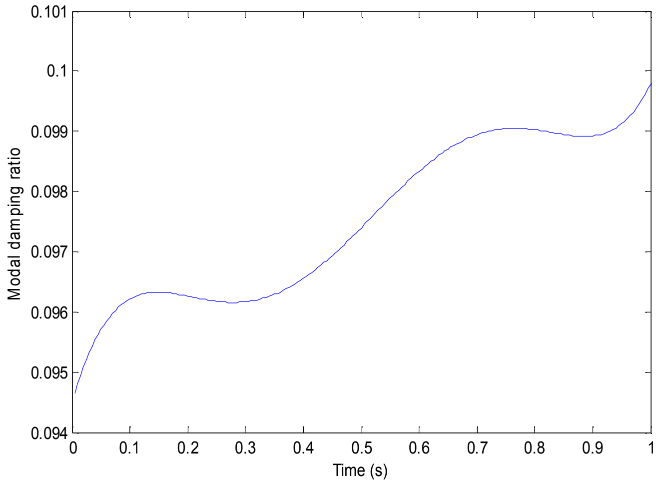

(e) The fifth mode

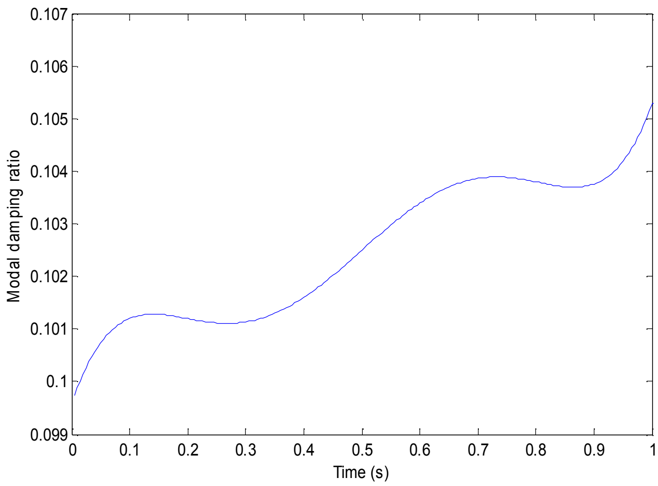

(f) The sixth mode

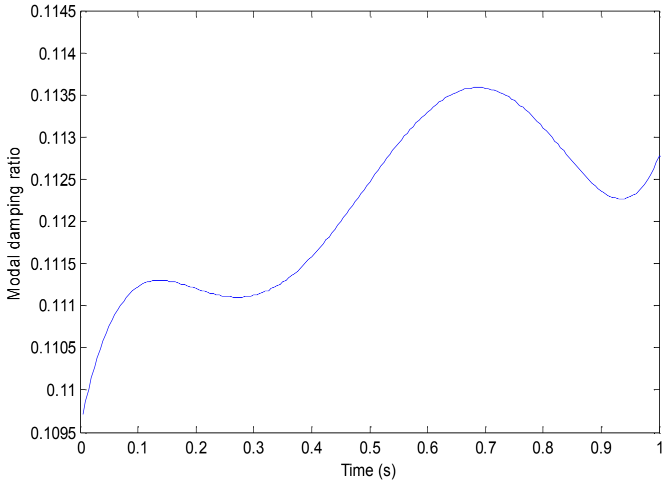

(g) The seventh mode

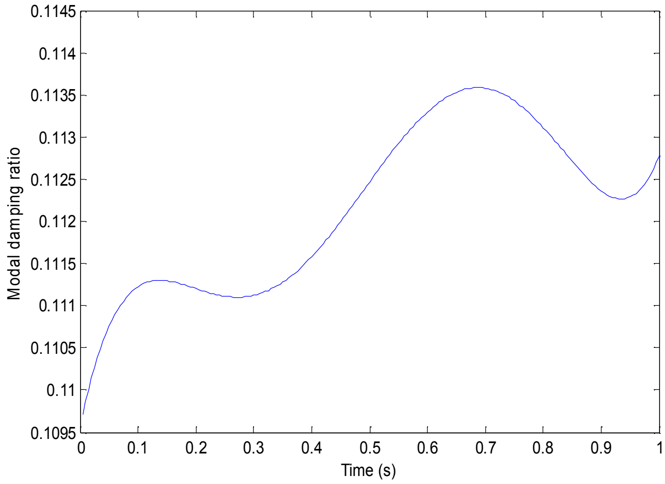

(h) The eighth mode

Figure 5.10 Fluctuating time history of modal damping ratios

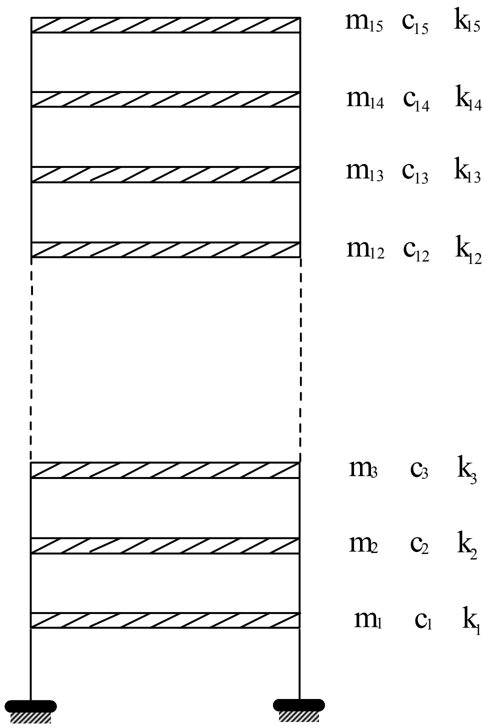

Figure 5.11 - Fifteen-storey shear frame

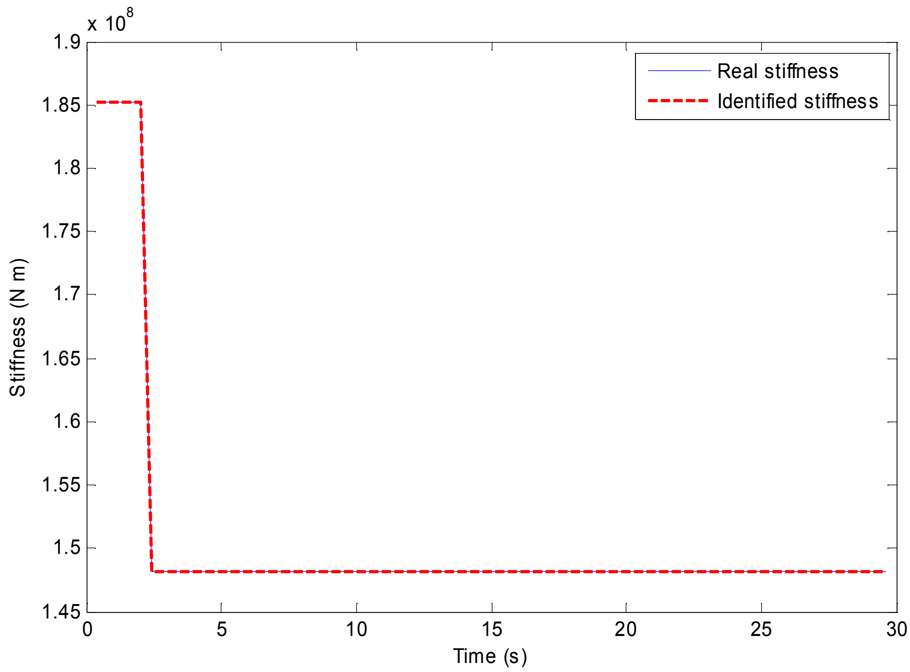

(a) The stiffness of the 2nd floor

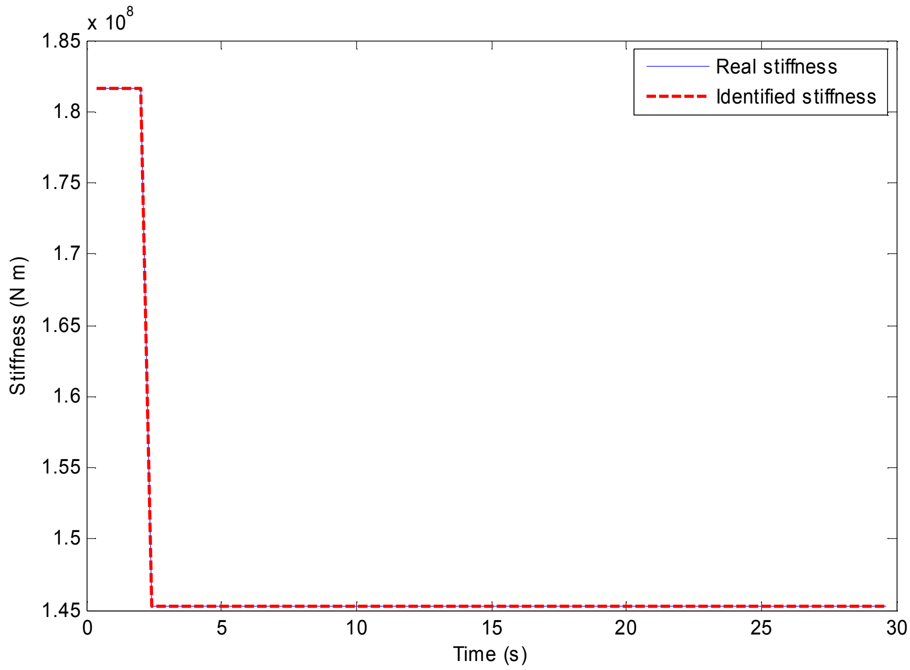

(b) The stiffness of the 5th floor

Figure 5.12 - Time-variant stiffness identification result without noise

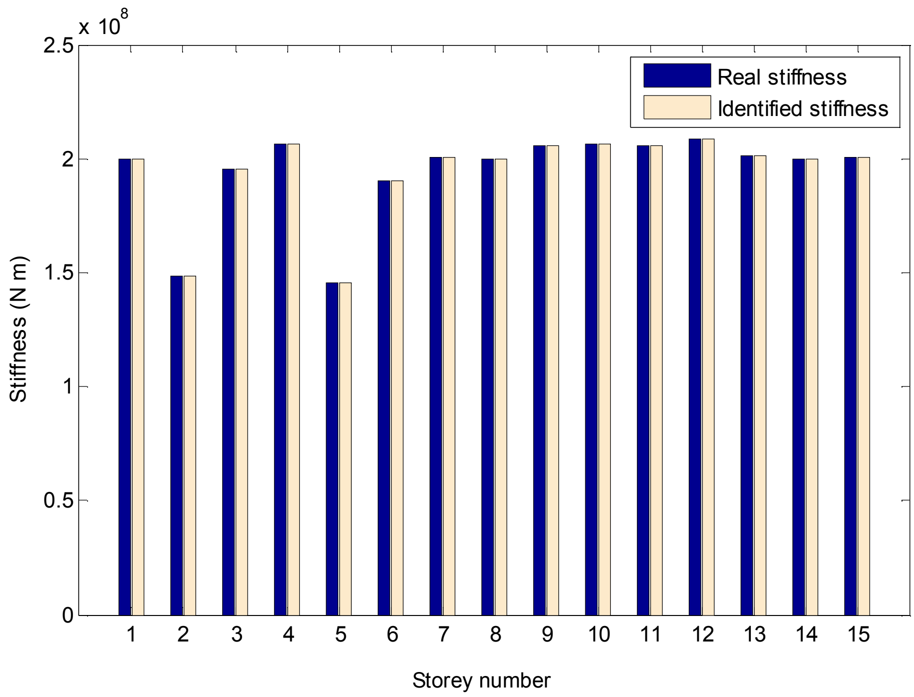

Figure 5.13 - Time-variant stiffness identification result of the last time step without noise

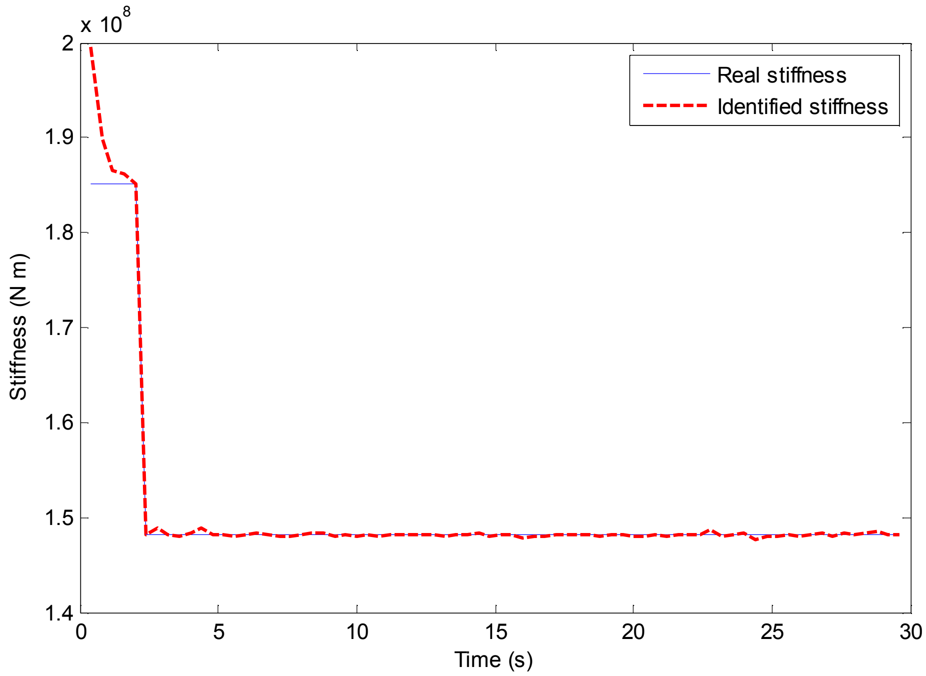

(a) The stiffness of the 2nd floor

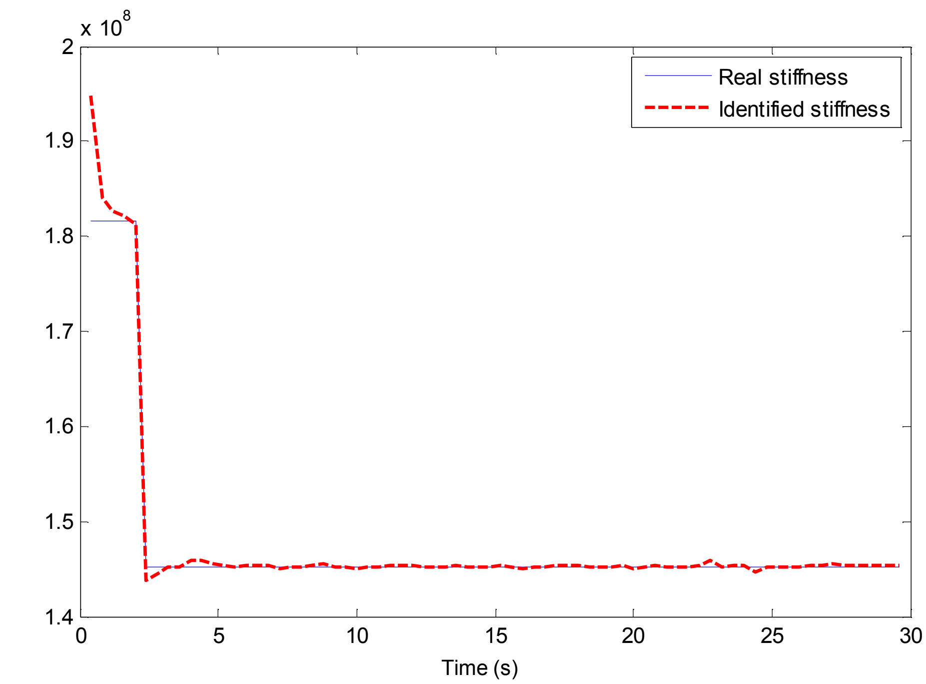

(b) The stiffness of the 5th floor

Figure 5.14 - Time-variant stiffness identification result with 10% noise

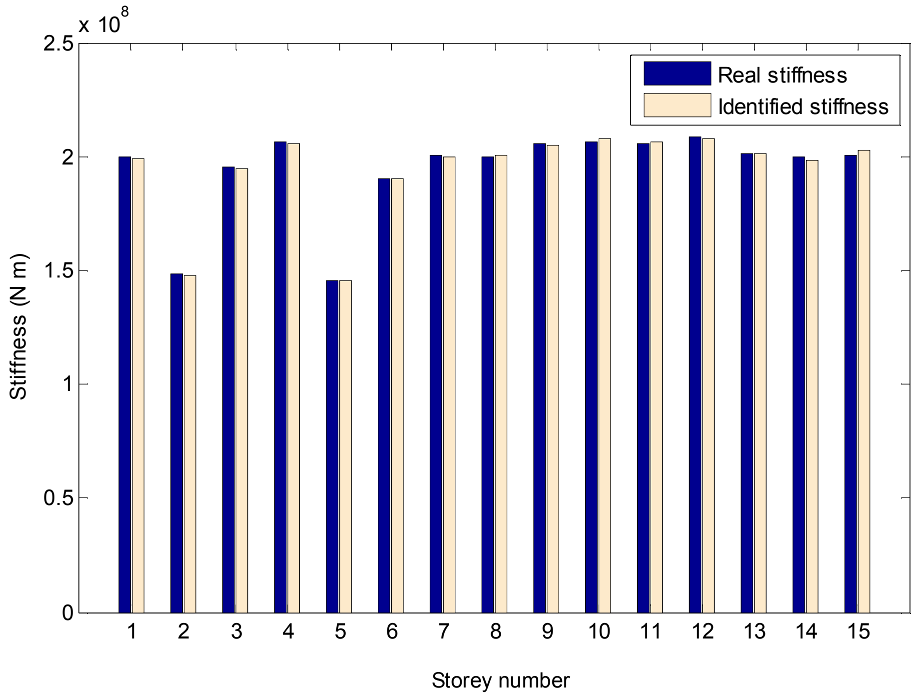

Figure 5.15 - Time-variant stiffness identification result of the last time window with 10% noise

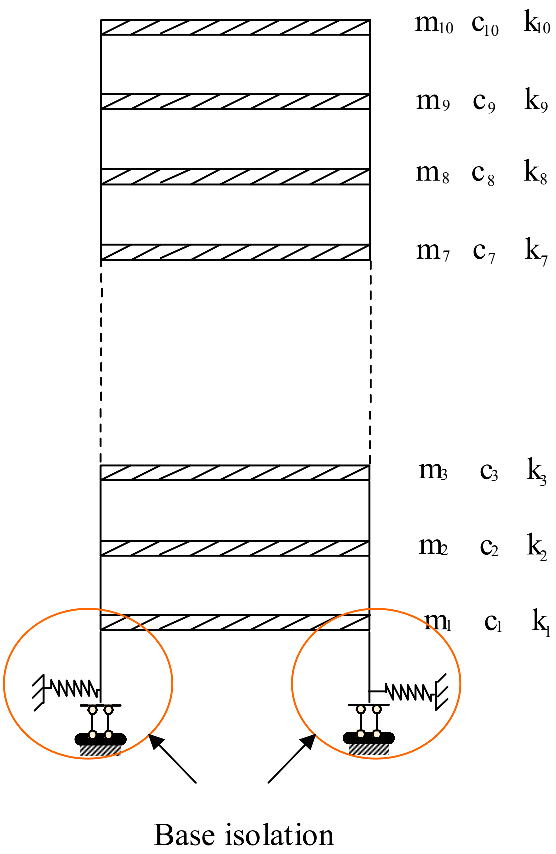

Figure 5.16 - Ten-storey shear frame with nonlinear base isolation

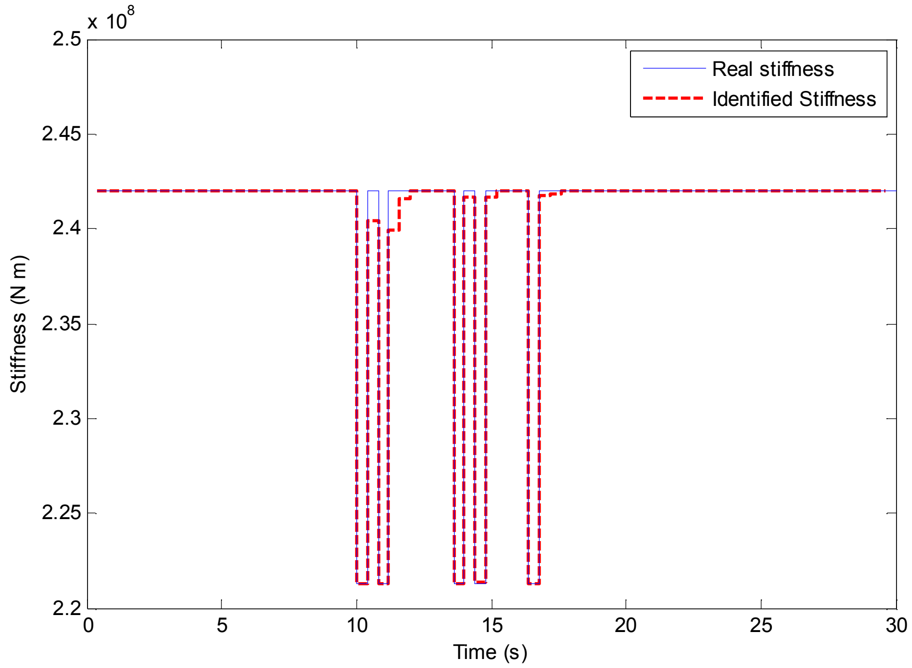

Figure 5.17 - Nonlinear time-variant stiffness identification result without noise

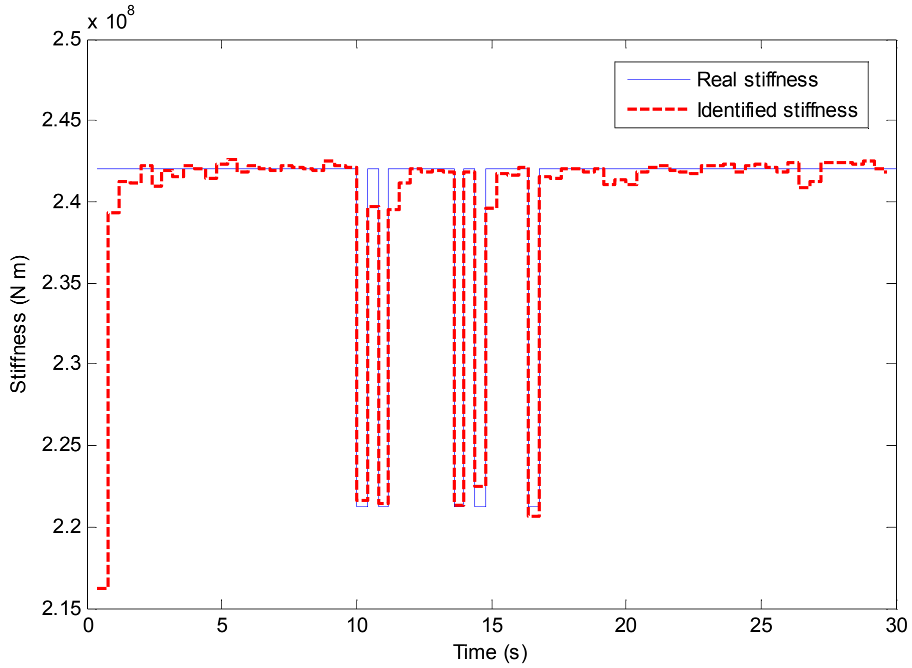

Figure 5.18 - Nonlinear time-variant stiffness identification result with 10% noise

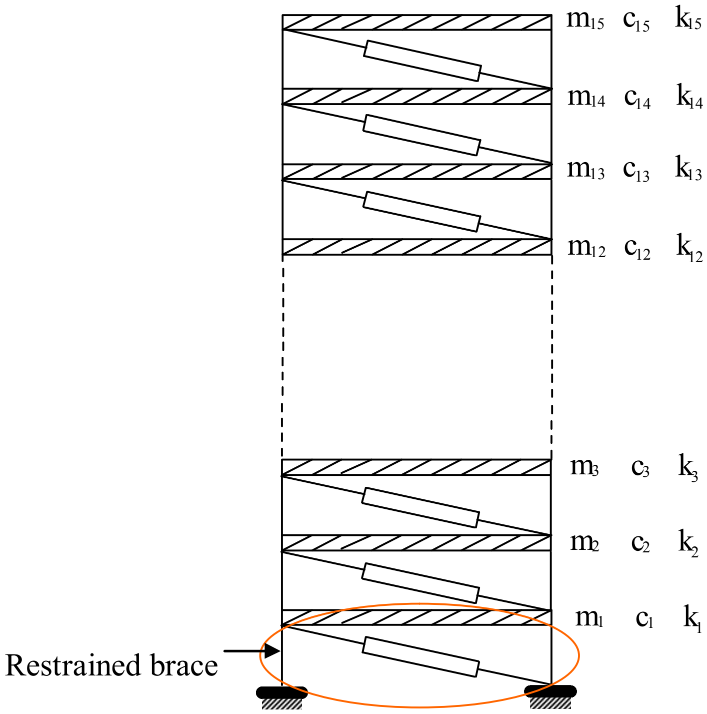

Figure 5.19 - Ten-storey shear frame with resisting bracings at each floor

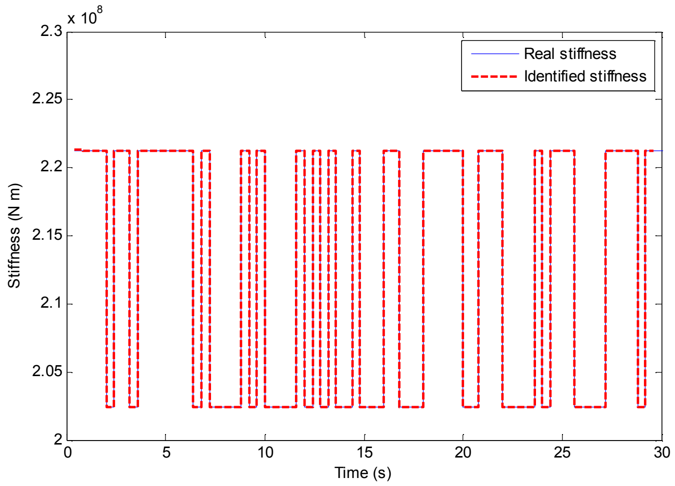

(1) Stiffness of 1st floor

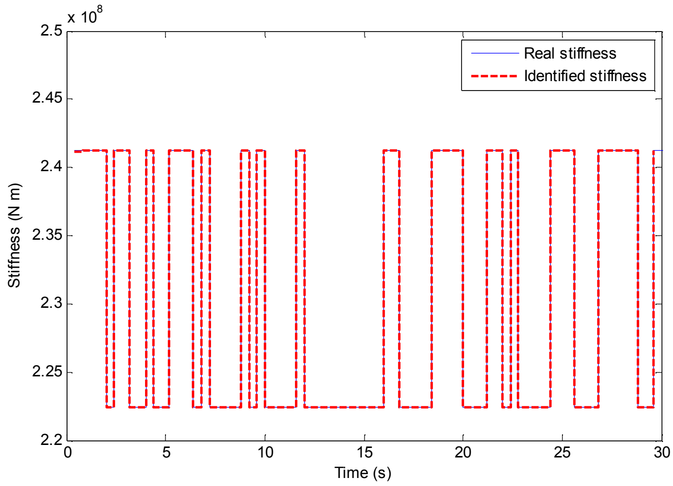

(2) Stiffness of 2nd floor

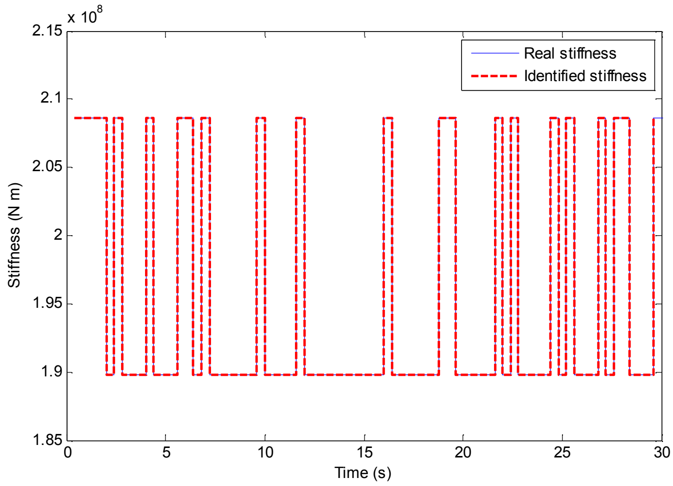

(3) Stiffness of 3rd floor

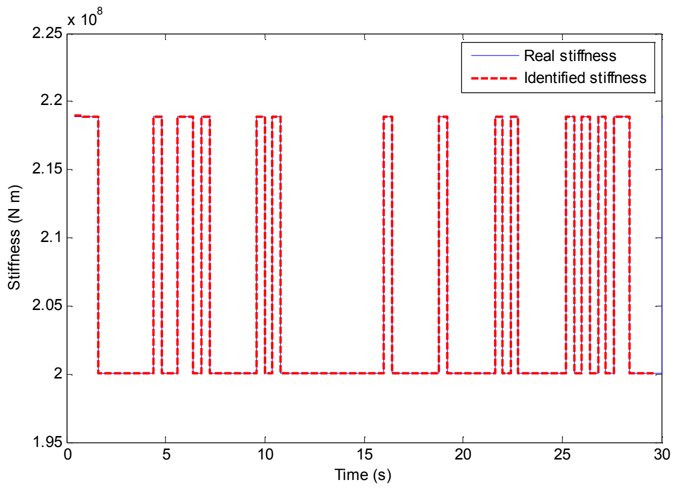

(4) Stiffness of 4th floor

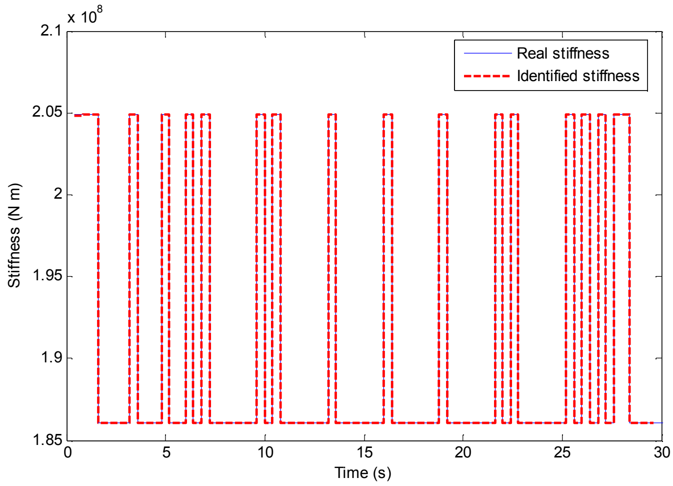

(5) Stiffness of 5th floor

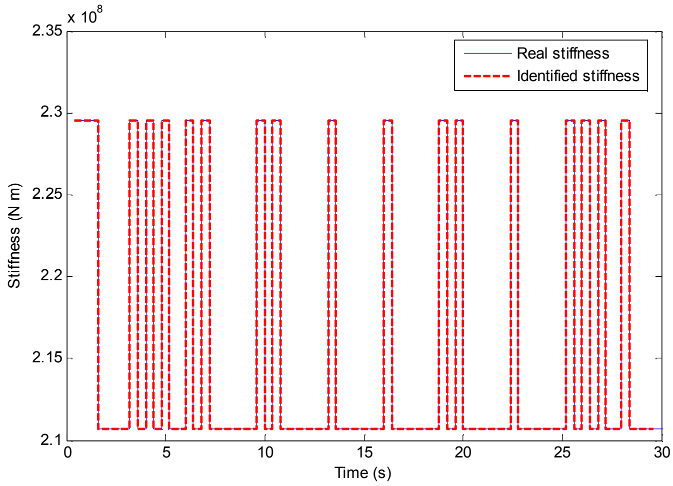

(6) Stiffness of 6th floor

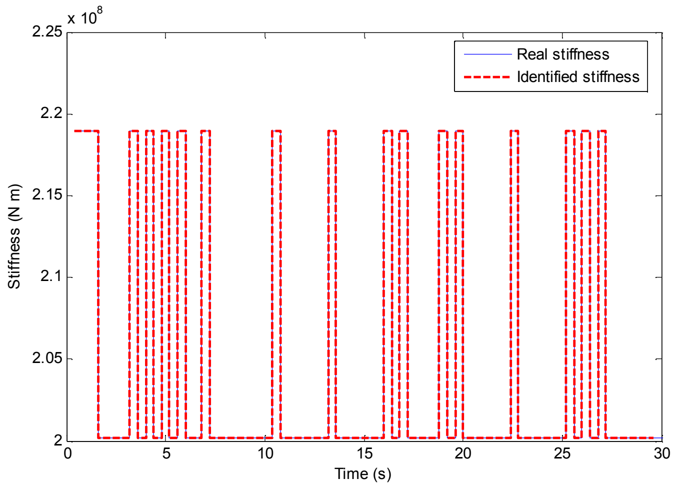

(7) Stiffness of 7th floor

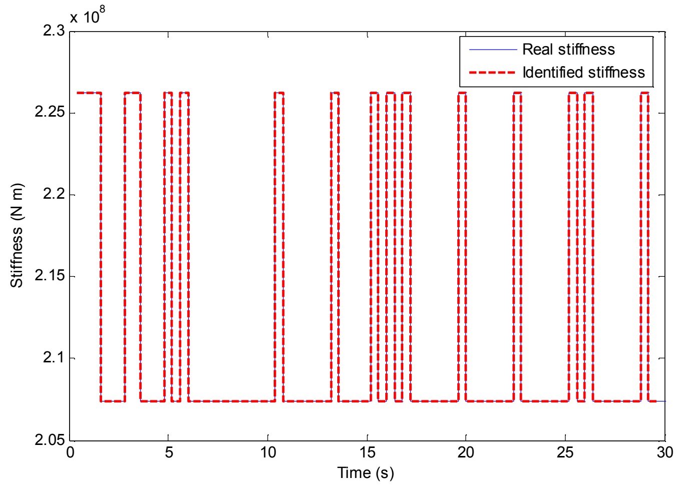

(8) Stiffness of 8^{th} floor

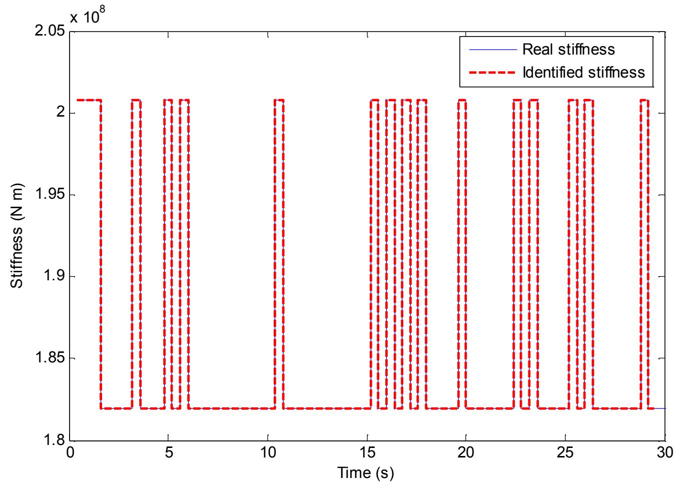

(9) Stiffness of 9^{th} floor

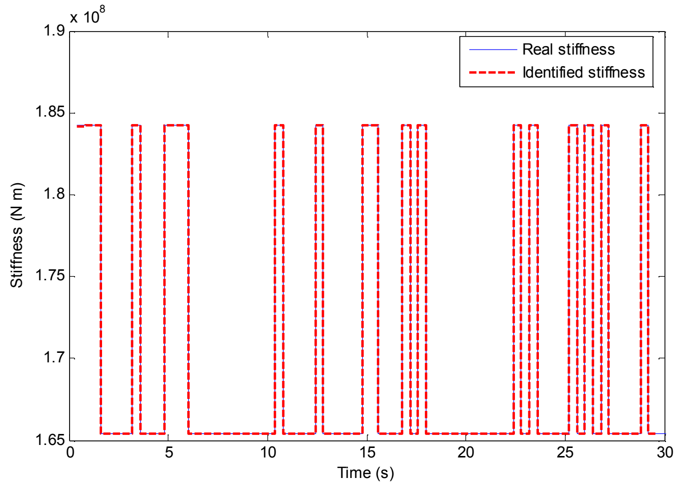

(10) Stiffness of 10^{th} floor

Figure 5.20 - Nonlinear time-variant stiffness identification result without noise

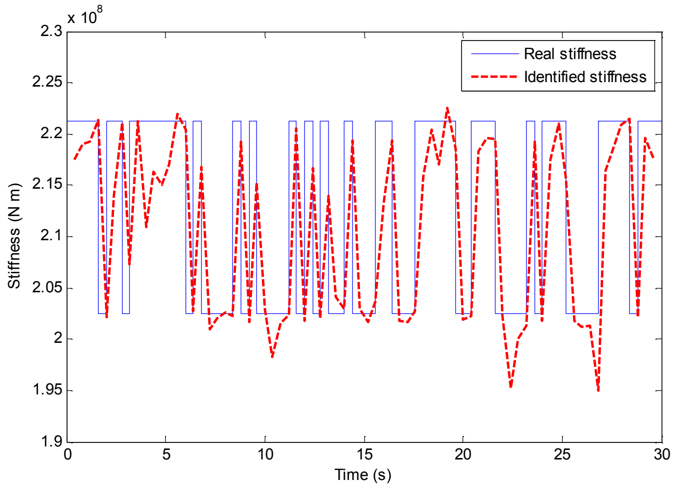

(1) Stiffness of 1st floor

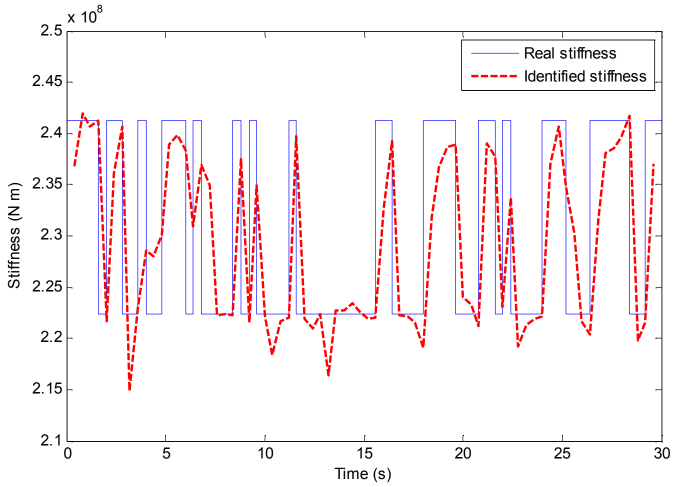

(2) Stiffness of 2nd floor

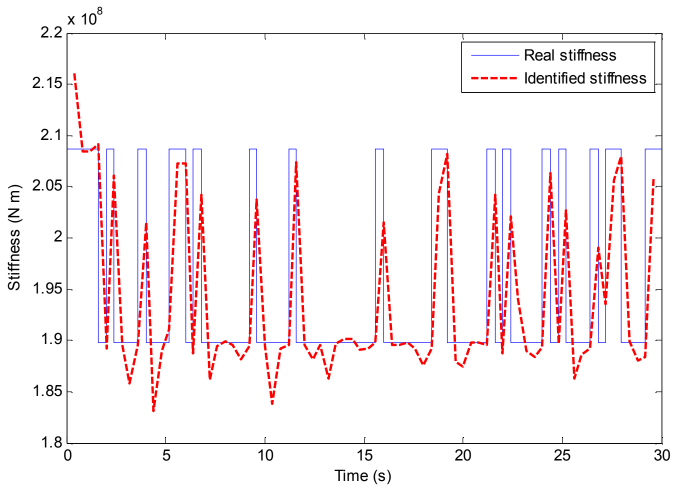

(3) Stiffness of 3rd floor

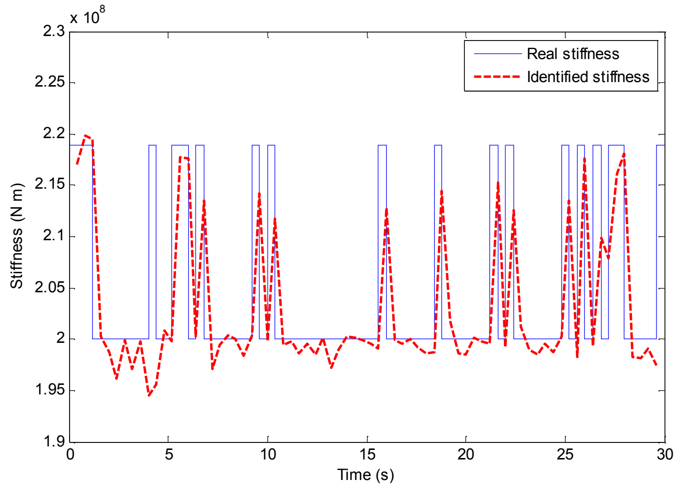

(4) Stiffness of 4th floor

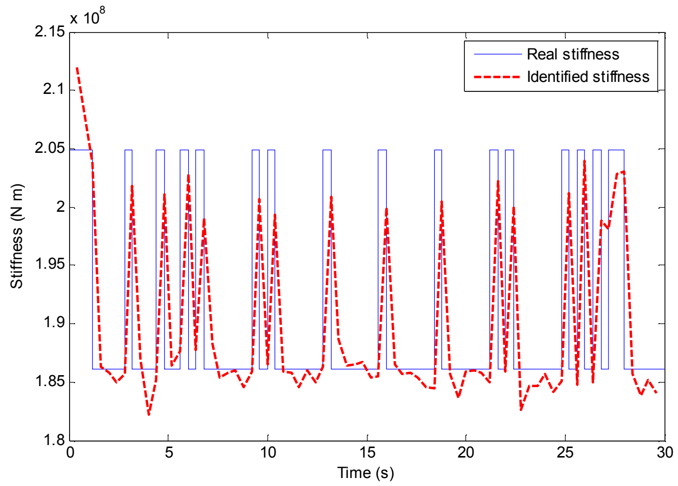

(5) Stiffness of 5th floor

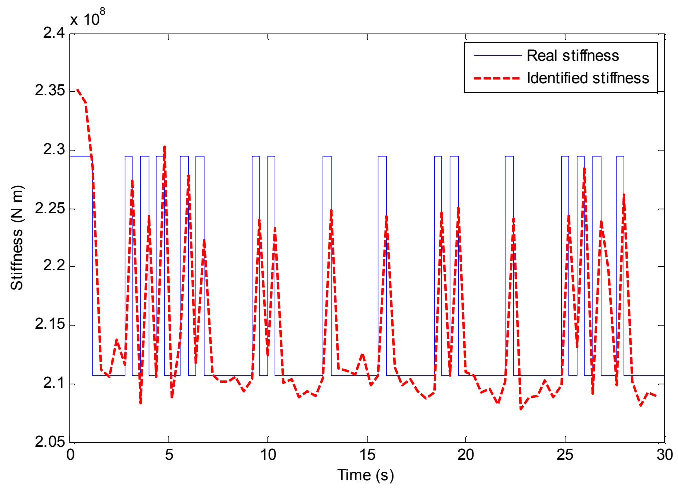

(6) Stiffness of 6th floor

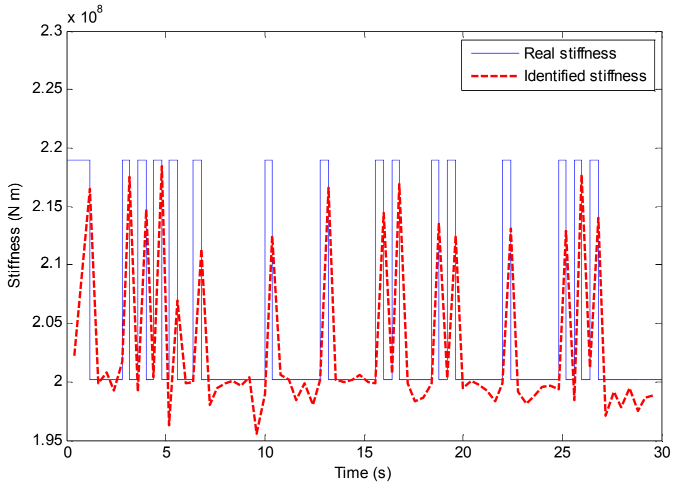

(7) Stiffness of 7th floor

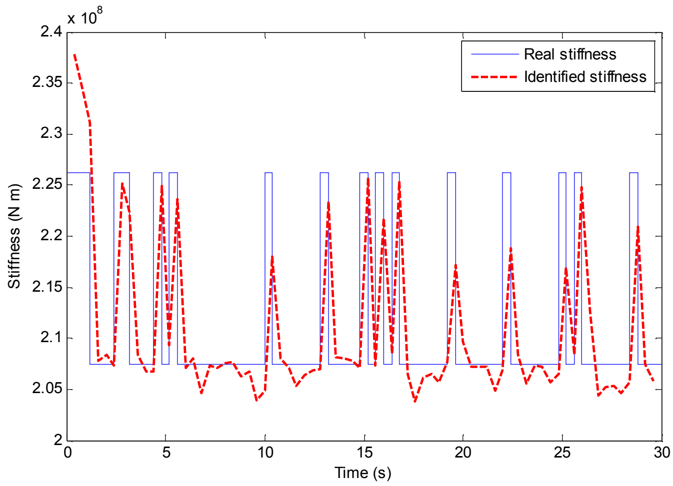

(8) Stiffness of 8th floor

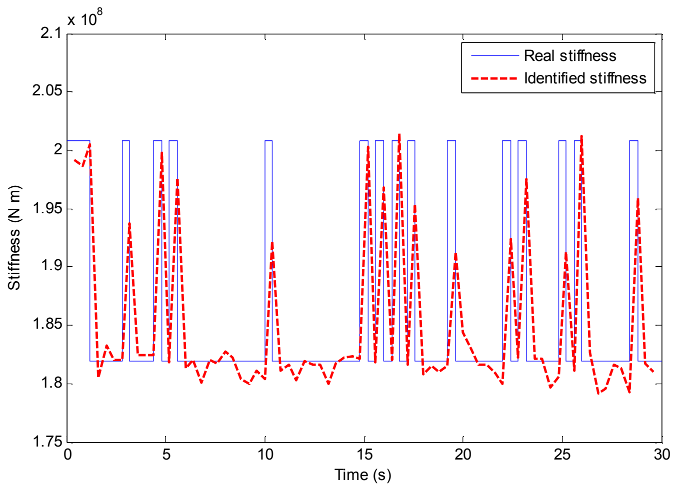

(9) Stiffness of 9th floor

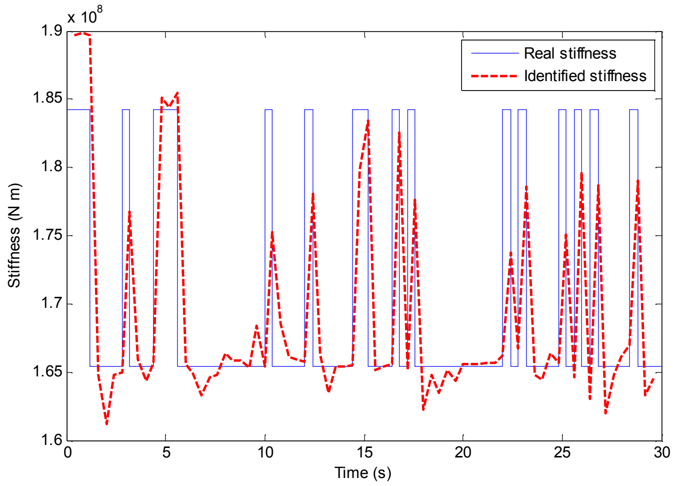

(10) Stiffness of 10th floor

Figure 5.21 - Nonlinear time-variant stiffness identification result with 10% noise

CHAPTER 6

INTEGRATION OF STRUCTURAL CONTROL AND STRUCTURAL EVALUATION FOR LARGE SCALE STRUCTURAL SYSTEM

6.1 Introduction

An integrated system of structural control and health monitoring can be implemented in modern structures with multi-purpose sensor system. The integration system not only promotes the reliability of the smart structure but also provides information on the condition of the smart structure. Both the structural vibration control and evaluation are important areas of structural engineering and they are of great importance for the structural safety and reliability. The combination of these two techniques is necessary since the structure control algorithm is always based on the parameters of the structural system. When the initial finite element model of the structure is inaccurate, the effect of structural control may not be effective. Existence of model errors and local damage will influence the optimal control effect.

The integration of structural parameter identification and semi-active control has been investigated by Xu and Chen (2007a, 2007b) where the concept of an integrated system with semi-active friction dampers is introduced. The integrated system is centralized and the parameter identification is conducted in frequency domain which needs plenty of measurement data. The on-line implementation of structural control and evaluation of a large scale structure are difficult due to the complicated calculation with large mass, damping and stiffness matrices. Moreover, the reliability of the structural control and evaluation results will also reduce in a large scale structural system during severe earthquake with centralized control system.

In control theory, the linear-quadratic-Gaussian (LQG) control problem is one of the most fundamental optimal control problems. It concerns uncertain linear system disturbed by additive white Gaussian noise, having incomplete state information (i.e. not all the state variables are measured and available for feedback) and undergoing control subject to quadratic costs. Moreover the solution is unique and constitutes a linear dynamic feedback control law that is easily computed and implemented. The LQG controller is also fundamental to the optimal perturbation control of non-linear systems (Athans 1971).

Negative stiffness control has been investigated with active and semi active control system (Iemura and M. Pradono 2003; Li and Ou 2006; Wu, Shi and Ou 2010) with the absolute acceleration of a structure reduced effectively. But the structural system with the control force will become unstable when the negative stiffness performed on the structure is more than the real stiffness of the structure. The pseudo negative control method would guarantee the stability of structural control with a constraint on the negative stiffness. The design of the pseudo negative stiffness control is always based on the structural parameters. An accurate model of the structure is always not available in practice or the structure may exhibit some local damages, which will lead to unfavorable effect on the structural control. Therefore, the control algorithm will be more reliable with more information on the structural parameters. Structural evaluation should update the structural parameters before appropriate structural control is implemented. The final integrated system of structural control will therefore be adaptive to this information.

In this Chapter, a new combined system of decentralized autonomous and structural evaluation is proposed. Section 6.2 reviews on two structural control algorithms which will be used in the proposed integrated system. Section 6.3 will illustrate the methodologies of centralized autonomous control and decentralized control algorithm. Implementation procedure will be provided for the proposed algorithm in Section 6.4. In Section 6.5 gives the numerical to validate the proposed control algorithm. A modified adaptive regularization method proposed in Chapter 5 will be used in the solution of the structural evaluation via model updating in Section 6.5. Conclusions on the proposed integrated system will be presented in Section 6.6.

6.2 Structural Control Algorithm

6.2.1 LQG Control

LQG control is convenient to implement in practice. When only part of the structural response can be measured, the LQG method can be applied based on state space equation of the system. Considering the state space equation of the structural system as

$$\dot{\mathbf{z}}(t) = \mathbf{A}\mathbf{z}(t) + \mathbf{B}\mathbf{U}(t) + (-\mathbf{M}\mathbf{G}\ddot{x}_g) + \varepsilon_1(t) \tag{6.1}$$

where $\varepsilon_1(t)$ is the system noise, $\mathbf{z}(t)$ denote the state vector, **U**(t) is the time history of control force, **B** is the location matrix of the control force and $\ddot{\mathbf{x}}_g(t)$ is the horizontal earthquake ground acceleration. $\ddot{\mathbf{x}}$, $\dot{\mathbf{x}}$ and $\mathbf{x}$ are vectors of acceleration, velocity and displacement of the structural system respectively. $\mathbf{z} = \begin{bmatrix} \mathbf{x} \\ \dot{\mathbf{x}} \end{bmatrix}$, $\mathbf{A} = \begin{bmatrix} 0 & \mathbf{I} \\ -\mathbf{M}^{-1}\mathbf{K} & -\mathbf{M}^{-1}\mathbf{C} \end{bmatrix}$ and $\mathbf{G} = \begin{bmatrix} 0 \\ \mathbf{M}^{-1} \end{bmatrix}$. A Kalman filter can be constructed as:

$$\dot{\hat{\mathbf{z}}}(t) = \mathbf{A}\hat{\mathbf{z}}(t) + (-\mathbf{M}\mathbf{G}\ddot{x}_g) + \mathbf{K}_e(\mathbf{Y} - \hat{\mathbf{Y}}) \tag{6.2}$$

$$\mathbf{K}_e = \mathbf{P}\mathbf{C}_0^T\mathbf{R}^{-1} \tag{6.3}$$

where $\mathbf{K}_e$ is the control gain of the LQG control, **P** is the Riccati matrix, **Y** and $\hat{\mathbf{Y}}(t)$ are the measured vector of **x** and the estimation vector of **Y** from the Kalman filter respectively. **R** is the weighing matrix of LQR method. The objective function applying the Kalman filter can be constructed as:

$$J = E\{[\mathbf{z}(t) - \hat{\mathbf{z}}(t)]^T[\mathbf{z}(t) - \hat{\mathbf{z}}(t)]\} \tag{6.4}$$

where $\hat{z}(t)$ is the estimation matrix of $z(t)$. The control system can be represented in state space as

$$\dot{\hat{\mathbf{z}}}(t) = (\mathbf{A} - \mathbf{B}\mathbf{G} - \mathbf{K}_e\mathbf{C}_0)\hat{\mathbf{z}}(t) + \mathbf{K}_e\mathbf{Y} \tag{6.5}$$

$$\hat{\mathbf{Y}}(t) = \mathbf{C}_0\hat{\mathbf{z}}(t) \tag{6.6}$$

where $\mathbf{C}_0$ is the transformation matrix. A negative stiffness could be added to the structure with this control algorithm (H. J. Liu 2007).

6.2.2 Pseudo Negative Stiffness (PNS) Control

The negative stiffness control method introduces the negative stiffness and viscous damping to the structural system. It has been shown that when the value of the negative stiffness equal to the structural stiffness but with an opposite sign, the system would have the maximum reduction effect in the acceleration response. To conduct the stable vibration control, the absolute value of the negative stiffness should be constrained to be smaller than the true value of the stiffness of the structure with the PNS control method.

With the PSN control, the control force applied on the first floor can be represented as

$$\mathbf{U}(t) = \begin{cases} k_{ns}x(t) & |f_0(t)| \geq k_{ns}x(t) \ \& \ f_0(t)x(t) < 0 \\ f_0(t) & |f_0(t)| < k_{ns}x(t) \ \& \ f_0(t)x(t) < 0 \\ 0 & f_0(t)x(t) \geq 0 \end{cases} \tag{6.7}$$

where $f_0(t) = -k_{ns}x_1 + c_{ns}\dot{x}_1$ (B. Wu et al. 2009), and k_{ns} and c_{ns} are the pseudo negative stiffness and the damping in the device.

6.3 Autonomous Control

6.3.1 Centralized Autonomous Structural Control System

The equation of motion for a structural system subject to earthquake with installation of control devices can be written as

$$\mathbf{M\ddot{x}} + \mathbf{C\dot{x}} + \mathbf{Kx} = -(\mathbf{MG})\ddot{x}_g + \mathbf{DU} \tag{6.7}$$

where matrices **M**, **C**, and **K** are the mass, damping and stiffness matrices of the structural system respectively, and **D** is the location matrix of the control forces. A 16-storey planar shear frame shown in Figure 6.1 serves as an example to illustrate the proposed integration system. In this centralized autonomous structural system, the controller will control all the actuators installed on the structural system.

The centralized autonomous control system consists of the function of structural vibration control and structural condition evaluation. With the integrated system, identifying and updating the structural parameters is necessary to ensure the effectiveness of the structural control. Various model updating methods could be alternatively applied in this function as proposed by Xu and Chen (2007a) according to the practical condition. The structural control could be conducted with the updated model and implemented with the sensor system, data acquisition system and data transmission system. As illustrated by Xu and Chen (2007a) the updated structural model facilitates the implementation of structural vibration control and provides a reference state for subsequent damage detection.

The flow chart of the centralized structural control could be shown as Figure 6.2. At the beginning the structural control is based on the initial model of the structure. It would then base later on the updated structural parameters transferred from the stage of structural evaluation. The value t_0 in Figure 6.2 denotes the required time duration for the structural evaluation and it depends on the computing speed of the computer and the number of DOFs of the structural system.

6.3.2 Decentralized Autonomous Structural Control System

Though the centralized autonomous structural control system is adaptive to the structural model and parameters the decentralized autonomous structural control system is more reliable and stable than the centralized structural control system. The rest of this Chapter will focus on decentralized autonomous control algorithm which is implemented with the integrated distributed control system and structural evaluation system based on substructure methods proposed in Chapter 4. A 16-storey planar shear frame in Figure 6.3 serves as an example to illustrate the proposed decentralized autonomous control algorithm. In this Section, control forces based on PNS control and LQG control are applied on the 1^{st} floor and on the 11^{th} floor and 12^{th} floor respectively as shown in Figure 6.3. The LQG control algorithm, PNS control algorithm introduced earlier in this Chapter and the substructure method proposed in Chapter 4 are integrated to implement the decentralized autonomous structural vibration control.

The decentralized autonomous structural vibration control is conducted with separate controller on each substructure. The structural system can be divided into substructures with independent controller and control forces. Figure 6.3 shows the division of the building frame structure into two substructures linked at the interface DOFs. Based on this sub-division of the structure, Equation (6.7) can be rewritten as

$$\begin{bmatrix} \mathbf{M}_{11} & \mathbf{M}_{12} \\ \mathbf{M}_{21} & \mathbf{M}_{22} \end{bmatrix} \begin{bmatrix} \ddot{\mathbf{x}}_1 \\ \ddot{\mathbf{x}}_2 \end{bmatrix} + \begin{bmatrix} \mathbf{C}_{11} & \mathbf{C}_{12} \\ \mathbf{C}_{21} & \mathbf{C}_{22} \end{bmatrix} \begin{bmatrix} \dot{\mathbf{x}}_1 \\ \dot{\mathbf{x}}_2 \end{bmatrix} + \begin{bmatrix} \mathbf{K}_{11} & \mathbf{K}_{12} \\ \mathbf{K}_{21} & \mathbf{K}_{22} \end{bmatrix} \begin{bmatrix} \mathbf{x}_1 \\ \mathbf{x}_2 \end{bmatrix} = \begin{bmatrix} -(\mathbf{MG})_1 \\ -(\mathbf{MG})_2 \end{bmatrix} \ddot{x}_g + \begin{bmatrix} \mathbf{D}_1\mathbf{U}_1 \\ \mathbf{D}_2\mathbf{U}_2 \end{bmatrix} \quad (6.8)$$

Equation of motion of Substructure 1 can then be rewritten as

$$\mathbf{M}_{11}\ddot{\mathbf{x}}_1 + \mathbf{C}_{11}\dot{\mathbf{x}}_1 + \mathbf{K}_{11}\mathbf{x}_1 = -(\mathbf{MG})_1\ddot{x}_g + \mathbf{D}_1\mathbf{U}_1 - (\mathbf{M}_{12}\ddot{\mathbf{x}}_2 + \mathbf{C}_{12}\dot{\mathbf{x}}_2 + \mathbf{K}_{12}\mathbf{x}_2) \quad (6.9)$$

The right-hand-side of Equation (6.9) consists of three parts which are the seismic excitation, control force and interface forces. $\mathbf{D}_1\mathbf{U}_1$ is the control force which is also a part of external force of the target substructure and the term $-(\mathbf{M}_{12}\ddot{\mathbf{x}}_2 + \mathbf{C}_{12}\dot{\mathbf{x}}_2 + \mathbf{K}_{12}\mathbf{x}_2)$ is the vector of internal forces associated with the interface DOFs. In fact, this vector of interface forces can be taken as another set of external forces acting on the substructure. The responses $\ddot{\mathbf{x}}_1$, $\dot{\mathbf{x}}_1$ and $\mathbf{x}_1$ in Equation (6.9) can then be solved using the step-by-step Newmark-β integration method. For Substructure 2 the equation of motion can also be represented as

$$\mathbf{M}_{22}\ddot{\mathbf{x}}_2 + \mathbf{C}_{22}\dot{\mathbf{x}}_2 + \mathbf{K}_{22}\mathbf{x}_2 = -(\mathbf{MG})_2\ddot{x}_g + \mathbf{D}_2\mathbf{U}_2 - (\mathbf{M}_{21}\ddot{\mathbf{x}}_1 + \mathbf{C}_{21}\dot{\mathbf{x}}_1 + \mathbf{K}_{21}\mathbf{x}_1) \quad (6.10)$$

In the stage of structural evaluation, it is time consuming to identify the interface forces between substructures. To avoid this obstacle, the interface forces of the substructure are calculated from the structural responses of the initial finite element model in the first step of structural evaluation. In the subsequent steps, the interface forces are calculated with the updated structural model. The flow chart of the decentralized autonomous system of each substructure is the same as the centralized autonomous system shown in Figure 6.2. The structural control is based on the initial model of the structure at the beginning of the control operation, and it is then based later on the updated structural parameters transferred from the stage of structural evaluation.

6.4 Implementation Procedure

The implementation procedure of the decentralized autonomous structural control of the structure during an earthquake is described as follows. The stage of structural evaluation is followed with the stage of structural control.

Stage of substructural evaluation:

Step 1: Divide the structure into substructures and obtain the mass, damping and stiffness matrices of substructures.

Step 2: Conduct dynamic measurement on the substructures.

Step 3: Compute the interface forces from the intact finite element model (in the first iteration) or the updated FEM (in other iterations).

Step 4: Compute responses of substructures from Equations (6.9) and (6.10) and the sensitivity of responses with respect to structural parameters of the substructure from Equation (4.6) in Chapter 4.

Step 5: The changes of the substructure parameters are solved with the adaptive Tikhonov regularization in Equation (4.30) of Chapter 4.

Step 6: Repeat Steps 3 to 6 until the convergence condition defined in Chapter 4 is met.

Step 7: Update the FEM and transfer the FEM to the control system.

Stage of structural control:

Step 1: Perform structural control on each distributed substructure with the initial FEM of the structure at time steps when $t \leq t_0$ and with the updated FEM when $t > t_0$. t_0 is taken to be 2.65 s in this study.

6.5 Numerical Simulation

A 16-storey planar shear frame structure is investigated to illustrate the proposed adaptive integrated system. The sampling rate of measurement is 100Hz. The mass of each floor is 4×10^5 kg and the stiffness of each floor is 2×10^8 N/m.

The excitation is the earthquake ground motion record of N-S El-Centrol (1940) with the peak ground acceleration scaled to 0.3*g*. The horizontal accelerations on the 2^{th}, 5^{th}, 7^{th}, 10^{th}, 13^{th} and 15^{th} floors are taken as the “measured” responses for structural control and model updating. Two cases are studied in the simulation. Case (a) there is 10% stiffness reduction of the structure in the 3^{rd} floor and 11^{th} floor. It is assumed that the initial structural model is the intact. In Case (b) the uncertainty in the storey stiffness is assumed to follow a normal distribution and simulated the same way as the measurement noise. The mean value is taken as 2×10^8 N/m and standard deviation is taken as $0.05\times2\times10^8$ N/m. The initial stiffness of the finite element model is taken as 1.2 times of the mean value for application of the modified adaptive regularization method.

In the simulation, the first 2.5 second acceleration of the measured data is used for the structural evaluation. Since the time required for model updating of the structure is 0.15 s (depending on the computing speed of the CPU), the structure control is therefore conducted with the initial structural parameters in the first 2.65 s, and structural control after the first 2.65 seconds is based on the updated structural parameters.

The damage detection results of the first case are shown as Figure 6.4 without noise in the measurement and in Figure 6.5 with 10% noise in the measurement. Though there are some small errors in the identified result with noise in the measurement, the structural parameters are closer to the real structural model than the initial structural model. The acceleration response of the 16th floor is shown in Figure 6.6. It is shown that the acceleration is reduced more effectively with the updated model parameters. The parameters identification results of the second case are shown in Figure 6.7 without noise in measurement and in Figure 6.8 with 10% noise. The identified results are fairly accurate from contaminated measurement with some small errors. The structural control with the updated model parameters performs more effectively as shown in Figure 6.8.

6.6 Conclusions

A general decentralized autonomous control algorithm is proposed based on a general integration of structural control and structural evaluation system. A substructure technique is applied in the integrated system. Time response sensitivity method for damage detection is presented for the structural evaluation of each substructure in the time domain. A modified adaptive Tikhonov regularization method is applied to identify the structural model error and local damage. Due to the computational time required for the structural evaluation, the control force is calculated from the initial structural model at the beginning and with the updated structural parameters after the structural evaluation system transfers the updated parameters to the control system. In the numerical simulation, the structural parameters could be identified accurately with 10% noise in the measurement and the structural control is noted to be more effective with the updated model. The integrated decentralized autonomous system could be implemented with wireless sensor technology or hybrid sensory system to have a reduced cost and more convenience for the long-term structural health monitoring and structural control.

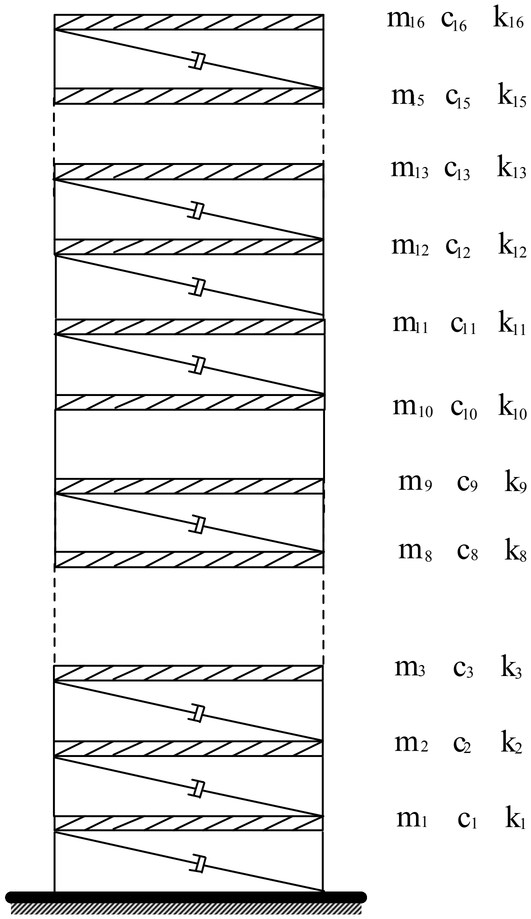

Figure 6.1 16-storey of shear frame with control device

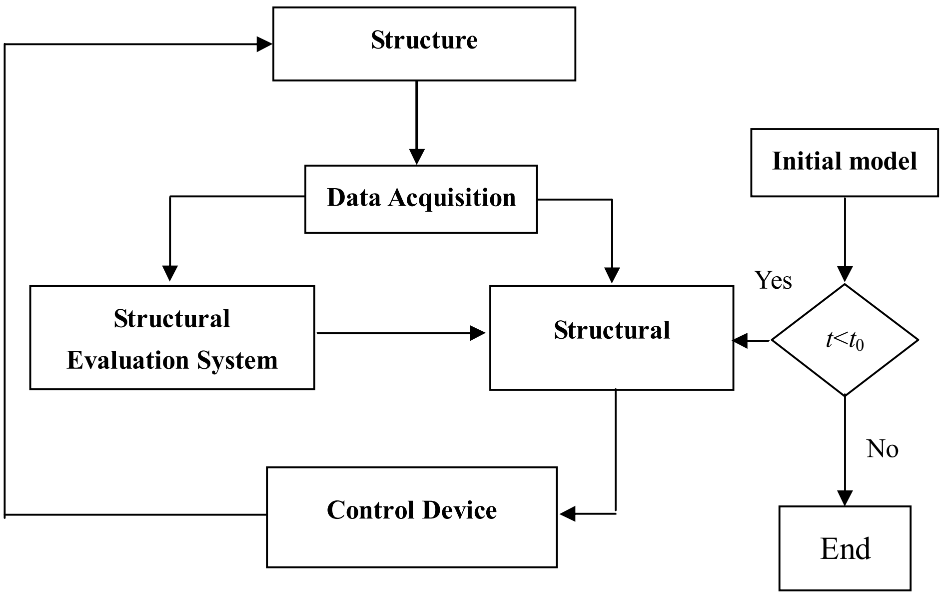

Figure 6.2 - Flow chart of the integration system

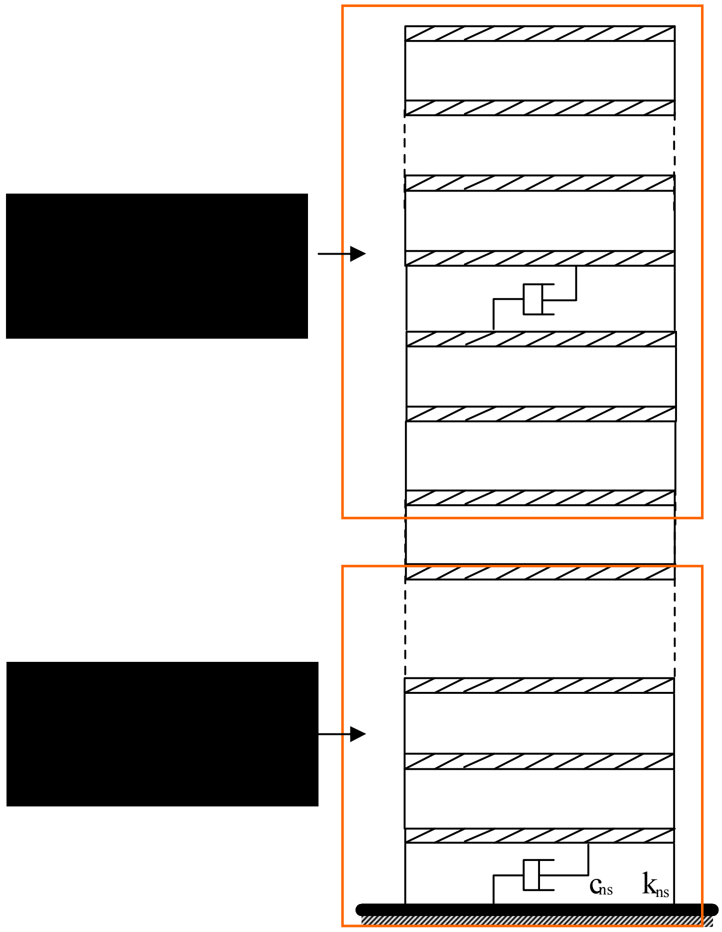

Figure 6.3 - 16-storey of shear frame with decentralized control method

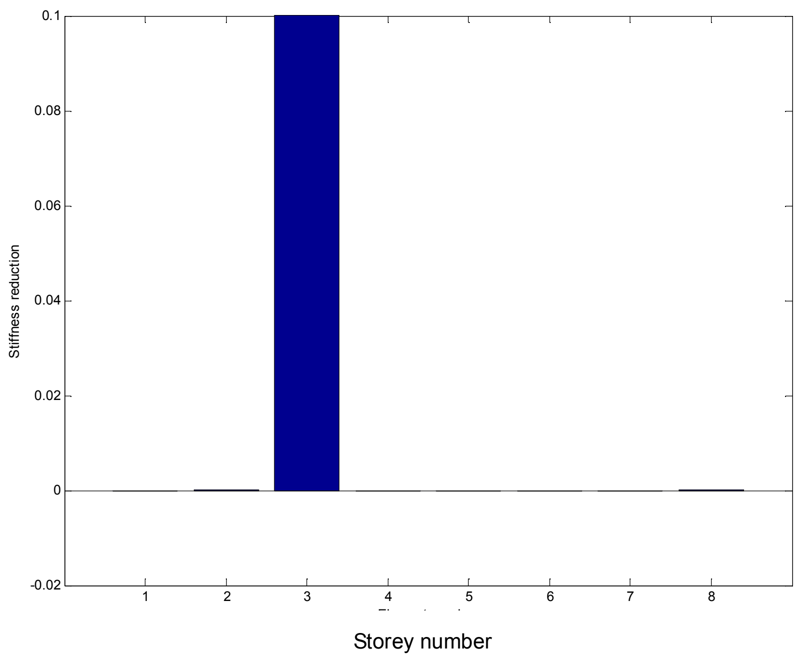

(a) Substructure 1

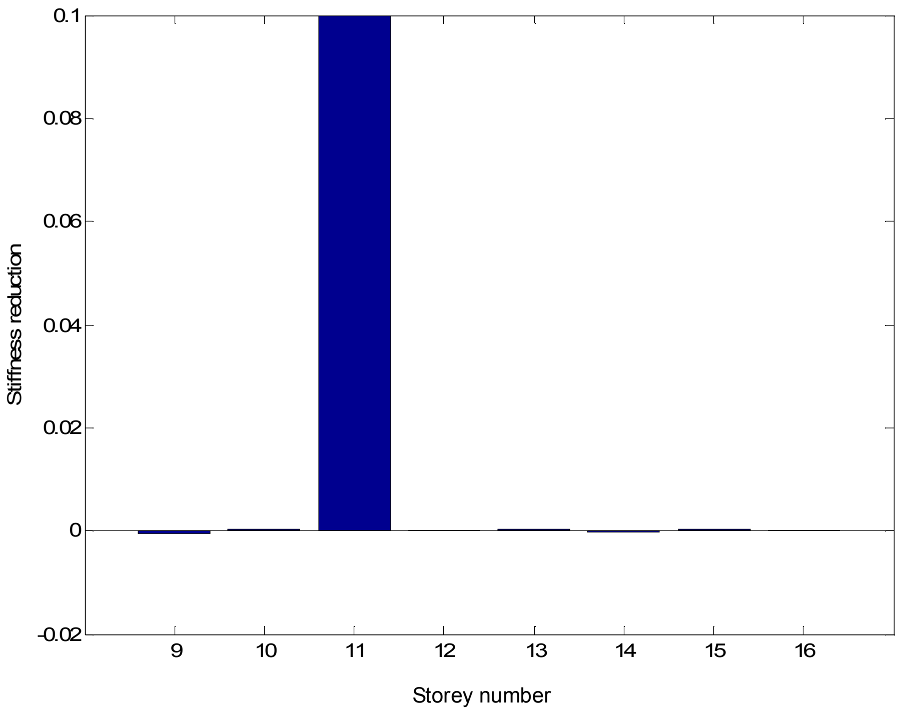

(b) Substructure 2

Figure 6.3 - Damage detection results without noise

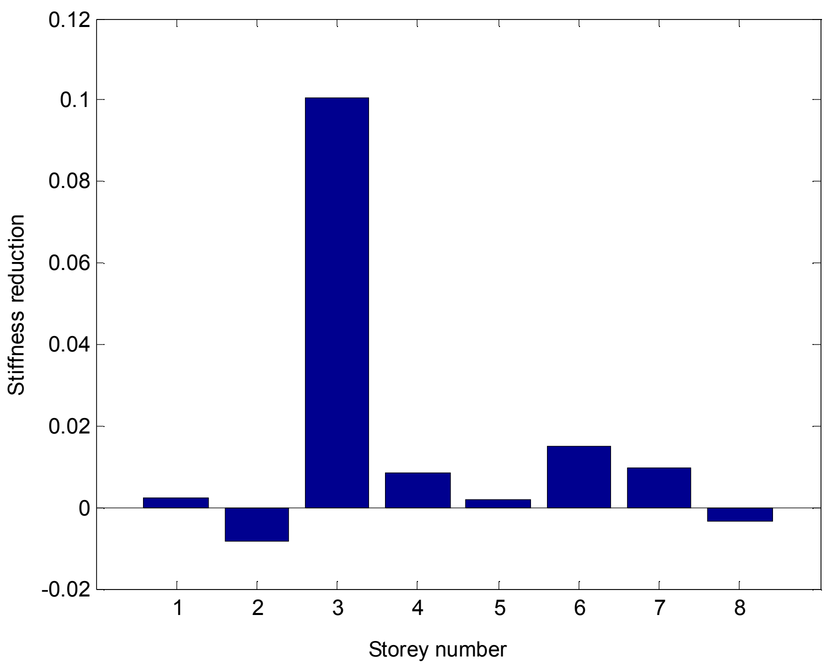

(a) Substructure 1

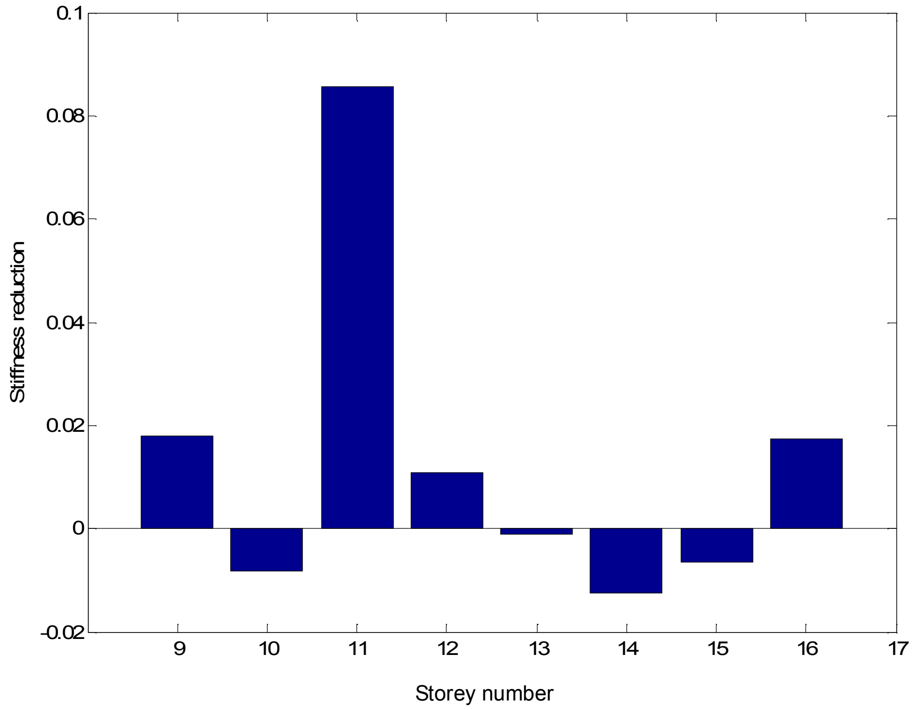

(b) Substructure 2

Figure 6.4 - Damage detection results with 10% noise

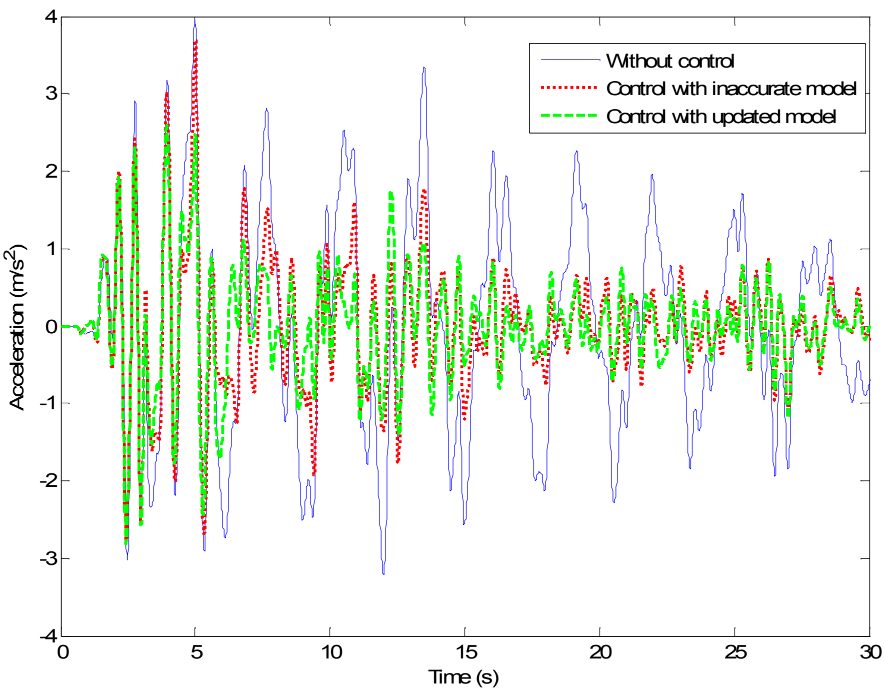

Figure 6.5 - Comparison of acceleration of the 16th floor (Case a)

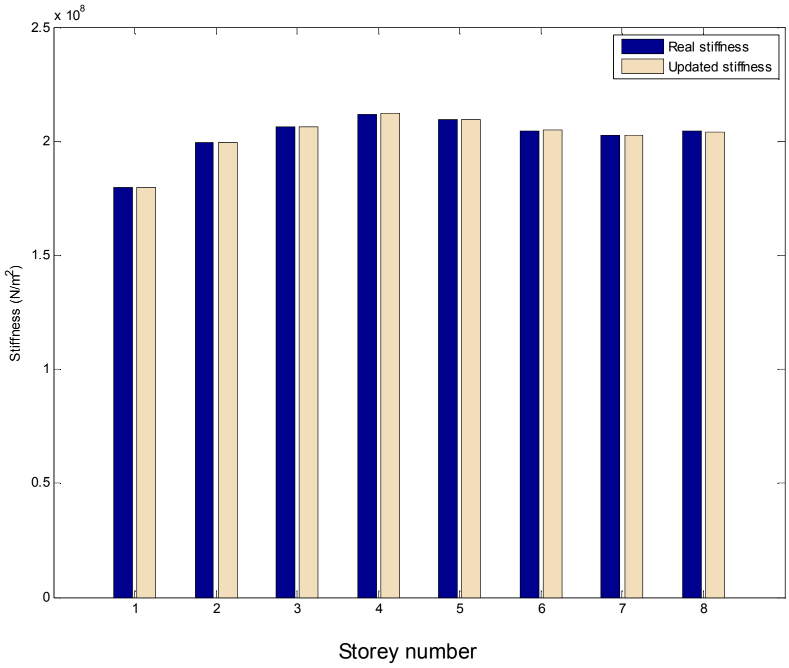

(a) Substructure 1

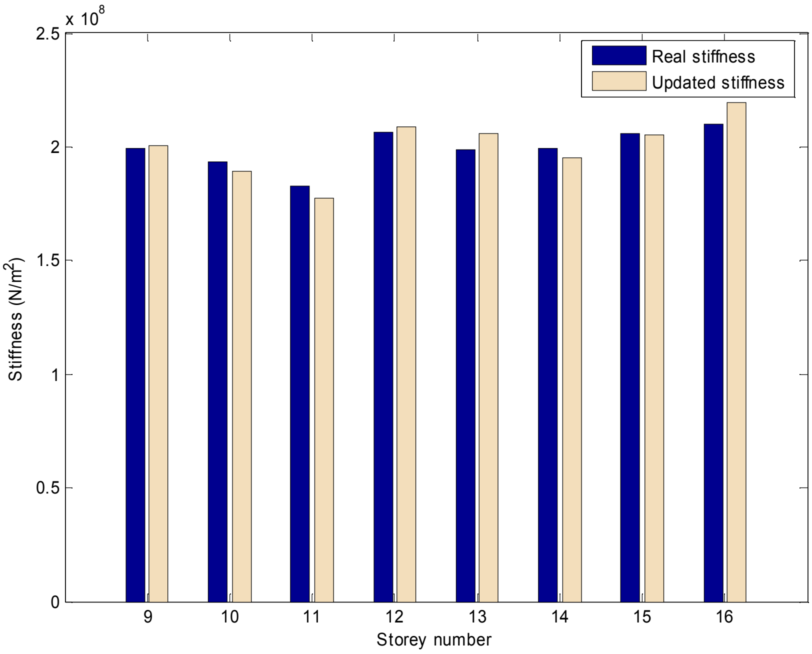

(b) Substructure 2

Figure 6.6 - Parameters identification results without noise

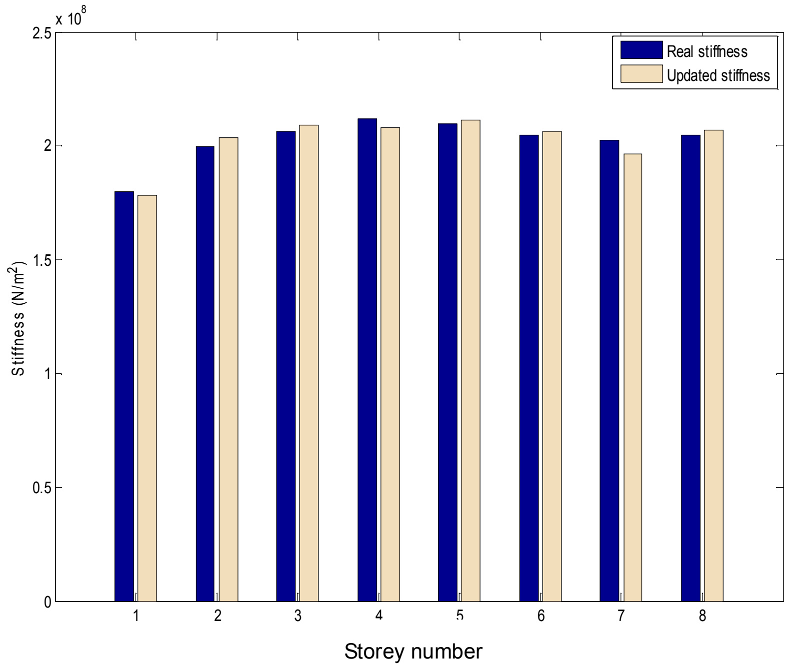

(a) Substructure 1

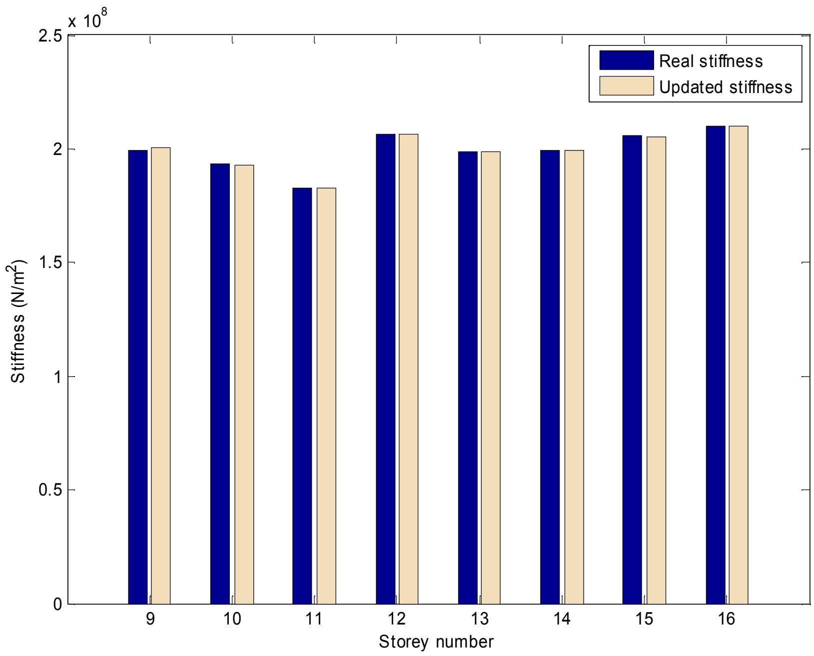

(b) Substructure 2

Figure 6.7 - Parameters identification results with 10% noise

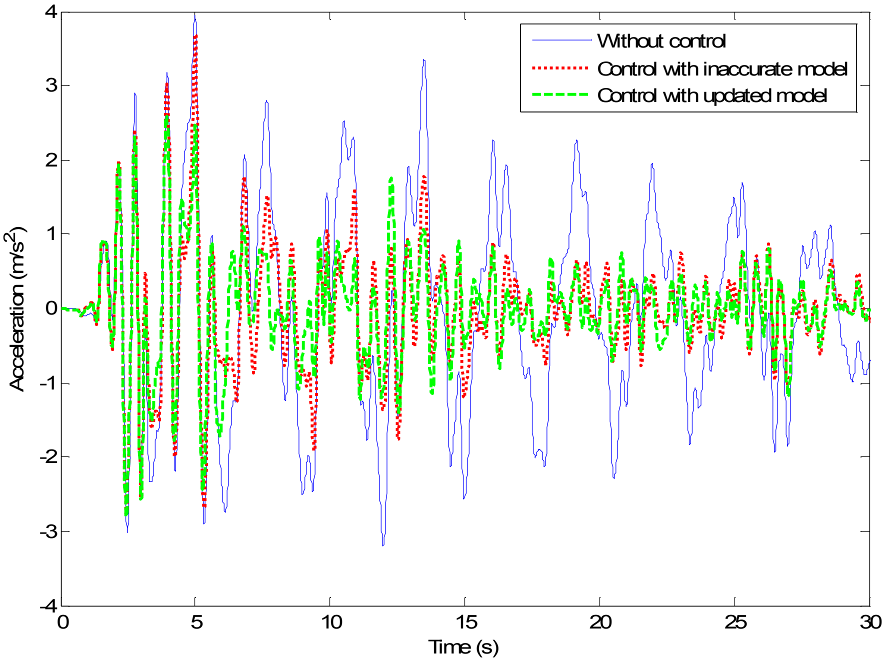

Figure 6.8 - Comparison of acceleration of the 16th floor Case 2

CHAPTER 7

LABORATORY WORK VALIDATION

7.1 Introduction

New structural condition assessment methods have been proposed and extensive numerical studies have been performed in the previous three Chapters. The numerical results demonstrated that the proposed method is sensitive to local structural parameters identification but insensitive to measurement noise, and model errors. This method can identify both location and severity of structural stiffness reduction satisfactorily. Nevertheless, the experimental investigation is necessary before the applications of these methods to practical engineering. This Chapter will present experimental investigations on some of these methods. Two structures, which are nine-bay space frame structure and two-dimensional frame, were built in the laboratory of The Hong Kong Polytechnic University for the methods validation. Measurements from the nine-bay cantilever space frame structure are used to validate the effectiveness of the proposed damping identification method with very accurate results. The experimental work with the two-dimensional frame was conducted to validate the proposed force identification methods and the two-stage substructural condition assessment method.

7.2 Experimental Work for Damping Identification

7.2.1 Dynamic Test of the Frame Structure

The nine-bay cantilever space frame was fabricated and tested in the laboratory as shown in Figure 7.1 (a). Members of the space frame were alloy steel tubes and they were connected to the ball joints as shown in Figure 7.1 (b) with a screw shown in Figure 7.1 (c). All the connection bolts were tightened with a torque wrench which provided the same torque for all joints to reduce human errors in the model fabrication. The physical properties of material and geometric properties are shown in Table 5.1 in Chapter 5. The finite element model with node number and member number systems is shown in Figure 5.1. A mass of 3.72kg was released freely from Node 29 to generate free vibration of the space frame. The vertical acceleration at Node 18 was measured with a B&K 4371 piezoelectric accelerometer. The sampling rate was 1000Hz and a one-second data was collected for the identification of damping models as described in Sections 5.1 and 5.2. The vertical acceleration from Nodes 18 and 23 were measured for the modal damping identification as described in Section 5.3 where the sampling rate was 200 Hz and also a one-second duration of data was used. The number of identification equations and unknowns for studies on different damping identification is the same as those shown in Table 5.4.

7.2.2 Damping Identification of the Space Frame Structure

Figure 7.2 gives the measured response and the calculated response of the vertical acceleration at Node 18 for the time-invariant Rayleigh damping model. Figure 7.3 shows the comparison of responses based on the time-variant Rayleigh damping model. In the first 0.5s of the time history, the fluctuation of the measured response is large which is due to the impulsive action of the free falling mass which might induce a broad spectrum of excitation. There are differences close to the peaks of the curves throughout the whole time duration. This can be explained as the effect of environmental noise in the measurement. Model errors distributed in the mass, stiffness of the structure and connection of base support might also contribute to this differences. The error of the constructed response is calculated as

$$error_{acc} = \left\| \ddot{\mathbf{x}}_{mea} - \ddot{\mathbf{x}}_{cal} \right\| / \left\| \ddot{\mathbf{x}}_{cal} \right\| \times 100\% \tag{7.1}$$

where $\ddot{\mathbf{x}}_{mea}$, $\ddot{\mathbf{x}}_{cal}$ are the measured and re-constructed accelerations respectively. The errors in the first second of identification for the three types of damping models are 43.6%, 37.2% and 26.3% respectively.

The above observations show that the time-variant modal damping identification is more accurate but it is also time consuming due to a large number of unknowns to be identified when all the modes are considered. It may be concluded that the time-variant damping is more accurate to describe the dynamic property of the structure and the time-variant modal ratio gives a more general description on the structural damping.

7.2.3 Discussions

It should be noted that the laboratory test was subject to excitations from operating mechanical systems in the surroundings. The test structure was slightly vibrating all the time, and the initial response of the structure was not zero at the beginning of the recorded data. The study was repeated with a longer duration of measurement for the time-variant damping identification to try to reduce the influence of initial value of the structural response caused by the environmental excitation. The sampling rate was changed to 200Hz and 3s measured acceleration from Node 18 was used in the two types of time-variant damping identification. The differences between the measured and re-constructed response curves on both the time-variant Rayleigh damping model and the time-variant modal damping model improve towards the end of time history but there are still some noticeable differences in the peaks at the beginning of the time history. The modal damping model gives better prediction in the first second of the time period than the other model. The errors of identification for the time-variant Rayleigh and time-variant modal damping models are respectively 35.6% and 22.4% which are slightly less than that from previous study with 1s response measurement.

The error of damping identification with experimental measured data is noted to be larger than those from the numerical studies due to the measurement noise and initial model errors. Also the type of damping is unknown in experiment while the type of damping is known with the simulation matching the type of damping model in the identification algorithm.

7.3 Tests of a Two-dimension Frame for Structural Condition Assessment

7.3.1 Experimental Arrangement

In this section the proposed structural external excitation identification methods described in Section 3.3 and the two-stage structural condition assessment method proposed in Chapter 4 will be validated with the experimental studies of a two-dimensional frame. The seven-story two-dimensional steel frame as shown in Figure 7.4 was fabricated and tested in the laboratory of The Hong Kong Polytechnic University. The finite element model consists of 56 elements and 51 nodes as shown in Figure 7.5. The tests of data were recorded with DEWESoft software and NI data acquisition equipment. The physical properties of the 7-storey steel frame are listed in Table 7.1. Two lumped mass were placed on each floor of the frame structure to simulate the effect of the floor slab, and the weight and their locations are of the lumped mass is listed in Table 7.2. The two supports of the frame were welded to the steel base plate and the plate was connected firmly to the ground simulating rigidly fixity to the ground. The finite element model consists of 56 elements and 51 nodes as shown in Figure 7.5. The test data was recorded with DEWESoft software and NI data acquisition equipment.

The intact structure was tested with free vibration tests and hammer impact tests respectively. Only the acceleration responses were used for the external excitation identification and structural model updating. The first seven frequencies of the intact structure are shown in Table 7.3. The stiffness of the structure was updated based on the first seven frequencies and mode shapes with the optimal function ‘fmincon’ of MATLAB. The initial Young’s modulus is set as 2.0×10^{11} N/m^2 for all components of the frame structure. The updated Young’ modulus of beam is 2.2×10^{11} N/m^2 and the updated Young’s modulus of column is 1.9×10^{11} N/m^2. The first seven frequencies of the updated structure and the percentage of the errors are shown in Table 7.3. It is noted that the updated modal parameters are very close to the tested frame structure.

Firstly, with the measured acceleration responses from the intact structure was used to estimate the external excitation with the proposed force identification method with FOH discrete method as presented in Section 3.3 of Chapter 3. Secondly, the two-stage model updating method as the described procedure in Section 4.5.2 was conducted on the intact structure. It is noted that the updated model of the structure may be still inaccurate though the model has been updated with the modal parameters in frequency domain. The model updating based on the time domain information could obtain more accurate model for the next stage of study. Thirdly a single-damage scenario was inflicted to a column in the 4th floor of the 7-storey frame with the width of the left column on the 4th floor was reduced from 49.89mm to 40mm with 5.0 mm from both sides of the left columns as shown in Figure 7.6. The structural condition assessment of the frame was conducted with free vibration tests. Finally a multi-damage scenario was studied with a similar the structural damage to the left column in the 2nd floor. The damage levels are the same at the 2nd floor and the 4th floor. The model updating was conducted on the damaged structure with hammer impact tests applying. Both the free vibration tests and hammer impact tests will be described in the following Sections.

7.3.2 Force Identification of the Intact Structure with FOH Discrete Method

The whole structure was divided into two parts for the force identification with substructure method as shown in Figure 7.5. The target substructure consists of the Elements from 5 to 56 and Nodes 4-51 except Node 9.

The impact force of hammer was identified based on the measured acceleration response. The acceleration responses in the x-direction were measured at Nodes 4, 11, 15, 18, 25, 32, 39 and 46 for the force identification in this section and the Nodes positions are shown in Figure 7.5. The impact force is applied horizontally on Node 50 with a hammer. The sampling rate is 1000Hz and as few as 160 sampling points are used for the impact force identification. There is no information on the interface forces. Figure 7.7 shows the external force identification result of the hammer impact force on Node 50 and the measured force from the hammer. It is noted that the measured force and the identified force are similar but there are also some fluctuations in the time history of the identified force, which are mainly from the effect of operational mechanical system in the laboratory. It is should be noted that the manual hitting of the hammer may be not absolutely horizontal, which may cause that the identified force is a little different from the measured force at the peak. The errors between the numerical response and measured acceleration response calculated from Equation (7.1) are 10.42% with ZOH discrete method and 7.53% with FOH discrete method as presented in Chapter 3. It is demonstrated that the force identification accuracy of substructure with FOH method is acceptable. In the following study, the FOH method is applied in force identification for higher accuracy.

7.3.3 Model Updating with Two-stage Method

7.3.3.1 Two-stage Model Updating on the Intact Structure

The free vibration test is conducted by the free falling of a hanging mass to update the structural model of the intact frame. The force of the hanging mass is 40N and it is applied in x-direction horizontally at Node 50 with a mechanism as shown in Figure 7.8. The positions of sensors are the same as those for the previous study. The sampling rate is 1000Hz and 0.8s of the data was used for force identification and the last 0.5s of the date was used for the structural model updating to avoid the very high frequency response generated by the impact action. The implementation procedure of the method in Chapter 4 was adopted. It is noted that the model updating in this section is for the whole frame to obtain a more accurate structural model.

The force identification result of from the falling mass tests based on the FOH discrete method is shown in Figure 7.9. It is shown that the force time history applying on Node 50 is nearly 40N before the falling which is consistent with the weight of the mass. It is also indicated that the time of the release of the mass is at around 0.265s from the beginning. The indentified result of the external force could reflect the whole process of the falling of the mass. But there are some fluctuations in the time history of the force especially close to the release of the mass. There may be three sources that cause such the fluctuations. The first one is that the hanging mass was not absolutely still and was interacting with the frame all the time. The second one is the operating mechanical systems in the surroundings as mentioned in Section 7.2. It is shown in Figure 7.9 that the fluctuation near the abrupt release of the string becomes a little larger. This may be due to the manual cutting of the string. The model updating result is shown in Figure 7.10. The model error of the intact structure may mainly be caused by the uncertainties of geometric property and Young's modulus and the welding of the beam and column joints. The updated structural parameters of the intact structure could be used as initial reference for the successive model updating.

7.3.3.2 Two-stage Model Updating on the Damaged Structure

The frame structure was divided into two substructures as shown in Figure 7.5 for validation of the two-stage substructural condition assessment method validation. The structure is divided into two substructures similar to the in Section 7.3.2. Two cases are studied in this Section. A single damage case is studied firstly with free vibration generated by the abrupt release of the hanging mass as shown in Figure 7.8. Accelerometers are placed on the Nodes 18, 25, 29, 32, 36, 39, 43 and 46 in the x-direction. The sampling rate is 1000Hz. 0.8s measured acceleration responses were used for the force identification while last 0.4s measured acceleration were utilized for the structural model updating. Reason of this selection is the same as for study in Section 7.3.3. The external force identification result is shown as Figure 7.11 and the damage detection result is shown in Figure 7.12. The characteristics of the identified force identification are consistent with the external force identification result in Section 7.3.3.1. The time history of the identified force is consistent with the measured force though there are some fluctuations and a little difference at the peak. Local damage could be located at Element 26 and the damage level is demonstrated as 5.56%. This value is less than the true condition of this experiment calculated as 8.3 % from an equivalent element with the same displacement under a transverse load. It is noted that the summation of the damage of Element 26 and Element 28 nearly equal to the true damage level of the structure. This is because both of these elements are at the same level contributing to the same storey stiffness.

Secondly, a multi-damage case was studied with the initial structural model obtained in Section 7.3.3.1. The horizontal acceleration responses in the x-direction under the horizontal hammer impact at the 7^{th} floor at Node 50 were measured at Nodes 11, 17, 22, 29, 36, 38, 43 and 46. Also, 0.8s measured data was used for the force identification and last 0.5s measured data was used for model updating. The impact force applied on the damaged structure is identified as Figure 7.13. It is shown that the peak of the impact force is very clear but there are also some small fluctuations before and after the peak of the impact force. As illustrated in Section 7.3.2, the fluctuations may be due to the excitations from operating mechanical systems in the surroundings and manual hitting with the hammer. Figure 7.14 is the model updating result. It is demonstrated in that the damage could be located on Elements 10 and Element 26 with the proposed method while there are some errors in other components, especially in Elements 12 and Element 28. This observation is similar to that for the single damage case as Elements 10 and 12 are at the second storey while Elements 26 and 28 are at the 4^{th} storey and they are performed together to contribute to the storey stiffness at each level. The total summations of damages at these two levels are 5.62% and 2.60% respectively which are close to the equivalent value of 8.3%.

7.4 Summaries

The time-variant damping identification method and the two-stage substructural condition assessment method described in previous Chapters were experimentally examined in this Chapter. A nine-bay space frame and a seven-storey two-dimensional frame were fabricated for hammer impact tests and free vibration tests.

Firstly, the nine-bay space frame structure is tested with free vibration tests to identify the damping of the structure. The parameters of time-invariant

Rayleigh damping, time-variant Rayleigh damping and time-variant modal damping were identified with the measured data to examine the accuracy of damping model as well as the proposed damping identification method. It was found that the time-variant modal damping was more accurate than the time-variant Rayleigh damping model when conducting the structural dynamic analysis. When the modal damping ratios are difficult to estimate or there is some innovative energy dissipation devices installed in the structural system, it is suggested that the damping can be initially assumed as time-invariant Rayleigh damping for a rough estimation to form a set of reference values for the subsequent more accurate time-variant damping identification. It is also recommended that the time-variant modal damping be utilized for the long-term structural health monitoring because there may be significant changes in the damping mechanism with time due to the changing environmental conditions and structure in the service life of the structure.

Secondly, the experimental data of a seven-storey frame were analyzed to conduct the external force identification and substructural model updating. A substructural external force identification method based on the equation in state space with the FOH discrete was experimentally studied in this Chapter. This method only needs acceleration responses measurement, and information on the finite element model of a substructure. The external force could be identified satisfactorily with the substructure method. It was also found that the proposed force identification method based on FOH discrete method was more accurate than the existing force identification method with ZOH discrete method. With the proposed two-stage method, the location and severity of the single damage scenario and multi-damage scenario could be identified satisfactorily though there are some errors in the intact elements. It is also found in this study that the symmetry of the structure affects the identification results with time domain method. It should be noted that the theoretical value of the damage may be different from the real case, but the identified results are close to the true values.

Table 7.1 - The property of the seven-storey frame

Properties	Member
Area of the beam (mm^2)	49.98×8.92
Area of the column (mm^2)	49.89×4.85
Density of the beam (kg/m^3)	7850
Density of the column (kg/m^3)	7734
Poisson ratio	0.3
Moment of area I_z (m^4)	3.645×10^{-9}
Torsional rigidity J [m^4]	7.290×10^{-9}

Table 7.2 - The weight and location of the lumped masses

Storey number	Node number	Weight (Kg)	Node number	Weight (Kg)
1	5	3.9456	7	3.9631
2	12	3.9231	14	3.9199
3	19	3.9568	21	3.9350
4	26	3.9247	28	3.9372
5	33	3.9476	35	3.9772
6	40	3.9682	42	3.9687
7	47	3.9571	49	3.9321

Table 7.3 - The first seven frequencies comparison

No. of frequency	Intact structure (Hz)	Updated numerical model (Hz)	Error (%)
1	2.53	2.53	0.0
2	7.66	7.67	0.13
3	12.85	12.86	0.077
4	18.04	18.00	0.22
5	22.98	22.90	0.35
6	26.98	27.01	0.11
7	29.91	29.88	0.10

(a) A nine-bay space frame in laboratory

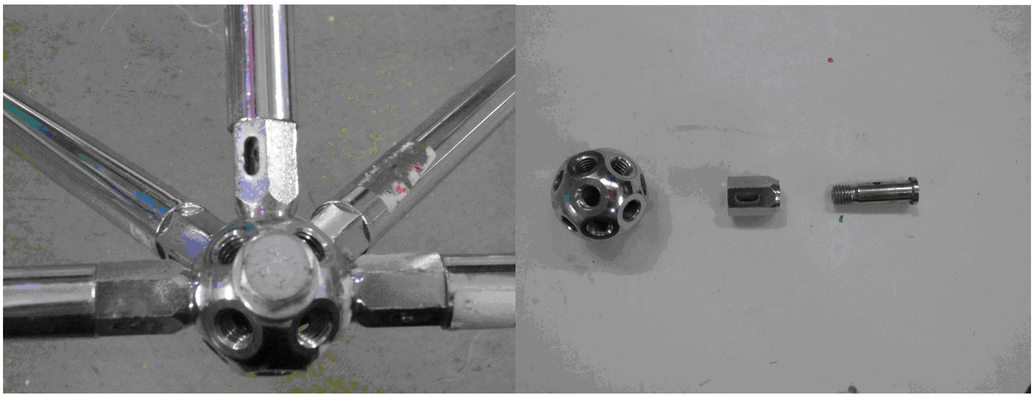

b) The joint connection (c) The ball joint of the connection

Figure 7.1 - Photographs of the three-dimensional space frame

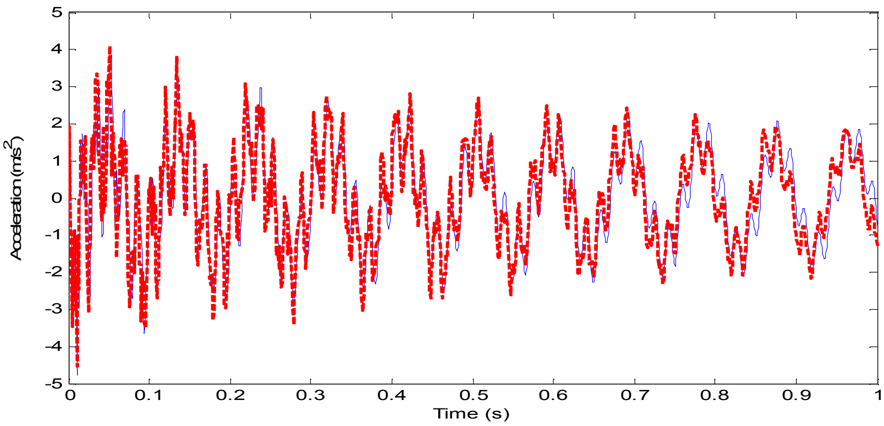

Figure 7.2 - Comparison of acceleration at Node 18 with time-invariant Rayleigh damping model laboratory work (___real, ---- reconstructed)

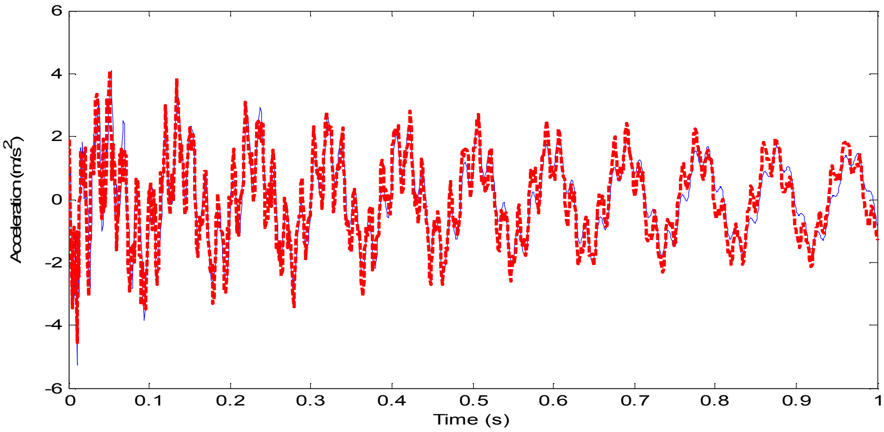

Figure 7.3 - Comparison of acceleration at Node 18 with time-variant Rayleigh damping model laboratory work (___real, ---- reconstructed)

Figure 7.4 - Photographs of the two-dimension frame

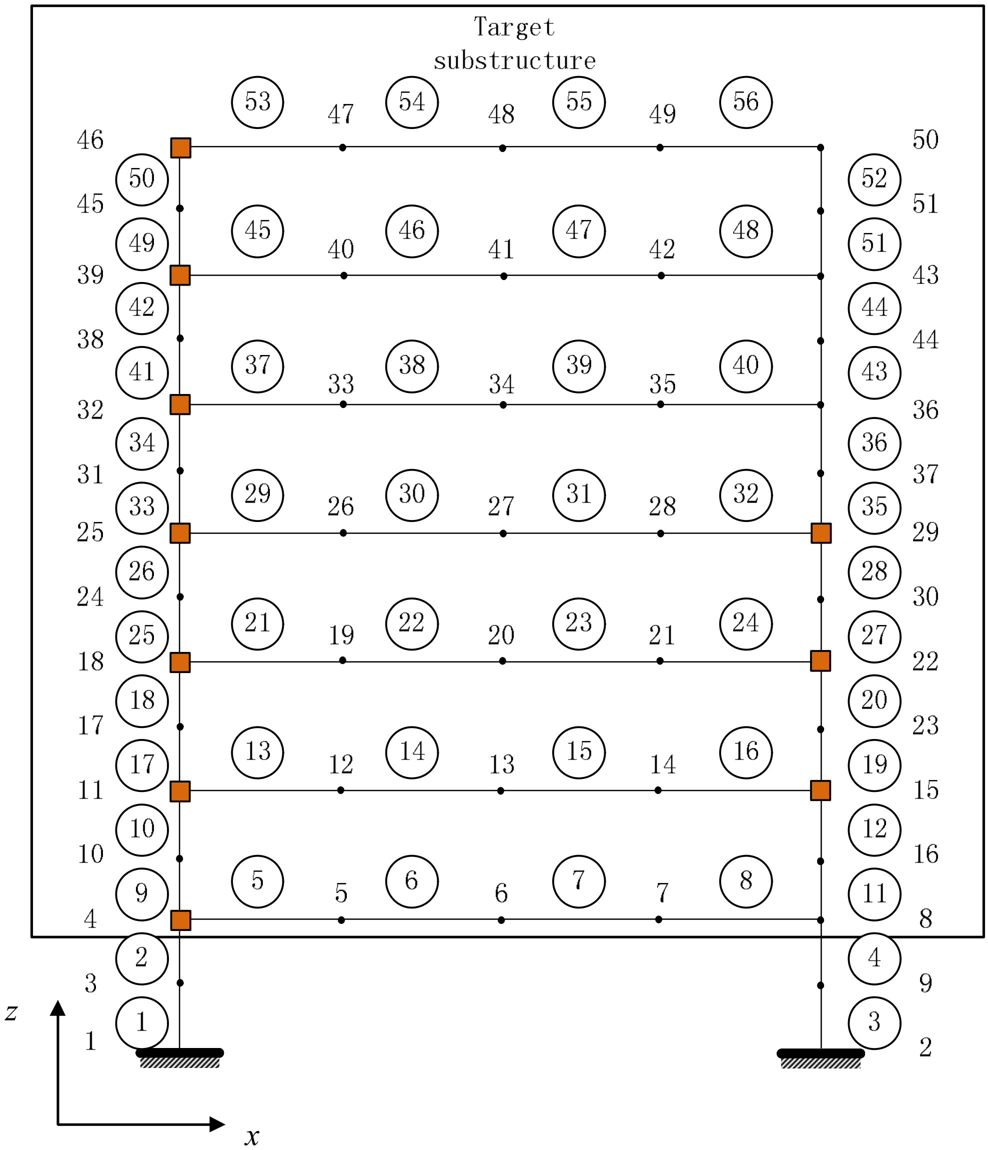

Figure 7.5 - Two-dimension seven-storey frame structure

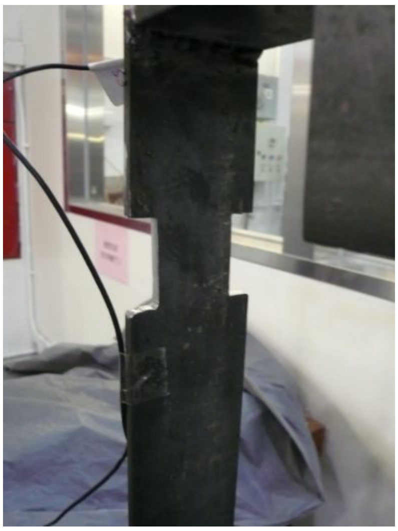

Figure 7.6 - Photographs of the damaged column

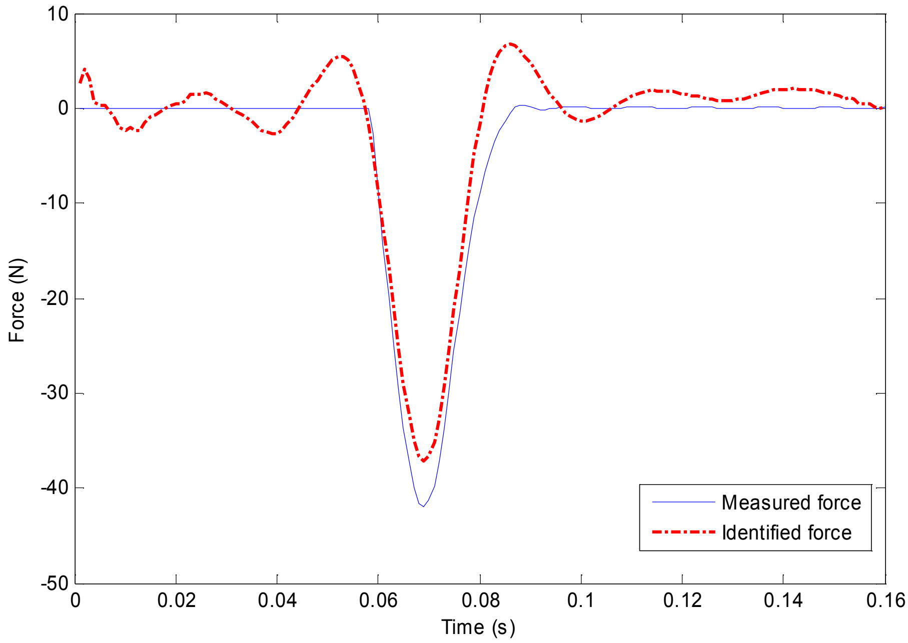

Figure 7.7 - Impact hammer force identification of intact structure with FOH discrete method

Hanging mass

Figure 7.8 - Photographs of the hanging mass on the two-dimension frame

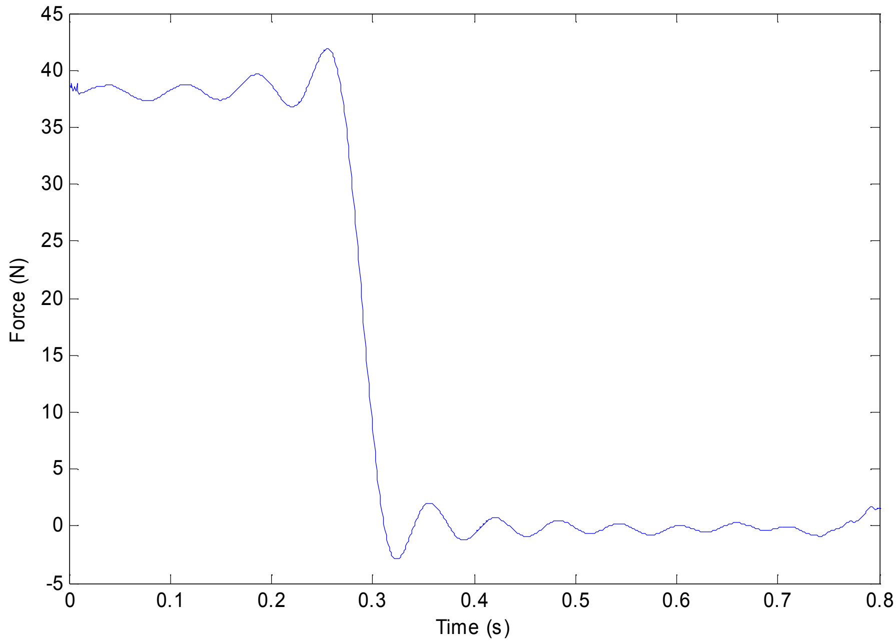

Figure 7.9 - Force identification of the abrupt falling of the mass on the intact structure with FOH discrete method

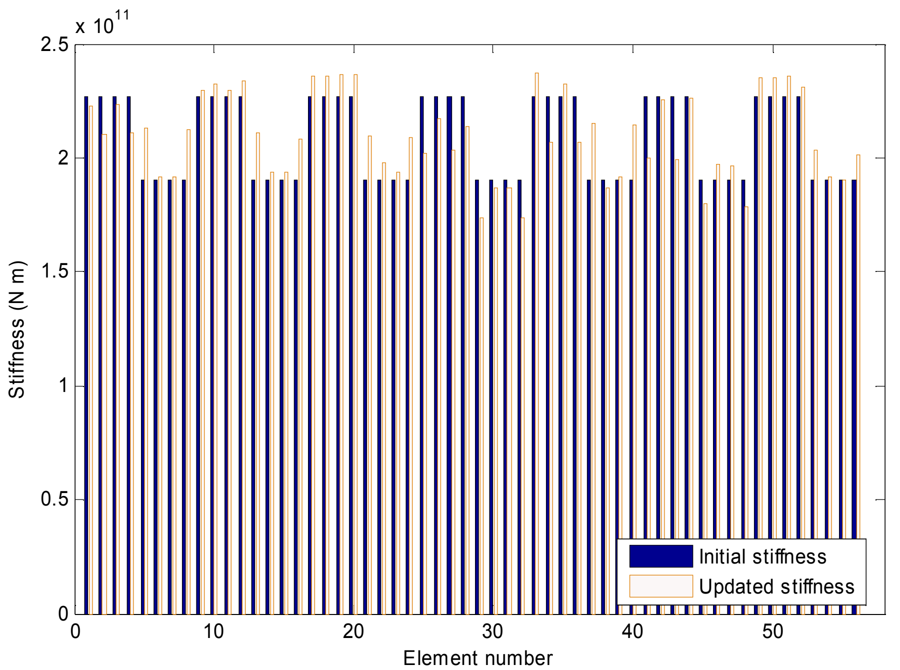

Figure 7.10 - Model updating result of the intact structure

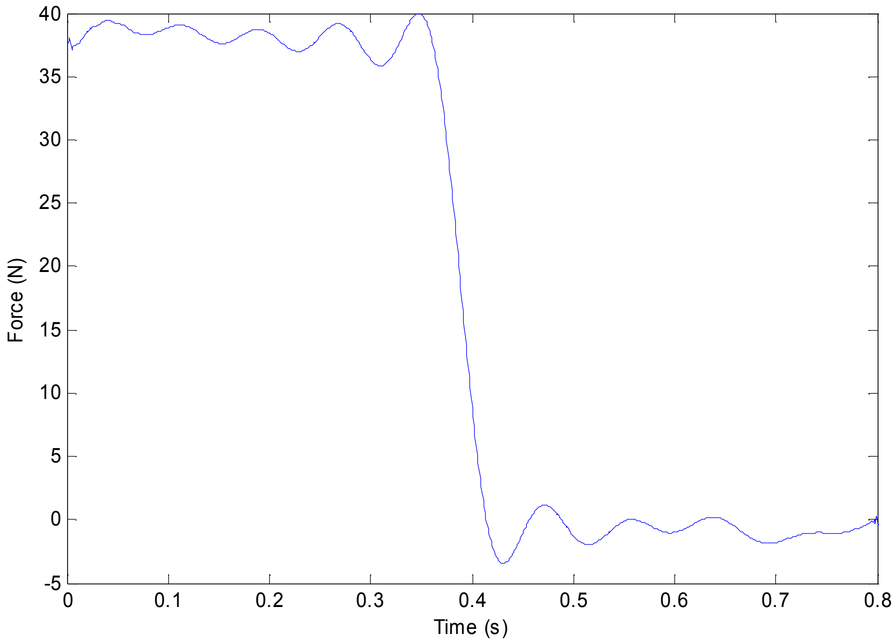

Figure 7.11 - Force identification of the abrupt falling of the mass on damaged structure with FOH discrete method

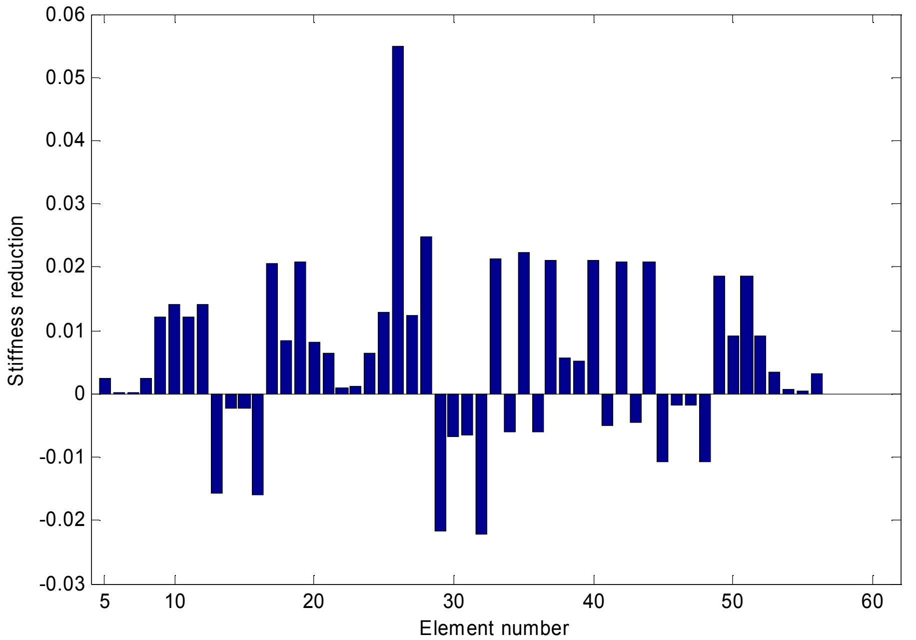

Figure 7.12 - Damage detection of the single damage scenario

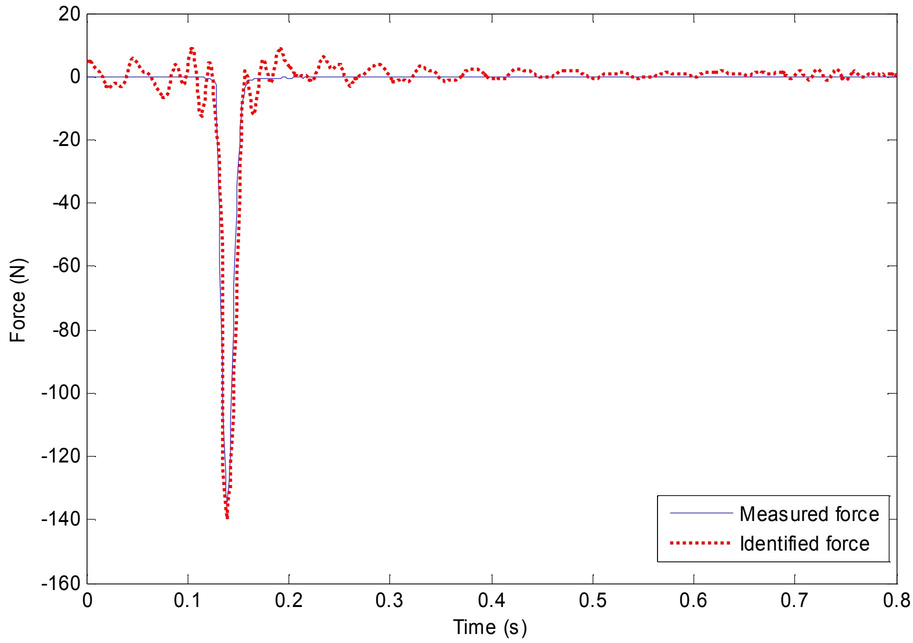

Figure 7.13 - Impact hammer force identification of damaged structure with FOH discrete method

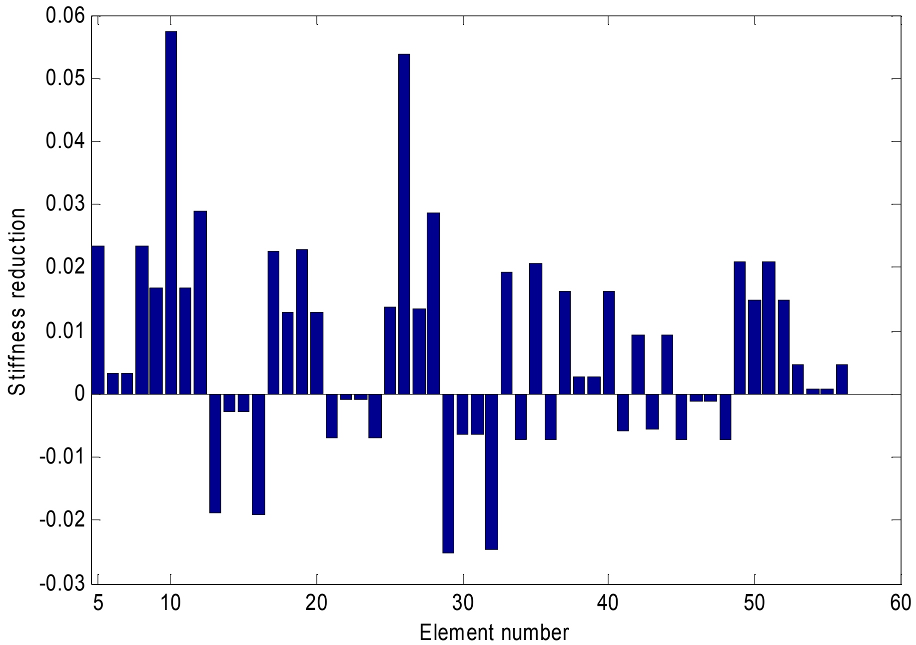

Figure 7.14 - Damage detection of the multi-damage scenario

CHAPTER 8

CONCLUSIONS AND RECOMMENDATIONS

8.1 Conclusions

The dissertation has established a frame work aiming to systematically propose and develop structural condition assessment method and structural vibration control algorithm with substructure techniques. A detailed illustration and proof to substructural condition assessment method with time domain response sensitivity method is provided which contributes to the development of the substructural methods with structural response in time domain. On the basis of this detailed proof and illustration two substructural condition assessment methods are presented with two-stage identification method. In the first method, the FEM of the whole structure is needed while only the FEM. This method could improve the computational efficiency with less unknown structural parameters. In the second method only the FEM of the target substructure is required. This method enables structural health monitoring of the large-scale structure only with the information from target substructure. Two new computational techniques are proposed to improve the first stage identification, which are: a time window force identification method to reduce the computation effort; and a method for the simultaneous identification of the unknown interface force and the initial structural responses of each time window. The time window identification method is originated from the average acceleration integration method. And the time window identification method is developed for the time-variant parameter identification and nonlinear parameter identification. A decentralized autonomous structural control system is proposed with the first substructure method. Numerical simulations and experimental works are conducted to investigate the effectiveness and efficiency of the partially proposed methods. The results and findings are summarized as follows.

Firstly, a force identification method with FOH discrete method was proposed for a substructure with the FEM of the substructure only. The formulation of the force identification with FOH method is derived numerically. Numerical simulation studies have been conducted with three cases of a force applied on a fixed position, a moving force only on the target substructure and a moving force on the whole structure for general application purpose. The results of the numerical examples indicate that the external force can be identified accurately though there are some errors in the interface forces of the target substructure. The simulation studies also demonstrate that the number of the sensors could be less than the number of forces relative low level of measurement noise. A laboratory work of a seven-storey frame is investigated to validate the proposed force identification method. The identification results indicate that the external force could be identified accurately with the proposed method and noisy measurement in laboratory.

Secondly, a detailed proof and illustration to substructural condition assessment method with the analogous evolution of a pseudo substructure in the model updating process in time domain is provided. The formulation presented in Section 4.3.2 provides a basis on the substructural sensitivity matrices and removes the limitations with ideal modeling of the boundary condition of substructure. The presented approach is capable for general application with substructures in the sensitivity approach of analysis. Based on the proof and illustration, two general substructural condition assessment methods are proposed based on the two-stage identification method. In the first method, the finite element model of the whole structure is required and a selected substructure is assessed for its structural conditions. In the second method, only the finite element model of the selected substructure is required with the dynamic measurement and excitation within the same substructure. This method could be applied for substructural model updating considering the nonlinear support-structure interaction. Exact knowledge on the boundary conditions of the substructure is not necessary. The proposed method is analogous to the evolution of a pseudo structure with iterative model updating. The numerical simulations in Section 4.6 indicate that the structural damage could be located and quantified with the proposed two-stage substructural condition assessment method. A two-dimensional seven-storey frame is tested in laboratory with the second two-stage method. The identification results show that the method is applicable to locate and quantify the structural damage.

Thirdly, two new computational techniques are proposed to improve the force identification, which are: a time window force identification method to reduce the computation effort; and a method for the simultaneous identification of the unknown interface force and the initial structural responses of each time window. Formulations for the simultaneous identification of unknown interface force and initial structural responses are derived in Section 4.4.2. Simulations in Section 4.6 also illustrate that the new techniques could improve the computational efficiency and remove the *priori* assumption of initial structural response satisfactorily.

Fourthly, two methods are developed for time-variant structural condition assessment. In the first method, the time history of time-variant parameter is represent with Chebyshev polynomial and the coefficients of polynomial is identified based on the difference between the measured response and calculated response. Experiments of nine-bay space frame are studied to validate the proposed time-variant damping identification method. The identification results indicate that the time-variant modal damping is more accurate than the time-variant Rayleigh damping model when conducting the structural dynamic analysis. In the second method, a time window identification method is developed for the time-variant parameter identification. A two-phase identification algorithm is presented to conduct the identification in each time segment. In the first phase, the initial structural response is identified with iterative Tikhonov regularization method while the structural model is updated with a modified adaptive regularization method. The occurrence time, location and severity of local changes in the storey stiffness can be identified with acceptable results even when the measurement is polluted by noise. The presented work indicates that the proposed method can be applied to conduct the post-earthquake structural condition evaluation.

Finally, a new decentralized autonomous control algorithm is proposed based on a general integration of structural control and structural evaluation system. A substructure technique proposed in Section 4.5.1 is employed in the integrated system. Time response sensitivity method for damage detection is employed for the structural evaluation of each substructure. A modified adaptive Tikhonov regularization method is applied to identify the structural model error and local damage. In the numerical simulation, the structural parameters could be identified accurately with 10% noise in the measurement and the structural control is noted to be more effective with the updated model. It is indicated that the integrated decentralized autonomous system could be implemented with distributed wireless sensor technology to have a reduced cost and more convenience for the long-term structural health monitoring and structural control.

8.2 Recommendations

Structural condition assessment and structural vibration control with substructure methods has developed in this thesis. And some aspects can be improved and expended as follows:

1 The inverse analysis may be adversely are affected by the uncertainties of

structural system, excitation and measurements. This thesis only considered the uncertainties of materials and measurements. The uncertainties need to be fully considered in the further research including the temperature effect. The recommendations to search the optimal parameter with regularization methods due to different sources of uncertainties are desirable.

2 Time-variant stiffness identification method is only validated by numerical simulation. Experimental work is required before the engineering application of this proposed method. Experimental verification of the proposed method on large-scale structure is also necessary.

3 In this thesis the linear damage model is assumed to be permanent reduction of stiffness and the nonlinear damage model is assumed to be bilinear model. However there are a number of patterns of the crack or damage in practice, especially the nonlinear structural damage model. More damage model is needed to be considered in the further research.

4 The time-variant model of Rayleigh damping and modal damping ratio may be different from the practical condition. More research work is required to obtain an accurate model to describe the damping mechanism of civil structural system.

5 The proposed substructural condition assessment methods are applied to shear building, truss structure and two-dimensional frame. Further

investigation aiming to extend this method to complicated structure with more interface forces is recommended.

6 The proposed two-stage substructural condition assessment methods can be utilized to identify the external forces and detect the damage. The accuracy of the force identification in the first stage may affect the damage detection result. Further investigation of a simultaneous identification of external force and damage is recommended. The influence of model uncertainties could be mitigated with this idea.

7 The measurement in both numerical simulation and experimental investigation are the acceleration responses from translational degree-of-freedom. The rotational measurement may be more sensitive to the changes of structure. It is recommended that rotational measurement could be utilized in further inverse problem with the development of data acquisition system and sensors. Hybrid measurement from the structural could provide more information about the changes of structure. Methodology based on the hybrid measurement is recommended to be developed for the structural condition assessment. Dynamic strain measured by FBG is also alternative measurement.

8 The decentralized autonomous control system based on the presented substructure method is proposed in this thesis. Further experimental validation is needed and other types of decentralized autonomous control system based on frequency domain structural condition assessment

method is suggested.

Appendix A

Impulse response of the extrapolation filter (Franklin et al. 1998) for the modified first-order hold (triangle hold) is shown as the following figure

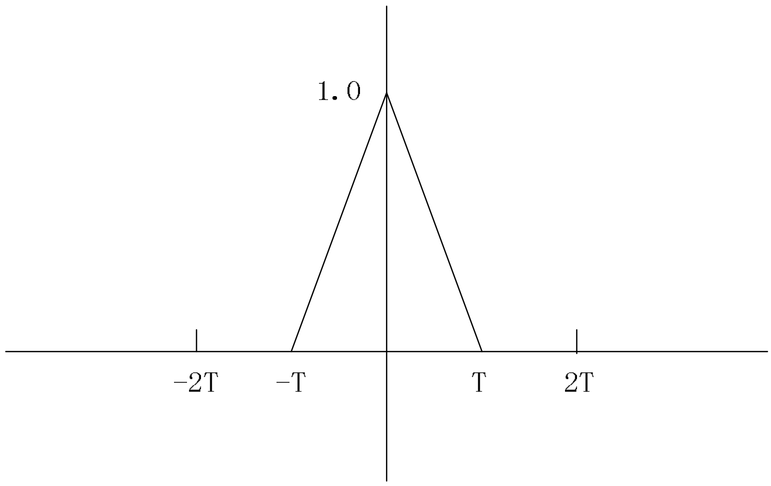

Figure A-I - Impulse response of the extrapolation filter

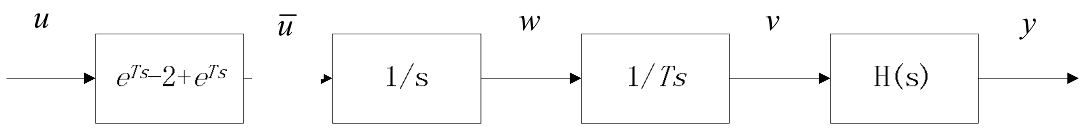

Figure A-II - Block diagram of the triangle-hold equivalent

Appendix B

Convergence on the Newmark's Constant Average Acceleration Method (Koh, 2010) is presented in this Appendix.

The Equation of motion could be written as

$$\mathbf{M}\ddot{\mathbf{x}} + \mathbf{C}\dot{\mathbf{x}} + \mathbf{K}\mathbf{x} = \mathbf{L}\mathbf{F} \tag{B.1}$$

With Newmark constant step-by-step integration method, the velocity and displacement could be represented by the following two equations

$$\begin{aligned} \dot{\mathbf{x}}_{k+1} &= \dot{\mathbf{x}}_k + (\frac{\ddot{\mathbf{x}}_k + \ddot{\mathbf{x}}_{k+1}}{2})\Delta t \\ \mathbf{x}_{k+1} &= \mathbf{x}_k + \dot{\mathbf{x}}_k \Delta t + (\frac{\ddot{\mathbf{x}}_k + \ddot{\mathbf{x}}_{k+1}}{2})\Delta t^2 \end{aligned} \tag{B.2}$$

Substitution in to the equilibrium equation and the following equation could be obtained:

$$(\frac{4}{\Delta t^2}\mathbf{M} + \frac{2}{\Delta t}\mathbf{C} + \mathbf{K})\Delta\mathbf{x} = \mathbf{F}_{k+1} + \mathbf{M}\ddot{\mathbf{x}}_k + (\mathbf{C} + \frac{2}{\Delta t}\mathbf{M})\dot{\mathbf{x}}_k - \mathbf{K}\mathbf{x}_k \tag{B.3}$$

The stability can be investigated with free vibration of the undamped single degree of freedom as follows:

$$\ddot{x} + \omega^2 x = 0 \tag{B.4}$$

Written the Equation (B.3) with F=0, C=0, $\ddot{x}_k = -\omega^2 x_k$ and $\omega^2 = k/m$

$$\Delta x = \frac{4}{4 + \Delta t^2\omega^2}\dot{x}_k - \frac{2\Delta t^2\omega^2}{4 + \Delta t^2\omega^2}x_k \tag{B.5}$$

So

$$x_{k+1} = \frac{4\Delta t}{4 + \Delta t^2\omega^2}\dot{x}_k + \frac{4 - \Delta t^2\omega^2}{4 + \Delta t^2\omega^2}x_k \tag{B.6}$$

And

$$\dot{x}_{k+1} = \frac{4-\Delta t^2\omega^2}{4+\Delta t^2\omega^2}\dot{x}_k + \frac{4\Delta t\omega^2}{4+\Delta t^2\omega^2}x_k \tag{B.7}$$

Equations (B.6) and (B.7) can be written in state space as

$$\begin{pmatrix} x_{k+1} \\ \dot{x}_{k+1} \end{pmatrix} = \begin{bmatrix} \dfrac{4-\Delta t^2\omega^2}{4+\Delta t^2\omega^2} & \dfrac{4\Delta t}{4+\Delta t^2\omega^2} \\ \dfrac{4\Delta t\omega^2}{4+\Delta t^2\omega^2} & \dfrac{4-\Delta t^2\omega^2}{4+\Delta t^2\omega^2} \end{bmatrix} \begin{pmatrix} x_k \\ \dot{x}_k \end{pmatrix} \tag{B.8}$$

The eigenvalues of Equation (B.8) can be written as

$$\lambda = \frac{4-\Delta t^2\omega^2}{4+\Delta t^2\omega^2} \pm \frac{4\sqrt{-\Delta t^2\omega^2}}{4+\Delta t^2\omega^2} \tag{B.9}$$

λ is always complex due to $\Delta t^2\omega^2 > 0$. The spectral is

$$|\lambda| = \sqrt{\left(\frac{4-\Delta t^2\omega^2}{4+\Delta t^2\omega^2}\right)^2 + \left(\frac{4\sqrt{\Delta t^2\omega^2}}{4+\Delta t^2\omega^2}\right)^2} = 1 \tag{B.10}$$

Therefore, the Newmark constant average acceleration method is unconditionally stable.

REFERENCES

Abdalla, M. O., Grigoriadis, K. M. and Zimmerman, D. C., (1998), "Enhanced structural damage detection using alternating projection methods", *AIAA Journal*, 36(7), 1305-1311.

Abdalla, M. O., Grigoriadis, K. M. and Zimmerman, D. C., (2000), "Structural damage detection using linear matrix inequality methods", *Journal of Vibration and Acoustics*, 122(4), 448-455.

Abdel, Wahab, M. M. and Roeck, G. D., (2001), "Effect of modal curvatures in damage detection using model updating", *Mechanical Systems and Signal Processing*, **15**(2), 439-445.

Abdel Wahab, M. M., Roeck, G. D. and Peeters, B., (1999), "Parameterization of damage in reinforced concrete structures using model updating", *Journal of Sound and Vibration*, 228(4), 717-730.

Abdo, M. A. B. and Hori, M. (2002), "A Numerical Study of Structural Damage Detection Using Changes in the Rotation of Mode Shapes", *Journal of Sound and Vibration,* 251(2), 227-239.

Adeli, H. and Saleh, A., (1998), "Integrated structural/control optimization of large adaptive/smart structures", *International Journal of Solids and Structures,* 35(28), 3815-3830.

Ahmadian, H., Gladwell, G. M. L. and Ismail, F., (1997), "Parameter selection strategies infinite element model updating", *Journal of Vibration and*

Acoustics, 119(1), 37-45.

Aktan, A. E., Lee, K. L., Chuntavan, C. and Aksel, T., (1994), "Modal testing for structural identification and condition assessment of constructed facilities", Proceedings of the 12th International Modal Analysis Conference, Honolulu, Hawaii, 462-468.

Anger, G., (1990), Inverse problems in differential equations, Plenum, New York.

Balageas, D.L. (ed.), (2002), *Proceedings of the 1st European Workshop on Structural Health Monitoring*, Cachan, France.

Bakir, P. G., Reynders, E. and De Roeck, G., (2007), "Sensitivity-based finite element model updating using constrained optimization with a trust region algorithm", *Journal of Sound and Vibration,* 305(1-2), 211-225.

Boller, C. and Staszewski, W.J. (eds) (2004), *Proceedings of the 2nd European Workshop on Structural Health Monitoring*, Munich, Germany.

Brock, J. E., (1968), "Optimal matrices describing linear systems", *AIAA Journal,* **6**(7), 1292-1296.

Busby H. R. and Trujillo D. M., (1998), "Optimal regularization of an inverse dynamics problem", *Computers and Structures*, 63, 243-248.

Cannon, J.R. and Hornung, U., (1986), Inverse Problems, Birkhauser Verlag, Vauser.

Cantieni, R., (1983), "Dynamic load tests on highway bridges in Switzerland – 60 years of experience", *Report* 211, *Federal Laboratories for Testing of Materials*, Dubendorf, Switzerland.

Cantieni, R., (1992), "Dynamic behaviour of highway bridges under the passage of heavy vehicles", *Report No.*220, *Swiss Federal Laboratories for Materials Testing and Research* (*EMPA*).

Casciati, F., Faravelli, L., and Borghetti, F., (2003), "Wireless links between sensor-device control stations in long span bridges", *Proceedings of SPIE – Smart Structures and Materials: Smart Systems and Nondestructive Evaluation,* 5057, 1-7.

Cawley, P. and Adams, R. D., (1979), "The location of defects in structures from measurements of natural frequencies", *Journal of Strain Analysis*, 14(2), 49-57.

Cebon, D., (1987), "Assessment of the dynamic wheel forces generated by heavy road vehicles", *Symposium on Heavy vehicle Suspension and Characteristics, Australian Road Research Board.*

Chan, T. H. T., Law, S. S. and Yung, T. H., (1999), "An interpretive method for moving force identification", *Journal of Sound and Vibration,* 219(3), 503-524.

Chan, T. H. T. and O' Connor, C., (1990), "Wheel loads from highway bridge strains", *Journal of Structural Engineering Division-ASCE,* 116, 1751-1771.

Chan, T. H. T., Yu, L., Law, S. S. and Yung, T. H., (2001) "Moving force identification studies, I: Theory", *Journal of Sound and Vibration,* 247(1), 59-76.

Chance, J., Tomlinson, G. R. and Worden, K., (1994), "A simplified approach to the numerical and experimental modeling of the dynamics of a cracked beam", *Proceeding of 12th International Modal Analysis Conference*, 778-785.

Chang, T. P., Lin, G. L. and Chang, E., (2006), "Vibration analysis of a beam with an internal hinge subject to a random moving oscillator", *International Journal of Solids and Structures*, 43, 6398-6412.

Chatterjee, P. K., Datta, T. K. and Surana, C. S., (1994) "Vibration of continuous bridge under moving vehicles", *Journal of Sound and Vibration*, 169, 619-632.

Chaudhry, Z. and Ganino, A.J., (1994), "Damage detection using neural networks-an initial experimental study on debonded beams", *Journal of Intelligent Material Systems and Structures*, 5(4), 585-589.

Chaudhuri, A. and Chakraborty, S., (2006) "Reliability of linear structures with parameter uncertainty under non-stationary earthquake", *Structural Safety*, 28, 231-246.

Chen, J.C. and Garba, J.A., (1980), "Analytical model improvement using modal testing results", *AIAA Journal*, **18**(6), 684-690.

Chu, S. Y., Soong, T. T. and Reinhorn, A. M., (2005), Active, Hybrid and Semi-active Structural Control, Wiley: New York, NY.

Collins, J.D., Hart, G.C., Hasselman, T.K. and Kennedy, B., (1974), "Statistical identification of structures", *AIAA Journal*, 12(2), 185-190.

Constantinou M. C., Soong T. T. and Dargush, G. F., (1998), "Passive energy dissipation systems for structural design and retrofit", *Multidisciplinary Center for Earthquake Engineering Research*, U.S.A., Monograph Series.

Cooley, J. W. and Tukey, J. W., (1965). "An algorithm for the machine calculation of complex Fourier series", *Mathematics of Computation*, 19, 297-301.

D"Ambrogio, W. and Sestieri, A., (2004), "A unified approach to substructuring and structural modification problems", *Shock and Vibration*, 11(3-4), 295-309.

Davis, P. and Sommerville, F., (1987) "Calibration and accuracy testing of weigh-in-motion systems", *Transportation Research Record,* 1123, 122-126.

Doebling, S.W., Farrar, C.R. and Prime, M.B., (1998), "A summary review of vibration based damage identification methods", *The Shock and Vibration Digest*, **30**(2), 91-105.

Faravelli, L. and Yao, T., (1994), "Applications of an adaptive-network Networkbased fuzzy inference system (ANFIS) to active structural control", *Proc., First World Conf. Struct. Control*, WPI. 49-58.

Farrar, C.R., Baker, W.E., Bell, T.M., Cone, K.M., Darling, T.W., Duffey, T.A., Eklund, A. and Migliori, A. (1994), "Dynamic Characterization and Damage Detection in the I-40 Bridge over the Rio Grande", *Los Alamos National Laboratory, Los Alamos, New Mexico*, Report No. LA 12767-MS.

Farrar, C.R., Doebling, S.W. and Nix, D.A., (2001), "Vibration-based structural damage identification", *Philosophical Transactions of the Royal Society of*

London Series A-Mathematical Physical and Engineering Sciences, 359(1778), 131-149.

Fletcher, R., (1987), Practical methods of optimization, *John Wiley & Sons*, New York.

Fox, C.H.J., (1992), "The location of defects in structures: a comparison of the use of natural frequency and mode shape data", *Proceeding of 10th International Modal Analysis Conference*, 522-528.

Fox, R.L. and Kapoor, M.P., (1968), "Rates of Change of eigenvalues and eigenvectors", *AIAA Journal*, **6**(12), 2426-2429.

Franklin, G. F., Powell, J. D. and Workman, M. L., (1998), *Digital Control of Dynamic Systems*, Third Edition, Addison-Wesley.

Freund, D. M. and Bonaquist, R. F., (1989), "Evaluation of a weigh-in-motion device at the pavement testing facility", *Public Roads,* 52, 97-106.

Friswell, M. I., (2007), "Damage identification using inverse methods", *Philosophical Transactions of the Royal Society*, 365 (1851), 393–410.

Friswell, M. I. and Mottershead, J. E., (1995), *Finite element model updating in structural dynamics*, Kluwer Academic Publishers.

Golub, G. H., Heath, M. and Wahaba G., (1979). "Generalized cross-validation as a method for choosing a good ridge parameter", *Technometrics*, 21(2), 215-223.

Hajela, P. and Soeiro, F., (1990), "Recent Developments in Damage Detection Based on System Identification Methods", *Structural Optimization*, 2(1), 1-10.

Hansel, E., (1991), Inverse Theory and Applications for Engineers. Prentice Hall, Englewood Cliffs.

Hansen, P. C., (1992), "Analysis of discrete ill-posed problems by means of the L-curve", *SIAM Review*, 34(4), 561-580.

Hansen, P. C., (1998), "Rank-Deficient and Discrete Ill-Posed Problems", *SIAM*, Philadelphia.

Haykin, S., (1996), Adaptive Filter Theory, Third Edition, Englewood Cliffs, NJ: Prentice-Hall.

Heaviside, O., (1892), "On the Forces, Stresses, and Fiuxes of Energy in the Electromagnetic Field", *On Operators in Physical Mathematics Part I*, Proc. *R. Soc.* London A. 52, 504-529.

Hemez, F.M. and Farhat, C., (1995), "Structural damage detection via a finite element model updating methodology", Modal Analysis: *The International Journal of Analytical and Experimental Modal Analysis*, 10(3), 152-166.

Housner, G. W., Bergman, L. A., Caughey, T. K., Chassiakos, A. G., Claus, R. O., Masri, S.F., Skelton, R.E., Soong T. T., Spencer, B. F. Jr., and Yao, T. P., (1997), "Structural control: past, present, and future", *J Engng Mech, ASCE*, 123(9), 897–971.

Housner, G. W., Soong, T. T. and Masri, S. F., (1994), "Second generation on active structural control in civil engineering", *In: Proc. 1st World Conf. on Struct. Control*. Pasadena (CA), FA2, 3–18.

Huang, H. W. and Yang, J. N., (2008), "Damage identification of substructure for local health monitoring", *Smart Structures and Systems*, 4(6), 795-807.

Ibrahim, S. R., (1986), "An approach for reducing computational requirements in modal identification", *AIAA Journal*, 24 (10), 1725-1727.

Ibrahim, S. R. and Mikulcik, E.C., (1977), "A method for the direct identification of vibration parameters from free response", *Shocked Vibration Bulletin*, 47(4), 183–198.

Iemura, H. and Pradono, M. H., (2003), "Application of Pseudo-negative Stiffness Control to the Benchmark Cable-stayed Bridge", *Journal of Structural Control*, 10(3), 187-203.

Imregun, M. and Robb, D., (1992), "Structural modification via FRF coupling using measured data", *Proceedings of the 10th International Modal Analysis Conference*, Society for Experimental Mechanics, Bethel, CT, 1095–1099.

Inoue, H., (2001), "Review of inverse analysis for indirect measurement of impact force", Applied Mechanics Reviews, 54(6), 503-524.

Jacob, B. A., (1994), "European research activity COST 323—weigh-in-motion of road vehicles." *Preceedings of NATDAC '94*.

Jacob, B. A. and O'Brien, E. J., (1996), "WAVE—a European research project on weigh-in-motion." *National Traffic Acquisition Conference* (*NATDAQ'96*), 659-668.

Jahn, H.A., (1948), "Improvement of an approximate set of latent roots and modal columns of a matrix by methods akin to those of classical perturbation theory”, *Quarterly Journal of Mechanics and Applied Mathematics*, **1**, 132-144.

Jin, S., Livingston, R.A. and Marzougui, D., (2000), “Energy index approach for damage detection in nonlinear highway structures”, *Proceedings of SPIE - The International Society for Optical Engineering*, v3995, *Nondestructive Evaluation of Highways, Utilities, and Pipelines IV*, Newport Beach, CA, USA, 52-63.

Joseph, L. and Minh-Nghi, T., (2005), “A wavelet-based approach for the identification of damping in non-linear oscillators”, *International Journal of Mechanical Sciences*, 47(8), 1262–1281.

Juan, C., Dyke, J.S. and Erik, A.J., (2000), “Health monitoring based on component transfer functions”, *Advances in Structural Dynamics,* Elsevier Science Ltd., Oxford, UK, 11, 997-1004.

Kareem, A., (1994), “The next generation of tuned liquid dampers.” *Proc.. First World Conf. on Struct. Control*, FP5, 19-28.

Kareem, A., Kijewski, T., and Tamura, Y., (1999), “Mitigation of motions of tall buildings with specific examples of recent applications.” *Wind Struct.*, 2(3), 201–251.

Kerschen, G., Peeters, M., Golinval, J. C. and Vakakis A. F., (2009), “Nonlinear normal modes, Part I: A useful framework for the structural dynamicist”, *Mechanical System and Signal Processing*, 23(1), 170-194.

Kerschen, G., Worden, K., Vakakis, A. F. and Golinval J. C. (2006), “Past, present and future of nonlinear system identification in structural dynamics", *Mechanical System and Signal Processing*, 20(3), 505-592.

Ko, J. M., Wong, C.W. and Lam, H.F., (1994), "Damage detection in steel framed structures by vibration measurement approach", *Proceedings of the 12th International Modal Analysis Conference*, Society for Experimental Mechanics, Bethel, 280-286.

Kobori, T., (1990), "Technology development and forecast of dynamical intelligent building (D. I. B.)", *Intelligent Struct.*, Elsevier Appl. Sci.,New York, N.Y., 42-59.

Koh, C. G. and Perry, M. J., (2010), *Structural Identification and Damage Detection using Genetic Algorithms*, Boca Raton, London : CRC Press.

Kolousek, V., Pirner, M. and Fischer, O., (1984), Wind effects on civil engineering structures, Amsterdam: Elsevier; Prague: Academia.

Kron, G., (1963), Diakoptics, Macdonald and Co., London.

Kucharski, T., (2000), "A method for dynamic response analysis of time-variant discrete systems", *Computers and Structures*, 76(4), 545-550.

Lai, X. P., (2005), "Projected Least-Squares Algorithms for Constrained FIR Filter Design", *IEEE Transactions on Circuits and Systems-I Regular Papers*, 52(11), 2436-2443.

Lam H. F, Ko J. M. and Wong C. W., (1995), "Detection of damage location based on sensitivity analysis", *Proceedings of 13th International Modal Analysis Conference*, 1499-1505.

Lardies, J., (1998), “State-space identification of vibrating systems from multi-output measurements”, *Mechanical Systems and Signal Processing*, 12, 543-558.

Law, S. S., Bu, J. Q. and Zhu, X. Q., (2005), “Time-varying wind load identification from structural responses”, *Engineering Structures*, 27(10), 1586-1598.

Law, S. S., Chan, T. H. T. and Wu, D., (2001), “Efficient numerical model for the damage detection of large scale structure”, *Engineering Structures*, 23(5), 436-451.

Law, S. S., Chan, T. H. T. and Zeng, Q. H., (1997), “Moving force identification: A time domain method”, *Journal of Sound and Vibration*, 201(1), 1-22.

Law, S. S., Li, X.Y., Zhu, X.Q. and Chan, S.L., (2005), “Structural damage detection from wavelet packet sensitivity”, *Engineering Structures*, 27(9), 1339-1348.

Law, S. S., Chan, T. H. T. and Zeng, Q. H., (1999), “Moving force identification: A frequency and time domains analysis.” *Journal of Dynamic Systems, Measurement, and Control-ASME*, 12(3), 394-401.

Law, S. S., Fang, Y. L. (2001), “Moving force identification: Optimal state estimation approach”, *Journal of Sound and Vibration*, 239(2), 233–54.

Law, S. S. and Li, X.Y., (2006), “Structural Damage Detection from Wavelet Coefficient Sensitivity with Model Errors”, *Journal of Engineering Mechanics*, *ASCE*, 132(10), 1077-1087.

Law, S. S. and Li, X.Y., (2007), Wavelet-based Sensitivity of Impulse Response Function for Damage Detection, *Journal of Applied Mechanics, ASME*, 74(2), 375-377.

Law, S. S., Shi, Z.Y. and Zhang, L.M., (1998), "Structural damage detection from incomplete and noisy modal test data", *Journal of Engineering Mechanics*, 124(11), 1280-1288.

Law, S. S., Waldron, P. and Taylor, C. (1992), "Damage detection of a reinforced concrete bridge deck using the frequency response function", *Proceedings of 10th International Modal Analysis Conference*, 772-778.

Li, J. and Law, S.S., (2011), "Substructural Response Reconstruction in Wavelet Domain", *Journal of Applied Mechanics, ASME*, 78(4), 041010, 1-10.

Li, H. and Ou, J. P., (2006), "A Design Approach for Semi-active and Smart Base-isolated Building", *Structure Control and Health Monitoring*, 13, 660-681.

Liu, H. J., "Dynamic model of MR dampers and optimal control of acceleration", Master Thesis, Harbin Institute of Technology, 2007 (in Chinese).

Li, J. and Roberts, J. B., (1999a), "Stochastic structural system identification, Part 1: Mean parameter estimation", *Computational Mechanics*, 24(3), 206-210.

Li, J. and Roberts, J.B., (1999b), "Stochastic structural system identification, Part 2: Variance parameter estimation", *Computational Mechanics*, 24(3), 211-215.

Li, X. Y. and Law, S. S., (2009), “Identification of structural damping in time domain”, *Journal of Sound and Vibration*, 238(1), 71–84.

Li, X. Y. and Law, S. S., (2010), “Adaptive Tikhonov regularization for damage detection based on nonlinear model updating”, *Mechanical Systems and Signal Processing*, 24(6), 1646-1664.

Lim, C. W. and Liew, K. M., (1995), “A Higher Order Theory for Vibration of Shear Deformable Cylindrical Shallow Shell”, *International Journal of Mechanical Sciences*, 37(3), 277-295.

Lin, C. J., (2007), “Projected gradient methods for non-negative matrix factorization”, *Neural Computation*, 19(10), 2756-2779.

Lin, R.M., Lim, M.K. and Du, H., (1995), “Improved inverse eigensensitivity method for structural analytical model updating”, *Journal of vibration and Acoustics*, *ASME,* 117(2), 192-198.

Loh, C. H, Lynch, J. P., Lu, K. C., Wang, Y., Chang, C. M., Lin, P. Y. and Yeh. T. H., (2007), “Experimental verification of a wireless sensing and control system for structural control using MR dampers”, *Earthquake Engng. Struct. Dyn.*, 36, 1303-1328.

Lu, Z. R. and Law, S. S., (2007a), “Features of dynamic response sensitivity and its application in damage detection”, *Journal of Sound and Vibration*, 303(1-2), 305-329.

Lu, Z. R. and Law, S. S., (2007b), “Identification of system parameters and input force from output only”, *Mechanical Systems and Signal Processing*, 21(5), 2099-2111.

Lunze, J, (1992), Feedback control of Large-scale Systems, Prentice Hall, New York.

Lynch, J. P. and Law, K. H., (2002a), "Decentralized control techniques for large-scale civil structural systems", *Proceedings of the20th International Modal Analysis Conference*, Los Angeles. Bellingham: Society of Photo-Optical Instrumentation Engineers.

Lynch, J.P. and Law, K. H., (2000b), "Market-based control of linear structural systems", *Earthquake Engineering and Structural Dynamics*, 31(10), 1855-1877.

Mares, C., Friswell, M. I. and Mottershead, J. E., (2002), "Model updating using robust estimation", *Mechanical Systems and Signal Processing*, 16(1), 169-183.

Mayes, R.L., (1992), "Error localization using mode shapes: An application to a two link robot arm", *Proceedings of 10th International Modal Analysis Conference*, 886-891.

Mayes, R.L., (1995), "An experimental algorithm for detecting damage applied to the I-40 bridge over the Rio Grande", *Proceedings 13th International Modal Analysis Conference*, 219-225.

Messina, A., Jones, I.A. and Williams, E. J., (1996), "Damage detection and localization using natural frequency changes", *Proceedings of conference on Identification in Engineering Systems*, Swansea, U. K., 67-76.

Messina, A., Williams, E.J. and Contursi, T., (1998), “Structural damage detection by a sensitivity and statistical-based method”, *Journal of Sound and Vibration*, 216(5), 791-808.

Mindlin, R. D. (1955), “An Introduction to the Mathematical Theory of Vibrations of Elastic Plates”, Fort Monmouth, NJ: U.S. Army Signal Corps Engineering Laboratories.

Moses, F., (1979), “Weigh-in-motion system using instrumented bridges”, *Transportation Engineering Journal of ASCE*, 105(3), 233-249.

Mottershead, J. E. and Foster, C.D., (1991), “On the treatment of ill-conditioning in spatial parameter estimation from measured vibration data”, *Mechanical Systems and Signal Processing*, 5(2), 139-154.

Mottershead, J. E. and Friswell, M. I., (1993), “Model updating in structural dynamics: a survey”, *Journal of Sound and Vibration*, 167(2), 347-375.

Mottershead, J. E., Mares, C., James, S. and Friswell, M. I., (2006), “Stochastic model updating: Part 2--application to a set of physical structures”, *Mechanical Systems and Signal Processing*, 20(8), 2171-2185.

Nelson, R. B., (1976), "Simplified calculation of eigenvector derivatives", *AIAA Journal*, 14(9), 1201-1205.

Nishitani, A. and Inoue, Y., (2001), “Overview of the application of active/semiactive control to building structures in Japan”, *Earthquake Engineering & Structural Dynamics*, 30(11), 1565–1574.

Nwosu, D.I., Swamidas, A.S.J., Guigne, J.Y. and Olowokere, D.O., (1995), "Studies on influence of cracks on the dynamic response of tubular T-joints for nondestructive evaluation", *Proceedings of 13th International Modal Analysis Conference*, 1122-1128.

Ojalvo, I.U. and Ting, T., (1990), "Interpretation and improved solution approach for ill-conditioned linear equations", *AIAA Journal*, 28(11), 1976-1979.

Pall, A. S., and Marsh, C., (1982), "Response of friction damped braced frames", *J. of Struct. Div., ASCE*, 108(6), 1313-1323.

Pandey A.K. and Biswas M., (1994), "Damage Detection in Structures Using Changes in Flexibility", *Journal of Sound and Vibration*, 169(1), 3-17.

Pandey A.K., Biswas M. and Samman M.M., (1991), "Damage detection from changes in curvature mode shapes", *Journal of Sound and Vibration*, 145(2), 321-332.

Parloo E., Guillaume P. and Van Overmeire M., (2003), "Damage assessment using mode shape sensitivities", *Mechanical Systems and Signal Processing,* 17(3), 499-518.

Park N.G. and Park Y.S., (2003), "Damage detection using spatially incomplete frequency response functions", *Mechanical Systems and Signal Processing*, 17(3), 519-532.

Pascual R., Schälchli R. and Razeto M., (2005), "Improvement of damage-assessment results using high-spatial density measurements", *Mechanical Systems and Signal Processing*, 19(1), 123-138.

Penny, J.E.T., Wilson, D. and Friswell, M.I., (1993), "Damage location in structures using vibration data", *Proceedings of the 11th International Modal Analysis Conference* 1, 861-867.

Phani, A. S. and Woodhouse, J., (2007), "Viscous damping identification in linear system", *Journal of Sound and Vibration*. 303(3-5), 475–500.

Pong, W. S., Tsai, C. S., and Lee, G. C. (1994a), "Seismic study of building frames with added energy-absorbing devices", NCEER Rep. No. 94-0016, State Univ. of New York at Buffalo, Buffalo. N.Y.

Pong, W. S., Tsai, C. S., and Lee, G. C., (1994b), "Seismic study of viscoelastic dampers and TPEA devices for high-rise buildings", *Proc., First World Conf. on Struct. Control*, Vol. 1, WP3-23-WP3-32.

Pong, W. S., Tsai, C. S., Tsai, K. C., and Lee, G. C. (1994c), "Parametric study of TPEA devices for buildings", *Proc., First World Conf. on Struct. Control*. Vol. 1. WP3-33-WP3-42.

Prandina M., Mottershead, J. E. and Bonisoli, E., (2009a), "An assessment of damping identification methods", *Journal of Sound and Vibration*, 323, 662–676.

Prandina, M., Mottershead, J. E. and Bonisoli, E., (2009b), "Damping identification in multiple degree-of-freedom systems using an energy balance approach", *7 th International conference on Modern Practice in Stress and Vibration Analysis*, *Journal of Physics: Conference Series*, 181, 012006. 27, 1586-1598.

Raghavendrachar, M. and Aktan, A.E., (1992), “Flexibility by multireference impact testing for bridge diagnostics”, *Journal of Structural Engineering, ASCE*, 118(8), 2186-2203.

Ratcliffe, C.P., (1997), “Damage detection using a modified laplacian operator on mode shape data”, *Journal of Sound and Vibration*, 204(3), 505-517.

Reissner, E., (1945), “The effect of transverse shear deformation on the bending of elastic plates”, *ASME, Journal of Applied Mechanics,* 12, 69-76.

Ren, W. X., (2005), “A singular value decomposition based on truncation algorithm in solving the structural damage equations”, *Acta Mechanica Solida Sinica*, 18(1), 181-188.

Rizos, P.F., Aspragathos, N. and Dimarogonas, A.D., (1990), “Identification of crack location and magnitude in a cantilever beam from the vibration modes”, *Journal of Sound and Vibration*, 138 (3), 381-388.

Rothwell, E. and Drachman, B., (1989), “A unified approach to solving ill conditioned matrix problems”, *International Journal for Numerical Methods in Engineering*, 28(3), 609-620.

Rytter, A., (1993), “Vibration based inspection of civil engineering structures, Doctoral Dissertation”, *Department of Building Technology and Structural Engineering*, University of Aalborg.

Salawu, O.S., (1997a), “Detection of structural damage through changes in frequency: A review”, *Engineering Structures*, 19(9), 718-723.

Salawu, O.S., (1997b), “An integrity index method for structural assessment of engineering structures using modal testing", *Insight: The journal of the British Institute of Non-Destructive Testing*, 39(1).

Salawu, O.S. and Williams, C., (1994), "Damage location using vibration mode shapes", *Proceedings of 12th International Modal Analysis Conference*, 933-939.

Samman, M.M., Biswas, M. and Pandey, A.K., (1991), "Employing pattern recognition for detecting cracks in a bridge model", *Modal Analysis: The International Journal of Analytical and Experimental Modal Analysis*, 6(1), 35-44.

Sandell, N., Varaiya, P. and Athans, M., (1978), "Survey of decentralized control methods for large scale systems", *IEEE Transactions on Automatic Control*, 23(2), 108-128.

Sandesha, S., (2009), "Time domain identification of structural parameters and input time history using a substructural approach", *International Journal of Structural Stability and Dynamics*, 9(2), 243-265.

Sandesha, S. and Shankarb, K., (2009), "Damage Identification of a Thin Plate in the Time Domain with Substructuring-an Application of Inverse Problem", *International Journal of Applied Science and Engineering* 7(1), 79-93.

Shi, Z.Y., Law, S.S. and Zhang, L.M., (1998), "Structural damage localization from modal strain energy change", *Journal of Sound and Vibration*, 218(5), 825-844.

Shi, Z.Y., Law, S.S. and Zhang, L.M., (2000a), "Damage location by directly using incomplete mode shapes", *Journal of Engineering Mechanics*, ASCE, 126(6), 656-660.

Shi, Z.Y., Law, S.S. and Zhang, L.M., (2000b), "Structural damage detection from modal strain energy change", *Journal of Engineering Mechanics*, 126(12), 1216-1223.

Shi, Z.Y., Law, S.S. and Zhang, L.M., (2002), "Improved damage quantification fromelemental modal strain energy change", *Journal of Engineering Mechanics,* 128(5), 521-529.

Simiu, E., Scanlan, R.H., (1996), Wind effects on structures. 3rd ed. New York, Wiley.

Simonian, S.S., (1981), "Inverse problems in structural dynamics", *Int. J. Numer. Methods Eng.*, 17(3), 357-365.

Skelton, R. E., (1988), Dynamic systems control: linear systems analysis and synthesis, *John Wiley & Sons, Inc.*, New York, N.Y.

Skinner, R. I., Tyler, R. G., Heine, A. J. and Robinson, W. H., (1980), "Hysteretic dampers for the protection of structures from earthquakes", *Bull. N.Z Soc. Earthquake Engrg.*, 13(1), 22-36.

Skjaeraek, P.S., Nielsen, S.R.K., and Cakmak, A.S., (1996), "Identification of damage in reinforced concrete structures from earthquake records: Optimal location of sensors", *Soil Dynamics and Earthquake Engineering*, 15(6), 347-358.

Soong, T. T. and Spencer, B. F. Jr., (2000), "Active, semi-active and hybrid control of structures", *Bulletin of the New Zealand National Society for Earthquake Engineering*, 33(3), 387-402.

Soong, T. T., (1990), Active structural control: theory and practice, Longman Wiley, London, England.

Spencer, B.F.Jr. and Nagarajaiah, S., (2003), "State of the art of structural control", *Journal of Structural Engineering*, 129(7), 845–856.

Srinivasan, M.G. and Kot, C.A., (1992), "Effects of damage on the modal parameters of a cylindrical shell", Proceedings of the 10th International Modal Analysis Conference, 529–535.

Steltzner, A.D, Kammer D.C., (1999), "Input force estimation using an inverse structural filter", *Proceedings of the 17th International Modal Analysis Conference*, 954–960.

Stevens, K. K., (1987), "Force identification problems-an overview", *Proceedings of the 1987 SEM Spring Conference on Experimental Mechanics*, Houston USA, 838–844.

Stubbs, N. and Osegueda, R., (1990), "Global damage detection in solids: Experimental verification", *Modal analysis: The International Journal of Analytical and Experimental Modal Analysis*, 5(2), 81-97.

Stubbs, N. and Kim, J.T., (1996), "Damage localization in structures without baseline modal parameters", *AIAA Journal*, 34(8), 1644-1649.

Stubbs, N., Kim, J.T. and Topole, K., (1992), "An efficient and robust algorithm for damage localization in offshore platforms", *Proceedings of the ASCE*

10th Structures Congress, 543-546.

Stubbs, N., Park, S., Sikorsky, C. and Choi, S., (1998), "A methodology to nondestructively evaluate the safety of offshore platforms", *Proceedings of the 8th International Offshore and Polar Engineering Conference*, The International Society of Offshore and Polar Engineers, California, 71-79.

Stubbs, N., Park, S., Sikorsky, C., and Choi, S., (2000), "A global non-destructive damage assessment methodology for civil engineering structures", *International Journal of System Science*, 31(11), 1361-1373.

Swartz, R.A. and Lynch, J.P., (2006), "Redundant Kalman Estimation for a Distributed Wireless Structural Control System", *Processing of the US-Korea Workshop on Smart Structures for Steel Structures*, Soul, Korea.

Tang, H. S., Xue, S. T., Chen R. and Sato, T., (2006), "Online weighted LS-SVM for hysteretic structural system identification", *Engineering Structures*, 28(12), 1728-1735.

Tee, K. F., Koh, C. G. and Quek, S. T., (2005), "Substructural first- and second-order model identification for structural damage assessment", *Earthquake Engineering and Structural Dynamics*, 34(15), 1755-1775.

Tee, K. F., Koh, C. G. and Quek, S. T., (2009), "Numerical and experimental studies of a substructural identification strategy", *Structural Health Monitoring*, 8(5), 397-410.

Tikhonov, A.M., (1963), "On the solution of ill-posed problems and the method of regularization", *Soviet Mathematics*, **4**, 1035-1038.

Tikhonov, A.N. and Arsenin, V.Y., (1977), *Solutions of ill-posed problems*, John Wiley & Sons, New York.

Tikhonov, A.N. (1995), *Numerical Methods for the Solution of Ill-posed Problems*, Kluwer Academic Publishers, Dordrecht, Boston.

Toksoy, T. and Aktan, A.E., (1995), "Bridge-condition assessment by modal flexibility", *Workshop on Instrumentation and Vibration Analysis of Highway Bridges*, University of Cincinati, Ohio.

Topole, K.G. and Stubbs, N., (1995), "Nondestructive damage evaluation of structure from limited modal parameters", *Earthquake Engineering and Structural Dynamics*, 24(11), 1427-1436.

Uzgider, F.A., Piroglu, F., Sanli, A.K., Caglayan, B.O., (1993), "Identification of railway bridges using locomotive induced vibrations", *International Conference on Bridge Management*, University of Surrey, Guildford, UK.

Uhl, T., (1998), *Computer Assisted Identification of Mechanical Structures* (in Polish), WNT, Warszawa.

Uhl, T., (2007), "The inverse identification problem and its technical application", *Archive of Applied Mechanics,* 77(5), 325–337.

Vandiver, J.K., (1975), "Detection of structural failure on fixed platforms by measurement of dynamic response", *Proceedings of 7th Annual Offshore Technology Conference*, 243-252.

Vandiver, J.K., (1977), "Detection of structural failure on fixed platforms by measurement of dynamic response", *Journal of Petroleum Technology*, 29(3), 305-310.

Wang, Y., (2007a), "Wireless sensing and decentralized control for civil structures: theory and implementation", Ph.D. Thesis, *Department of civil and Environmental Engineering*, *Stanford University*, Stanford, CA.

Wang, Y., Swartz, R. A., Lynch, J. P., Law, K. H., Lu, K. C. and Loh, C. H. (2007b), "Decentralized civil structural control using real-time wireless sensing and embedded computing", *Smart Structures and Systems*, 3(3), 321-340.

Wang, J. H. and Liou, C. M., (1991), "Experimental identification of mechanical joint parameters", *Journal of Vibration and Acoustics, ASME*, 113(1), 28-36.

Weber, B., Paultre, P. and Proulx J., (2009), "Consistent regularization of nonlinear model updating for damage identification", *Mechanical Systems and Signal Processing*, 23(6), 1965-1985.

West, W.M., (1984), "Illustration of the use of modal assurance criterion to detect structural changes in an orbiter test specimen", *Proceedings of Air ForceConference on Aircraft Structural Integrity*, 1-6.

Whittaker, A. S., Bertero, V. V., Thompson, C. L., and Alonso, L. J., (1991), "Seismic testing of steel plate energy dissipation devices", *Earthquake Spectra*, 7(4), 563-604.

Widrow, B. and Lehr, M. A., (1990), "Thirty years of adaptive neural networks: perceptron, madaline and backpropagation", *Proc.. IEEE*, 78(9), 1415-1441.

Wojnarowski, M.E., Stiansen, S.G. and Reddy, N.E., (1977), “Structural integrity evaluation of a fixed platform using vibration criteria”, *Proceedings of 9thAnnual Offshore Technical Conference*, 247-256.

Worden, K., Farrar, C.R., Manson, G. and Park, G., (2005), “Fundamental axioms of structural health monitoring”, *Structural Health Monitoring 2005: Advancements and Challenges for Implementation*, Chang, F. K. (editor), DEStech Publications, Lancaster, Pennsylvania, 26-41.

Wu, B., Shi, P. F. and Ou, J. P., (2010), “Performance of Structures Incorporating MR Dampers with Pseudo-negative Stiffness”, *5th World Conference on Structural Control and Monitoring*, 5WCSCM-279.

Wu, D. and Law, S. S., (2004), “Damage localization in plate structures from uniform load surface curvature”, *Journal of Sound and Vibration*, 276(1-2), 227-244.

Wu X, Ghaboussi, J. and Garrett, J. H., (1992), “Use of neural networks in detection of structural damage”, *Computers and Structures*, 42(4), 649-659.

Wu, J. J., (2006), “Use of moving distributed mass element for the dynamic analysis of a flat plate undergoing a moving distributed load”, *International journal for numerical methods in engineering*, 71(3), 347-362.

Xu, B., Wu, Z.S., Chen G.D. and Yokoyama K., (2004), “Direct identification of structural parameters from dynamic responses with neural networks”, *Engineering Applications of Artificial Intelligence*, 17(8), 931-943.

Xu, Y. L. and Chen, B., (2007), “Integrated Vibration Control and Health

Monitoring of Building Structures using Semi-Active Friction Dampers: Part I - Methodology”, *Engineering Structures*, 30(7), 1789-1801.

Xu, Y. L. and Chen, B., (2007) “Integrated Vibration Control and Health Monitoring of Building Structures using Semi-Active Friction Dampers: Part II - Numerical investigation”, *Engineering Structures*, 30(3), 573-587.

Yang, J. N. and Lin, S., (2004), “On-line identification of non-linear hysteretic structures using an adaptive tracking technique”, *International Journal of Non-Linear Mechanics*, 39(9), 1481-1491.

Yang, J. N. and Huang, H. W., (2007), "Substructure damage identification using a damage tracking technique", *Proceedings of SPIE - The International Society for Optical Engineering*, San Diego, California, USA, Article No. 65292R.

Yao, G.C., Chang, K.C. and Lee, G.C., (1992), “Damage diagnosis of steel frames using vibrational signature analysis”, *Journal of Engineering Mechanics*, 118 (9), 1949-1961.

Yu, L. and Chan, T. H. T., (2003), “Moving force identification based on the frequency-time domain method”, *Journal of Sound and Vibration*, 261(2), 329-349.

Yuen, M.M.F., (1985), “A numerical study of the eigen-parameters of a damaged cantilever”, *Journal of Sound and Vibration*, 103, 301-310.

Yun, C. B. and Bahng, E. Y., (2000), “Substructural identification using neural networks”, *Computers and Structures*, 77(1), 41-52.

Yun, C. B. and Lee, H. J., (1997), "Substructural identification for damage estimation of structures", *Structural Safety*, 19(1), 121-140.

Zadeh, L. A., (1965), "Fuzzy sets", *Information and control*, 8, 338-353.

Zhang, J. L., (2003), "On the convergence properties of the Levenberg-Marquardt method", *Optimization*, 52(6), 739-756.

Zhang，K. and Law，S. S., (2010), "Structural Damage Detection from Coupling Forces between Substructures under Support Excitation", *Engineering Structures*, 32(8), 2221-2228.

Zhang, K. Y., Gu, A. J. and Li, J. W., (1992), "Diagnosis of a slot fault on a frame structure", *Proceedings of 10th International Modal Analysis Conference* 1, San Diego, California, 549-553.

Zhang, K. Y., Cheng, L. J. and Jin, T. X., (1993), "Research on the diagnosis of defect on a building foundation piles", *Proceedings of 11th International Modal Analysis Conference* 1, Kissimmee, Florida, 690-695.

Zhi, X., Shalaby, A. and Middleton, D., (1999), "Evaluation of Weigh-in-motion in Manitoba", *Canadian Journal of Civil Engineering*, 26(5), 655-666.

Zhu, X. Q. and Law, S. S., (2000), "Identification of vehicle axle loads from bridge dynamic response", *Journal of Sound and Vibration,* 236(4), 705-724.

Zhu, X. Q. and Law, S. S., (2001), "Identification of moving loads on an orthotropic plate", *Journal of Vibration and Acoustics-ASME*, 123(2), 238-244.

Zhu, X. Q., Law, S. S. and Bu, J. Q., (2006), "A state space formulation for moving loads identification.” *Journal of Vibration and Acoustics-ASME*, 128(4), 509-520.

Zhu, X. Q. and Law, S. S., (2002b), “Moving loads identification through regularization”, *Journal of Engineering Mechanics*, 128(9), 989-1000.

Zhu, X. Q. and Law, S. S., (2003), “Identification of moving interaction forces with incomplete velocity information”, *Mechanical Systems and Signal Processing*, 17(6), 1349-1366.

Zhu, X. Q., Law, S. S. and Bu, J. Q., (2006), “A state space formulation for moving loads identification”, *Journal of Vibration and Acoustics*, 128(4), 509-520.

Zhu, X. Q. and Law, S. S., (2007a), “Identification of system parameters and input force from output only”, *Mechanical Systems and Signal Processing*, 21(5), 2099-2111.

Zhu, X. Q. and Law, S. S., (2007b), “Damage Detection in Simply Supported Concrete Bridge Structure Under Moving Vehicular Loads”, *Journal of Vibration and Acoustics*, 129(1), 58-64.

Ziaei-Rad, S. and Imregun, M., (1999), “On the use of regularization techniques for finite element model updating”, *Inverse Problems in Engineering*, 7(5), 471-503.